Life-time monitoring of in service switches and crossings through field experimentation

ANDREW TOM CORNISH

Future Railway Research Centre

Department of Mechanical Engineering
Imperial College London

Imperial College London

Supervisors
Professor Roderick Smith
Professor John Dear

Submitted for the degree of Doctor of Philosophy to
Imperial College London

May 2014

DECLARATION

I can confirm that the work completed in this thesis report is my original work, and whilst gaining information from some relevant sources that are referenced, the words, format and processes have been generated by me.

Andrew Tom Cornish

ABSTRACT

In financial year 2011/2012, Switches and crossings (S&C) cost the UK rail infrastructure owner, operator and maintainer, Network Rail, over £220m in maintenance and £189m in renewals. This represented 24% of the total track maintenance budget, whilst accounting for only 5% of the network mileage. The large costs are due to the complex S&C design that allows network flexibility whilst supporting a vehicle traversing from the switch rail to the stock rail and through the crossing. The motivation for undertaking this research was to understand how S&C reacts to dynamic loading imposed by the vehicles, and to gain a better knowledge of the deterioration of the asset. The understanding and measurement of S&C degradation has never been scientifically measured in real time before, which means that currently the maintenance schedules are cyclic or reactive. The outcome from this investigation could be used to provide a finely calibrated pre-emptive schedule for more effective S&C maintenance and investment.

Eight sites were outlined in the design of experiments, of which four were instrumented as part of the first phase of the research in this thesis. High wear and fatigue rates from prior failure statistical analysis showed the need to understand the loading and degradation of S&C. Strain gauges, geophones and accelerometers were used to understand the system reaction to loading, through strain and the sleeper deflection within S&C.

The results show that the largest increase in strain over time was at the stock rail with the closed switch rail. The degradation is due to the increased dynamic forces of the vehicle transferring from one line to another. The change in strain indicates that the additional vibrations / frequencies will occur over time, increasing the rate of material change. As speed increases through switches and crossings, a reduction in the strain generated is seen at the gauge locations. This indicates that switches demonstrate lower levels of wear with a higher speed at the locations of the gauges. Degradation of vertical motion of sleepers at the crossing is shown, with no change in the bending strain generated due to the whole asset deforming at a similar rate.

Key words: S&C instrumentation, deterioration, strain gauge, vertical displacement

ACKNOWLEDGEMENTS

I would like to thank everyone who has supported me during this process; Network Rail for the funding and financial support, with Engineering function and Switch and Crossing team support and great foundation knowledge, Phil Winship for the application knowledge and organisational skills that he has shown throughout the project. Prof Roderick Smith, Dr Elias Kassa and Prof John Dear for their academic applications, guidance and belief in the project. I would also like to thank Catherine Griffiths for her excellent guidance on writing.

Whilst completing the research, often talking things through have clarified issues. For his help in general discussions and assistance, I would like to thank Ian Coleman – with whom I hope to continue in collaboration for many years to come.

I would like to honour my family for the mental support and encouragement that they have shown: Joanne Cornish (Wife) and Sally Cornish (Mother) for their significant support; Hannah Elizabeth Cornish (daughter) and Jacob Patrick Cornish (son) for enduring the missed bedtimes with understanding and constant affection.

Thank you.

NOMENCLATURE

Symbol	Unit (SI)	Meaning
$\in'_{\frac{T}{O}}$		Thermal output adjusted for instrument gauge factor setting
$\in_{\frac{T}{O}}$		Thermal output from gauge package data sheet
113A	lb/y	Weight of rail, same rail weight as 56kg/m
Angle of attack	o	The difference between the position of the axle and the angle to the centre of the curve
C		C length switch (c.f. Table 5-1)
Cant	mm	Difference in elevation between one rail and the other
Cant deficiency	mm	Reduction in cant below the design cant outlined in Network Rail standard TRK/L2/001
Creepage		The relative velocity between the wheel and the rail
D		D length switch (c.f. Table 5-1)
F_I		Instrument gauge factor during strain measurement
G		G length switch (c.f. Table 5-1)
mV		milli-Volts, unit of voltage from the strain gauges before conversion
SCx		Switch and Crossing X (c.f. Table 5-1)
SGX		Strain gauge number
Train		Any number of vehicles, running on the network
TX	Tonnes	Tonnage level X, defined by certain parameters (c.f. Table 5-1)
Tγ	J/m	The contact patch energy, Creep Force x creepage
Unsprung mass	kg	The mass of a vehicle between the contact of the rail and the first suspension system
V	m/s	Velocity

Vehicle		A single carriage
VX	m/s	Velocity level X, defined by certain parameters (c.f. Table 1)
x	m	Displacement
ε	$\mu\varepsilon$	Change of length of material against the original length
ε_{actual}	$\mu\varepsilon$	Strain calculated through use for the gauge factor
ε_{axial}	$\mu\varepsilon$	Axial strain (longitudinal)
ε_{raw}	$\mu\varepsilon$	Strain recorded from gauges and converted from volts to strain
$\varepsilon_{transverse}$	$\mu\varepsilon$	Transverse strain (Vertical and compressive)
υ		Poisson's Ratio

ABBREVIATIONS

Abbreviation	*Meaning*
Abaqus/CAE	*Complete Abaqus Environment – Finite Element Analysis software programme to complete the analysis found in section 8*
BRR	*British Rail Research – a section of British Rail funded to complete research for the railway industry*
CEN	*European Committee for Standardisation – use European standards to create similar policies for technical boards*
CPU	*Central Processing Unit – hardware within a computer the carries out the operations requested*
DAQ	*Data AQusition system*
DOE	*Design of Experiment*
EMC	*Electro Magnetic Current – Electromagnetic current generates a noise through the electrical system at 50Hz. Currents are undesirable due to the impedance of the metal cable running through the electromagnetic field generating an electrical noise and distorting any signal.*
EMGTPA	*Equivalent Million Gross Tonnes Per Annum – a method of normalising track damage. Axle number, Axle load and speed are multiplied by factors to generate a annual figure for each vehicle. A good reference for the potential damage that will be seen over the site*
FEA	*Finite Element Analysis*
HST	*High Speed Train – the original high speed train in the UK, with the configuration of a class 43, Mk3 coaches and a class 43 locomotive*
LHS	*Latin Hypercube Sampling – a semi-randomised sampling technique, using probability to define bins for random sampling*
LLP	*Louis Le Pen – member of the University of Southampton (UoS) which calibrated for some of the geophone research and processing*
LMWS	*Load Measuring Wheelset – Strain gauges are attached to a wheel to gain the loading from the vehicle into the track*
NMT	*New Measurement Train – a train used by Network Rail to dynamically measure the track geometry*
PPM	*Public Performance Measure – train performance measure, usually as a percentage, of trains arrival against the schedule*
POE	*Points Operating Equipment – manoeuvres the switch rail to allow for functionality and holds in position*
Pway	*Permanent way – features of the railway, including the rails, ballast,*

	sleepers and switches and crossings
RMS	*Root mean squared – a mathematical term of taking the mean of the squared values from the data and square rooting. This allows for the more larger, and more significant, data points to have greater influence.*
S&C	*Switch and Crossing*
TOC	*Train Operating Company – franchise owners that operate the trains*
UoS	*University of Southampton – collaboration was completed with Louis Le Pen at the UoS on the geophone conversation and analysis*

CONTENTS

FIGURES

TABLES

This page was left intentionally blank

1. INTRODUCTION

This chapter gives a preface and the motivation for the research. An overview of the approach of the thesis is described before the aims are presented. The chapters of the thesis have been summarised to show the research that has been completed.

On the UK railway infrastructure, there are 20,327 sets of switches and crossings (S&C), with over 200 variations in design due to design parameters such as switch lengths and angle of the diversion route (turnout route). S&C's have historically taken 24% of maintenance and 23% renewal budgets (c.f. Chapter 4) against 5% of representative track miles. This is due to complex wheel to rail interaction and machined longitudinal rail profiles. Internationally, switches and crossings have separately been the subject of research to understand their degradation, focusing on the contact patch (contact conditions between wheel and rail on a localised level), the ground conditions or using historic renewal data. The full switch and crossing rail design and deterioration were not considered in the previous research.

There have been two major incidents in recent years within S&C due to missing / damaged components (stretcher bars and bolts) causing the switch blade to be uncontrolled and the vehicle derailed [1]. The incidents occurred at Potters Bar in Hertfordshire, and Grayrigg (sometimes referred to as Lambrigg due to the nearby town) in Cumbria. The fines imposed by the Office of Rail Regulation (ORR) on the infrastructure owner, operator and maintainer, Network Rail, were £3m and £4m respectively, plus prosecution fees. This research was initiated from the lack of Network Rail's knowledge of forces being imparted to the S&C from the vehicles. The ORR and Rail Accident and Investigation Branch (RAIB) report on the Grayrigg derailment states;

"Section 414. ... Network Rail's incomplete understanding of the design and performance of S&C, and it's inspection and maintenance requirements, was an underlying factor in the accident at Grayrigg." [1]

A typical S&C unit will be replaced after 25 to 60 years, with the period of renewal dependant on the speed and tonnage of the route. For routes with high speeds, above 128mph,

or 25EMGTPA (Equivalent Million Gross Tonnes Per Annum – c.f. Figure 2-8), the expected life is 25 years which is 2.1% of the total S&C population. The typical life increases incrementally up to 60 years for routes with speeds below 25mph and 6EMGTPA, which make up 23% of the S&C population.

Figure 0-1 shows some of the damage that occurred at Lambrigg due to the missing and damaged components. These components were not found in the current routine inspection due to unknown reasons [2, 3].

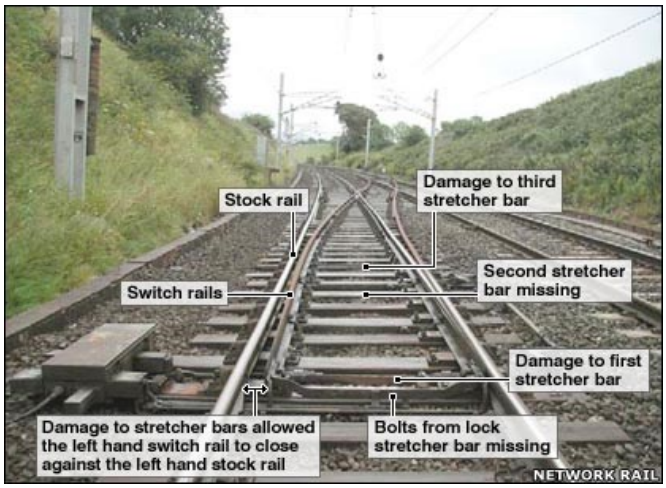

(i)

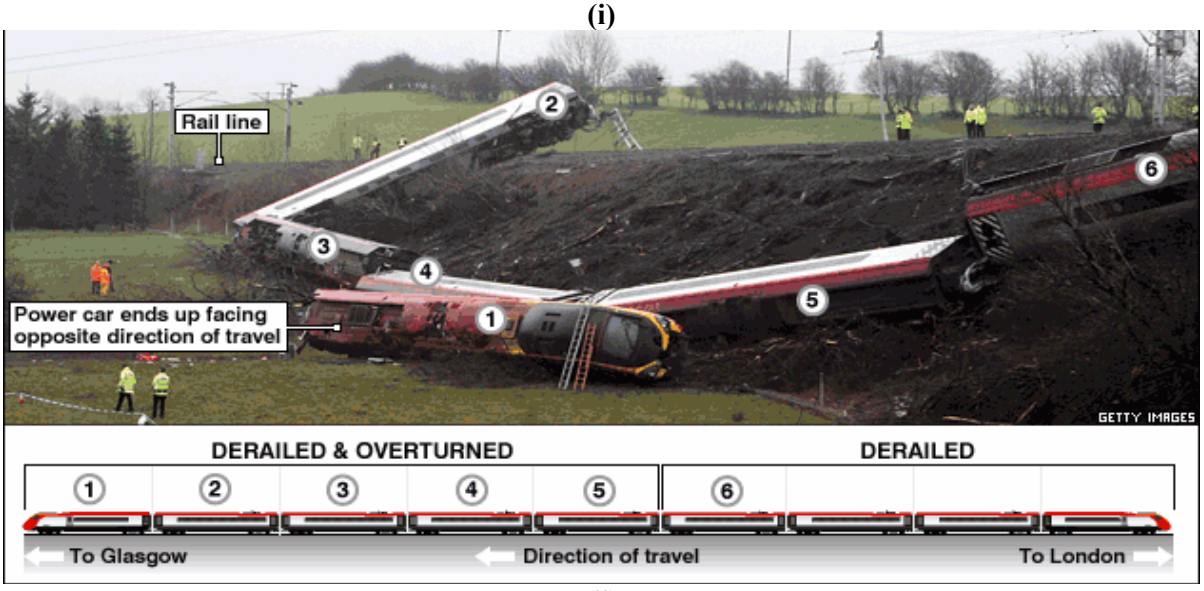

(ii)

Figure 0-1: Images of the Lambrigg incident in February 2007 (i) a short description of the incident [2]and (ii) showing the vehicles in their resting position after the incident [3]

1.1 RAILWAY FINANCE AND REGULATION OBJECTIVES

As a result of the accident investigation and funding deliverables, Network Rail was given a set of targets to improve efficiencies by the ORR with a target completion date of April 2014 [4], and recently been given additional targets until 2019 [5]. The targets until April 2014 include increasing the availability of the infrastructure for passenger vehicles by 37% (by reducing the expected disruption to passengers from the lines being closed), without detrimentally affecting freight services. Between April 2014 and April 2019, the target for passenger train journeys increased by an additional 14% by 225 million and by 16% for freight, as the expected demand for the railway continues to grow for the next five years. To achieve these targets, the infrastructure must run more efficiently, with less useable maintenance time. The increase in efficiency of maintenance practices will be achieved by focusing on key components, identified through a study on train delay statistics. The government funding between 1986 and 2013 is shown in Figure 0-2**.** There was a significant increase in the funding from £1.4bn after the Hatfield rail incident [6] in 2000, up to a maximum of £6.3bn in 2006 to find and replace rail that were showing similar damage mechanisms, rolling contact fatigue, and continued improvement for inspections and rectifications. Currently, the government investment in the railway infrastructure is annually £4bn. On the secondary axis of Figure 0-2**,** the passenger kilometres travelled have increased steadily from 29 billion km/annum in 1994 to 54 billion km/annum in 2013 [7].

A ‘Railway Value for Money’ study was completed in 2012 to compare the UK against other European railways to understand how the UK could become more efficient in operating the railway [8]. The McNaulty report states that the UK railway infrastructure is approximately 30% more expensive than equivalents across Europe due to high labour costs, inefficient practices and the current company structure. Maintenance practices need to be streamlined to achieve a £1bn saving per year in railway operational costs by 2019. Degradation and failure knowledge of S&C is necessary to create a structured approach to maintenance by focusing the inspection to specific assets.

The aim of this research is to understand the change in material strains through the life cycle of S&C, and monitor the deterioration of the asset. Understanding of forces in S&C allows the industry to increase the reliability and efficiency of maintenance procedures. Greater understanding of the assets reaction to certain loading types and ground conditions is necessary for the deterioration knowledge.

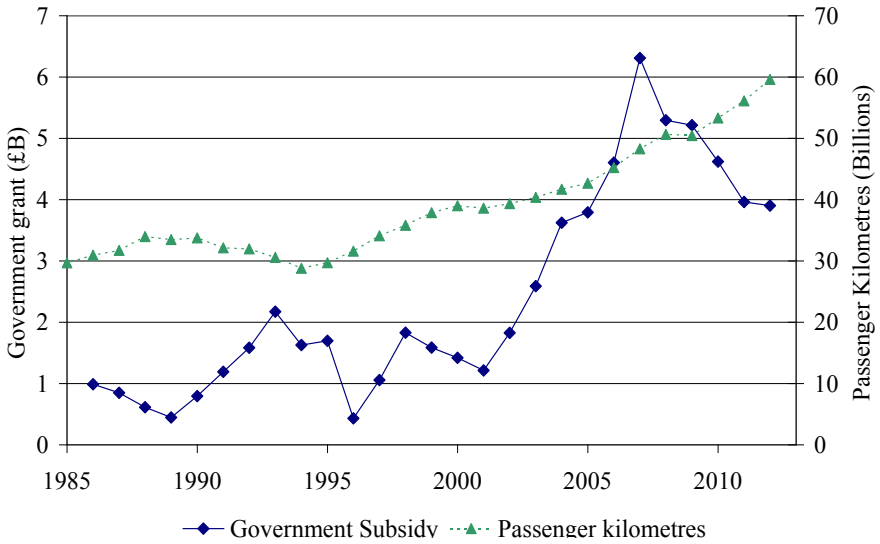

Figure 0-2: Total government funding to the infrastructure companies from 1985 – 2012 and passenger kilometres (secondary axis)

There are four main expenditures for Network Rail from the government grant – Operational, Maintenance, Renewal and Enhancements. Over the past four years, the mean percentages for expenditures are:

- Operational, 20.8% - non-maintenance costs incurred for operating the railway, including signalling staff and managing stations [10].
- Maintenance, 15.5% - Maintenance work is critical to the safety and performance of the network as it allows for the assets to be kept at an operational level.
- Renewal, 35.3% - Network Rail's renewals are planned operations to replace the life expired infrastructure assets.
- Enhancements, 28.4% - Enhancements are projects that improve the capacity or capability of the network. This includes projects such as electrifying sections of track, for example, the Great Western Main Line running from London Paddington to the South West of England and Wales.

1.2 INTRODUCTION TO SWITCHES AND CROSSINGS

S&C's enable vehicles to travel from one line to another, allowing for increased capacity and operation of the network. Generally, S&C units comprise of 17 components, with variations

throughout the design of the layout, including points operating equipment (POE). Figure 0-3 shows a generalised overview of a switch and crossing unit.

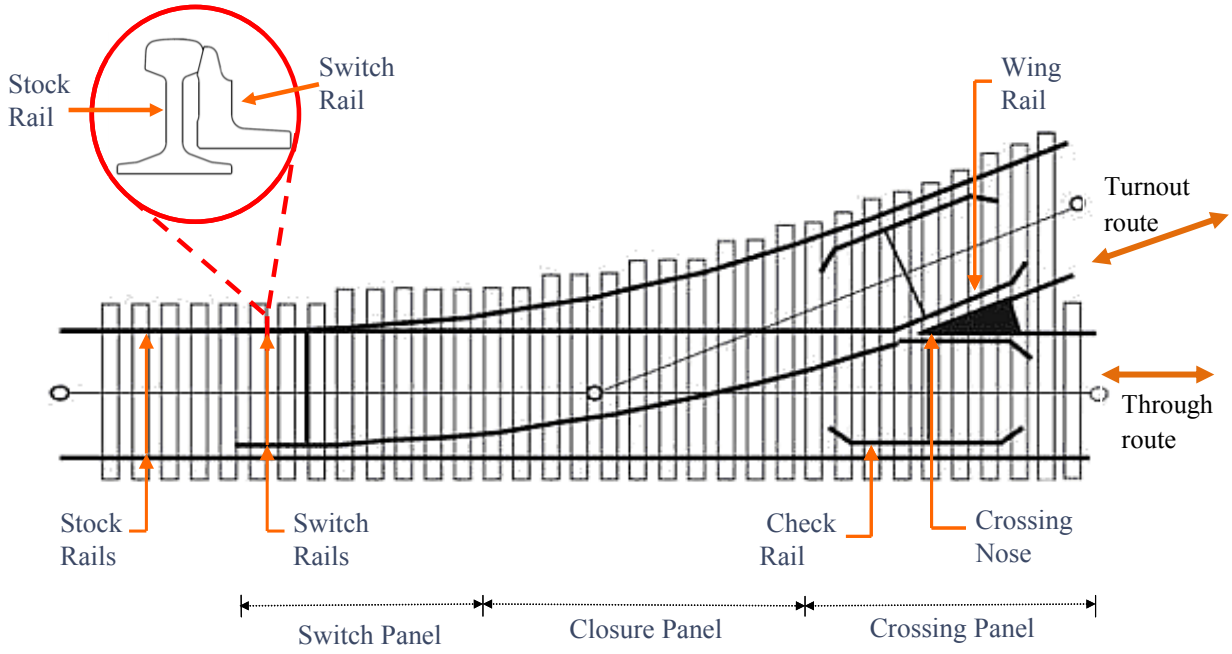

Figure 0-3: General switch and crossing unit [9]

The complexities of the research originate from over 200 different options for an S&C unit. The variables are described in Chapter 2.

1.3 RESEARCH AIMS

With the issues outlined above, the aims are to;

- Determine the forces / loading that are in the S&C units. With the number of contact points and location altering through the switch, it is needed to understand the development of the asset reaction as the train traverses.
- Evaluate current performance of in-service S&C. Once the instrumentation results are collected, the material response to the current loading and design can be studied to understand the pertinent parameters for switches and crossings.
- Determine the trend of deterioration. With strains being collected, a monitoring of the change over time can be recorded and used to determine any key stages in the life cycle. To gain a full life cycle, the instrumented S&C's need to represent various

stages of the life. A full life cycle monitoring will allow for forward predictions of deterioration through existing knowledge and trends.

1.4 APPROACH OF RESEARCH

The research was initiated to understand the forces in S&C's under dynamic loading from a vehicle. The complete project outcome is to understand the damage processes and causes of different damage mechanisms, which will allow for a degradation model to be developed. Collecting strain of the material and the change in response through the life cycle of in service S&C is complex due to the dynamic nature of the loading and the 100mm^2 contact patch. Studying changes in the strain in S&C over a prolonged period of time takes large amounts of computational time and power to model as the switch and crossing has many variable components and longitudinal profiles. Field instrumentation allows for instantaneous outputs which were collected and stored in large quantities on site.

Instrumentation data from the field is fundamental in understanding the change of loading over time. Strain gauges, geophones (to monitor velocity) and accelerometers (only on some sites due to their expense) have been collecting the S&C response to loading, with the aim to cover the key types of S&C. The S&C's instrumented were found through failure statistics and design of experimentation techniques to ensure deterioration is followed from installation and includes the pertinent parameters found through industrial knowledge and failure analysis.

In the thesis presented here, the field experimentation method is used to realise the research aims mentioned in Section 1.3. The reason for using the approach is:

- Train loading data can be collected in service, covering industry relevant S&C's on the network. This allows for operating vehicles and their loading to be monitored as they travel through the S&C unit. The high cost of the instrumentation and installation are considered a negative to this methodology, but are out-weighed by the outputs of the data collected;
- Parameters and levels can be set and analysis of the various parameters can be completed to understand the reason for degradation in greater details through S&C. The deterioration rate and response to loading is not known and so monitoring of field

experimentation outputs can follow the change in response over time with respect to the various parameters. A two level design of experiments was chosen over a larger number as the increased number of levels and parameters would further complicate the instrumentation design and increase the cost of the experimentation system;

- Field instrumentation was chosen as laboratory experimentation was not practical due to the complex nature and variable profiles of S&C. The advantages of laboratory testing, such as high volume of loading cycles, cannot be implemented on a whole S&C unit due to the large size and the rolling nature of the contact. Field instrumentation allows for these disadvantages and monitors in-situ vehicles with varying loads including various vehicles and passengers.

1.5 STRUCTURE OF THESIS

The thesis will be structured as follows;

Chapter 2 – Switch and Crossing Introduction

A background into S&C is described, from their original design in 1832 to the current preferred design and components.

Chapter 3 – Literature review

A review of the relevant literature has shown that there are three gaps in the current knowledge of the switch and crossing system. The review focuses on the literature on switches and crossings; S&C design, current maintenance techniques, damage characteristics and statistical analysis. Knowledge development expected from the research is described with the novelty of the research outlined.

Chapter 4 – Statistics and failure analysis

Understanding the previous failure statistics allows for focused instrumentation. The analysis is completed over the past 3 years of failure statistics of the infrastructure, and population of S&C in the UK.

Chapter 5 – Design of experimentation

The design of experimentation chapter is a methodological section to show the use of statistics in the experimental design. The design of field experimentation is explained,

describing the technique, the parameters used for the design chosen and their justification, sampling techniques, instrumentation used in the design, and field experimentation design.

Chapter 6 – Field experimentation results

The outputs from the instrumentation lead to data processing, conversion from the instrumentation to useable data and their error levels, filtering techniques and application. A review of each of the instrumented sites is completed. Peak to peak strains are analysed at each site against speed and weight.

Chapter 7 – Analysis of results

The material response is shown through strain for the whole asset to give an understanding of the reaction to loading locations and vehicle types. The change in the strain and displacement from instrumentation is analysed through monitoring the tonnage that has traversed the asset and how the response of the material has altered. The design of experiments technique, outlined in Chapter 5, has been analysed to understand which parameter has greater significance in the change of strain.

Chapter 8 – Modelling and validation

A finite element model has been created with variable suspension elements to represent sleeper stiffness. The model is of a plain line section of rail but is used to validate some of the strains seen at the gauge with the expected vertical displacements that are seen from the output of instrumentation. The purpose of this section is to ensure that the gauges are in the correct location for maximum strain, and to monitor the deflection change with sleeper stiffness and compare against strain that is occurring on the network.

Chapter 9 – Conclusions and future work

A review of the thesis is completed, summarizing the main findings and discussing the main outputs from the instrumentation and the trends identified. The development of the industry knowledge is stated, followed by recommendations for further work and development of the trend analysis, which will continue to increase confidence in the strength of the trends found.

REFERENCES

1. Rail Accident Investigation Branch, *Rail Accident Report: Derailment at Grayrigg, 23 February 2007*: Rail Accident Investigation Branch, Report No: 20/2008, Department for Transport The Wharf, Stores Road, Derby, UK, DE21 4BA. 2009.

2. BBC News. Available from: http://news.bbc.co.uk/1/hi/england/cumbria/6978220.stm [Accessed: 28/01/2013].

3. BBC News (in-depth). Available from: http://news.bbc.co.uk/1/hi/in_depth/629/629/6393023.stm [Accessed: 28/01/2013].

4. Network Rail, *CP4 Delivery Plan 2009; Enhancements programme: statement of scope, outputs and milestones*: Network Rail, Kings Place 90 York Way, London, N1 9AG. 2009.

5. Network Rail, *Strategic Business Plan for England and Wales*: Network Rail, Kings Place 90 York Way, London, N1 9AG. 2013.

6. Office of Rail Regulators, *Train Derailment at Hatfield: A Final report by the Independent Investigation Board*: Office of Rail Regulation, 1 Kemble Street London, WC2B 4AN. 2006.

7. Office of Rail Regulators. *Passenger Numbers; National Rail Trends Portal*. From Crown Copyright; 2010 Available from: http://dataportal.orr.gov.uk/ [Accessed: 09/04/2013].

8. McNaulty R, *Realising the Potential of GB Rail - Report of the Rail Value for Money Study - Summary Report*: Department of Transport, Great Minster House 76 Marsham Street, London SW1P 4DR. 2011.

9. Kassa E, Wiest M, Daves W, Nielsen JCO & Ossberger H, Assessment of methods for calculating contact pressure in wheel-rail/switch contact, *Wear - An international journal on the science and technology of friction, lubrication and wear*, 2008; 265(9-10): 1439-1445.

10. Ofiice of Rail Regulation, *Periodic Review 2013: Final determination of Network Rail's outputs and funding for 2014 - 2019,* Crown, 2013

2. SWITCHES AND CROSSINGS

Switches and crossings are essential for allowing capacity on the network through flexibility of movement of trains. This chapter is to give a preface to the known aspects of switches and crossings, parameters and current maintenance. The history of switches and crossings design is explained, whilst outlining the complexities, such as the transfer zone, that are present and pertinent to understanding the current maintenance. The knowledge has been used to influence the locations of the instrumentation and the design of experiments.

S&C's enable vehicles to travel from one line to another, allowing for increased capacity and flexibility on the network. The asset is made of many components, with many variations throughout the design of the layout. Figure 2-1 shows a fully profiled stock rail with a 'closed' switch rail (pushed against the stock rail) and points operating equipment.

Figure 2-1: Picture of a 'half set' of switches, showing the variation profile longitudinally for the switch rail and the contact conditions (light sections on the head of the rail)

2.1 HISTORY OF SWITCH AND CROSSING

S&C's were originally designed in 1832 by Sir Charles Fox, to allow for manoeuvrability from one line to another through the use of a lever to switch the direction of the route. The profiled rails superseded the previous sliding rail that were used on the infrastructure [2, 3]. The switch blades were moved mechanically, which remained unchanged until the widespread availability of electricity [4], with the maximum distance from the points to the signal box being 300 yards [3]. Francis Fox (son of Charles) states that

> *"prior to [the invention of the switch] the ordinary sliding rail was the only device, but it had this great disadvantage, that, if a train were shunted when the rail was moved, it ran off the metals and was derailed; whereas with 'Fox's patent switch' the train remained safe on the line."* [5].

Fox had designed the variable longitudinal profile that would allow a vehicle to travel down either route by manoeuvring the location of the switch blade, compared with having to either transfer the vehicle or slide a full rail into position. The profiled rail design is still in current use on the railway throughout the world.

This research is focused on the permanent structure of the rail and the attached components within switches and crossings. The point operating equipment (POE), the mechanism that pushes the rail into the required position, will not be covered in this research as the rail (and missing components) was the major contribution to incidents mentioned in Chapter 1**.** Figure 2-2 shows some of the complexities and dimensions (in mm) of the design.

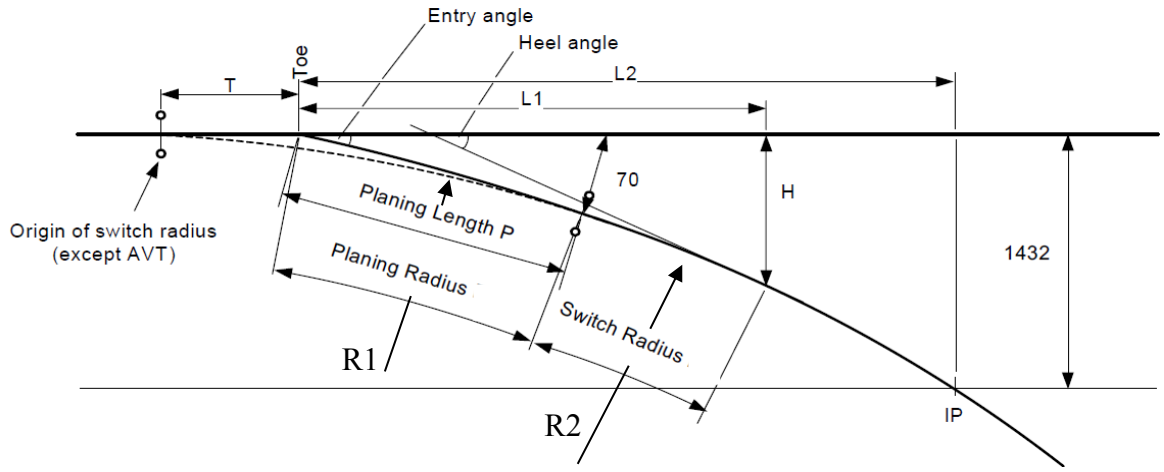

Figure 2-2: Design and geometry of switches and crossings [6]

Where; T – Distance origin of R2 to switch toe

P – Planing length

R1 – Planing radius; radius of switch blade, planned for vehicle entry

R2 – Turnout radius, measured between region shown

L1 – Heel length; Heel of switch is where the switch panel ends

L2 – Lead toe to intersecting point of crossing

H – Heel offset

1432 – This is the gauge, distance between running rails 14mm below top of rail. 1432mm is a typical distance for a set of vertical S&C. Inclined rails are at 1435mm to adjust with the reduction from inclination.

In 1988, shallow depth switches were introduced into service on the UK mainline infrastructure after 20 years of testing in the UK [7] and use in countries across Europe [8]. Shallow depth switches are named after the reduced height of the switch rail, as shown in **Figure 2-3** (b), which allows for a common shape and size rail to be used. Vertical shallow depth switches were introduced to give increased reliability due to reduced stress of the vertical loading in the rail. They were less likely to suffer from bolt interference issues due to the change in switch blade profile and locations of the bolts [9]. The increased life of the S&C was due to the ability of the infrastructure to cope with vertical forces as the stock rail has the full foot design, reducing the number of stress raisers in the cross-section design and fractures.

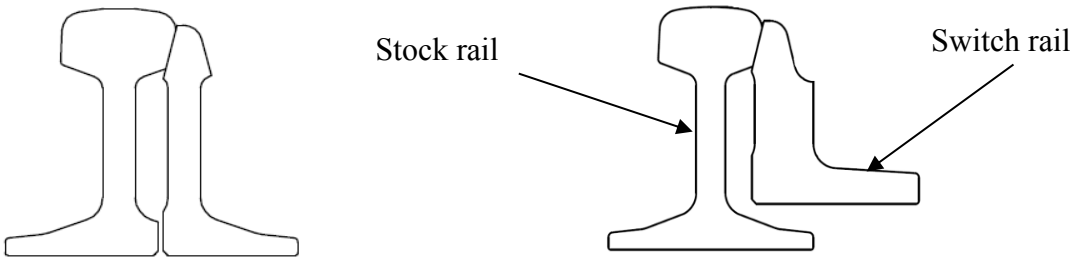

Figure 2-3: The comparison between (a) full depth vertical switches (b) and shallow depth vertical switches (flat bottom)

2.2 SWITCHES AND CROSSINGS DESIGN OPTIONS

The complexities of the investigation originate from the eight variables in the switch and crossing layout. The variables are placed into three categories, Geometry, material and operations:

2.2.1 Geometry

Geometry can be split into two groups: local geometry, which affects the contact between the wheel and the S&C units such as the rail design and length of profiled rail; and global geometry, which has an effect on the vehicle dynamics and includes the design of the curve.

Local geometry; The local geometry is critical as it allows the contact patch to transfer from one line to another. The turnout length (Table 2-3), is determined by the allowable space and contributes to the speed allowed on the turnout route (shown in Figure 1-3), with the longer turnout length tending to smooth the transition of the wheel between the contact on the switch and the stock rail.

The crossing angle, the rate of increase of the crossing usually defined as 1:x, contributes to the transfer from crossing nose to wing rail, with a shallower angle increasing the transition length. This has a similar effect on the contact conditions as the turnout length.

Inclination of the rails changes the contact location and size of contact between the wheel and the rail. The UK has two inclinations on the network, vertical and 1:20. Both are currently used on the network as there is transformation process to change the rail inclination, which is completed through enhancements to the railway. All switch rails are currently designed vertically as the lateral motion for inclined switch rails would be too complex for the point operation. Inclined switch rails would deliver small benefits of larger contact patch but would be complex to deliver. Currently, a design exists for 1:20 stock rails, but there is a higher risk of rolling contact fatigue through transfer zone due to the over-stressing of the rail material close to the surface through changing contact conditions. 68% of S&Cs are vertical, 23% inclined, and 9% unknown due to the collection of information on the database not being updated after a replacement.

Global geometry;

Poor geometry increases the magnitude of vertical loading from the vehicle through misalignments and discontinuities in the running path. Misalignments and discontinuities are necessary through switches and crossings to allow for wheels to pass from one line to another for the operation of the network to be completed.

The turnout geometry design changes the rate of curvature that is applied to the turnout route. Three geometry design are available; secant, clothoidal or tangential [10], with the clothoidal

(linearly increasing curve) the commonly used design currently as it reduces the angle at which the vehicles axles travels through the turnout route.

The transition between the switch and crossing, and crossing and running line can be supplemented through a curved rail before and after the crossing. The curvature of the rail can provide a transition between the switch and crossing and the proceeding rail. This is wholly dependent on the local layout of the route and the available space.

2.2.2 Materials

Currently, Austenitic Manganese Steel (AMS) is the most commonly used material for crossing, with switches made from 240 HB Steel. Two additional materials are currently being trailed in UK for both switch and crossing: high performance (HP) steel at 350 Brinnel throughout the material; Micro Head Hardened (MHH) steel at 400 Brinnel at the surface and reduced to 320 in the main rail material section. The advantages of these include longer wear resistance, but come at an increased initial cost and are susceptible to rolling contact fatigue (RCF). Explosive Depth Hardened (EDH) is an additional option which uses 240Brinnel steel and work hardens through explosives on the surface. The different rail material and hardened crossings are not currently widely available.

2.2.3 Operations

The switches are necessary to allow the trains to transfer from one line to another. Points Operating Equipment (POE) positions the switch rails in the correct locations for the vehicle to travel in the correct direction. The POE type has not been included in this research as they do not affect the contact between the wheel and the rail.

From all of these parameters, the preferred type of S&C that is being installed by the infrastructure company is the vertical, 56kg/m rail; 12.4m switch length with a 333m turnout radius, with clothodial turnout and straight to straight 1:13 crossing design.

2.3 CURRENT IN-SERVICE SWITCH AND CROSSING

S&C are a hugely versatile asset with 15 components and eight design variables. S&C cause c. 10% of the delays on the network whilst being c. 5% of the track mileage. This is due to the complexities of the discontinuities in the rail and running path, and the criticality to the capacity of the network that would cause cumulative delays to trains if failure occurs.

2.3.1 Switches and Crossings Structure

The S&C unit can be categorised into three main panels as shown in Figure 1-3 and Figure 2-4.

- The switch panel is comprised of four rail sections, two are fixed, fully profiled stock rails, and two are the associated asymmetrical manoeuvrable rails, called switch rails. The switch blade (profiled section of the switch rail) starts being initiated at the toes of the unit, Figure 2-9, and has an increasing cross-section until fully profiled, with the variation in profile shown in Figure 2-7. The switch blades are the moveable components within S&C's that allow the vehicle to transfer from one line to another in a continuous motion as the switch rail creates a different rail for the vehicle to run.

- The closure panel is the rail section between the switch panel and the crossing panel. The section of rail allows the vehicles to transfer between the two sides of the S&C unit with fully profiled rails.

- Crossing panel, separating the through route from the turnout route in the UK, also called 'diverging' route in some European countries. 'Common crossings' are part of the layout that provides the intersection of the two opposite gauge lines of track and are acute in angle [9]. According to GEOGIS (Section 4.2) 78.5% of crossings on the infrastructure are 'common' type. The crossing type is highly dependent on the switch panel design and the allowable space.

2.3.2 Functions of Switches and Crossings

S&C were designed to increase the manoeuvrability of trains by allowing vehicles to move from one line to another [11]. The flexibility allows for an increase in the capacity of the network by freeing train paths that other vehicles can use. Figure 2-4 shows an image of the switch and crossing panels on a common turnout design.

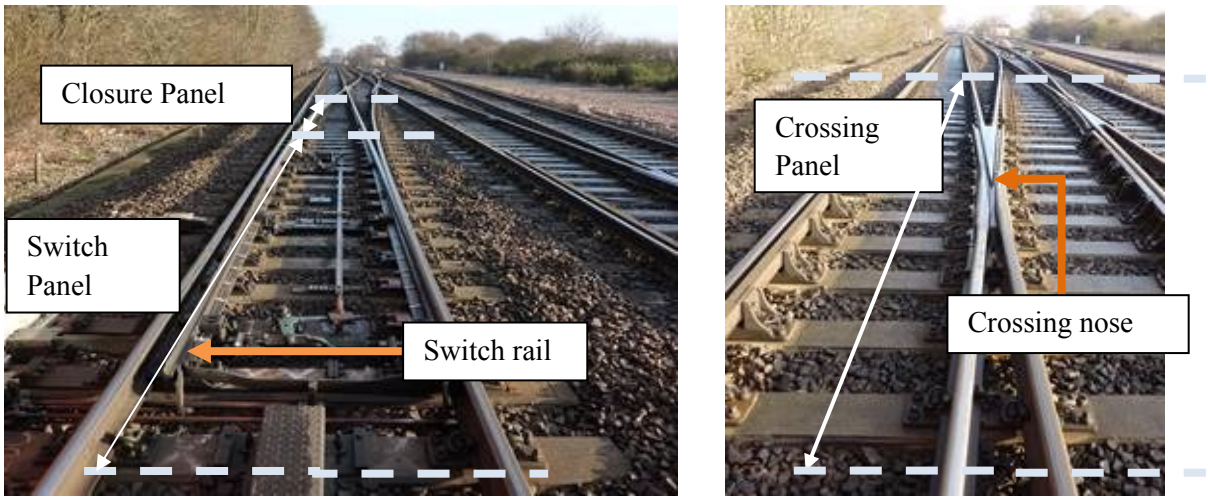

(i) (ii)

Figure 2-4: (i) A standard right-turn railway turnout, switch and closure panel and (ii) the crossing panel

Figure 2-5 shows the four functions of S&C, allowing vehicles to:

a) Manoeuvre between various tracks to continue their way in different directions

b) Join multiple tracks or to split up a single track into multiple track

c) To change tracks but continue in the same direction on different lines

d) To cross other tracks.

All of the functions allow the trains to either travel in various directions to other destinations, manoeuvre an obstruction, or increase the capacity by finding new sections of rail to run along. Therefore the maintenance of these assets is essential to ensure that these functions continue to operate and allow the trains the flexibility of the network.

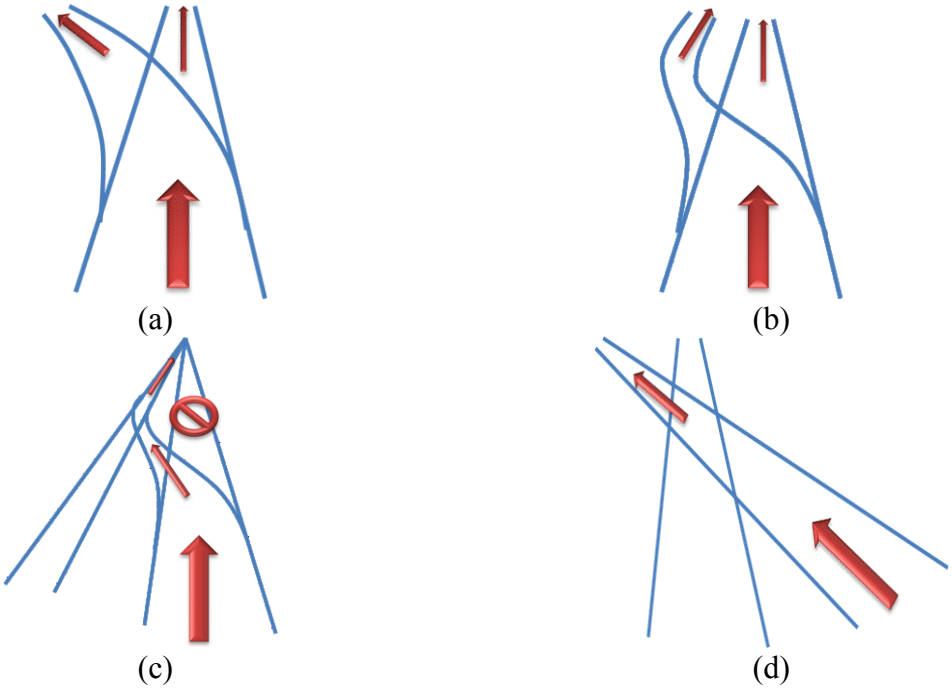

Figure 2-5: Switch and Crossings functions [12]

2.3.3 Switches and Crossings layouts

S&C can be configured into layouts which allow the functions in Figure 2-5 to be completed. There are four main types; Standard Turnout, Crossing, Crossover and Slips (of which there are single and double) which can be seen in Figure 2-6 [13].

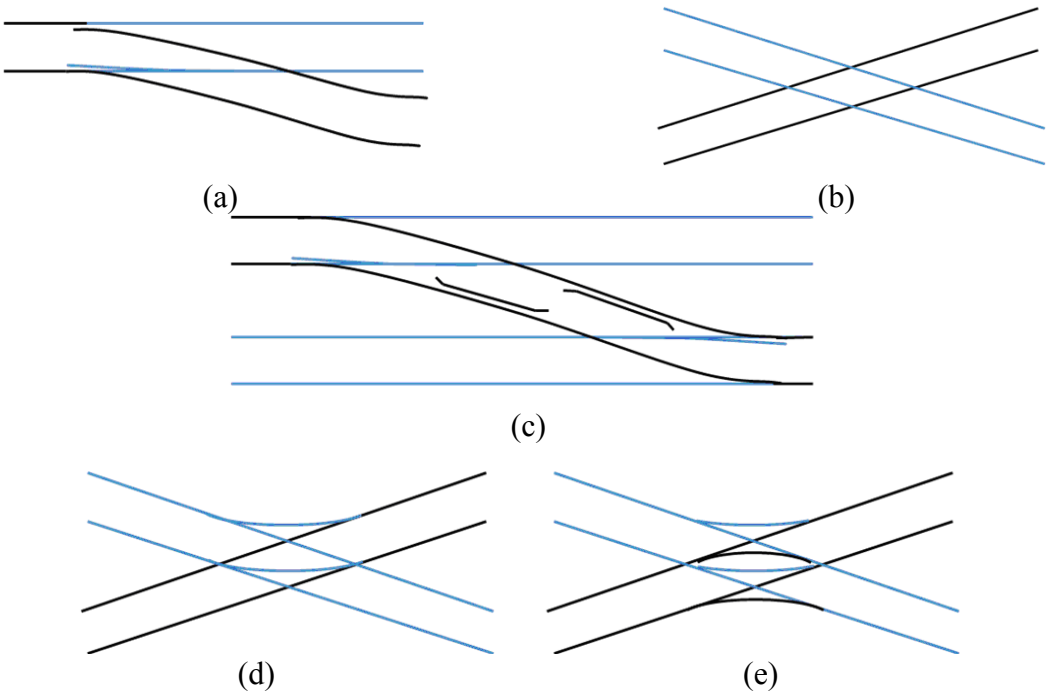

Figure 2-6: Layout of (a) turnouts (b) crossing (c) crossover and (d) single and (e) double slip [10]

Turnouts (Figure 2-6 (a)) comprise of a set of switches, a closure rail and a common crossing. These designs cover the basic and most frequently used layout of S&C.

A crossing (b) has four crossing noses which contributes to high magnitude loading on four occasions, rather than a single crossing discontinuity for the turnout design.

A crossover is two turnouts aligned back to back. This contributes to the changing track and continuing in the same direction function (c. in Figure 2-5) and allows for increased operations of the railway if a blockage occurs.

The single and double slips crossings, such as (b), have additional complexities of switches (or slips) which increase the availability of the railway. They have the four crossing noses, and four (or eight for a double slip) switch ends which combines the functions of crossing over and manoeuvring between various tracks to carry on it different directions.

In this research, the focus is going to be on turnouts as they are the most common type with 88% of the S&C population.

A full switch design is shown in Figure 2-9. A half set of switches include a single switch rail and a single stock rail.

The turnout has variable profiles along the length of the planing section (up to the end of the planning radius). Figure 2-7 shows the changes in the profiles along the length of the variable profile section using Miniprof (cross-section profile tool) measurements from an instrumented site.

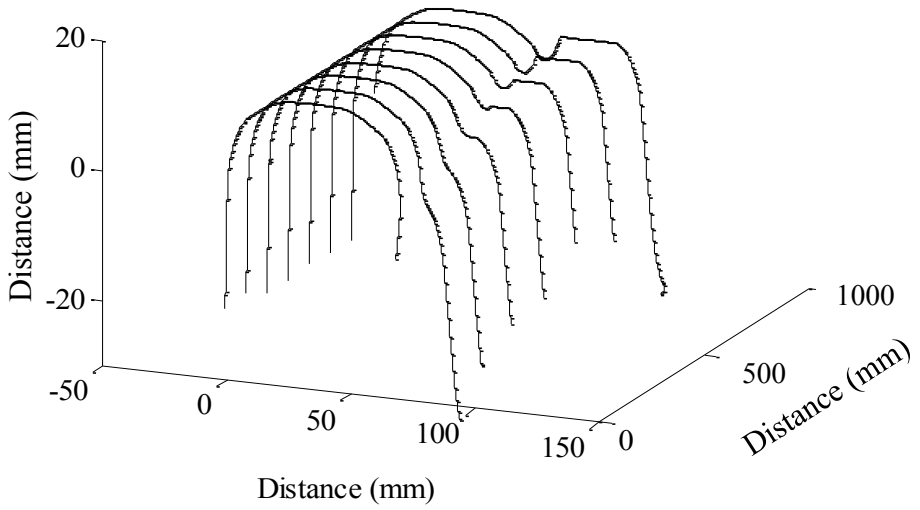

Figure 2-7: A variation in the profile of a switch through the wheel transfer zone

2.4 CURRENT MAINTENANCE INSPECTION PROCEDURE

Network Rail uses three specifications for inspection of switches and crossings: the inspection of permanent way, the inspection and repair to reduce derailment risks at switches, and inspection of cast crossings in track [14-16]. The standards outline the frequency and level the inspection that has to be carried out.

The *inspection of permanent way* [16] describes the levels of the inspections, and the frequency that the monitoring should be completed. Specific measurements for switches are shown in the *'inspection and repair to reduce the derailment risk at switches'* specification [15]. The main potential cause of a derailment outlined in the specification is cross-section deterioration of profile (commonly deformed through abrasion of the material on the inside of the switch blade) that allows the wheels to climb the rail [15]. Table 2-1 gives details of the level and frequency of inspection, aligned with Figure 2-8. The 'track category' are based on industry standards, classified against speed and Equivalent Million Gross Tonnes Per Annum (EMGTPA), which is based on speed and vehicle type, as found in GC/RT5023 [22].

Table 2-1: Track inspection frequency in weeks

Inspection interval (weeks)	Track Category						
Inspection types	1a	1	2	3	4	5	6
Visual Inspection	1	1	1	2	2	4	4
Ultrasonic	8	12	25	52	52	52	104
Geometry train	12	12	25	52	52	52	52
Supervisor Cab ride	4	8	12	25	25	23	25
Supervisor visual inspection	8	8	8	12	12	12	12
Track maintenance engineer cab ride	8	12	24	52	52	52	52
Train maintenance engineer visual inspection	104	104	104	104	104	104	104

The current standard for the inspection to reduce the risk of derailments in switches, NR/L2/TRK/0053, was originally developed in 1973, which was introduced due to the flange climb derailments that were occurring through switches [17]. The purpose of the standard is

to identify derailment hazards and highlight the remediation that is necessary to fix the problem and to ensure that the hazards / risks are removed.

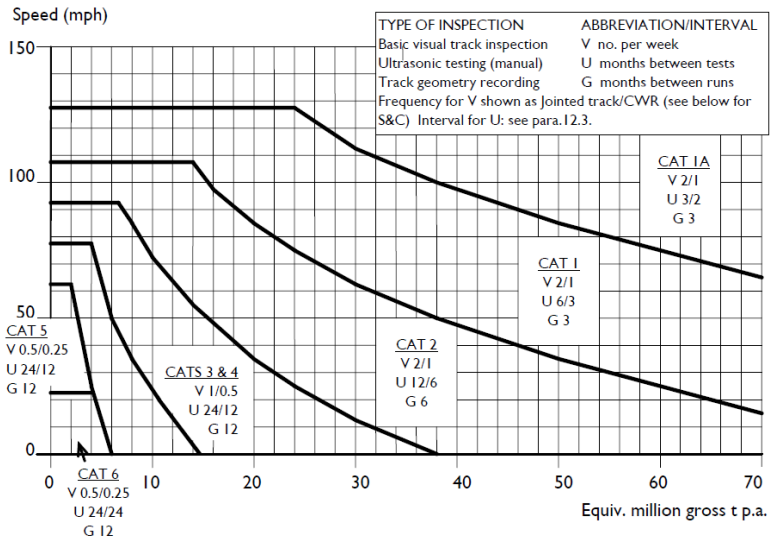

Figure 2-8: Track category definition and abbreviation for inspections taken from standards [16]

Track Categories are calculated using speeds and tonnage, and vehicle types. The boundaries for the categories below 25EMGTPA were generated through past experiences, with above 25EMGTPA extrapolated from the curves [16].

2.5 SWITCH AND CROSSING POPULATION AND DESIGN

Switches and crossings are assets that are used around Europe and the world since their design in 1832. Table 2-2 shows a comparison of the current population of S&C's around European countries on which information is publically available [18, 19] and through personal communication [8, 20] with employees of the railway infrastructure company within the countries.

The UK has a fairly highly populated network of S&C's, with just over 3 units / 5 kilometres of mainline track. These figures of S&C units do not include sidings (non-mainline), as the failure data used in Chapter 4 does not include sidings.

Table 2-2: Switch and crossing populations around Europe and their equivalent unit per track kilometre [18]

Countries	Mainline track kilometre	Mainline S&C population	S&C units per mainline track kilometre	Density - Railway km / 1000km^2
Germany	41,315	69,983	1.69	106
Austria	10,800	15,700	1.45	68
Switzerland	4,800	5,290	1.11	128
Belgium	6,500	6,505	1.01	118
Netherlands	5,090	4,460	0.88	89
Norway	4,230	3,680	0.87	14
United Kingdom (UK)	31,100	20,325	0.65	67
Italy	27,100	14,100	0.52	57
France	32,450	25,600	0.48	47
Sweden	12,150	4,560	0.38	27

The best trend that was found was the number of S&C units per kilometre aligned similarly to the density of the railway in the country. Table 2-2 focuses on European countries information was publically available.

With the design of the infrastructure varying in terms of length and radius, it is important to understand the population of the different classifications of railway switches.

Table 2-3 shows the design characteristics of S&C used in the UK, and their associated classification. In the UK, the letter classification are used for signifying certain turnout lengths and radii. European infrastructure companies tend to use more descriptive classifications for their switches, for example: 56kg/m rail, with a 750m switch radius shown at 56E1:750, with other switch lengths and rail types available.

For the population of S&C in the UK, the higher speed switches (+98kph) have been combined into a single functional switch length, ‘G+’, because of the insignifiant population

of the separate high speed switch lengths. This classification for the higher speed switch will be used for the remainer of the investigation.

Table 2-3: The designs of the switches and crossings for CEN56 vertical (V) design [10] in line with the schematic shown in Figure 2-2

Switch Classification	Turnout length , L2 (m)	Switch radius, R2 (m)
A	7.3	141.1
B	8.7	184.0
C	11.9	245.8
D	12.4	332.7
E	17.3	645.1
F	20.8	980.9
G+	24.4	1264

Figure 2-9 shows the switch in a panel with increased detail, including more components.

The population of the switch designs are necessary as the failure statistics are aligned to the switch length and design classification. The population of the classifications allow a normalisation of delays to be completed. Figure 2-10 shows the population in percentage of all S&C in UK for the various switch classifications and their associated maximum speeds on the secondary axis. Maximum allowable speed is taken from the design for the CEN56E1 vertical S&C from the 2049 standard [10].

1. Fixed stretcher bar

2. Left hand stock rail

3. Left hand switch rail (closed)

4. Lock stretcher bar

5. Right stock rail

6. Right switch rail (open)

7. Baseplates

8. Sleeper / bearer

9. Switch spacer block

10. Heel block

11. Transition between shallow depth switch rail profiles and full depth stock rail profiles

12. Switch tips

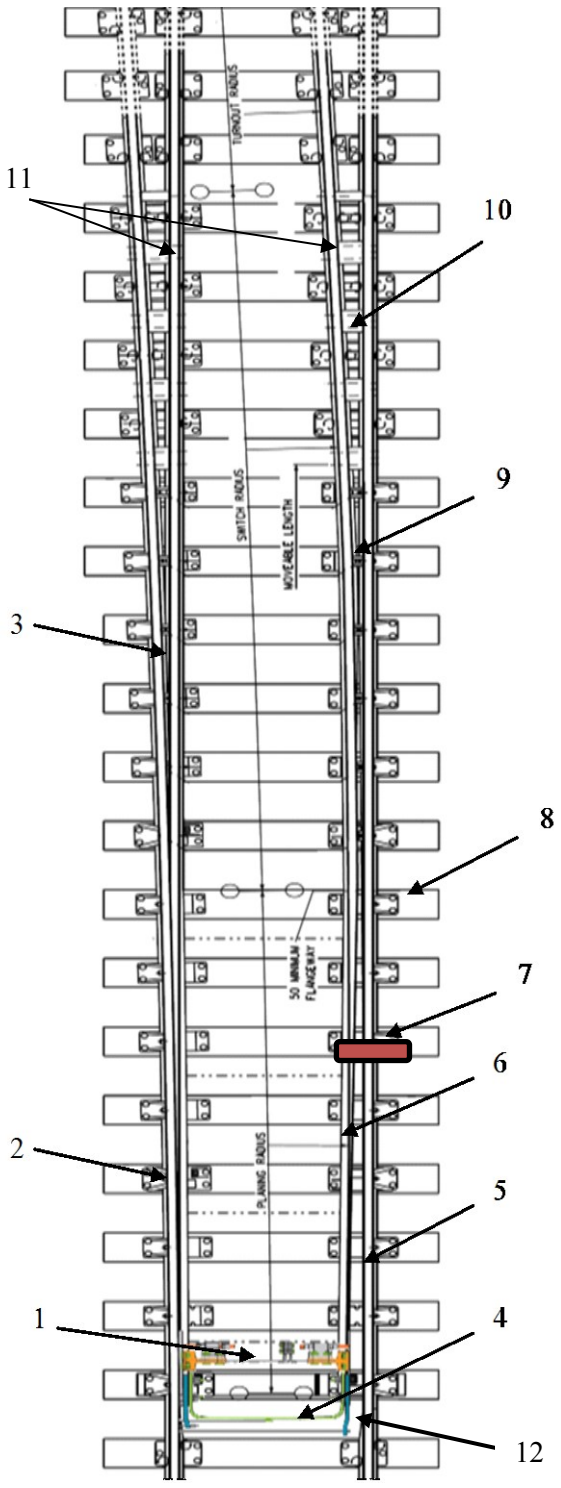

Figure 2-9: Components of the common switch unit in the through direction, with the left hand half set closed and the right hand half set open

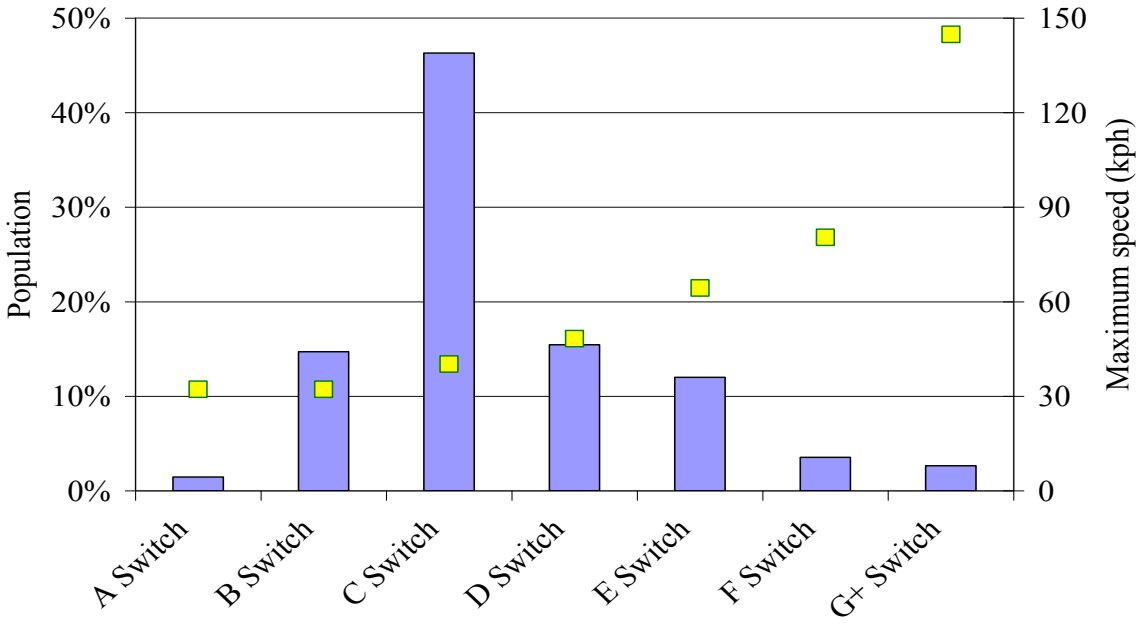

Figure 2-10: Population percentage of design of switches and their associated design maximum speeds (on secondary axis)

The population percentages show that the high speed (140kph+) switches and the slow switches (max 31kph) have a small percentage population, with 2.8% and 1.4% respectively. The limited number of high speed switches is due to the small distance (550 miles) of track that is classed as high speed (+200kph) in the UK. The slower speed switches are aimed at the access / egress to the sidings, such as train depots and freight to manoeuvre the vehicles around the infrastructure within limited space.

The dominant population is mid-speed (35kph to 60kph, C and D length) switches, with 63% of the total population. The mid speed switches are used in the majority of stations as they allow for trains to leave at a reasonable speed whilst allowing for limited geographical space to be used for the track. For enhancements of track (new track designs), the current preferred design of switch and crossing is the D length switch, with concrete sleepers, vertical and shallow depth [21]. The mid speed design has a slightly higher design speed than the C length switch due to the higher / longer radius of the turnout. The length of the switch is 87m longer, but the reduced dynamics of the longer radius allow for a reduced wear and deterioration at the head of the rail.

2.6 CONCLUSION OF SWITCHES AND CROSSINGS

S&C's allow vehicles to transfer from one line to another. This gives the necessary flexibility to increase the capacity of the network, to run and operate an efficient railway service. The effective and reliable operation of the S&C is crucial to the service that the infrastructure owner provides. S&C and the maintenance are critical to the operation of the railway, but the current S&C design is still based on the original, created in the 1830s.

It is necessary that the forces going through the S&C unit are understood with the knowledge of the deterioration of the life cycle maximising the effect of a predictive maintenance schedule. The life time monitoring of the in-services switches and crossings will allow for an effective maintenance regime to be set up by understanding the critical areas of the S&C unit and the deterioration rate. Currently, maintenance is completed by a cyclic and routine maintenance regime and reactive response to failure.

The current population of S&C shows that the mid-speed switches are the most common with greater than 60% in the speed range of 35kph to 60kph, and are highly relevant to the infrastructure due to the population and design focus.

REFERENCES

1. Kassa E, Wiest M, Daves W, Nielsen JCO & Ossberger H, Assessment of methods for calculating contact pressure in wheel-rail/switch contact, *Wear - An international journal on the science and technology of friction, lubrication and wear*, 2008; 265(9-10): 1439-1445.

2. Grace's Guide. *Charles Fox*. [online]: 2012 Available from: http://www.gracesguide.co.uk/Charles_Fox [Accessed: 09/04/2013].

3. Carter EF, *The Railway Encyclopedia*. London: Harlod Starke Ltd; 1963.

4. Absolute Astronomy. *Railroad Switches*. [online]: 2013 Available from: http://www.absoluteastronomy.com/topics/Railroad_switch [Accessed: 09/04/2013].

5. Fox F, *River, road and rail - Some engineering reminiscences*. London: John Murray; 1904.

6. Ventry D, RE/PW/729, *BS113A / CEN56E1 Verical switches general arrangement AV-EV*, Network Rail, 40 Melton Street, London, NW1 2EE, 2005.

7. South G. *History of British Rail Vertical S&C*. 2003 (Unpublished).

8. Nissen A. Track Expert, Trafikverket, Sweden. Personal communication. 20/03/2012.

9. Cope DL & Ellis JB, *British Railway Track, Design, Construction and maintenance*. 7th ed: The Permanent Way Institution; 2007.

10. Network Rail. NR/L2/TRK/2049, *Track Design Handbook,* 40 Melton Street, London, NW1 2EE. Network Rail; 2008.

11. Zwanenburg WJ. *Modelling Degradation Processes of Switches & Crossings for Maintenance & Renewal Planning on the Swiss Railway Network.* PhD Thesis: Delft University of Technology, École Polytechnique Federale De Lausanna; 2009.

12. Zwanenburg WJ. The Swiss experience on the wear of railway switches and crossings. In: *7th Swiss Transport Research Conference - STRC 07*, Patterson Z. (eds.); September; Monte Verita / Ascona 2007. p. 15.

13. Cope GH, *British Railway Track: Design, Construction and Maintenance*: The Permanent Way Institution; 1993.

14. Network Rail. RT/CE/S/054, *Inspection of Cast Crossings and Cast Vees in the Track,* 40 Melton Street, London NW1 2EE. Network Rail; 2003.

15. Network Rail. NR/L2/TRK/0053, *Inspection and repair to reduce the risk of derailment at switches,* 40 Melton Street, London, NW1 2EE. Network Rail; 2008.

16. Network Rail. NR/L2/TRK/001, *Inspection and maintenance of permanent way,* 40 Melton Street, London, NW1 2EE. Network Rail; 2008.

17. Paling KD, *Investigation into derailments on facing switches by flange climbing*. Derby: British Rail Research and Development Division, Report No: 203-81-29, Board British Railways. 1974.

18. European Commission - eurostat. *Railway transport - Length of tracks*. From Eurostat; 2013 Available from: http://appsso.eurostat.ec.europa.eu/nui/show.do?dataset=rail_if_tracks&lang=en [Accessed: 03/09/2013].

19. Deutsche Bahn AG. *Annual Report of BD Netz AG*. From DB Netze; 2013 Available from: http://www.db-netz.de/fahrweg-en/start/company/about_us/2736928/annual_report.html [Accessed: 03/09/2013].

20. Bjornseth H. Inspector of Accidents, Accident Investigation Board, Norway. Personal communication. 9th August 2013.

21. South G. Principal Switch and Crossing Engineer. Personal communication. 7th January 2011.

22. Railtrack PLC. GC/RT/5023. *Categorisation of Track.* Floor DP01, Railwaytrack House, Euston Square, London, NW1 2EE. Railtrack PLC; 1999

3. LITERATURE REVIEW

Existing research on switch and crossing instrumentation, S&C design, current maintenance techniques, damage characteristics and statistical analysis has been reviewed. The literature shows a gap in the understanding of trend analysis and forces through switches and crossings under loading. Gaps were found in research within deterioration of S&C, performance of current S&C and field experimental studies. The research aimed to fill the gaps through improving knowledge of field instrumentation, deterioration of S&C over time and key parameters of the current design.

The literature review is categorised into five topics. The five topics are: the deterioration of S&C that are commonly used in the UK; the mechanisms of deterioration common within S&C; current maintenance practices in the UK; statistical analysis of S&C; and field experimental studies within S&C. There is overwhelming evidence that S&C's are a major contributor in the maintenance of the rail infrastructure and take a disproportionate amount of the budget, 24% of the track maintenance budget, for 5% of track [1].

The evidence presented here shows that none of the existing research monitors the condition of the S&C unit over time. The historic experimentation uses either instrumentation that has been placed onto the vehicle, monitoring S&C through a single loading cycle, or focused on field instrumentation on crossings for a few train passages. The current literature available fails to cover the complexity of the wide range of S&C that are available in the UK or monitor the condition of the asset over time to follow the degradation. With the research outlined, the development of knowledge increases expertise in UK field instrumentation of S&C, understand the current performance of present S&C units and understand the key parameters in the degradation of the units.

Currently, S&C only had limited research coverage due to the highly complex modelling computational requirements and the limited knowledge of contact forces through S&C. The research focus has shifted towards S&C and components due to rail incidents in Potters Bar (2002) and Grayrigg (2007) [2].

The aim of the research is to inform infrastructure owners and operators the strains being generated within the asset at various stages of the life cycle.

3.1 DAMAGE CHARACTERISTICS OF S&C

When a new profiled wheel comes into contact with a new profiled rail, the surface area in contact is circa 100mm^2 [3]. The 'contact patch' that is formed between the two surfaces transmits traction and braking forces, and large contact and loading forces from the vehicle into the rail. The attributes of the wheel / rail contact forces generated in the contact patch are determined by their location, frequency of the loading, magnitude of the forces, and orientation of the resultant force. The characteristics of the contact between the two non-conformal surfaces determine the damage mechanism that is generated. Material damage characteristics have been studied by various authors [4-10]. Enblom [11] produced an overview of material damage characteristics, focusing on the wheel / rail interface mechanics which included wear prediction. Zerbst et al. [27] gave a thorough overview of the fatigue crack propagation and changes in contact forces from thermal residual stresses. The research describes literature showing the three stages of crack propagation; initiation, accelerated grown and branching. They also showed that larger residual stresses are from flash butt welding after grinding compared with roller straightening and in service loading. Sawley et al. [12] separated the damage characteristics into two categories to differentiate between the 'micro' effect of contact on the head of the surface and the 'macro' effect of the loading on the surrounding material for focusing the knowledge. The categories are: within the influence of the wheel / rail contact force (those close to the contact location and within / near the contact patch); and the damage generated away from the contact location, resulting from higher bending stresses. Both of the categories, the localised loading and the deterioration through change in structure, are found within the S&C units due to the high magnitude loading.

3.1.1 Wear

Wear is the loss of material from contacting surfaces [13]. Wear can be described within several categories from the tribology field: Adhesive (surfaces bond under load), Abrasive, Corrosive (rubbing removes surface under corrosive environment), Surface fatigue (removal

of material near surface due to cyclic loading) and minor types (including erosion) [13]. Two of the wear categories are covered within the wheel / rail context, abrasive and mild (surface fatigue) wear [14]. Abrasive wear is more severe as is caused by the asperities between the running surfaces, removing the top layer of the materials in contact [15]. The removal of the work hardened layer alters the contact conditions and exacerbates any degradation. Mild wear is the removal of rust, or oxidised layer on the rail steel and results in the surfaces being made smoother than before, but does not remove layers of the rail material. This is completed through multiple passes of wheel in the same location of the rail laterally (with circa 0.0015µm of material removal per wheel [13]) [15].

Currently, authors [16-18] have researched wear and other surface damages, such as corrugation and fatigue cracks, as railway vehicles traverse various radii curves. The higher rate of deterioration tends to occur on the high rail of curves due to the vehicle dynamics generating a curving / lateral force causing the leading wheelset to 'attack' the high (outside of curves) rail [19, 20]. The variation of the axle from the line to centre of radius is called the angle of attack, with a larger angle of attack generating high frictional wear, RCF and fatigue due to the rail not being able to cope with the creepage (relative velocity between the rail and the wheel) between the wheel and the rail and overstressing the surface.

3.1.2 Plastic Deformation

As cyclic loading increases above the elastic limit of the material, contact stresses between the wheel and rail exceed the yield limit. The material within the contact region flows plastically [22, 23], allowing the profile to alter shape. The adaption of shape and material properties modifies the contact location and pressure between the two surfaces. Williams et al. [24] describes the effect of hardening of the material as the loading exceeds the elastic limit, raising the effective yield strength for subsequent loads. The material reacts to loads above the elastic limit with element of elastic response and plastic deformation. Williams states that material responds to the excessive localised loading by deforming. The increase in the yield stress limit, and plastic deformation, is due to the loads exceeding the elastic limit and generating an increased residual stress within the material. The shakedown theory gives values for the upper limit of load to the deflections, below which the material will respond elastically [24-28]. When the magnitude of the loading exceeds the plastic shakedown limit, the material responds through incremental accumulations in plastic deformation under every

load cycle. This 'ratchetting' of the material continues to increase the strain until the material fails.

Figure 3-1 shows the material response to the loading cycles at various levels of plastic deformation. Plastic deformation is influenced by the high normal and tangential loading that occurs between the wheel and the rail [6]. The severity of the deformation is determined by the repeated cyclic loading, hardness and maximum stresses (residual and bending) compared with the yield stress of the material involved [6].

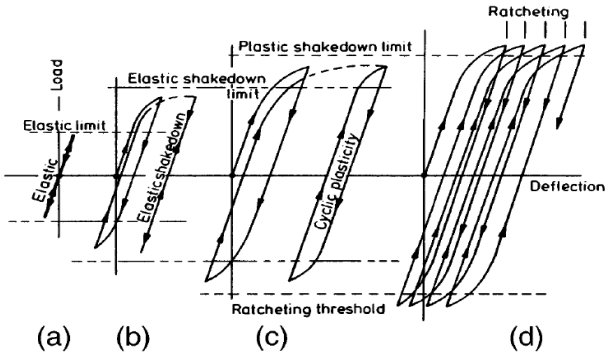

Figure 3-1: Development of plastic deformation through ratchetting [6]

Corrugation, a wave like pattern on the head of the rail through wheel / rail contact, can be formed through a cyclic formation of plastic deformation. High dynamic loading encourages slip between the wheel and rail, resulting in plastic cyclic deformation [29, 30]. Grassie states the long and short wavelength corrugation is due to 'triggers' and irregularities in the running path, such as change in material stiffness (welds for example) causing the wheel / rail contact to 'slip' [29]. The slip areas are regions of reduced contact between the wheel and rail, causing the contact patch to decrease in area. The slip regions are followed by larger area of contact, or stick, as the wheel gains traction with the rail. The 'stick-slip' condition produced a wave of plastic deformation along the track laterally.

3.1.3 Rolling contact fatigue (RCF)

Rolling contact fatigue (RCF) is initiated in two different ways, either through surface initiated cracks and high impact loading or through sub-surface cracks generated in the manufacturing process [31]. Surface initiated cracks happen within the influence of the contact, at the head of the rail, and subsurface below the head of the rail, and throughout the rail.

Subsurface manufacturing cracks within rail are becoming increasingly rare in service due to the increase in accuracy of inspection and testing, combined with improved quality of rail being produced [3]. Contact patch loading can initiate surface cracking through exceeding the material yield limit of elasticity. The cracking continues to grow due to the ratchetting (Figure 3-1 (d)) showing the incremental deflection increase with every pass of the plastic shakedown limit) under the cyclic contact.

Cannon [32] describes the generation of head checks, gauge corner cracking (GCC) and squats (categories of RCF) as a result of severe shearing of the surface layer. Burstow [33] developed a simplified RCF criteria, using the damage function Tγ (creep force (T) x creepage (γ)) for the 'Whole Life Rail Model' (WLRM) in 2003. WLRM is able to predict the initiation of cracks, locations and severity over a period of time through an indicative function. The size of the contact patch on the rail and the work done at the contact patch through creepage is predicted. The model has been validated and is currently in use by Network Rail and other research organisations.

3.1.4 Fracture

Fracture is the exceeding of the ultimate point of the material and is caused by the high bending stresses generated through point loading. The fracture cracks are often found around stress raisers, such as bolt holes, or at maximum bending, such as the web of the rail. The initiation of the crack is usually by a fatigue mechanism, which then fails through exceeding the material properties. Figure 3-2 shows the rail's stress categories [27] in a 2D longitudinal plain line rail, including the thermo, bending, shear and residual stresses. The bending stress under loading at the top and at the bottom of the rail is at maximum due to the compression and tension. The shear stress in the rail is due to the contact pressure / axle loading so has a strong relationship to the loading characteristics. The limitations of this model are that the values of the stresses, the severity of the loading are not included which means that there is some ambiguity to the levels of the stresses that are present in the rail through loading, and the additional complications of residual stresses.

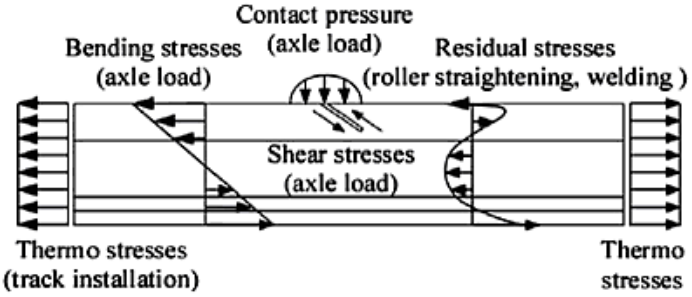

Figure 3-2: The variation in the stresses that are generated through plain line rail sections [27], not to scale

The profile of the residual strength changes through as the material alters and the profile changes. The effect that this has on the fatigue length of the material was studied using X-ray and FEA [52]. This showed that for an un-used section of rail, the residual strain varies longitudinally, depending on manufacturing, with the ends of the material holding higher residual stresses, as well as through the cross-section, which will affect the rail's ability to cope with loading. Crossing fracture is becoming increasingly rare in the field (seven instances in 2010) due to alteration in material and manufacturing processes [34]. When fracture does occur, safety is compromised to the vehicles and instant rectification action must be taken.

3.2 STIFFNESS THROUGH SWITCHES & CROSSINGS

Research covering stiffness through switch and crossing units have been covered in various countries, including UK, German and Sweden. Hunt [53] completed a literature review in 2005 for the Rail Safety and Standard Board (RSSB) on the track stiffness effect on track performance, which focused on mainline track and excluded other assets including S&C. Hunt showed that there is various optimum track stiffness;

- 80 – 130kN/mm for 'typical' rail, variable speeds (130 – 200kN/mm excluding rail pads)
- 70 – 80kN/mm for high speed rail
- 25 – 50kN/mm for freight traffic. This allows the track to absorb some of the freight vehicle loading, particularly with flat spots of the wheels that increase the loading on the system.

The value of stiffness was calculated through Beam on Elastic Foundation (BOEF) calculations, with more information shown by Bowness et al. [54-55]. This method was selected by Hunt as it was used most commonly used for rail stiffness calculations. Typically, the experimental measurements that

were taken have shown that typical stiffness of sleeper ends in the UK is 75kN/mm, whilst in Europe, the stiffness is in the region of 150kN/mm.

Limitations on the research reviewed by Hunt included the value of the change in cost for the maintenance of the various stiffness levels, remediation to deteriorating assets and the range of stiffness that had been found to be 'optimum'. The research did not cover the effect that the change in stiffness had on the life of the assets, or the deterioration of stiffness over time.

In the UK in 1977, Pennycook [56] used a rolling load rig over a 15 sleeper track section. Pennycook found that a constant stiffness over the 15 sleepers gives the maximum sleeper deflection, with the maximum deflection of 1.46mm with a 23t axle load on 113A rail at 600mm concrete sleeper centres. This is due to the constant stiffness allowing minimum compactions between the various sleepers. The sleeper reaction calculated through a computational programme, which showed the sleeper vertical reaction was 50 – 70kN. The method of stiffness calculation was not explained, and the method for measuring deflection was not disclosed in the paper. Only small amounts of data were available for this paper.

Internationally, Nicklisch et al. [42, 57-58] completed measured stiffness experimentally and through computational modelling as part of the INNOTRACK project on a switch in Sweden and a crossing in Germany. The vertical displacements was measured experimentally through track receptance (dynamic displacement/unit force) using a vehicle with instrumented wheels. Through the switch, the rail, rail pads and sleeper vertical stiffness varies. Three points were monitored, at 4.5m from toes, 9.1m and 21.85m. They showed that the point at 9.1m was 40% larger and 21.85m was 70% larger than the initial point at 4.3m. Using Multi-Body Simulation (MBS) software, SIMPACK, the switch and crossing were modelled to understand the stiffness under the assets, which were validated through the instrumented wheels. Through the modelling, it was found that the smaller the variance, through adjusting stiffness by using elastic rail pads, gave a 30% reduction in the vertical forces. A similar trend was found through the crossing, reducing the stiffness from 500kN/mm to 85kN/mm using elastic rail pads reduced Normal contact forces from 330kN to 185kN. Whilst this modelling was validated, the change in the stiffness over time and the deterioration has not been monitored.

3.3 STATISTICAL ANALYSIS OF SWITCHES AND CROSSINGS

Williams et al. [35] completed a statistical analysis of the UK infrastructure in 2007 regarding failure and delay minutes due to S&C. From the delay data that was obtained, a strong relationship between the scale of delays and the traffic type was found. Delays

affecting passenger vehicles were ten times longer than freight due to the lower number of freight trains on the network in comparison with passenger.

Williams explained that all lengths of S&C show an increase in the failure rates due to increasing the tonnage over the units. The increase of tonnage has a detrimental effect on the failure rate on the S&C wear due to the higher gross tonnage that the unit is subjected to the switch.

Higher failure rates were seen with a decrease in vertical track alignment [35], with a rapid rate of change demonstrating the highest failure rate. The vertical alignment and tonnage relationships found by Williams showed a need to increase the procedures to maintain the track for the parameters as they increase the dynamic forces by the vehicle experiencing discontinuities through the S&C. Fisher [36] states that the results from statistics should be comparable with the experimental aspect to give validation to the statistics and to show repeatability. The refinement allows for objective sampling data by studying the historical components of the statistics and increasing the confidence through experimental design and studies. Hanna [37] shows that the use of statistics and the merit of this data is only the starting point in the process of obtaining quality, accurate and reliable results; using the data in a process of design and development of experimental testing and production.

Zwanenburg completed a statistical study of S&C units replaced on the Swiss rail network [38]. Zwanenburg's study shows that the geometrical degradation increases renewal rates due to the increased deflection. This causes the S&C unit to experience increased stresses through larger deflections and degrade the rail material to a state that the unit needs replacement in a short duration. From the statistical analysis completed by Zwanenburg, the ages of the S&C when replaced fluctuated between 10 years in service in 1993 to 21 years in 2005, when the study ended. The explanation for the increase in duration in service is due to higher quality components, such as hard wood and concrete sleepers instead of timber sleepers. Maintenance policy to replacing smaller components was considered for another explanation as it kept components at their optimum level in a cyclic renewal. The rebuttal of the industry experts to this conclusion was that the policy had not changed in that timeframe.

3.4 FIELD EXPERIMENTAL STUDIES IN SWITCHES AND CROSSINGS

Experimentation is completed in two different areas; laboratory and field testing. Experimentation completed in British Rail Research (BRR) and other research organisations

will be reviewed, describing the level of detail and type of experimentation used in the investigation and conclusions, highlighting the gaps in the current knowledge.

Previously, twin disc testing has been completed for railway applications [39] to monitor the wear and degradation of surfaces between the wheel and rail with the advantages of reduced time and quick changes in testing parameters. The twin disc tests are completed on plain line rail and used to monitor the wear, RCF development (and initiation), adhesion conditions and degradation, with the ability to add 3rd body materials [8] in a lab environment.

S&C lab testing is very complicated and has not been found to have been completed due to the size of the asset and loading complexities of multi-point contact. Field experimentation studies have been completed across the world to understand certain aspects of switch and crossing dynamic behaviour.

Field experimentation can be separated into two sections; vehicle based and infrastructure based.

3.4.1 Vehicle based field experimentation

Vehicle based instrumentation allows for a dynamic loading of the infrastructure to be recorded. This would highlight the vehicles reaction to a change in the contact conditions and the discontinuities in the running path. The advantage of this would be for a single passage over an asset or to compare the different types of infrastructure assets. Disadvantages include it being very complicated to align multiple runs to monitor deterioration and only monitoring of a single vehicle.

S&C field experimentation has been completed in Europe as part of a joint study INNOTRACK European project, but the UK infrastructure was not included. The project is analysed, followed by other European experimental studies and studies from other countries around the world. The international project INNOTRACK was set up to understand and study the life cycle costs (LCC) of specific assets of railway infrastructure [40]. The output of the project was to optimise and increase the life of key assets such as S&C, rail, welds and their geometry. The INNOTRACK project showed a reduction in the lifecycle costs of 29% through innovation in design and material, POE and condition monitoring. In the UK, this

isn't a directly comparable turnout design, but the turnout radius is somewhere between a 'D length' and an 'E length' switch.

Kassa [42] completed research in Sweden using a load measuring wheelset (LMWS) showing that an increase in the velocity would increase the lateral and vertical forces being generated by the vehicle as it traversed the S&C unit. 16 strain gauges were attached to a single wheel on a freight vehicle Y25 bogie, as shown in Figure 3-3, allowing for vertical and lateral forces being applied to the wheel to be calculated. As the vehicle traversed the crossing at increasing speeds, it was found that the maximum lateral (Ymax) and the maximum vertical (Qmax) increased. With the increase in the lateral forces (from 70kN at 10kmh to 87kN at 80kmh), there was also a change in the location along the crossing that the force was found, which was due to the vehicle dynamic. There was a high frequency content to the LMWS outputs were found at the change (or transition) between the shallow depth and full depth rail due to the stiffness change and the peak force dynamically loading the vehicle. There were small inaccuracies in the model created at this location due to the unknown stiffness content through the transition. Whilst the forces going through a single switch and crossing were found, the change in force through degradation was not investigated due to instrumentation repeatability over a single site.

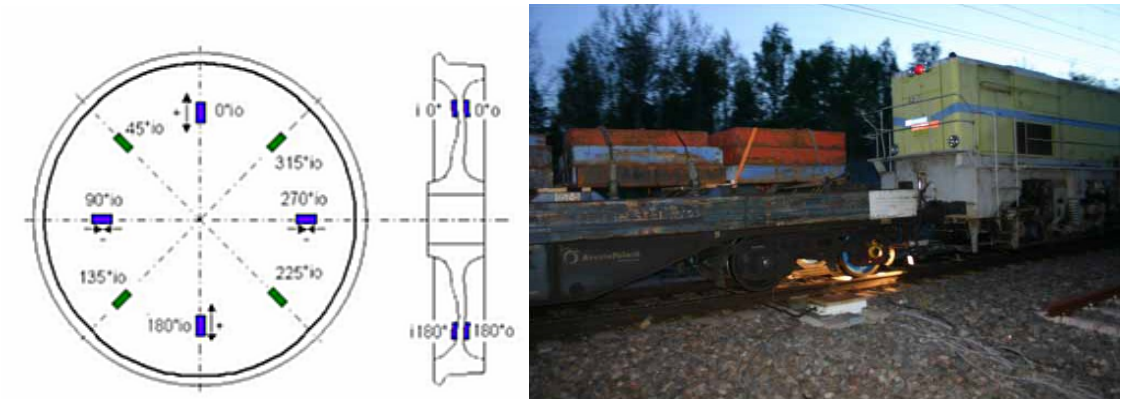

(a) (b)

Figure 3-3: Instrumented wheelset on a Y25 bogie (a) strain gauge locations and (b) location on freight vehicle

In British Rail Research (BRR), Cheesewright [43] used a load measuring wheelset (LMWS, 4 wheel, 2 axle freight wagon of 30 tonnes (cf. Figure 3-4)) over various types of crossing to compare the vertical forces. Cheesewright explained that the largest dynamic vertical forces of 180kN (twice the static load at 106kmh) are at the interruptions in the running surface due to the transfer of forces increasing the peak forces. The interruptions include the crossing

nose in the facing direction, and the wing rail in the trailing direction, which are the regions that the wheel transfers from one rail to another. Troup [44] used the same LMWS to monitor switch diamonds and swing nose crossings in the UK, with additional strain gauges and accelerometers on the vehicle for validation. It was found that vertical loading increased with worn wing rails, which generated additional contact points.

Clarke [45] showed on a vertical S&C unit in 1981 that a higher entry speed into the switch on the diverging route had a reduced lateral force due to the increased radii of the turnout using the LMWS. Clarke studied nine designs of S&C, at 20 sites. The higher speed, however, sees a detrimental dynamic effect, which damaged the heel of the switch (through the wheel transfer zone). The vehicle used had a long wheelbase, a two axle vehicle, and so there will be different result for the currently used bogie / four axle design. The long wheelbase reduces the curving behaviour of the vehicle which increases the damaging effect the leading axle has on the curved track. At the sites, the natural frequency of the 'unsprung mass', mass in contact with rail before any suspension element, was within the 13 – 26Hz. Due to the design of the LMWS used, the unsprung mass was large, and the vehicle had a large wheelbase, which reduces the curving ability behaviour of the wagon, increasing the damage expected [31, 46].

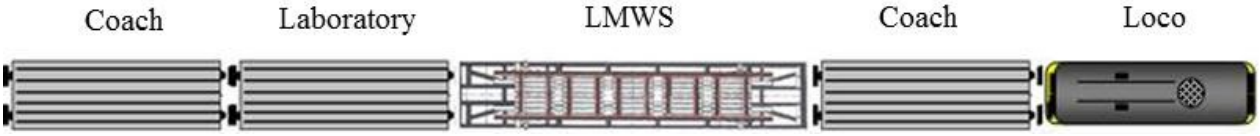

Figure 3-4: Design of load measuring recording train [44]

3.4.2 Infrastructure based field experimentation

Infrastructure based field experimentation use instrumentation that are fixed to the asset over a period of time and monitor each loading cycle. Advantages of this method include the continued and monitoring of the asset over a period of time and collecting many different loading types / vehicles. Disadvantages are the limitations on locations that a fixed instrument covers, with gauges in particular c. 15mm wide, or accelerometers in a fixed position. This means that the information from one gauge to another is not fully known.

Six test sites were set up in the INNOTRACK European project, with varying level of instrumentation and location, with sites on Deutsche Bahn (Germany infrastructure),

Banverket (Sweden infrastructure – now Trafikverket). An example of the research completed using strain gauges on a crossing was on German infrastructure in Haste [41], where a crossing was installed with no switch panel. Using 16 strain gauges in a rosette style, the investigators were able to calculate the vertical wheel / rail contact forces for a single locomotive. The maximum wheel-load of 172kN was found. The force measured was for a 1:12 crossing. This crossing angle is not found in the UK and there was no research completed on the strain within the switch in these tests. The switch testing was to demonstrate the horizontal and vertical stiffness of the switch, with no published conclusions.

Licciardello [47] used displacement transducers to study the lateral displacements through S&C and comparing the static and dynamic loads being applied in Italy. The study was to understand the low frequency content of the S&C structure and the displacement under loading. Through the experiment, one site was studied with limited alteration to the contact conditions, with a mixture of traffic. The lateral switch blade deflections are not significantly affected by the increasing wheel load, with vertical displacements of 2.5mm peak to peak.

Further, Li [48] used lasers to monitor lateral displacement of track on a high speed line in China, comparing the switch and the crossing. The switch blade moved laterally up to 8mm under traffic (high speed (200kph) passenger line), which was significantly more than 3mm of lateral movement seen at the crossing. The decreased lateral movement in the crossing can be explained by the much stiffer crossing unit in comparison with this thin switch blade with the ability to move.

Strain gauges on crossings only have been completed in the UK in the 1970s [49, 50]. Boutle [49] compared bending strains of two crossings (with gauges applied on the bottom of the crossing) in Watford in the early 1978. The aim was to compare the manufacturing of two competitive companies. 39 strain gauges of 120ohms, with a sample rate of 1500 samples/second were used on new crossings. Boutle claimed that two designs generated very similar strains with a similar trace, peaking around 1000με due to loading. It was found that at higher speeds, the spread of strains reduced, with a heavier locomotive and lighter carriages inducing similar strains. A fatigue limit for austenitic manganese steel (AMS, used for current crossings) of 2000με was described by Boutle through laboratory testing, which is well over the 1000με found. Groom [50] states that the difference in strain that is seen in a crossing due to speed is minimal. In his research in 1973, strain gauge were placed on speed restricted sites and design of the crossing on East Coast Main Line. Type 4 trains were

monitored over the site with speeds ranging from 60kph to 125kph, which gave strains of between 55με and 400με. He states that the higher strain levels are exacerbated due to poor ground conditions.

Track21, a project between three UK universities; University of Southampton, University of Birmingham and University of Nottingham, and industrial partners, including Network Rail, has many instrumentation work streams. The project uses train born instrumentation and ground vibration analysis. The project is in the initial stages, and has not yet drawn any conclusion to date [51]. The ground borne vibration analysis uses some of the outputs from the instrumentation in this research to build the knowledge through critical parameters, such as S&C.

3.5 CRITICAL REVIEW OF CURRENT LITERATURE

There is limited literature available on the S&C instrumentation, with the main focus historically focused on crossings or train borne measurements and for a short duration. The literature reviewed has shown that there is a current gap in the knowledge for deterioration of S&C in service over the life cycle of the asset. The knowledge gap needs to be reduced to ensure that the life cycle of S&C units can be extended through efficient maintenance regimes. This will in turn reduce major incidents and risk-based inspections.

The review of the relevant literature has shown that there are currently low levels of knowledge in the switch and crossings instrumentation topic. S&C design, material degradation and previous statistical analysis are well documented. Research using field instrumentation in the UK is limited, with two papers completed in 1980s on the bending strains through crossings in the UK to compare two manufacturers' design at a single location. The research focuses on bending strains in crossing units and doesn't compare age and the impact on the strain. The focus on crossings was due to the material, manufacture and installation costs being the industry priority in the 1980s.

Additional research is needed to gain a clearer understanding of how the structure responds to the dynamic loading of a train passage through the switch and crossing. The best application of monitoring loads currently is through field experimentation as in-service outputs can be collected and are repeatable to monitor changes of the instruments over time. The outcome

from the field instrumentation gives a greater knowledge of the magnitude of the current loading and a deterioration process of S&C.

Damage mechanisms are well documented with wear, plastic deformation and RCF researched extensively. The degradation knowledge specifically within S&C has only been researched through failure statistics and renewal rates, due to the available data and the lack of field instrumentation outputs.

Currently, no research has combined the statistical analysis of failures with field experimental processes on S&C in the U.K. Field experimentation on crossings has been completed as part of the INNOTRACK European railway infrastructure research project, and in the UK in the 1980s. The UK infrastructure has different turnout radius and length of the switch design so the research that was completed on European design will have different contact locations. The changes in the infrastructure design have a significant effect on the vehicle dynamics that would occur as the vehicle passes through the unit with longer turnouts generating reduced lateral loading. This means that the research that has been reviewed has not given a relevant representation of switch and crossing response for the current design in the UK.

The literature review has shown that the areas of development of knowledge include the study of field experimentation through the S&C unit and the deterioration through in-service loading.

3.6 KNOWLEDGE DEVELOPMENT

From understanding the knowledge currently available and the gaps in the knowledge, this thesis aims to increase the knowledge in four areas. These areas are;

- UK field instrumentation of S&C – field instrumentation has been completed; however, not through S&C in the UK. Field instrumentation output comparisons with various design parameters have not been researched previously. Field instrumentation will allow for a change in the response of the switch and crossing asset to loading to be monitored in service.

- Performance of current S&C in UK – Understanding the performance through field experimentation will allow for a critical analysis of the design which will develop the industries understanding.

- Critical Parameter Study – Design parameters for switches and crossings will be evaluated through the deterioration and will lead to on-going knowledge of the critical nature of the design.
- Optimisation of maintenance for switches and crossings – repetitive inspections are understood, but optimisation could be researched after developing knowledge on the dynamic loading and material degradation of current designs.

3.7 NEXT STEPS

The thesis aims to bridge the gaps in the field instrumentation knowledge of switches and crossing based on the structure set out in Chapter 1.

The design of experiments (DOE) that will be needed for the instrumentation design for the trend analysis relies on statistical reasoning and understanding. In Chapter 4, data from historic failures seen within the S&C units will be analysed from Network Rail databases, giving parameters and levels used in the DOE techniques in Chapter 5.

REFERENCES

1. Cornish A, Kassa E & Smith RA. Investigation of failure statistics for switches and crossings in the UK. In: *Railway Engineering - 2011*, Forde M. C. (eds.), University of Westminster, 2011, 1-14

2. Rail Accident Investigation Branch, *Rail Accident Report: Derailment at Grayrigg, 23 February 2007*: Rail Accident Investigation Branch, Report No: 20/2008, Department for Transport The Wharf, Stores Road, Derby, UK, DE21 4BA. 2009.

3. Schmid F, Burstow M, Clark S, Eickhoff B, Hiensch M, Hsu SS & Kent S, *Best Pratice in Wheel-Rail Interface Management for Mixed Traffic Railways*. 1st ed: University of Birmingham Press; 2010.

4. Andersson S, *Friction and Wear Simulation of Wheel-Rail Interface*. In: Lewis R., Olofsson U., (eds.) *Wheel-Rail Interface Handbook*. Woodhead Publishing Limited; 2009.

5. Ayasse JB & Chollet H, *Wheel-Rail Contact*. In: Iwnicki S., (eds.) *Handbook of Railway Vehicle Dynamics*. Taylor & Francis Group; 2006. p.85-120

6. Bower AF & Johnson KL, Plastic flow and shakedown of the rail surface in repeated wheel-rail contact, *Wear - An international journal on the science and technology of friction, lubrication and wear*, 1991; 144(1-2): 1-18.

7. Busquet M, Chollet H, Baillet L, Dagorn C, Ayasse JB & Berthier Y, From railway dynamics to wheel/rail contact mechanics, an approach for the modelling of the wheel/rail contact: elasto-plastic response of the railhead, *Proceedings of the Institution of Mechanical Engineers - Part F - Journal of Rail & Rapid Transit*, 2006; 220(3): 189-200.

8. Fletcher DI, Franklin FJ & Kapoor A, *Rail surface fatigue and wear*. In: Lewis R., Olofsson U., (eds.) *Wheel-Rail Interface Handbook*. Woodhead Publishing Limited; 2009.

9. Garciavadillo E, Gimenez J & Tarrago J, Wheel Rail Contact - Geometrical Study, *Vehicle System Dynamics - International Journal of Vehicle Mechanics and Mobility*, 1984; 13(4): 207-214.

10. Johnson KL, *Contact Mechanics*. Cambridge University: The Press Syndicate Of The University of Cambridge; 1985.

11. Enblom R, Deterioration mechanisms in the wheel–rail interface with focus on wear prediction: a literature review, *Vehicle System Dynamics: International Journal of Vehicle Mechanics and Mobility*, 2009; 47(6): 661-700.

12. Hiensch M, Heaton N, Sawley K, Burstow M, Kapoor A, Fletcher DI, Franklin FJ, Jones C, Jones R, Taylor J & Eickhoff B, *Wheel-Rail Deterioration and its Impact*.

1st ed. In: Hiensch M., (eds.) *Wheel-Rail Best Practice Handbook*. University of Birmingham Press; 2010. p.1-94

13. Halling J, *Principles of Tribology*. 1 ed: The MacMillan Press Ltd; 1975.

14. Olofsson U & Lewis R, *Tribology of the wheel-rail contact*. In: Iwnicki S., (eds.) *Handbook of Railway Vehicle Dynamics*. Taylor and Francis Group; 2006. p.pp121-142

15. Johansson A & Andersson C, Out-of-round railway wheels - a study of wheel polygonalization through simulation of three-dimensional wheel-rail interaction and wear, *Vehicle System Dynamics - International Journal of Vehicle Mechanics and Mobility*, 2005; 43(8): 539-559.

16. Jin XS, Wen ZF, Zhang WH & Shen ZY, Numerical simulation of rail corrugation on a curved track, *Computers & Structures*, 2005; 83(25-26): 2052-2065.

17. Wang WJ, Guo J, Liu QY, Zhu MH & Zhou ZR, Study on relationship between oblique fatigue crack and rail wear in curve track and prevention, *Wear - An international journal on the science and technology of friction, lubrication and wear*, 2009; 267(1-4): 540-544.

18. Telliskivi T & Olofsson U, Wheel-rail wear simulation, *Wear - An international journal on the science and technology of friction, lubrication and wear*, 2004; 257(11): 1145-1153.

19. Wickens AH, *Static and Dynamic stability of railway vehicle wheelsets having profiled wheels*. Derby: British Rail Research (BRR), Report No: TN-DYN-90, (BRR) British Rail Research. 1968.

20. Wickens A, *A refined theory of the lateral stability of a four wheeled railway vehicle having a flexible, undamped suspension*: British Rail Research (BRR), Report No: 261-032-023, 1966.

21. Cornish A, *Development of Predictive Maintenance of Switches and Crossings based on Experiemental Analysis and Numerical Modelling*, Future Railway Research Centre Department of Mechanical Engineering, February, 2011.

22. Garnham JE & Davis CL, *Rail Materials - Part 1*. In: Lewis R., Olofsson U., (eds.) *Wheel-Rail Interface Handbook*. Woodhead Publishing Limited; 2009. p.125-171

23. Garnham JE & Davis CL, *Rail Materials - Part 2*. In: Lewis R., Olofsson U., (eds.) *Wheel-Rail Interface Handbook*. Woodhead Engineering; 2009.

24. Williams J, Dyson I & Kapoor A, Repeated Loading, residual stresses, shakedown and tribology, *Journal of Materials Research*, 1998; 14(4): 1548-1559.

25. Burstow M, *Whole Life Rail Model Application and Development for RSSB - Continued Development of an RCF Damage Parameter*: Rail Safety & Standards Board, AEA Technology Rail, September, Report No: AEATR-es-2004-880, 2004.

26. Johnson KL, Contact mechanics and the wear of metals, *Wear - An international journal on the science and technology of friction, lubrication and wear*, 1995; 190(2): 162-170.

27. Zerbst U, Lunden R, Edel KO & Smith RA, Introduction to the damage tolerance behaviour of railway rails - a review, *Engineering Fracture Mechanics*, 2009; 76(17): 2563-2601.

28. Kapoor A & Williams JA, Shakedown limits in rolling-sliding point contacts on an anisotropic halfspace, *Wear - An international journal on the science and technology of friction, lubrication and wear*, 1996; 191(1-2): 256-260.

29. Grassie SL, *Rail Corrugation*. In: Lewis R., Olofsson U., (eds.) *Wheel-Rail Interface Handbook*. Woodhead Publishing Limited; 2009.

30. Grassie S & Elkins JA, Tractive effort, curving and surface damage of rails: Part 1. Forces exerted on the rails, *Wear - An international journal on the science and technology of friction, lubrication and wear*, 2005; 258(7-8): 1235-1244.

31. Burstow M, *Background the to Tgamma RCF damage function*, Railway Systems Engineering Network Rail, 2006.

32. Cannon DF, Edel KO, Grassie SL & Sawley K, Rail defects: an Overview, *Fatigue & Fracture of Engineering Materials & Structures*, 2003; 26(10): 865-886.

33. Burstow M, *A Tool to Predict Rolling Contact Fatigue*: AEA Technology Rail, Jubilee House 4 St. Christophers Way, Pride Park, Derby, DE24 8LY. 2004.

34. Network Rail, *Annual Return 2010, Moving ahead; Investing in the future*, Network Rail Kings Place, 90 York Way, London, N1 9AG. 2010.

35. Williams J, Gordon D & Harrison J, *S&C Failure and Delay Analysis*, Report No: SA/TSS/17754/S3/R001, Serco Assurance Thornson House, Birchwood Park, Warrington, Cheshire, WA3 6GA. 2007.

36. Fisher RA, *Statistical methods, Experimental design and Scientific inference*. 7th ed. Bennett J.H, (eds.). Oxford: Oxford University Press; 1990.

37. Hanna TH, *Field instrumentation in geotechnical engineering*. 13th ed: Trans Tech Publications Ltd; 1985.

38. Zwanenburg WJ. *Modelling Degradation Processes of Switches & Crossings for Maintenance & Renewal Planning on the Swiss Railway Network.* PhD Thesis: Delft University of Technology, École Polytechnique Federale De Lausanna; 2009.

39. Zhang W, Dai H, Shen Z & Zeng J, *Roller Rigs*. In: Iwnicki S., (eds.) *Handbook of Railway Vehicle Dynamics*. 2006. p.457-506

40. Ekberg A & Paulsson B, *Concluding Technical Report - INNOTRACK, Innovative Track Systems*: Intellecta Infolog; 2010.

41. Nicklisch D, Nielsen JCO, Ekh M, Johansson A, Palsson B, Reinecke JM & Zoll A. Simulation of Wheel-Rail Contact Forces and Subsequent Material Degradation in Switches & Crossings. In: *21st International Symposium on Dynamics of Vehicles on Roads and Tracks*, (eds.), Stockholm, Sweden, 2009, 1-14

42. Kassa E & Nielsen JCO, Dynamic interaction between train and railway turnout: full-scale field test and validation of simulation models, *Vehicle System Dynamics - International Journal of Vehicle Mechanics and Mobility*, 2008; 46(1): 521-534.

43. Cheesewright PR, *Wheel/Rail Forces Measured at Crossings of Cast Manganese and Built-up Types*, British Railways Research and Development Division - Track Group, June, Report No: 263-191-24, British Rail. 1977.

44. Troup R. M., *Measured Wheel-Rail Forces through switch diamonds and swing nose crossings*, British Rail Research Board (BRRB), Report No: TM VDY 003, 1985.

45. Clarke R. A., *Measurement of wheel-rail contact forces at a selection of switches and crossings using the HSFV1 equipped with load measuring wheelsets*: British Rail Research (BRR), Report No: TM DA 39, 1981.

46. Wickens A, *Fundermentals of Rail Vehicle Dynamics: Guidance and Stability*. Ma F., Kreuzer E., (eds.). Loughborough University, UK: Swets & Zeitlinger; 2003.

47. Licciardello RV, Bruner M, Corazza GR, Cosiotti E, Malavasi G, Malavasi G, Troisi R & Musella S. Some experience on the dynamincs of turnouts due to passing trains. In: *8th World Congress on Railway Research*, (eds.), Seoul, Korea, 2008, 1-9

48. Li H, Xu Y & Zhou Y. Field Measurement and Performance evaluation of High-Speed Railway Turnouts on Ballasted Track of Passenger Dedicated line. In: *Railways Engineering 2011*, Forde M. C. (eds.), University of Westminster, Engineering Techics Press, 2011, 1-6

49. Boutle NF, *A Fatigue-Orientated Analysis of Strains Measured from Two Crossings of Different Design Installed at Watford Junction*: British Railways Board, British Railways Research and Development Division - Track Group, Report No: 263-190-16, 1978.

50. Groom GM, *Strain Gauge Survey of the E.C.M.L. Newark High Speed Square Crossing*, British Railways Research (BRR) - Track Group, Report No: 263-202-9, 1973.

51. Track21 - Railway Research - Funded by EPSRC EP/H044949/1. *Track21, Railway track for the 21st century*. Available from: http://www.track21.org.uk/ [Accessed: 025/05/2013].

52. Takahashi S, Sasaki T, Kondoh Y& Hirose Y, Residual stress evaluation of Railway rails, *International Centre for Diffraction data,* 2009; 240-247.

53. Hunt G, *T372 - Review of the effect of track stiffness on track performance,* Rail Safety and Standards Board (RSSB), AEATR-II-2004-018, 2005

54. Bowness D, Lock AC, Powrie W, Priest JA & Richards DJ, Monitoring the dynamic displacements of railway track, *Proceedings of the Institution of Mechanical Engineers - Part F - Journal of Rail & Rapid Transit*, 2007; vol. 221: 13-22.

55. Priest JA & Powrie W, Determination of Dynamic Track Modulus from Measurement of Track Velocity during Train Passage*, Journal of Geotechnical and Geoenvironmental Engineering,*2009, 135(11), 1732-1740.

56. Pennycook JT, *Investigation intoTrack Stiffness, Sleeper Load and settlement using Rolling Load Rig Experimental Results*: British Rail Research (BRR), Report No: TM-SM-45, 1977

57. Nicklisch D, Kassa E, Nielsen J, Ekh M, Iwnicki S, Geometry and stiffness optimization for switches and crossings, and simulation of material degradation, *Proceedings of the Institution of Mechanical Engineers - Part F - Journal of Rail & Rapid Transit*, 2010, vol. 224, 279-292.

58. Li MXD, Berggren EG, A study of the effect of Global Track Stiffness and its Variation on Track Performance: Simulation and Measurement, *Proceedings of the Institution of Mechanical Engineers - Part F - Journal of Rail & Rapid Transit*, 2010, vol. 224, 375-382.

4. FAILURE ANALYSIS

It is vital to instrument the correct components within the S&C to get pertinent outputs for deterioration. Failures and delays of trains were collected through the Operational Control between 2009 and 2012. The purpose of the failure analysis is to focus the instrumentation design to ensure the pertinent failure modes can be monitored through the next phase. This will increase the understanding the current deterioration in service through statistics. Delay minutes and cost are used with rectification costs to understand the most prolific failure mode.

S&C's have a higher failure rate compared to plain line because of the amplified dynamic forces that incur as vehicles negotiate through irregularities in the running surfaces. Currently, there is a limited industrial knowledge on the failures of S&C, with Williams et al. [1] showing increased tonnage getting increased failure rates due to the high wear and dynamic loading on the system. This chapter aims to increase the understanding of failure location, type of failure, and failure characteristics within current S&C's. Table 4-1 shows the annual delay minutes across the network, and the percentage within an S&C unit.

Table 4-1: The Network Rail delay statistics [2]

	Financial Years						
	2006/07	2007/8	2008/09	2009/10	2010/11	2011/12	2012/13
Network delay minutes (million)	10.53	9.5	8.84	8.18	8.95	8.34	8.80
S&C delay minutes				820,992	835,870	865,785	575,870[1]
S&C delay percentage				10.04	9.34	10.38	6.54

Infrastructure failures cost Network Rail £327 million/year in financial year 2012/13 (excluding the cost of replacing the damaged asset), which is a mean of £45/minute. Of these delay minutes, c. £32 million is due to failures from within S&C. The delay minutes are the

[1] This value is the points operation failures and does not include some of the switch and crossing rail material failure, but the points failure minutes are c.18,000 minutes lower compared with previous years

number of minutes later than the scheduled arrival time [3]. The Public Performance Measure (PPM) shows the percentage of trains arrived on their scheduled time 90.9% of occasions in 2012, which include trains less than 5 minutes delayed (and 10 minutes for long distance) [3]. The minutes incurred by the infrastructure company due to vehicles being delayed has shown a downward trend annually since 1994 (c.f. Figure 4-2). For the year 09/10 (aligned with the fiscal calendar), total delay minutes across the network were circa 8.18 million minutes. The number of train journeys being completed has increased during the same time period to record levels due to increased efficiencies in the time to train paths with improved timetable designs within Network Rail and maintenance practice of the infrastructure.

Between 2009 and 2013, 70-85% of the failures within S&C are from failures within POE. POE has an increased chance of failing due to the high frequency vibrations that occur through the asset which damage the electrical elements within the operating equipment. This research focuses on understanding the dynamic loading through S&C rail sections, and the resulting deterioration of rail steel and components. The deterioration is understood on plain line rail surfaces, but the knowledge is missing for S&C due to the lack of research currently completed.

4.1 COMMON FAILURE MODES IN SWITCHES AND CROSSINGS

In S&C the conventional wheel-rail contact interrupts at several locations due to the discontinuities, or irregularities. These irregularities cause disruption of the contact trajectories and results in complex dynamic responses. The main damage types that are in S&C are covered within the literature review. A summary of the common failure modes is given and their effect on the operation of S&C.

Damage characteristics can be separated into two categories based on the location and nature of damage: those within and close to the contact patch due to the large wheel-rail contact pressure, plastic deformation, wear and rail head cracks; and those away from the contact location, fracture usually in the web of the rail or rail foot due to higher bending stresses [4]. Figure 4-1 shows the common failure types that are seen in S&Cs.

4.1.1 Plastic deformation

Plastic deformation develops due to the dislocation movements in the grain structure of the material [5, 6]. As cyclic rolling loading exceeds the elastic limit of the material, contact

stresses exceed the yield limit and the grains become heavily deformed and elongated, leading to local material degradation with anisotropic properties. In switch panels and at the crossing nose, repeated and high magnitude cyclic contact forces on the rail leads to accumulated plastic deformation that changes the rail profile and can stop the operation of the switch through rail material blocking the closing mechanism. The rate and magnitude of the profile change depends on both the loading and the material behaviour of the rail steel. Large magnitude loading leads to a rapid change of the rail profile by plastic deformation. As a result of the plastic deformation, the contact location and contact pressure alters between the wheel and the rail. Initially plastic deformation occurs at the surface of the rail as the wheel and the rail become more conformal, through a combination of normal and tangential forces, to distribute the loads between the contacting surfaces and reduce some of the high intensity of the loading [21]. Friction coefficient contributes to the plastic deformation initiated cracks, with the coefficient 0.25μ initiating cracks in 38,000 cycles at the surface [22] found through modelling (damage accumulation), due to the increase in friction causing material failure to progress towards the surface. 1757,000 cycles were needed at 0.2μ to initiate cracks.

i) Plastic deformation – Section 4.1.1

ii) Wear through friction (switch rail) [7] – Section 0

iii) Fracture – Section 4.1.3

iv) Spalling / pitting – Section 4.1.4

Figure 4-1: i) Plastic deformation of a wing rail at a crossing, ii) wear through friction at a switch blade and through the wheel transfer zone, iii) a fracture in the foot of a cast crossing, and iv) rail head spalling / pitting through crack propagation on the crossing nose (and plastic deformation on the wing rail)

The friction levels are highly significant through switches and crossings, as turnout switch rails are well lubricated through maintenance practices and thus increase the number of cycles on the switch blade before plastic deformation and crack initiation. Non-switch rails are rarely lubricated as it would affect the rail head conditions and braking ability of the vehicles.

4.1.2 Wear

According to Bayer [8] wear can be divided into five categories, of which three are found through wheel / rail contact;

- Abrasion – material or particle removal through asperities in the running surface causing high friction levels between the surfaces
- Impact – high magnitude contact forces between bodies in contact lead to rapid changes in stress, causing plastic deformation, and initiation and propagation of cracks
- Delamination – thin layers of material removal from the surface.

These wear categories can happen independently or combined simultaneously through switches and crossings due to the high impact forces from the discontinuity of the geometry and various contact locations and magnitudes of loading.

Currently, whilst there are inspection criteria for side abrasion wear in the switch panel [7], there is limited industrial knowledge on the impact that this wear has on the dynamics between the wheel and rail. Optimising the design of the switch geometry has been undertaken [9] to reduce the wear through the switch by applying a gauge widening at the switch tip. The forces and wear of the gauge widening were calculated through a multi-body simulation package and showed that through the switch the normal contact force and the RCF prediction reduced with an optimal widening of 12mm. This is due to the change in the dynamic forces, with the profiles on the wheel generating a steering force away from the switch rail due to the change in contact between the wheel and the rail. This also changes the contact location away from the thinner section of the switch, which means that there is more rail material to withstand the contact forces.

4.1.3 Fracture at the web or foot of the rail

Fracture failure types can be categories depending on location within the rail: defect in the web of the rail; and those in the foot [10]. Fracture can happen either through repeated high loading exceeding the ultimate strength of the material, or through a single instant catastrophic loading. These loadings are affected by the wheel-rail contact forces causing the bending stress to focus on concentrated and weakened areas, particularly through increased dynamic loading from irregularities in the crossing. Longitudinal defects in S&C account for 23% of rail fractures or detected cracks [10]. Crossing fracture is becoming increasingly rare in the field due to changes in material composition and increased quality control in the manufacturing process [11, 12]. Crossings and bolt holes are the most likely locations for fracture, due to their localised stress raisers and high stresses from loading. Crossings have high magnitude loads from the irregularities generating high bending stress at the foot of the asset, with is the common location of fracture, as shown in Figure 4-1 (iii).

4.1.4 Rail head cracks

Rail gauge corner cracks, or 'head checks' are a group of fine surface cracks found on the outer rail of curved sections of tracks and switches and crossings. Head checks can cause spalling of pieces of material and transverse cracks leading to fracture of the rail [13]. Rolling Contact Fatigue (RCF) is initiated through high magnitude shear strains of the head of the material and close the contact surface [14]. Transient forces generate ratcheting of the material close to the surface, and then continued loading changes the crack growth rate (enhanced by fluid entrapment), before branching further into the rail material, which is undesirable due to the limitations on inspection techniques.

4.2 NETWORK RAIL DATABASES

Network Rail currently uses 16 different databases to collect, store and generate information for asset management and knowledge sharing. User uncertainty can cause inputted data to be erroneous, giving the current databases an 90% accuracy [1]. Errors in the asset location can potentially put failures outside of the asset location, which lead to unknown data entries. Historically, the asset databases were created and then populated through local groups, and

then were updated after a renewal occurred. This allowed for incorrect information to be inputted into the system and not validated.

Three databases have been used in this research for: asset information (GEOGIS); train delay information (TRUST); and infrastructure failures (FMS). These databases are independent, but can be aligned through joining the train delay data with the infrastructure fault data and location.

- GEOGIS – G*eography and Infrastructure System*
    - Asset information database, such as geographical locations, asset type and year of installation
    - The advantage of GEOGIS is that it stores all the asset data in a single location. This means that details of the asset will be able to be aligned with the delay information
    - GEOGIS is c. 90% accurate when locating S&C [1], due to initial input and updates of information within the system
    - For this research, GEOGIS is used to understand the population, and assets involved in the failures to give more details for the analysis.
- TRUST – *Train Running system TOPS (Total Operation Processing System)*
    - TRUST logs all details of running vehicle and aligns with the schedule of the vehicles, giving delays to trains and their associated failure
    - The database can cross-reference the fault description in *Fault Management System (FMS)* to give a full account of the delay and causes
    - Not all S&C failures record a delay to vehicles, either through being within a possession (line blocked to traffic), or rectified before a train traverses the points, which can lead to not recording all the delays and being omitted from the statistics
    - For this research, TRUST is used to determine failure costs and the reasons for the delay to the train.
- FMS – *Fault Management System*

- Manages and reports failures on the network infrastructure asset
- FMS shows and explains the detail behind the failure from an asset perspective
- FMS has to be linked with GEOGIS to align the infrastructure with the details of the failure. The alignment has error levels built in due to the accuracy issues mentioned in GEOGIS. FMS is directly related to the delays found in TRUST but needs to be aligned through post-processing
- For this research, the alignment of the asset failure is essential to understand which component is the cause of the delay and any additional comments that are from the inspector.

Within Network Rail there is a new database for asset management, ORBIS, *Offering Rail Better Information Services* [15], but this is not yet being fully implemented by all infrastructure groups. ORBIS is verifying the asset type and locations of all assets to improve the accuracy of the asset knowledge. The ORBIS programme has two main objectives; to improve the asset information quality of the current infrastructure and to deliver a validated plan for the next funding period to the ORR. This will increase the accuracy in the failure data in the future by updating the asset information and with increased detail.

If a failure is found through the various inspections, the National Operations Centre is informed. Once the detail of the fault has been transferred to the Operations Centre, a fault code is generated within the TRUST database. This is used to align the train running data and the delays that can be associated with the fault. The delay information and costs to the asset information are combined with the asset database, GEOGIS to have an account of the incidents and their associated asset(s). This database can be filtered to analyse the assets, such as S&C, the details of the delay, and the costs that have been associated to it. As the fault is processed over the phone, there is a chance of errors occurring through poor or mis-communication.

For this research, the data used is;

- January 2009 to May 2012 for all S&C failures, and the associated delay cost for the failures.

- Network Rail Business Plan which showed the historic maintenance and renewal figures.
- Historic delay information and costs from the *Annual Returns*, which are published by Network Rail [16].
- Network Rail asset information from 2011, total train miles, S&C type and population, and renewal information.

The information will allow the current failures in the infrastructure to be analysed. The statistics will focus the instrumentation to pertinent parameters that are representative of the current failures in service.

4.3 FAILURE STATISTICS ANALYSIS

Total train delays and train passenger miles against years are shown in Figure 4-2 using the National Rail Trends Portal [17]. Figure 4-2 shows that the number of trains increased from 450Mkm in 2000/01 to 536Mkm in 2012/13. Increased traffic heightens the possibility of failures through quicker deterioration and the high capacity means total delays could be exacerbated through a larger accumulated delay. Historically, the trend of increasing delays with passenger numbers has not been the case as delays on the network have decreased from 17Mmins to 8.7Mmins from 2001.

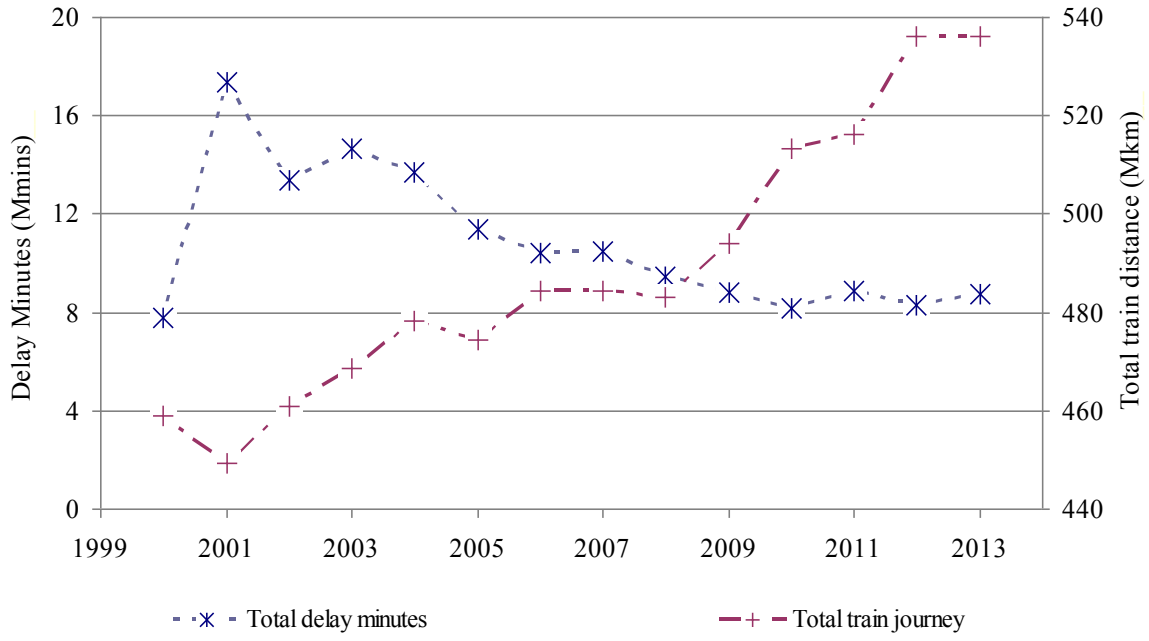

Figure 4-2: Annual delay minutes and annual train journeys since 2000 [17]

Figure 4-3 shows the total delays and cost of the delays against years. The failure statistics for 2012 are much reduced due only 5 months of data available at the time of research. In the figure, there is a small decrease in the delays minutes per year, but an increase in the cost of the delays rising on average £15 / 10 minute delay.

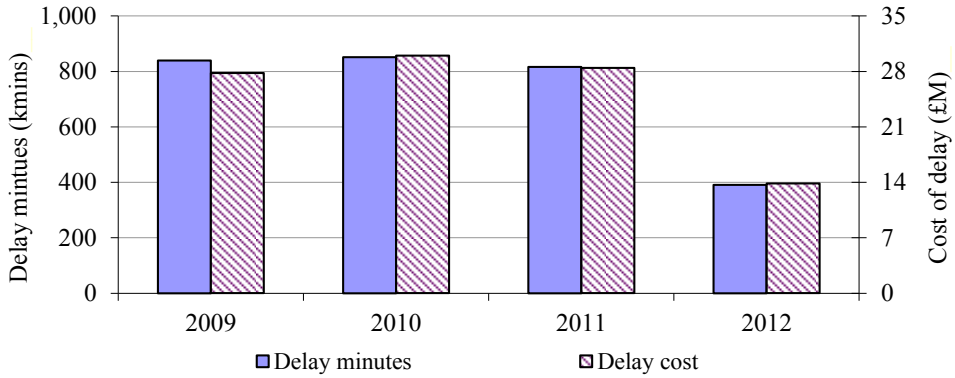

Figure 4-3: The delay minutes within S&C on primary axis, delay costs on secondary axis to give a representation on the changing of costs / minute / year – 2012 has a reduced time frame of 5 months due to the data available

Figure 4-4 shows the delays / month against the calendar years in reference to 2009. The figure shows that 2011 had reduced delay minutes / month, but 2012 had much worse delays / month. There were three significant snow falls that caused large number of delays through switches and crossings due to obstruction of the switch motion. These were in December 2010, January - February 2012 [2]. This would give some justification to the increase in the delay minutes per month associated to switches and crossings in 2010 and 2012. The 2012 is a smaller sample size (5 months) due to the available data, which means that it is influenced highly by the first few months of delays.

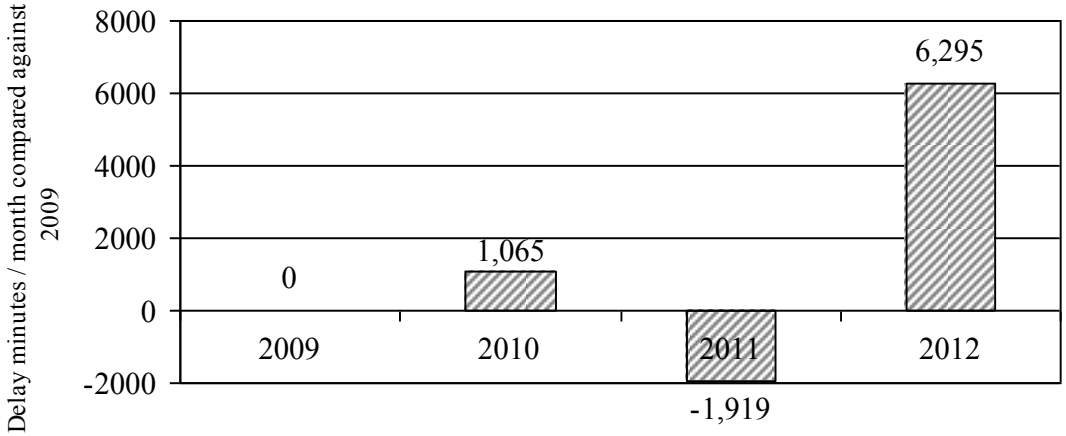

Figure 4-4: Annual delay minutes per month against the data from 2009.

Figure 4-5 shows the POE and Permanent way (Pway: rails, sleepers, ballast and adjoining assets) percentages / year. There are much larger failures specified within POE in comparison with the Pway, with POE seeing over 80% of the failures / year.

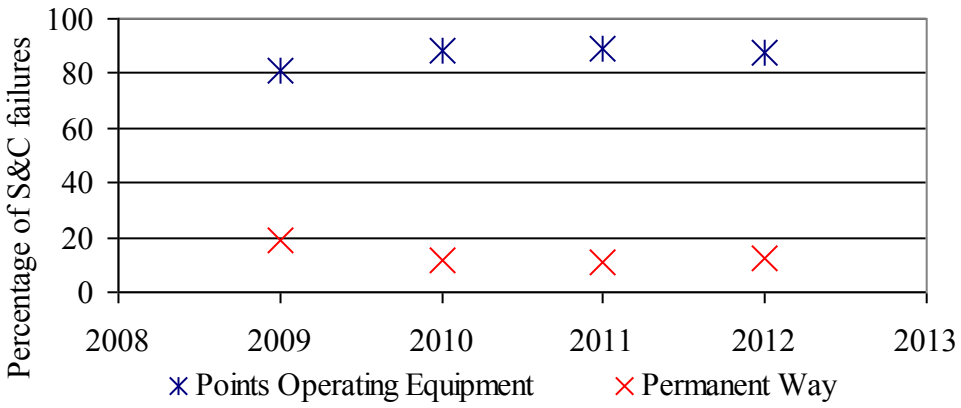

Figure 4-5: The annual split between points operating equipment and permanent way.

POE is much more likely to fail due to the electrical components and connections, with high frequency excitations causing the equipment to fail as the electronic components are unable to cope with the vigorous loading.

For the locations of the experimentation to create high quality and pertinent outputs, the delay statistics need to be refined to give validation to the selection of instrumentation locations. Geographical location gives a national perspective to the experimentation, to ensure that the deterioration has a national perspective.

4.3.1 Switch and crossing location failure analysis

Network Rail was devolved into ten regions after the McNaulty Report in 2012 [18] so that the local maintenance teams could focus their resources on regional issues. Figure 4-6 shows the delay minutes from Pway delay data available (January 2009 to May 2012) and divided by the number of S&C in each region, with the percentage per region shown in the numbers above the bars. Wales region has not been included in the analysis due to the small number of delay minutes that occurred within that region in S&C (0.38% of national). Network Rail class Anglia, Kent, Sussex and Wessex as ‘London and the South East’ due to the location and commuter routes. The delays minutes / unit is larger for these regions due to the increasing passenger numbers due to the proximity to London, and the poor weather that affected Anglia and Kent and Wessex in the winter months of 2010 and 2012. LNE is the

London North East route and runs from London St Pancras north into Edinburgh, Scotland. LNW is the London North West route and runs from London Euston, past Crewe and up to the Glasgow, Scotland.

Figure 4-6: Delays minutes against the number of switch units in the various routes, with percentage of total delay minutes

The delay minutes / unit are all within 10%, with the largest at 16.2% in Anglia and smallest 6.4% in the Midlands region. The largest delays per unit are on the commuter routes into London; such as the Kent, LNW and Wessex, due to the effect of high capacity on the routes, which can quickly accumulate delays. The impact of the regions is inconclusive, and whilst consideration should be taken for access to the site; to inspect and collect data, the geographical area is not relevant to the historic delays.

4.3.2 Switch and crossing layout failure analysis

As seen in Chapter 3, *Literature Review*, there are over 200 variations in switches and crossings. They are categorised by their length, with ‘A length’ being the shortest turnout and slowest, and ‘G+ length’ being the longest turnout and fastest.

Figure 4-7 shows the Pway cost per failure that occurred in each of the switch classifications from January 2009 to May 2012 to understand the influence of switch length on failure.

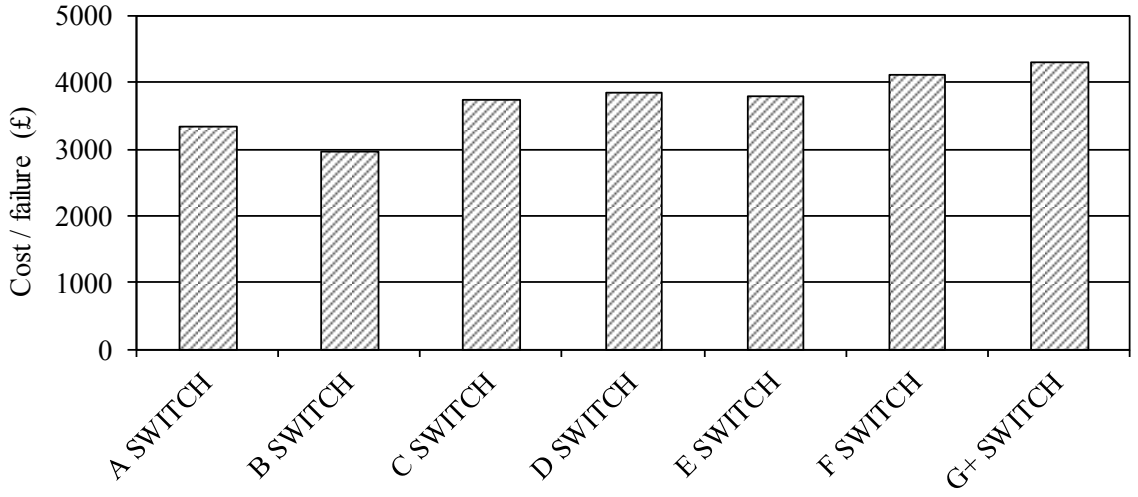

Figure 4-7: The delay cost of each failure seen within the various S&C classification

Over the full duration of the failure statistics available, the cost per failure tend to increase depending on the length of the asset, with the G+ switch being the longest, and the highest cost for each failure, with the smaller A and B switches showing lower costs. The higher cost per failure is due to the high speed switches causing longer delays due to having a greater effect on the running / capacity of trains, with the subsequent vehicles also encountering a delay, generating a cumulative effect on the delay at the end location.

4.3.3 Switch and crossing component failure

For the instrumentation to be installed in the correct areas on the switch and crossing unit, it is necessary to understand the failures of the components in S&C's. Figure 4-8 shows the failure location of the Pway component against the likelihood of the occurrence, as a cost percentage.

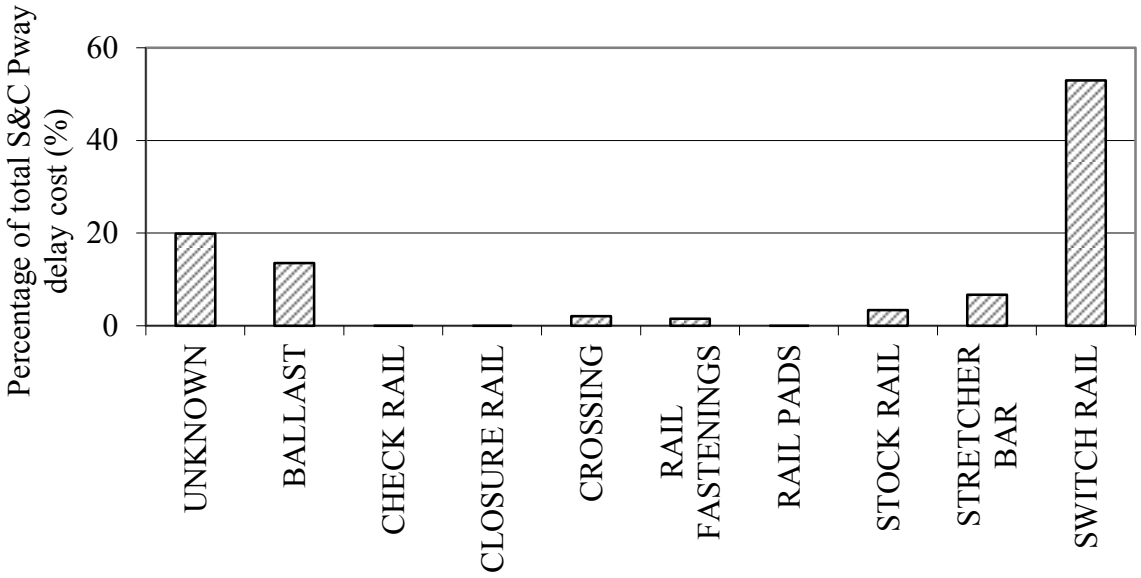

Figure 4-8: The percentage of permanent way S&C delay cost for the components

Figure 4-8 shows that the failure location is most likely to be within the switch blade, with 53% of Pway failures. The trend of the switch rail having the largest cost percentage is found in all switch lengths. This is due to the moveable section of rail emphasising the stress raisers / weaknesses of the asset and the failure of the switch to work, compromising the safety of the railway.

4.3.4 Switch and crossing failure cause

The cause of the failure is highly important in the location of instrumentation as it allows the degradation to be monitored in service over time. An understanding of the common failure types within S&C will allow the instrumentation to focus on areas that are most likely to degrade through change of material properties. Figure 4-9 shows the breakdown of the types of failure modes that were described in FMS and TRUST within the S&C unit that caused delays.

The cracked failures are the largest failure type with 68% of the failures recorded. This is due to the large variations of failures and assets that are put under the 'Cracked' classification, e.g. cracked detection rods, cracked stretcher bars and cracked weld repairs. Cracked rails are 24 of the 394 within Cracked category (6.1% within 'Cracked' are a rail, 4% of the overall delay minute percentage are cracked rails).

The variation in the definition of 'Cracked' has highlighted some issues with the recording and collection of the data. For the remainder of the research, the non-pertinent or non-rail cracked components have been ignored from the cracked category due to their non-relevance to the degradation of the rail material.

The '053 failure' includes five types of degradation within the switch panel, with the NR/L2/TRK/053 inspection to monitor for any issues that can derail a train [7]. The failure modes of the inspection include wear and plastic deformation in various formations on the stock and switch rail. There is not enough description in the databases to distinguish the detail of the failure mode. With the greater detail within the failure categories, Figure 4-9, lipping, a railway term for the physical appearance of plastic deformation, is the most common failure mode, and so the rails plastic reaction to loading is highly significant. As the rail head is not able to be instrumented to monitor the change in strain from the variable contact conditions, the change in the materials response to the loading is highly significant.

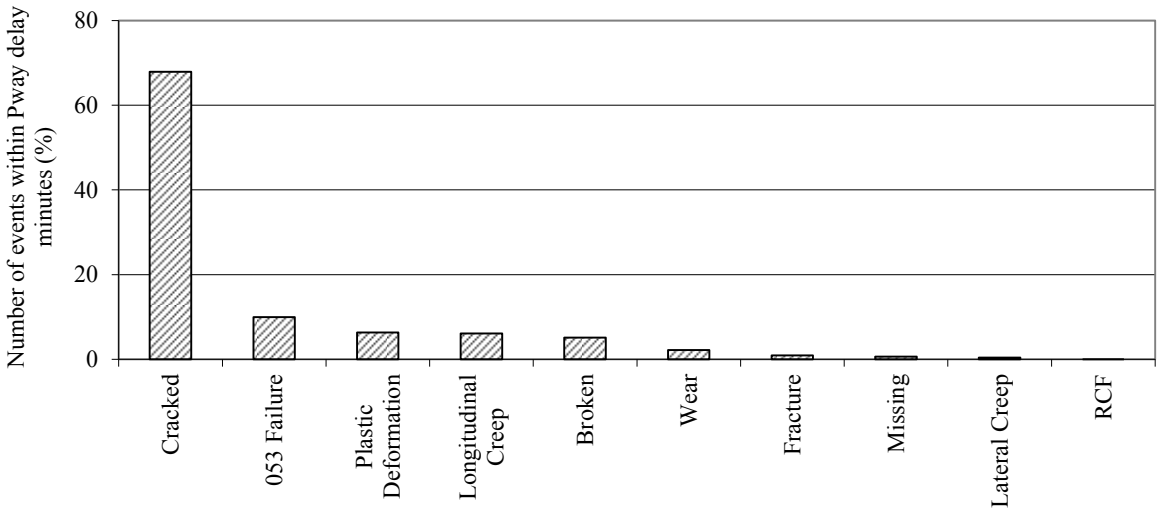

Figure 4-9: The percentages of failure modes that are seen within the failure minutes statistics

4.3.5 Failures, rectification and their costs

When failures occur in S&C, delays are felt across the network by cumulative delays to services. When the delay has stopped affecting the network and passages of vehicles, a cost is assigned to it, depending on the number of cancelled vehicles, delay minutes and train operating company (TOC). The TOC have associated delay fine costs against the infrastructure owner, depending on the route and contract agreement, ranging from £7 for a

minute delay on a suburban service to over £25,000 for a cancellation of a train on a high speed line [19].

Once the failure has been discovered, it is necessary to rectify the issues that have been raised. The common failure modes in Figure 4-9 have been grouped into three 'failure classifications': Plastic deformation, Fracture and Worn.

Table 4-2 shows the failure classifications that are described within Section 4.1, apart from rail head cracks and RCF. RCF is not included in the failure mode classification as the statistics show that less than 1% of failures were caused by RCF within S&C.

The rectifications give an indication on the type of repair and severity of the classification to rectify, with grinding being a cheaper and less drastic measure for repair than replacement. The plastic deformation rectification can be fairly cheap, with grinding the preferred option for the majority of the failures, removing the plastic deformation and returning the rail to the design cross-section. Usually, fractures need to replace the asset due to the safety critical nature of the asset and the severity of any exacerbation of the issue.

The rectifications are the process to fix the issue that caused the delay. This will give the instrumentation an overall cost relevance, or *failure cost*, to ensure that the correct areas are being instrumented. The costs include materials and labour to complete the rectification, and a percentage of the rectifications within each classification having a likelihood associated with the delay database.

From using the failure classifications, the associated switch lengths can be investigated to see if there is a variation of the classifications. Figure 4-10 shows the classifications of failure as a percentage of Pway failure cost. It shows that the C length switch has the largest percentage of failures over the network which is due to the high population of the C length switch.

Figure 4-10 shows the general failure classifications: Plastic deformation; Fracture and fatigue; and Wear, using the values from within Figure 4-9. Table 4-2 shows how the failure types of the components were put within the defined classifications.

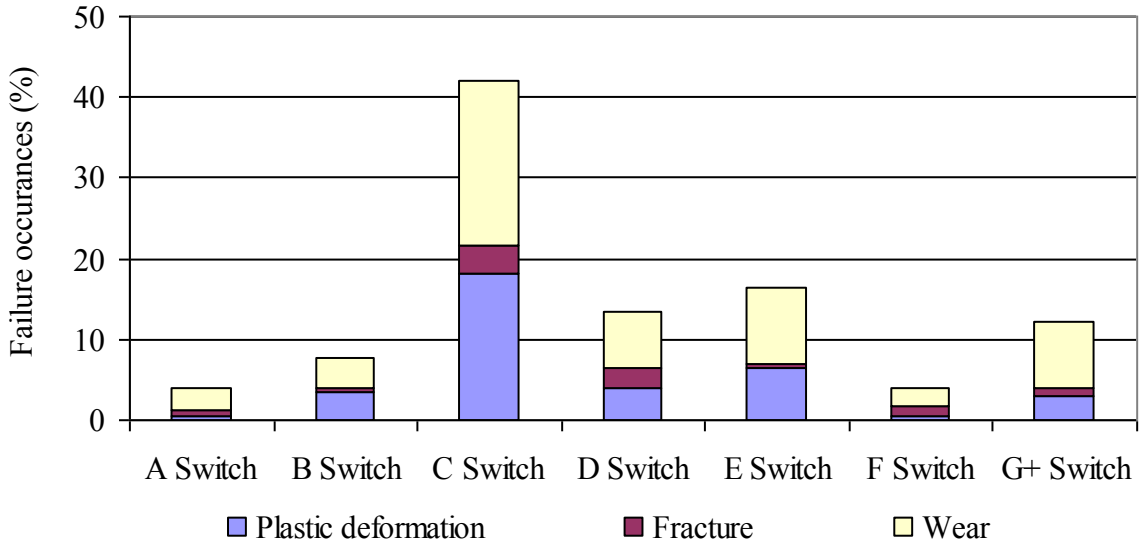

Figure 4-10: Percentage of Pway failure occurrences against switch length

Table 4-2: Description of failures and their associated classification in terms of failure modes

Failure classification	Failure Type	Rectification
Plastic deformation	Lipping	Grinding
	053 – Switch rail damage	Grinding
	053 – Switch rail with sharp gauge corner	Grinding
Fracture and fatigue	Fracture	Replacement / replace weld
	Rolling Contact Fatigue	Grind
	Broken	Replacement / weld repair
Wear	Hogged	Replace half unit
	Worn	Weld repair
	Creep	Gang for alignment
	Head missing	Weld repair
	053 – Sideworn stock rail associated with a little used switch rail	Weld repair / replace half unit
	053 – Stock rail and switch rail both worn	Weld repair / replace half unit
	053 – Stock rail headwear and associated with less head worn switch	Weld repair / replace half unit

Plastic deformation (38.6%) and worn (39.6%) classifications are the two largest in failure costs, with the occurrences of fracture less often (21%), but with greater costs for rectification.

The rectification costs are added to the delay costs to give a total failure cost.

$$Delay\ (TRUST\ cost) + Rectification(cost) = Failure(cost)$$

In some of the rectifications seen in Table 4-2 there are multiple modes of rectification for similar failure classification. The percentage of each rectification was calculated through a single year historic data and applied to the number of failures over the whole data available. Assumptions that have been used in the calculation of the rectification costs include;

- 89% of fractures happen within a weld (218 weld failures of 245 fractures); a replacement weld is completed rather than a replacement of a whole S&C unit. A broken rail is defined as fracture through the full cross section, or substantial cracks broken out of the rail head. The costs associated with fracture will be 89% the cost of a weld, 11 the asset cost that is replaced.
- 50% of 'Worn' can be completed with a weld repair (localised welding to reinstate the profile of the rail); the other 50% is unit replacement.

The combination of these failure costs are shown in Figure 4-11 against the various switch lengths and failure modes.

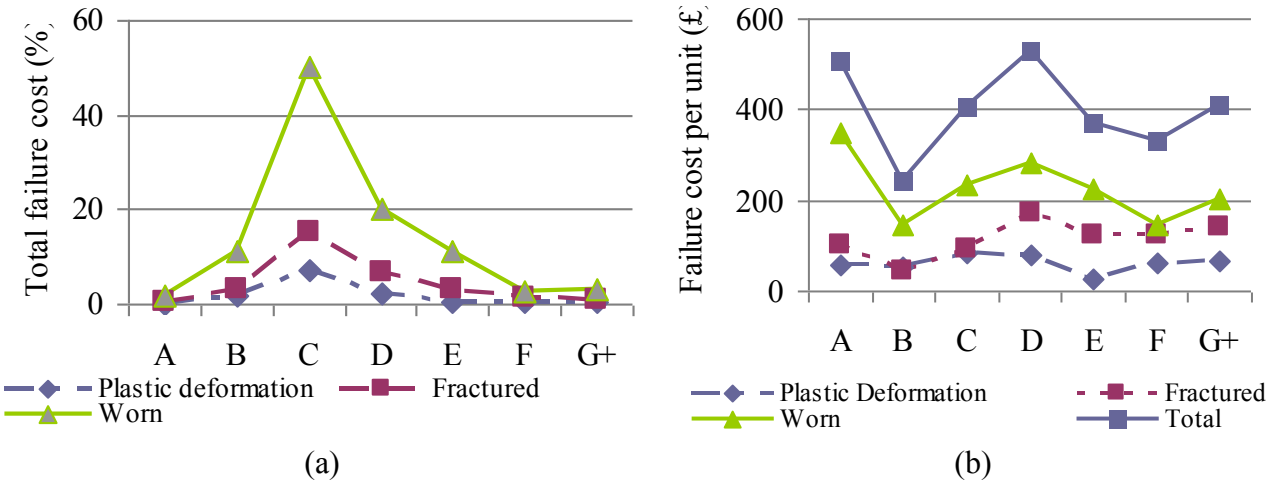

Figure 4-11: The costs of failures, (a) The percentage of total failure costs against switch length, and (b) the failure cost per unit for the various failure modes

From Figure 4-11 (a) it can be seen that the switch length C has the highest percentage of total failures costs. This is due to the large population of the C length switch. In general, the higher speed switches tend to see more wear damage due to the dynamic forces removing the top layers of the material. D length and slower switches experience more plastic deformation due to the vertical loading exceeding the elastic limit and plastically deforming. The A length switch tend to stay in service for longer durations [20] which means that the unit is replaced due to excessive wear. When normalising the cost against the number of S&C units Figure 4-11 (b) shows the high speed (G+ switch) and the low speed (A switch) have much higher costs / unit. Whilst they have a higher failure cost / unit, the population is small in comparison. As seen in Figure 4-7, the higher speed generating a higher failure cost per failure. The failure costs has a similar trend, with the cost per failure of the higher speed switches c. £200 / failure more expensive that the mid-speed switch. This is due to the higher percentage of failures per asset and the higher implications of the failures on the higher speed lines.

The mid speed (D length) switch is the most significant for the first phase of instrumentation excluding the extremes. This is due to 13.5% of failure costs against and £85 failures / unit, whilst having 16% of the total population.

4.4 DISCUSSION OF FAILURE STATISTICS OF SWITCHES AND CROSSINGS

In the financial year 2012/13, a total of 1500 failures were caused by S&C rail, causing a delay to the network of over 115,000 minutes. This equates to a cost of over £3 million to the infrastructure company, increasing to £22M for all delays within S&C, which includes POE. Failure statistics were analysed to understand the type of failure that occurs within the current design to ensure the instrumentation is positioned in the pertinent locations. S&C are highly complex assets, which have many components with a 5% track length against the total track distance of infrastructure. S&Cs have design classifications to generate eight allowable speeds and infrastructure constraints. The statistical analysis was completed to focus the instrumentation parameters and understand the current in-service degradation of S&C.

Within the highly functional S&C unit, there are three main failure modes; plastic deformation, fracture and fatigue, and wear. These are the failure modes also found on

railway plain line infrastructure. The instrumentation focuses on the switch panel, with the switch blade the highest failed component with 53% of the failures within S&C in the switch. Failure costs have shown that a range of switch designs will be instrumented as there is a similar normalised distribution. The highest population is the C length switch, with 55% of total switch numbers, with mid-speed having high industrial importance due to the population of the turnouts.

Statistical analysis has shown that the common failure mode of degradation depends on the length of the switch. The shorter switches (slower speed) are generating higher percentage of plastic deformation failures and the longer switches (higher speed) developing more wear failure mode. The change in the material degradation is due to the variation in tonnages and types of vehicles over the unit, with the slower switches seeing larger percentages of freight vehicles. Laden freight has higher tonnages, which generate more plastic deformation due to large vertical and lateral loading, deforming the head of the rail.

The delay costs have been aligned with rectification costs and it has been found that the highest 'failure' classification (summation of delay and rectification costs) is plastic deformation within the C length switch. The cost per unit is highly influenced by the population of the speed range, with the smallest (A switch) and the longest (G+ switch) having small populations percentages (less than 1%, and 7% respectively) and influenced by small numbers of failures. Excluding the extremes, the D length switch has the most significant normalised failure costs due to the population and high cost per unit.

Within failure cost per unit, plastic deformation was found to have the highest influence. This shows that the local contact between the wheel and the rail is critical in the deterioration of current S&C.

REFERENCES

1. Williams J, Gordon D & Harrison J, *S&C Failure and Delay Analysis*, Report No: SA/TSS/17754/S3/R001, Serco Assurance Thornson House, Birchwood Park, Warrington, Cheshire, WA3 6GA. 2007.

2. Network Rail, *Annual Return 2013, A technology-enabled future*, Network Rail Kings Place, 90 York Way, London, N1 9AG. 2013.

3. Office of Rail Regulators - National Rail Trends (NRT) Data Portal. *Public performance measure (PPM) by train operating company - table*. From Office of Rail Regulation, 1 Kemble Street, London, WC2B 4AN; Available from: http://dataportal.orr.gov.uk/displayreport/report/html/255f6c0e-f540-4b44-8686-db16270dde00 [Accessed: 28/02/2013].

4. Hiensch M, Heaton N, Sawley K, Burstow M, Kapoor A, Fletcher DI, Franklin FJ, Jones C, Jones R, Taylor J & Eickhoff B, *Wheel-Rail Deterioration and its Impact*. 1st ed. In: Hiensch M., (eds.) *Wheel-Rail Best Practice Handbook*. University of Birmingham Press; 2010. p.1-94

5. Garnham JE & Davis CL, *Rail Materials - Part 1*. In: Lewis R., Olofsson U., (eds.) *Wheel-Rail Interface Handbook*. Woodhead Publishing Limited; 2009. p.125-171

6. Garnham JE & Davis CL, *Rail Materials - Part 2*. In: Lewis R., Olofsson U., (eds.) *Wheel-Rail Interface Handbook*. Woodhead Engineering; 2009.

7. Network Rail. NR/L2/TRK/0053, *Inspection and repair to reduce the risk of derailment at switches,* 40 Melton Street, London, NW1 2EE. Network Rail; 2008.

8. Bayer RG, *Mechanical wear prediction and prevention*. First ed: Marcel Dekker, New York, USA; 1994.

9. Nicklisch D, Kassa E, Nielsen JCO, Ekh M & Iwnicki S, Geometry and stiffness optimization for switches and crossings, and simulation of material degradation, *Proceedings of the Institution of Mechanical Engineers - Part F - Journal of Rail & Rapid Transit*, 2010; 224: 279-292.

10. Zerbst U, Lunden R, Edel KO & Smith RA, Introduction to the damage tolerance behaviour of railway rails - a review, *Engineering Fracture Mechanics*, 2009; 76(17): 2563-2601.

11. Network Rail, *Annual Return 2010, Moving ahead; Investing in the future*, Network Rail Kings Place, 90 York Way, London, N1 9AG. 2010.

12. Office of Rail Regulators, *Train Derailment at Hatfield: A Final report by the Independent Investigation Board*: Office of Rail Regulation, 1 Kemble Street London, WC2B 4AN. 2006.

13. Cannon DF, Edel KO, Grassie SL & Sawley K, Rail defects: an Overview, *Fatigue & Fracture of Engineering Materials & Structures*, 2003; 26(10): 865-886.

14. Burstow M, *A Tool to Predict Rolling Contact Fatigue*: AEA Technology Rail, Jubilee House 4 St. Christophers Way, Pride Park, Derby, DE24 8LY. 2004.

15. Office of Rail Regulators, *Network Rail's output framework for 2014 - 19*, Office of Rail Regulation 1 Kemble Street, London, WC2B 4AN. 2012.

16. Network Rail. *Annual return web-pages*. Available from: http://www.networkrail.co.uk/Publications/Annual-return/Annual-Return-2012/ [Accessed: 05/01/2012].

17. Office of Rail Regulators National Rail Trends (NRT) Portal. *National Rail Trends*. From Office of Rail Regulation, 1 Kemble Street, London, WC2B 4AN; 2013 Available from: http://dataportal.orr.gov.uk/ [Accessed: 2013].

18. McNaulty R, *Realising the Potential of GB Rail - Report of the Rail Value for Money Study - Summary Report*: Department of Transport, Great Minster House 76 Marsham Street, London SW1P 4DR. 2011.

19. Salmon N. Performance Analyst Manager. Personal communication. 30/07/2013.

20. Zwanenburg WJ. *Modelling Degradation Processes of Switches & Crossings for Maintenance & Renewal Planning on the Swiss Railway Network.* PhD Thesis: Delft University of Technology, École Polytechnique Federale De Lausanna; 2009.

21. Bower AF, Johnson KL, Influence of strain hardening on cumulative plastic deformation in rolling and sliding line contact, *Journal of the Mechanics and Physics of Solids*, 1989; Vol. 37(4): 471 -493.

22. Wickramasinghe AIU, Hargreaves DJ, De Pellegrin DV, Predicting Crack Initiation Due to Ratchetting in Rail Heads using Critical Element Analysis, *International Journal of Chemical, Materials Science and Engineering*, 2013; Vol.7(5):149-154.

5. FIELD INSTRUMENTATION DESIGN

Field experimentation is necessary to measure large quantities of in-service loading data that would otherwise be unobtainable. The evidence from the literature review shows that there is a lack of knowledge on the current S&C on the UK network and the change in the material response to loading over time. The design of experiments procedure has outlined eight sites and locations for instrumentation. The design of the instruments on the switch and crossing unit show that the switch area should have gauges on the neutral axis mid-sleeper. The statistics show the crossing instrumentation should focus on the bending strains, with fracture being the largest failure mode. A sampling technique is completed to reduce the number of datasets for the investigation, to hasten the analysis whilst ensuring the analysis stays representative to the individual sites. The design of the instruments is essential to collecting high quality and pertinent results for deterioration analysis.

5.1 FIELD EXPERIMENTATION INTRODUCTION

The failure statistics and analysis shown in Chapter 4 – *Failure Analysis* demonstrate that the main area of focus through S&C should be in the switch area (area with profiles switch rails) with 68% of the permanent way failures. Historically, the deterioration rates of neither the switch nor the crossing have been researched thoroughly.

Field instrumentation is a key way to be able to collect and analyse strains and deflections from in-service loadings. Field instrumentation was selected over lab testing due to the large size of the asset to be analysed. A full S&C unit of 65m in length, creates complex conditions and contact locations through the length of the S&C unit due to the variable profiles and geometry. Representative testing of this magnitude would be highly complicated to replicate in a lab. The majority of other S&C research has been completed using modelling [1-4] with limited validation from in-field testing, which used vehicle based measurements which studies the instantaneous vehicle reaction to the contact. The trend of material response to

loading of in-service S&C has not been completed previously, with analysis of single loading from the point of view of the vehicle and crossing.

5.2 STRATEGIC DESIGN OF EXPERIMENTS TECHNIQUE

A Design of Experiments (DOE) technique was used to ensure that all parameters and levels, highlighted in failure statistics and historical research are covered within the experiment. The DOE technique allows the responses to the various levels within the parameters to be studied [5]. Previously a DOE methodology has been used to study the influence of parameters on the wheel-rail contact force using computer modelling [5], with friction and axle load having the largest effect on dynamic response. SC1 is the preferred design for switches and crossings and is the typical design for future enhancements to the infrastructure, and renewals. Two phases were set up due to the constraints of instrumention all sites simultaneously. The first four (SC1 – 4) sites were instrumented through this research, with the aim to continue the research to include units SC4 – 8. The continuation will complete the design of experiments and give increased confidence to the analysis. The strategy for the instrumentation was driven by the constraint of being able to install and monitor more than four sites simultaneously.

Table 5-1: The design of experiments completed through the failure statistics and parameter understanding (legend in Nomenclature)

Unit Name	Switch Design	Rail Inclination	Line Speed	Track Quality	Traffic Type	Annual Tonnage	
SC1	D	Vertical	V1	Good	Mixed	T1	Phase 1
SC2	D	Vertical	V2	Poor	Mixed	T3	
SC3	D	Vertical	V3	Satisfactory	Mixed	T1	
SC4	D	Inclined	V3	Good	Mixed	T2	
SC5	C	Vertical	V2	Satisfactory	Freight	T3	Phase 2
SC6	C	Inclined	V1	Poor	Freight	T2	
SC7	C	Inclined	V2	Satisfactory	Mixed	T2	
SC8	G+	Vertical	V3	Good	Passenger	T1	

Recently, through the INNOTRACK [7] project, instrumentation measurements have been carried out within S&C on the Swedish and German infrastructures. The measurements focused on switches and crossings that have different geometry to the common UK design of S&C and did not monitor the change of strain over time.

Table 5-1 outlines the DOE structure for the experimentation. A DOE procedure was set up in line with the results gained from the failures statistics [8] showing that the D length switch (13m switch rail length, 370m turnout radius [9]) has high industrial relevance with high delay and failure costs.

SC1 has been classified as the reference site, has been instrumented since installation, and has additional gauges as shown in Table 5-2. The focus in this section of the research is on the first phase of the instrumentation and experiment, the D switches, which are mid-speed, mid-population and high relevance for the future of the infrastructure owner and operator. The second phase (SC5 – 8) is focused on mid speed and high speed switches to understand the variance on the length of switch and additional dynamic responses.

5.2.1 Block design

A block design was set up to allow for multiple parameters to be compared over the duration of the project. The following sections explain the parameters, the various scalable levels, and the effect levels of the parameters were expected to have on the results from the various instrumentation sites [8].

5.2.1.1 National level

Traffic type; In this investigation, the focus is on the mixed traffic, however, there is a variety of the percentage of passenger and freight traffic that are currently going over the sites. The difference in the deterioration of the material due to varied loading has been studied in other investigations [2, 10]. Heavier axle loads have a larger wear and plastic deformation characteristic than lighter vehicles with equal total tonnage. This means that the heavier axle loads are more likely to pass the yield level of the material than the lighter axle loads, due to the vertical loading and creepage within the contact patch.

5.2.1.2 Local level

Train tonnage; Annual tonnages are dependent on the local areas capacity, through the number of lines and flexibility. The capacity is dependent on the number of trains that travel through the S&C unit and the speed that they traverse. In the experimental design, the highest annual tonnage includes mainly passenger trains.

Line speed; Many research papers have shown that line speed has a large effect on the material degradation process [3, 10]. The speed of the vehicle increases the dynamic force that is being generated as the vehicle passes over the S&C unit by generating higher rotational velocities and higher magnitude vertical loads at the crossing.

Track quality; Track Quality changes over the life of the infrastructure, and is very difficult to maintain at a steady level. The track quality is monitored through the use of track recording units. The track quality is variable with the ground materials and the sites have been set up at various locations over the country to understand the influence of ground conditions to the degradation of the track quality.

Inclination; Inclination changes the contact between the wheel and the rail due to the variation in the shortest distance between the profiled wheel and the rail. Inclination is either at 1:20, or vertical. The inclination will remain constant throughout the life of the infrastructure as the rail is held in position through the sleepers and / or baseplates.

5.2.1.3 Switch and crossing level

Switch design; The switch designs are dependent on the allowable space and the line speed of the infrastructure. The higher the allowable speed of the local area, the switch radius is longer to allow for the better curving dynamics of the vehicles. The S&C is to accommodate any moving traffic to increase the capacity of the line. Tighter radius curves on the slower routes increase the lateral vehicle dynamics as the vehicle passes through the diverging route.

5.3 INSTRUMENTATION

Strain gauges (measure change in strain), geophones (measure velocity) and accelerometers (measure accelerations) are used to understand the change in S&C material response to loading over time. The instrumentation used for the field experimentation are commonly used throughout the rail and other industries, such as oil, civil engineering and aeronautical. These instruments can be left on the infrastructure for continuous outputs due to their small size and small cost (£15 / gauge, plus installation). Table 5-2 shows a comparison between the instrumentation quantity on the reference site, SC1, and our non-references sites, SC2-8.

In Phase One, the sites have different sampling rates to make the data collection and data storage efficient, with the reference site, SC1, running at 3000 samples/second and the non-reference sites, SC2 – 4, running at 1000 samples/second. The purpose of choosing a high sampling rate was to include some of the high frequencies described in Figure 5-3. The high sampling rate will allow for the lower frequencies (0-100Hz) to be collected and will give the information needed to study the excitations within the medium (100-500Hz) to high frequency ranges (>500Hz).

The geophones and accelerometers are used on the reference site (SC1) to give a comparison with the velocity collected from the geophone and the derived velocities from the accelerometer. The instrumentations are in different locations through the S&C unit to give an understanding of the vertical displacements of the units, but means that the instrumentation is not directly comparable.

Table 5-2: Number of instrumentation at the various sites in the initial phase of the instrumentation investigation

Instrumentation	Quantity	Frequency	Reason for instrumentation
Strain Gauges	12 off on Non-reference sites 26 off on Reference (22 bi-directional, 4 uni-directional)	1000 samples/s at non-reference 3000 samples/s at reference, 0 - 1500Hz	Strain through material under loading. 1500Hz sampling rate includes some of the high frequency content (>500Hz) including the vehicle vibration in the wheel / rail contact. From analysis of the outputted data, it has been found that frequencies above 100Hz do not show significant occurrences.
Geophones	2 off on non-reference 5 off on reference site	0 – 300Hz	Velocity of connecting assets, such as bearers, and ground conditions. The natural frequency of the geophones was lowered to 1Hz, through using a low power electrical circuit to dampen the system [11]
Accelerometers	0 off on non - reference 5 off on reference	0 - 100Hz	Vertical acceleration of the instrumented unit
Thermocouples	2 off on all sites	--	Temperature sensors are necessary to compensate the strain values against the expansion of the gauge and rail. The two sensors are within the switch, which has some heating capability, and at the crossing, which is not affected by the heating element.

5.3.1 Strain Gauges

Strains, change in material length in comparison with original length, can be used to understand the material reaction to the loading. Strain gauges are used to collect the change in length at the neutral axis through the switch and the change of length at the foot of the crossing. At the neutral axis location, the strains due to bending are zero. Figure 5-1 shows the layout of the gauges and the variation of the transverse and the axial gauge direction as on the switch. Once a load is applied to the location of the gauge, a change of voltage is

recorded across the strain gauge due to the change in size and shape of the gauge. The voltage can be transformed back into micro strain (με) and stored.

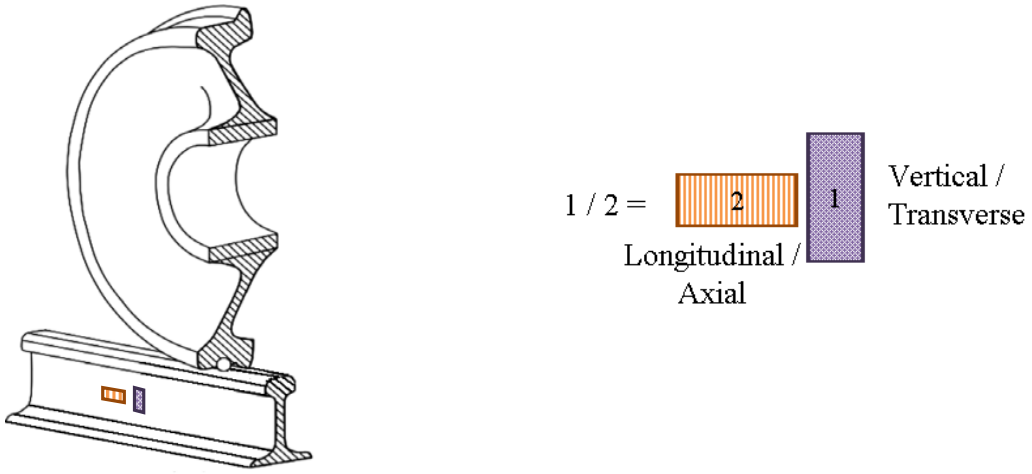

(a) (b)

Figure 5-1: The layout of strain gauges at (a) the neutral axis and (b)the names of the directions of the gauges, image from [12]

The process of transformation from gauge output, of millivolts, to strain is shown in Chapter 6. The gauges are axial and transverse to measure the vertical and longitudinal axial material response to loading. The position of the strain gauge on the neutral axis was to collect the shear strain from the loading of the rail. Within the research, the focus on the shear strain as it reflects any change in the contact loading and the response of the rail to the loading. The bending strain is zero at the neutral axis, this means that the outputs for the strain gauge at this location will only output the shear loading components. Therefore the neutral axis was instrumented with strain gauges to align with the peak of shear strain to give the closest alignment to the loading, i.e. with zero bending strain contribution.

5.3.2 Geophones

Geophones are instruments used to measure velocity of the structure. The velocity can be used to derive displacement of the structure. Geophones are an instrument that can measure velocity of an oscillating object through a linear transducer system [13]. A schematic of a typical geophone is shown in Figure 5-2

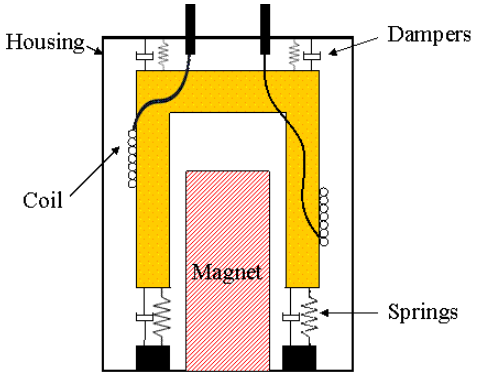

Figure 5-2: Geophone schematic

The geophone contains a magnetic mass, and an electric coil that generates a voltage with movement. A frequency response of the geophone is classified as a simple harmonic oscillator, giving a level of sensitivity to each geophone depending on the magnetic mass and forced damping. Typically, geophones have a natural frequency of around 10Hz. This frequency can be lowered through electrical damping using an equation of motion and reducing the ratio between the spring-damper system and the mass. Corner frequencies, or natural frequencies, below 1Hz are impractical due to the design of the instrument and the accuracy of the output being compromised.

5.3.3 Accelerometers

Accelerations within the rail system can decrease the stiffness of the asset through compaction and displacement of under sleeper ballast, or increase stiffness through contamination of ballast through debris of rubbing surfaces. Assets, such as POE that are attached to the switch rails and located on the adjoining sleeper, are susceptible to damage from these accelerations due to the high frequency content vibrating components beyond their limit. Accelerometers measure the rate of change of velocity, or vibration of a structure. The output of the instrument is proportional to the amplitude of the vibration [14]. The purpose for the accelerometers is to give on site validation for the vertical deflection. Additionally, the accelerometers are set up to be tri-axial, which allows for data to be recorded for the rotation and deflections in all directions. This gives additional information regarding the loading type that is causing changes in strain.

5.3.4 Simple processing overview of outputted data

The analogue output from the instruments must be converted to digital data for signal removal. All instruments on site are constantly generating data. To ensure that we collect all the necessary frequencies from instrumentation, the system frequencies must be known.

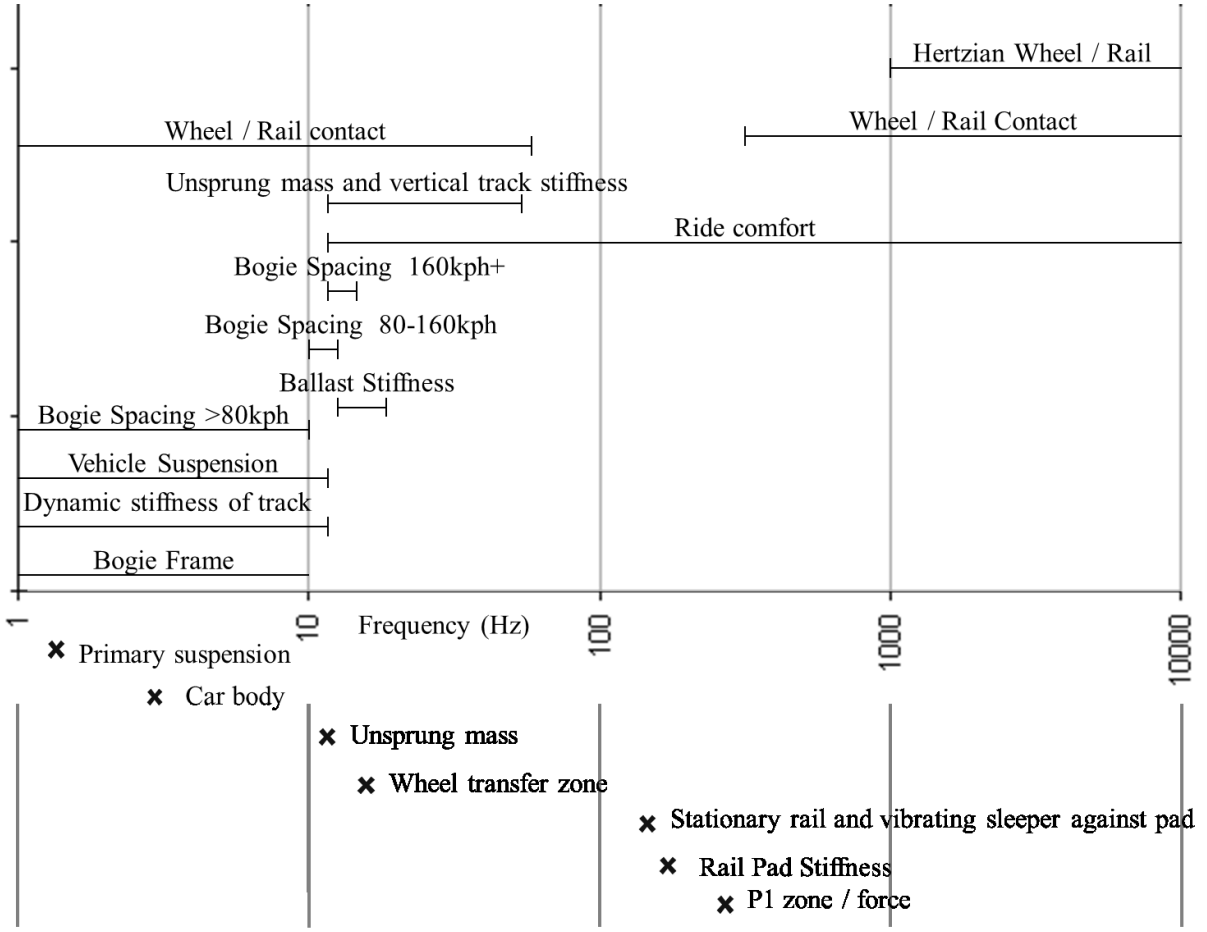

Figure 5-3: Frequencies that have been found within the railway system [1, 3, 4, 15-20]

Figure 5-3 shows the frequencies present in the S&C and general railway system, through previous modelling and instrumentation studies [1, 3, 4, 15-20]. For the instrumentation, the major contributions will be the lower frequencies (<100Hz), which have higher amplitudes than the medium and high frequencies. The lower frequencies show higher amplitude as they are the components of loading that will contribute more times to the strain values at the gauge. The medium and high frequencies are included within the figure to show the frequency content of loading that occurs within the wheel / rail interface and can affect the type of damage that occurs to the head of the rail.

With the non-reference sites sampling rate of 1000 samples/second, it is possible to include the dynamic effects of the vehicles and the response of the material. The Nyquist theory states that the sampling rate should be more than twice that of the frequency that is being monitored [21]. The Nyquist theory allows for the peaks and troughs to be collected due to the variance in the signal and data collection frequencies. With the frequencies going up to c. 500Hz, a sampling rate of 1000 samples/second is acceptable [22]. More information on the data processing can be found in Chapter 6. The process of collecting and analysing the data follows the flow chart process in Figure 5-4. The instrumentation is constantly generating a current that is passed back to the DAQ (Data Acquisition), but only stored when the trigger is activated.

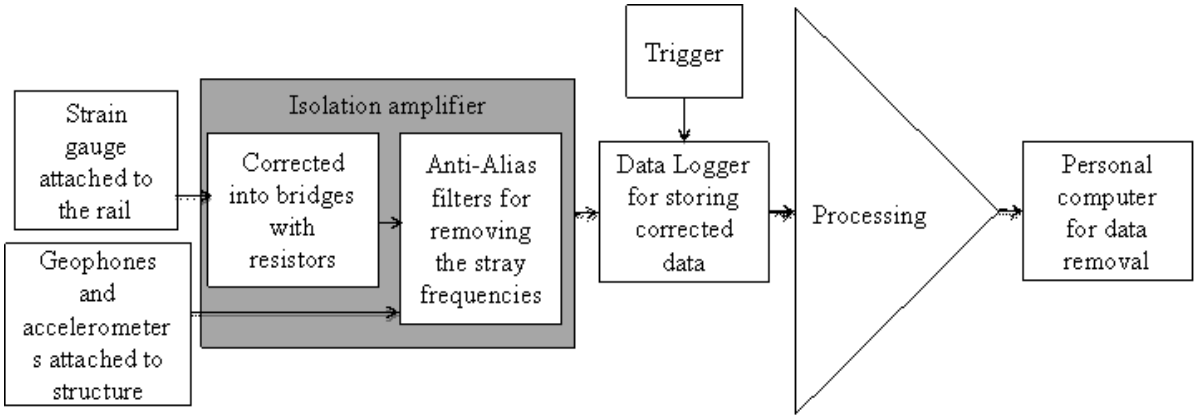

Figure 5-4: Process of data collection and storage within the DAQ

5.4 INSTRUMENTATION OUTPUTS AND CORRECTION FACTORS

The instrumentation outputs are a result of the change in voltage across the small area of the instrument, which are induced by the desired parameter. These outputs need to be converted into unit that represent the instrument purpose. The strain gauges, geophones and accelerometers (found on the fully instrumented sites) all output volts (mV) from instruments. The data output is converted into the units through specific sensitivities within the DAQ.

Strain gauges; Strain = $\frac{\text{Gauge output (mV)}}{\text{Maximum strain of gauge}}$

Geophone; Velocity = $\frac{\text{Geophone output (mV)}}{\text{Constant sensitivity response (V/ms}^{-1})}$

Accelerometer; Acceleration = $\frac{\text{Accelerometer output (mV)}}{\text{Constant sensitivity response (mV/g)}}$

The maximum strain of the gauges is 2000με, so the correction factor for the gauge is 0.005.

The constant sensitivity response of the geophone is 15V/ms^{-1}. This was chosen due to the low natural frequency (of 1Hz), which can record the low frequency measurements through the system.

The constant sensitivity response of the accelerometer is 10mV/g, which was chosen due to their ability to monitor small accelerations of the assets.

5.4.1 Thermal and environmental corrections

The outputs from the strain gauges help to understand the trends in the materials response to loading over the research. Along with the sensitivity corrections, strain gauge output needs to account for thermal influences, as the metal wire of the gauge can be affected by temperature.

Thermocouples have been added to two areas of the instrumentation region, at the switch and at the crossing to monitor the change in temperature and apply corrections to the gauge output. At the switch due to the effect of the copper heating strips are present that are activated in cold weather to allow the operation of the switch to continue. These heating strips have a thermal effect on the rail material which can cause a change in the response at the gauge. Temperature has the condition of being an annual parameter, to calculate the differences in the strain due to thermal variation; equation (5-1) can be used;

$$\in'_{T/O} = \in_{T/O} \frac{2.0}{F_I} \qquad (5\text{-}1)$$

Where $\in'_{T/O}$ = Thermal output adjusted for instrument gauge factor setting

$\in_{T/O}$ = Thermal output correction, found on data sheet TN-504-1 [23].

F_I = Instrument gauge factor during strain measurement [23]

Equation (5-1) gives a gauge factor of 2.115 at 24^{o}C (with the gauge factor given as it was calibrated at room temperature) for the strain gauge used, as shown in Figure 5-5.

The train traverses the S&C unit in typically less than 60s. Within this short time of the train passage, there is no thermal variation on the strains, and therefore equation (5-1) can be reduced by removing the thermal affects, to;

$$\varepsilon_{actual} = \varepsilon_{raw} \cdot \frac{2}{F_I} \qquad (5\text{-}2)$$

Where ε_{actual} = Comparable strain including the temperature compensation

ε_{raw} = Converted strain from the gauge.

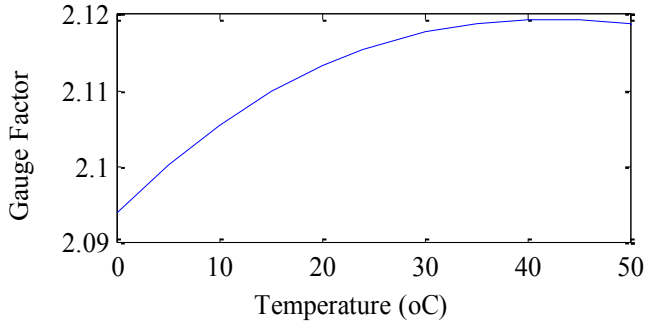

Figure 5-5: Gauge factor and its change depending on temperature

The strain data has been corrected using equations (5-2) at 24°C and using equation (5-1) at other temperatures. Removing the temperature from equation (5-1) reduces the processing time as the calculations uses less variables, which hastens the computational time.

5.5 HAND CALCULATIONS FOR STRAIN

Hand calculations can help design the location of the strain gauge on the rail, and validate further calculations. Bending moments were calculated on the cross-section, and shear stress and bending moments were calculated longitudinally. The outputs allow an understanding of the internal pressures from a point loading at the surface. Using the neutral axis, the second moment of area can be calculated. This is needed to understand the bending and shear stress generated though a cross-section rail profile.

5.5.1 Assumptions for hand calculations

For hand calculations to have a simplified method, a few assumptions have had to be made;

- The sleepers are 'point' boundary conditions as the location of connector between the sleeper and the rail is a clip. Longitudinally, the boundary conditions are positioned at the sleeper centres.
- The bottoms of the sleepers are considered rigid. In cross-section calculations, the bottom of the rail is rigid, to give a fixed point as to not include dynamic elements to the calculations.
- The sleeper spacing is the distance between the sleeper centres, 710mm; standard through the crossing at SC1.
- The wheel / rail contact is a small area, of c.100mm^2. As the size of this is small in comparison to the longitudinal length of the rail, it is considered a point loading.
- Rail profiles are simplified in the cross-section for quick calculation, with additional validation to ensure that the cross section is still relevant to the rail profile.
- Rail is assumed to be a beam for the longitudinal calculations.

5.5.2 Cross section calculation

The calculation of the cross section and the neutral axis is an essential part of the understanding of the location for the strain gauge. To begin the hand calculations, a simplified cross-section profile was generated, as shown in Figure 5-6 (a) against the real rail profile in (b). The neutral axis is used within the second moment of area calculations, and the strain and bending moment calculations. Equation (5-3) is used to calculate the neutral axis distance from the head of the rail.

$$\bar{y} = \frac{\sum y\, Ay}{A} \qquad (5\text{-}3)$$

Where $\bar{y}$ is the distance from the top to the neutral axis, y is the distance in mm from the neutral axis to the centre of the area of calculation, and A is the area of the shape.

From calculating the area of each of the sections seen in Figure 5-6 (a) a second moment of area was calculated to be 82.29mm from the crown of the rail. From using the computer

package Solidedge, the neutral axis was calculated at 82.17mm from the crown of the profile, which means that the simplified profile is within 1% of the modelled version. From the official NR drawing [24] for the 113a rail (56kg/m) drawing, the y value is 82.35mm from the top, so the simplified rail is within 1% of the standard rail profile. This gives confidence in the simplification will give errors within ±1% of the expected values from the official drawing.

There is a difference between the drawing in Solidedge and the Network Rail standard drawing of 0.2mm. This was due to the small errors in the generation of the part in Solidedge, but as the error is small, 0.3%, it is not considered to be a significant percentage against the full scale of the hand calculations.

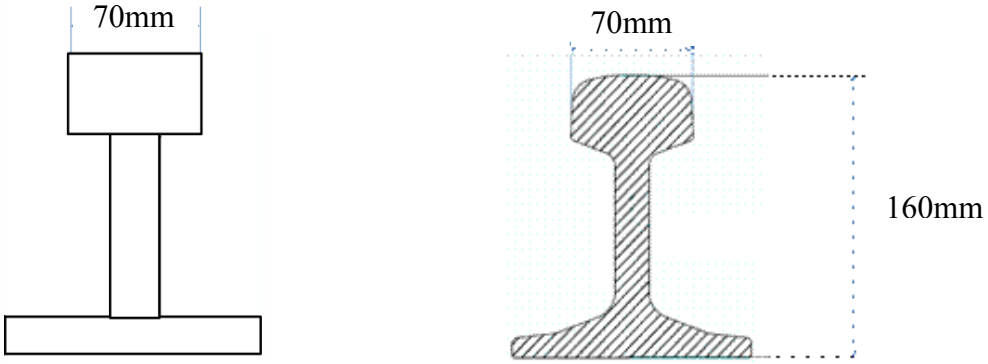

Figure 5-6: (a) Simplified rail used in the simplified calculations against (b) the profiles from Solidedge computation model

$$I = \frac{bd^3}{12} + Ah^2 \qquad (5\text{-}4)$$

Using the same simplified profile to calculate the second moment of area, using equation (5-4), it was calculated that the second moment of area of the beam is; $I_{RAIL} = 25.8 \times 10^{-6} m^4$.

$$\sigma = \frac{My}{I_{RAIL}} \qquad (5\text{-}5)$$

The second moment that has been used in in the drawing for rail [24, 25] shows that the value of the cross section of the usual profile is $23.49 \times 10^{-6} m^4$, so the assumptions are 10% to the fully designed profiled rail and deemed useable for hand calculations.

From the assumption that the maximum load is being used, the load applied to the head of the rail is;

- 25 tonnes / axle equate 12500 kilograms and 122625N per wheel. With a contact patch assumed to be 100mm^2, the pressure is applied to the head of the rail is 1226.25MN/m^2 (or MPa).

The values of bending strain that have been calculated are shown graphically in Figure 5-7. Table 5-3 shows the material properties for the Pearlitic material used on the railway application from Network Rail standard RT/CE/S/061 [25].

Table 5-3: The material properties for the standard Pearlitic rail used on the infrastructure [30]

Material	0.2% Proof Strength (MN/m2)	Ultimate Tensile Strength (MN/m2)	Tensile Ductility, %
260 grade carbon steel	470 - 620	979 - 998	10-12

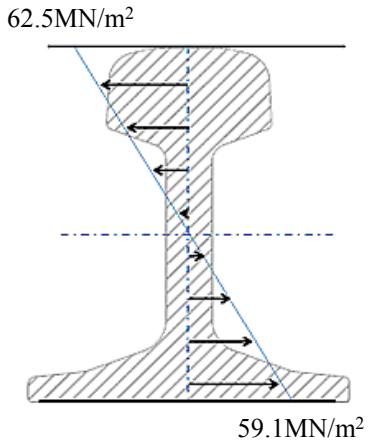

Figure 5-7: Stress distribution on the cross-section of the rail profile and load directly at the head

The stress distribution and cross section analysis shows that the location of strain gauge should be at the neutral axis to reduce the residual strain on the output and give the purest shear results, which excludes the bending on the cross section as the neutral axis is neither in compression or tension.

5.5.3 Longitudinal Calculations

The longitudinal calculations are used for location of the gauge along the track. It has been determined that there will be two gauges per location to get the vertical effect of the loading and longitudinal change in length due to the elongation of the material. For the longitudinal calculations, it is assumed that there is a single beam with supports at either end, acting as sleepers, labelled *A* and *B*. Assuming the wheel load at the centre, the point load, P, is constant in magnitude along the whole span with the location equal to the F/2. A free-body diagram, the shear stress and bending moments are shown in Figure 5-8 to understand the beam reaction to the point loading at the centre of the beam.

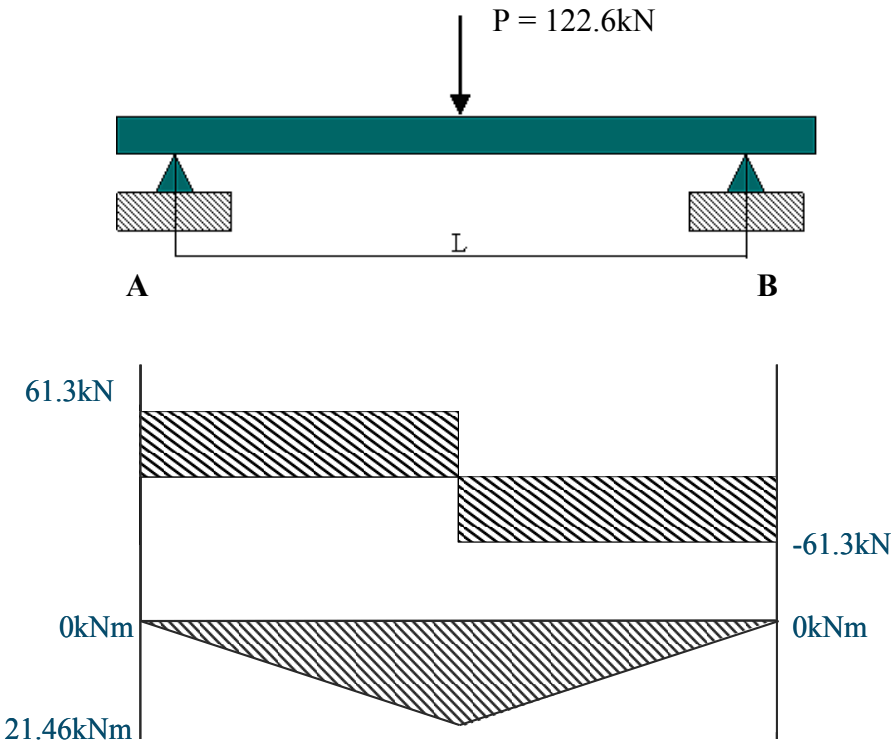

Figure 5-8: Shear stress (top) and bending moment (bottom) diagram for loading in the centre of the beam

The bending moment is maximum at the centre of the model as the reactionary forces at either end of the beam supports the structure. This relates to the location of the strain gauges as the maximum bending strain of the beam can be cancelled by placing the strain gauge on the neutral axis. This therefore removes the bending strain from the outputs and allow for the shear strain to be monitored easier and clearer.

5.5.4 Maximum shear strain and principal stresses

Mohr's circle is a graphic tool that enables stresses in the cross section of a body to be determined and visualised. It is used to determine the principal stresses and the shear stress at the strain gauge location. It calculated the minimum and maximum shear forces and bending at various points of the longitudinal beam.

From Figure 5-8, and assuming that the loading is on the mid-point of the beam, using the stress calculation, and $y_a = 0$, the bending moment at that location is $0N/m^2$. The shear strain and principal strains are calculated for the location of the gauge; centre of the sleeper spacing on the neutral axis.

Dissecting the beam at the mid-point and taking moments of shear about the midpoint gives;

$$\tau_{xy} = \frac{VQ}{bI} \qquad (5\text{-}6)$$

Where b = thickness of the section; in this situation this is the width of the web

V = vertical shear load

$Q = \Sigma A\bar{y}$

I = moment of inertia

Table 5-4: The shear stress calculation and associated values

V	Q	b	I	**Total** τ_{xy}^{A}
61.3kN	$1.9\text{x}10^{-4}m^3$	0.02m	$25.8\text{x}10^{-6}m^4$	**22.6MN/m**

To give the data points for the Mohr circle, principal stresses and maximum shear stress need to be calculated using equations (5-7) and (5-8).

$$\sigma_1 = \frac{\sigma_x + \sigma_y}{2} + \frac{1}{2}\sqrt{\left[\left(\sigma_x - \sigma_y\right)^2 + 4\tau_{xy}^2\right]} \qquad (5\text{-}7)$$

$$\sigma_2 = \frac{\sigma_x + \sigma_y}{2} - \frac{1}{2}\sqrt{\left[\left(\sigma_x - \sigma_y\right)^2 + 4\tau_{xy}^2\right]} \qquad (5\text{-}8)$$

At mid-point of the rail and mid-point of the beam the σ_x and σ_y are equal to zero, therefore

$\sigma_1 = +^{\tau_{xy}} = 22.6MN/m$ $\sigma_2 = -^{\tau_{xy}} = -22.6MN/m$

The maximum shear stress is shown in Figure 5-9.

$$\tau_{max} = \frac{1}{2}(\sigma_1 - \sigma_2) \quad (5\text{-}9)$$

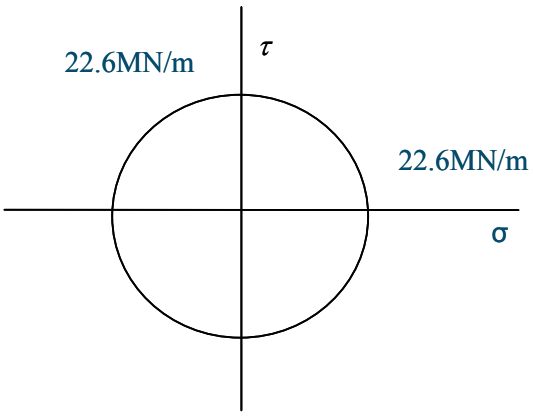

Figure 5-9: Mohr circle of the outputs from the calculations shown from eqn. (5-5) and (5-9)

The Mohr's circle represents all possible states of normal and shear stress on any axis. The diagram in Figure 5-9 shows that at the midpoint of the beam and the location of zero loading. This coincides with the location that the shear stress is at its maximum and from the Mohr circle is classed as pure shear. The ideal location for the strain gauge is at the centre to minimise the bending strain that would be applied to the gauge under loading directly over the gauge.

From the hand calculations, it has been found that the best position for the strain gauge is on the neutral axis of the cross-section and mid-point of the longitudinal sleeper spacing. The neutral axis would experience no bending strain on the cross section, but would allow for a shear strain to be encountered. The longitudinal loading shows maximum shear strain and maximum bending strains at the centre point of sleepers, but the bending strain can be counteracted by using the neutral axis.

These loading cases mean that with a gauge in the desired location, it would be possible to understand the outputs from the shear strain loading only as the bending would be minimum due to support conditions.

5.6 DISTRIBUTION OF INSTRUMENTATION OUTPUT DATASETS AND SAMPLING METHODOLOGY

The collection and analysis of field instrumentation data is key to the understanding of the changes in material response under loading over time. Due to the setup of the instrumentation and data logging, up to 100 trains/day worth of data is being collected and stored at each site, which exceeds the information than can be analysed. To reduce the number of datasets, a sampling method is completed. The method aligns the sampling method to the parameters that were outlined in Table 5-1. In this section, the probability of vehicle types at one site is shown and a demonstration of sample section that are used for analysis. A data selection process uses probability to ensure the selected datasets are representative of the total population. Analysis of the samples selected using Latin Hypercube (LHC or Latin Hypercube sampling, LHS) and Monte Carlo techniques are completed to show comparison between two sampling techniques. LHS was chosen due to the more systematic approach used during the selection process, which ensures that all the samples are considered within the selection, rather than selecting from the higher population section, which was the case for Monte Carlo.
For a thirty second trace and a sampling rate of the reference site being 1500 samples/second, the number of data points is roughly 45,000 per train.

5.6.1 Collection and sampling techniques

As each vehicle passes over the instrumentation site, the trigger records all instrumentation outputs and stores them as a database for analysis. The vehicles are identified through an initial visual monitoring to observe the configuration of the trains passing over the units. This is then used to compare number the peaks within the traces when not present.

Figure 5-10 shows all the data sets that have been collected at SC3. This shows a large break in the data between October 2011 and May 2012, and June 2012 and October 2012. The system was not active in these breaks due to hardware issues within the DAQ, and the data was not recorded.

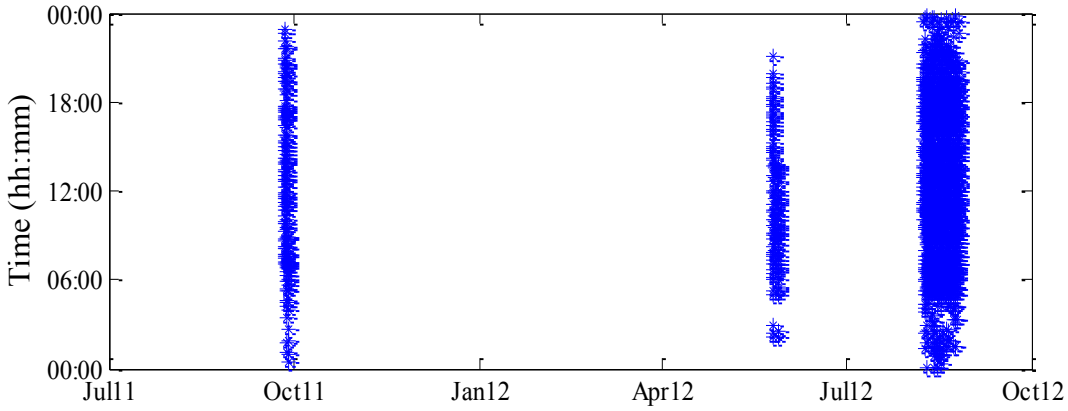

Figure 5-10: SC3 [4] data sets, each '' is a vehicle passing over the unit*

1355 samples have been collected for SC3 between September 2011 and October 2012. To reduce computational power and time, 100 samples are used for the analysis. Before the trigger limits were enabled, the datasets collected 10 minutes (600s) worth of data, which in some instances contained more than one vehicle. Additional vehicles have been taken into consideration for the prior probability, shown in Table 5-5, but not for the distribution. This is due to the sampling process using the time and date stamps of the samples as the primary parameter for the selection.

From the train sample data, a probability distribution can monitor the distribution of the vehicles through the day. The beta distribution had the best fit to the data compared with out distributions. The beta distribution is a process in the Bayesian analysis, where the variables calculated (called the observed distribution) can be used to calculate the unit probability [26].

Bayesian analysis is a statistical procedure which uses observed distribution to estimate parameters which can then project forwards [26]. The distribution combines the likelihood of the event occurring with the probability function. The Beta distribution function is used due to its compatibility LHS sampling techniques and it gives the best fit to the datasets. For the distribution function to be generated for the sites, variables α and β must be calculated, allowing for the variance and means to be used.

The probability density function of the beta distribution, with parameters $\alpha > 0$ and $\beta > 0$, is described as:

$$y(x) = \frac{(1-x)^{\beta-1}.x^{\alpha-1}}{B(\alpha,\beta)} \qquad (5\text{-}10)$$

$$y(x) = \frac{1}{B(\alpha,\beta)} x^{\alpha-1}(1-x)^{\beta-1} I_{(0,1)}(x) \qquad (5\text{-}11)$$

Where y(x) is the probability density function, $B(\alpha,\beta)$ is the beta distribution, and $I_{(0,1)}(x)$ is a parameter used to make sure that $0 < x < 1$ [26]. The beta distribution gives the curve shown in red in Figure 5-11 against the histogram of the train time distribution.

From the data sets that we have collected and the distribution that has been generated through Beta analysis, there is a 2.9% skew in the datasets towards the afternoon. This is due to the larger number of samples running over the site after 18:00 (19.7% of datasets), compared with before 06:00, where there are (10.3% of datasets) at SC3.

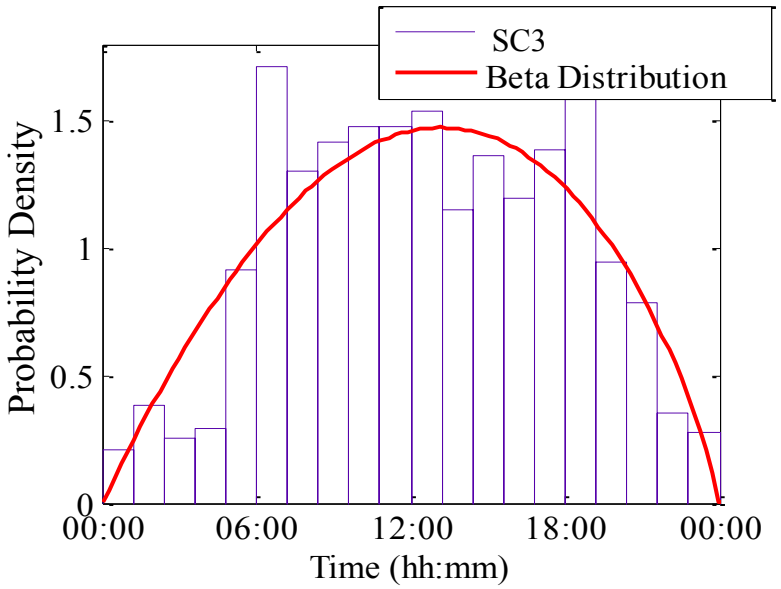

Figure 5-11: Histogram of the datasets and the Beta probability distribution for the vehicles over the instrumentation site SC3

Using the Matlab programme, the mean of the distribution was calculated to be at 0.524 and variance of 0.052, where $0 < x < 1$.

The variance shows that there is a very small spread of the datasets and distribution, and is repeatable data. Figure 5-12 shows the cumulative probability of datasets against the beta distribution applied to show the close fit of the two datasets. For the cumulative distribution, the data fit is 95%. The region before 06:00 and the Bayesian data does not fit to the data due to the steep increase in datasets and the distribution curve not following the trend.

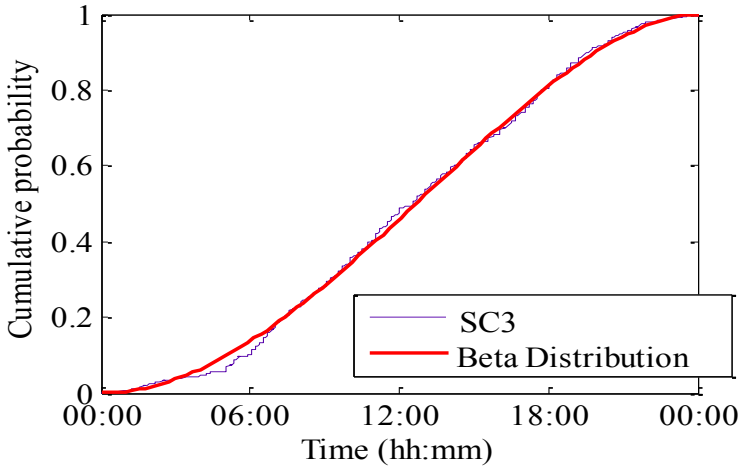

Figure 5-12: Cumulative probability of the beta distribution showing a 95% fit against the datasets

5.6.2 Train type analysis for data mining techniques

To focus the sampling, the trains were put into time 'bins'. This allowed the passenger and freight distributions to be analysed. Firstly, time classifications are generated. The Naive Bayes method combines the prior and conditional probabilities, and allows for a probability for each bin to be generated [27].

The datasets that were used for probability generation were from a single day at SC3 [28], on the 10th September 2012. The day was chosen due to it being a typical day on the network in terms of trains and their running times. The information consisted of 82 vehicles. An example of prior probability is;

P(Passenger = all day) = 58/82 = 0.707

P(Freight = all day) = 24/82 = 0.293

This means that the data that was seen over this site on this day was 71% passenger traffic. This understanding is important as Kassa et al [3] has previously shown that heavier axle loads, such as laden freight, cause higher wear rates than lighter vehicles. Table 5-5 is populated with conditional probabilities based on the time bins defined below. The time bins were set at four-hour intervals to compare some typical times for certain vehicles. E.g. *P*(Vehicle = Passenger | time = 12.00-15.59) is 0.9.

Table 5-5: The classification of the parameters set out and their associated probabilities

	00.00 – 03.59	04.00 – 07.59	08.00 – 11.59	12.00 – 15.59	16.00 – 19.59	20.00 – 23.59
Passenger	1/5 = 0.2	11/13 = 0.85	17/21 = 0.81	9/10 = 0.9	19/23 = 0.83	1/6 = 0.17
Freight	4/5 = 0.8	2/13 = 0.15	4/21 = 0.19	1/10 = 0.1	4/23 = 0.17	5/6 = 0.83
Prior Probability	**5/78 = 0.06**	**13/82 = 0.17**	**21/82 = 0.27**	**10/82 = 0.13**	**23/82 = 0.29**	**6/82 = 0.08**

The prior probability that has been populated at the bottom of the table is calculated to understand the influence of time on the train types traversing the points. This shows that the majority of vehicles travel between 16:00 and 19:59 per day, which would be due to commuter traffic. The value for the prior probability gives weighting to the trains over a full day rather than within a specific time sector.

$$P(x_i) = \prod^{n} P(vehicle = v_j \mid time = t_i) \qquad (5\text{-}12)$$

Where Π indicates the product of the multiplication of the *n* values for the variations in;

v_j = the classification of vehicle, either passenger of freight

t_i = the time of day, split into six bins, as shown in Table 5-5.

An example of the probability of a certain vehicle would be;

P(vehicle = passenger | time = 12.00-15.59) = 0.9*0.12 = 0.108

This shows that, at SC3, the probability of a selection of a passenger vehicle between 12:00 and 15:59 is 10.8%. These probabilities are used in the LHS technique to ensure the representative high probabilities get more samples selected.

5.6.3 Sampling technique analysis

The distribution of selected datasets should ensure the beta probability trains are covered. Sampling processes are used to ensure that a selection of the datasets are analysed, whilst covering a wide range of train types and date scale. A small description of Monte Carlo and LHS processes is below. Only one of these data sampling techniques is used for the selection of the instrumentation outputs analysis.

5.6.3.1 Monte Carlo method and application

Monte Carlo method is a random sampling technique that allows data sets to be sampled quickly with no limitations on the selection [29]. The Monte Carlo method selects samples through random selection which are independent from other samples previously selected [5]. This method allows for complete randomisation of the sampling. The Monte Carlo sampling tends to take the data from the higher probability sections as the randomised selection tends to select within the higher probability. This means that it is highly likely to miss some of the lower probability data, which is covered through LHC sampling.

5.6.3.2 Latin hypercube method and application

Latin hypercube sampling is a method of collecting random selected samples within regularly spaced intervals [5]. LHS involves splitting the datasets into evenly distributed, non-overlapping regions (n_r), which have probabilities distributed with the region of $1/n_r$. A sample is selected from the each region through random permutation.

$$\xi_i = [\xi_{i1}, \xi_{i2}, ..., \xi_{ik}], i = 1,2,.....n_r \qquad (5\text{-}13)$$

Where n_r is the region within which the variable is selected at random and k is the number of variables and ξ_i is the stored matrix of samples. Values from this equation are used in equation (5-14). $\boldsymbol{P}$ is the permutation matrix which is defined by each of k columns. The value selected is a random permutation of (1, 2, ..., n_r). $\boldsymbol{U}$, which is the same size as $\boldsymbol{P}$, consist of independent random numbers from the uniform (mean = 0, variance = 1) distribution. $F_{\xi j}^{-1}$ is the inverse of the target cumulative distribution function for variable j.

$$\xi_{ij} = F_{\xi j}^{-1}\left(\frac{P_{ij} - U_{ij}}{n_r}\right) \qquad (5\text{-}14)$$

Where i =1, 2, ... n_r and j =1, 2.....k

For each column, the N values are randomly distributed with one from each interval (0,1/N), (1/N,2/N),....(1-1/N,1). Equation (5-14) shows the method of sampling selection of the datasets within the site. This method reduces the randomness of the dataset selection and aligns with the probability and distribution.

5.6.4 Outputs from sampling techniques / selected samples

In this investigation, 100 samples were chosen from the 1355 datasets to compare the sampling methods. 100 samples were chosen as it covers the necessary vehicle types and the data available, whilst not being too computationally expensive.

Figure 5-13 shows the data sets that have been selected using the Monte Carlo (green blocks) and LHS (red rings) methods against all the data sets (+). Plotting a histogram of the samples selected from the two methods, Figure 5-14, shows that there is a better representation using LHS compared Monte Carlo when compared with the original dataset distribution as it includes more of the datasets in the extremes of the day.

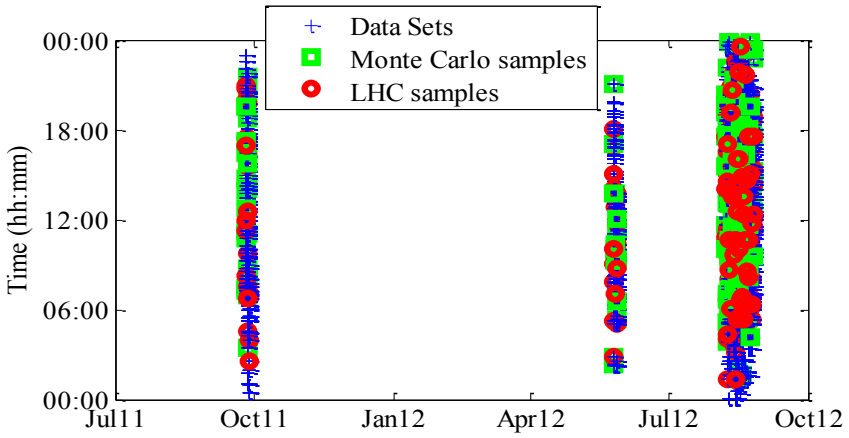

Figure 5-13: Data samples, in line with Figure 5-10, and the selection (red and green rings) of 50 datasets using the Latin Hypercube and Monte Carlo sampling methods

From the data, Monte Carlo data sampling technique did not randomly select any samples before 04:00 as the CPD in Figure 5-13 shows a low probability within that timeframe and Monte Carlo can miss the smaller probabilities due to the randomised nature. The lack of

samples in that time would not give a representation of freight, as it could miss out a fifth of the freight population (4 freight in 00:00-03:59 / 20 total freight). The LHS has included some samples from all time frames as it randomly selects data within smaller bins of samples. Therefore, LHS is used for data sampling throughout the investigation as it covers the full scope of the datasets available.

5.7 DESIGN OF EXPERIMENT DISCUSSION

Design of experiments (DOE) technique focuses the instrumentation into pertinent S&C units that the parameters and levels cover from the failure statistic outputs. Focus has been put onto the mid-speed switches due to the population and preferred design of the industry.

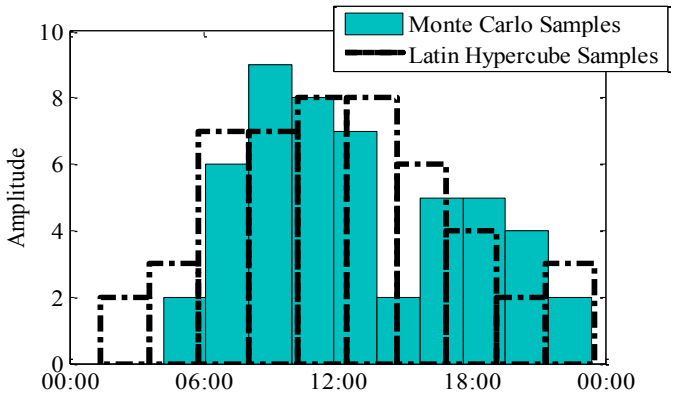

Figure 5-14: Histogram of 100 samples selected, (green block filled histogram) showing the Monte Carlo sample distribution over 24 hours against the (clear, dashed outlines) LHS samples

The DOE technique has used the analysis of failures statistics from Chapter 4, showing that the switch panel is highly relevant, along with annual tonnage and national location. The DOE procedure gave parameters and levels for eight sites, with three levels for six parameters covering the key assets within the huge variation that are available on the infrastructure network. The parameters are; switch length, inclination, tonnage, geometry, vehicle type and line speed.

Strain gauges, geophones and accelerometers have been designed on the S&C unit to monitor the transfer zones (and increased irregularities) of the switch panel and crossing nose. Strain gauges are used to measure the shear strain from loading at the neutral axis, geophones measure the vertical displacements of the sleepers and accelerometers measure the

acceleration of the connected assets in three axis. Data processing is a necessary phase of the analysis to ensure highly accurate results. These instruments are the most pertinent for the application of continuous system monitoring of in-service S&C due to their cost and availability.

The optimum location for a strain gauge would be at the neutral axis through the switch panel, and in the middle of the sleeper beds longitudinally. Hand calculations show the neutral axis has no bending stress and maximum shear strain longitudinally. Bending stress was found to be non-pertinent at switches due to the lack of cracking failures at the base of the switch units through bending strains from the failure statistics. Fracture was the highest failure costs at the crossing, therefore bending at the crossing is most pertinent and the strain gauges were placed at the foot of the crossing.

The triggered instrumentation datasets gets stored in the logger for manual removal and analysis. The corrected datasets have been collected and organised in time and date order. Sampling methods have to be used to reduce the total number of dataset to increase the time and computational levels available. Monte Carlo and Latin Hypercube sampling methods have been compared, with LHC found to cover the full probability of the vehicles at each site due to the semi-randomised nature of the technique.

REFERENCES

1. Bruni S, Anastasopoulos I, Alfi S, Van Leuven A & Gazetas G, Effects of train impacts on urban turnouts: Modelling and validation through measurements, *Journal of Sound and Vibration*, 2009; 324(3-5): 666-689.

2. Kassa E & Nielsen JCO, Dynamic train–turnout interaction in an extended frequency range using a detailed model of track dynamics, *Journal of Sound and Vibration*, 2009; 320(4-5): 893-914.

3. Kassa E & Nielsen JCO, Dynamic interaction between train and railway turnout: full-scale field test and validation of simulation models, *Vehicle System Dynamics - International Journal of Vehicle Mechanics and Mobility*, 2008; 46(1): 521-534.

4. Kassa E, Andersson C & Nielsen JCO, Simulation of dynamic interaction between train and railway turnout, *Vehicle System Dynamics - International Journal of Vehicle Mechanics and Mobility*, 2006; 44(3): 247-258.

5. Kassa E & Nielsen JCO, Stochastic analysis of dynamic interaction between train and railway turnout, *Vehicle System Dynamics - International Journal of Vehicle Mechanics and Mobility*, 2008; 46(5): 429-449.

6. Hanna TH, *Field instrumentation in geotechnical engineering*. 13th ed: Trans Tech Publications Ltd; 1985.

7. Innotrack - Innovative Track Systems, *D3.1.4 Summary of results from simulations and optimisation of switches*: UIC - International Union of Railways, 2009.

8. Cornish A, Kassa E & Smith RA. Investigation of failure statistics for switches and crossings in the UK. In: *Railway Engineering - 2011*, Forde M. C. (eds.), University of Westminster, 2011, 1-14

9. Network Rail. RE/PW/807, *Shallow depth switch machining details,* London. Network Rail, 40 Melton Street, London NW1 2EE; 2007.

10. Zwanenburg WJ. *Modelling Degradation Processes of Switches & Crossings for Maintenance & Renewal Planning on the Swiss Railway Network.* PhD Thesis: Delft University of Technology, École Polytechnique Federale De Lausanna; 2009.

11. ION Geophysical Corpotation. *LF-24 Low Frequency Geophone Sensor datasheet.* ION Geophysical Corpotation. 2010.

12. Zerbst U, Lunden R, Edel KO & Smith RA, Introduction to the damage tolerance behaviour of railway rails - a review, *Engineering Fracture Mechanics*, 2009; 76(17): 2563-2601.

13. Hons M. Accelerometer vs. Geophone Response: A Field Case History. In: *Back to Exploration - Joint Annual Conventions (Canadian Society of Petroleum Geologists, Canadian Society of Exploration Geophysicists and Canadian Well Logging Society)*, (eds.), Canada, 2008, 271 - 275

14. Dimension Engineering - Robotics Rc, Power electronics. *A beginner's guide to accelerometers*. 2012 Available from: http://www.dimensionengineering.com/accelerometers.html [Accessed: 17/01/2012].

15. Cheesewright PR, *Wheel/Rail Forces Measured at Crossings of Cast Manganese and Built-up Types*, British Railways Research and Development Division - Track Group, June, Report No: 263-191-24, British Rail. 1977.

16. Berggren E. G, Martin X.D. Li & Spannar Jan, A new approach to the analysis and presentation of vertical track geometry quality and rail roughness, *Wear - An international journal on the science and technology of friction, lubrication and wear*, 2008, 16th May; 265: 9.

17. Clarke R. A., *Measurement of wheel-rail contact forces at a selection of switches and crossings using the HSFV1 equipped with load measuring wheelsets*: British Rail Research (BRR), Report No: TM DA 39, 1981.

18. Bruni S & Braghin F, *Effect of Damage on Vehicle Dynamics*. In: Lewis R., Olofsson U., (eds.) *Wheel-Rail Interface Handbook*. Woodhead Publishing Limited; 2009.

19. Alfi S & Bruni S, Mathematical modelling of train–turnout interaction, *Vehicle System Dynamics: International Journal of Vehicle Mechanics and Mobility*, 2009; 47(5): 551-574.

20. Pålsson BA & Nielsen JCO, Wheel–rail interaction and damage in switches and crossings, *Vehicle System Dynamics - International Journal of Vehicle Mechanics and Mobility*, 2011; 50(1): pp.43-58.

21. Brandt A, *Noise and Vibration Analysis; Signal Analysis and Experimental Procedures*: John Wiley & Sons, Ltd; 2011.

22. Vishay Precision Group. TN-517, *Strain Gages and Instruments,* Micro-Measurements; 2010.

23. Vishay Precision Group. TN-504-1, *Strain Gage Thermal Output and Gage Factor Variation with Temperature,* Toronto. Micro-Measurements; 2010.

24. Ventry D, RE/PW/620, *BS113A Rail section and drilling details*, London. Network Rail, 40 Melton Street, London, NW1 2EE, 2005.

25. British Standard. EN 13674-1, *Railway Application - Track - Rail,* London. European Comittee for Standardization; 2003.

26. Weisstein EW. *Beta Distribution*. From *Mathworld* - A Wolfram Web resourse; Available from: http://mathworld.wolfram.com/BetaDistribution.html [Accessed: 23/08/2012].

27. Bramer M, *Principles of Data Mining*. Mackie Ian, editor. Portsmouth: Springer-Verlag London Limited; 2007.

28. Cornish A, Kassa E & Smith RA. Field Experimental Studies of Railway Switches and Crossings. In: *First International Conference on Railway Technology: Research,*

Development and Maintenance, Pombo J. (eds.), Civil-Comp Press, Stirlingshire, United Kingdom, 2012,

29. Weisstein EW. *Monte Carlo Method*. From MathWorld--A Wolfram Web Resource; Available from: http://mathworld.wolfram.com/MonteCarloMethod.html [Accessed: 18/01/2013].

30. Jay Jaiswal, *Material Properties - Property Comparisons,* Tata Steel, 2010.

6. FIELD EXPERIMENTAL OUTPUT

Data collection, conversion and filtering of the raw data collected from site is shown and analysed. Error levels are calculated and evaluated to understand the credibility level of the instrumentation data. The converted strain and geophone data is shown, focusing on the peak to peak values for the strain and vertical motion. The instrumentation data was stored on a data logger on site and manually downloaded, converted, filtered and then analysed in Matlab software. The purpose of this section is to show the converted results of the instrumentation. The correction factors and filters are described to demonstrate the processes and assumptions used to increase the accuracy of the outputted data.

6.1 FIELD EXPERIMENTATION INTRODUCTION

Field experimentation is vital in the understanding of the current assets and the reaction to in-service loading. The analysis is highly dependent on the quality of the data that has been collected. Correction factors are necessary to convert the data to useable units and increasing the quality of the data recorded, while understanding error levels allows for an increased credibility of the instrumentation outputs.

Figure 6-1: Site installation of field experimentation

Three types of instrument have been installed on four sites around the country in accordance with the design of experiments, to monitor the material response of S&C over time. Strain gauges, geophones and accelerometers output voltage, which is converted from analogue to digital signal, and then to units and amplified within a data acquisition system (DAQ). The

DAQ then stores the data on a hard-drive for data collection from site. The transfer of data would not be possible through a mobile data system as each file collected was c. 33Mb in size for the non-reference site. Other methods, such as a broadband system, were not considered due to the cost of putting in the cables necessary for the broadband system.

6.2 ERROR LEVELS

Error levels seen at the data logger are an accumulation of the small errors seen through the strain gauge and the cables. These errors include;

- An analogue strain gauge generates continuous analogue output with a tolerance resistance of 350Ω ± 0.4%: the resolution of the dataset (converted data) was determined by the DAQ with the use of amplifiers.
- Gauge factor - the sensitivity of the strain gauge, *k*, is the factor between the change in resistance and the strain outputted. For the batch of strain gauges used in the experimentation, the gauge factor is 2.12 ± 0.5% (or ± 0.01).
- Temperature tolerance to gauge factors - The maximum error is between 0 and 40 degrees centigrade is 1.5%. The change in gauge factor has been included in the calculation of strain. From the temperatures collected from the datasets, the temperature ranges from 10^{o}C to 40^{o}C, which has a change in gauge factor of 0.6%.
- Error within the installation location – The vertical location of the strain gauge is at 82.17mm from the bottom. Installation at this level of accuracy in the field is extremely complicated due to the profile of the rail. The gauges are attached to the rail (using a 0.13mm thick backing sheet) and vertical offset / misalignment includes bending strain within the output. It is assumed that the backing sheet does not affect the strain due to the relative thickness being insignificant.
- Fatigue of the strain gauge – Vishay Precision Group claim that the CEA gauges used have a life expectancy of $5x10^{6}$ loading cycles due to fatigue damage of the gauges and wiring. The field experimentation should not exceed the number of cycles needed to cause any change in the outputs [1] as the maximum number of axles on site would be 2000 / day, and would take almost 3000 days to exceed the gauge fade value.

Error levels contribute to a maximum uncertainty of the strain gauge output at ± 1.5%.

Geophones have additional correction complexities due to their design of a mass spring / damper electrical system. These complexities include;

- Electrical circuitry - for the geophones installed (ION LF-24) [2], a low power electrical circuit is used to allow for a reverse filter function to be applied. This lowers the natural frequency by damping the resonance of the system to allow for lower frequencies to be collected without additional post-processing and filtering. The electrical circuit will have an effect on the error levels by adding additional complexity to the system [2].

- Response - The response, sensitivity of the output, from the geophone is a variable output between 0 and 1.5Hz, and above 1.5Hz is constant at 15V/m/s, shown in Figure 6-2 (a). The variable sensitivity means that the output of the geophone at low frequencies needs to be scaled to give a linear sensitivity of 15V/m/s throughout the whole signal.

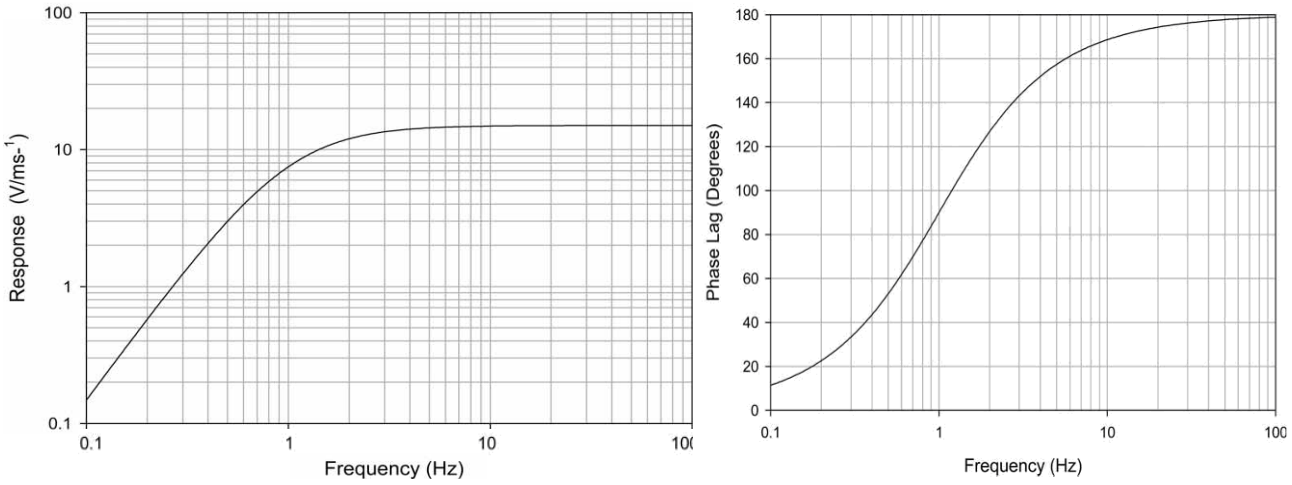

(a) (b)

Figure 6-2: The functions of geophones showing (a) typical sensitivity chart of geophones, with natural frequency of 1Hz using electrical damping and (b) the typical phase lag of the system [3, 4]

- Phase lag - Phase lag is due to the system of a geophone being a mass on a spring system and initial oscillations have lower accuracy as the mass counters the damping and stiffness. Figure 6-2 (b) shows the phase lag of the geophone and needs additional conversion of the data before the displacements are calculated.

The phase lag and the response functions have been obtained from the manufacturers

6.3 FILTER PROCESSING AND APPLICATION

The time domain is a non-linear process that constantly changes through the duration of the event. The outputs from the signals are in the time domain. The non-linear events are made up of multiple frequencies that can be studied through the linear domain by putting into frequencies 'bins'. FFT's (Fast Fourier Transforms) allow the time domain to be transferred into the frequency domain, and can highlight any dominant frequencies and irregularities in the data. To ensure that the data has limited uncertainty, a linear filter is applied to the data, i.e. above 50Hz, to remove the inaccuracies mentioned in *Error levels*. Non-linear filters, such as median filter, are commonly used to process images and can filter in the time domain. The median filter takes a group of data, ranks the data signal according to their value, then takes the extreme values and align those with the median. This reduces the impact of the impulse noise and spurious frequencies. The non-linear filters are more computationally and time consuming due to additional processing, and are not used in this thesis as the benefit compared with a linear filter would be negligible as the signal is 2 dimensional.

Filtering is a process of calculations that removes the 'undesirable' frequencies of a signal [5]. The ideal filter would have no removal of data within the required frequency levels, known as the 'cliff-edge' and shown in Figure 6-4. In reality, it is impossible to achieve the cliff edge with current techniques [6] as the roll off rate distorts the signal before the required cut off. There are four main types of filter shown in Figure 6-3;

- Low Pass filter; attenuates high frequency
- High Pass filter; attenuates low frequency
- Band Pass filter; attenuates component outside frequency band
- Band Stop filter; attenuates components inside frequency band

Throughout the processing of the data, the Butterworth filtering technique will be used to optimise the analysis by removing the unwanted frequencies (such as electrical noise). The Butterworth filter was originally designed in the 1930's and was applied to RC (resistor - capacitor) electrical circuits. A Butterworth filter manages to keep the data at maximum value before the cut off, and then applies a linear 'roll off' that continues towards zero at a rate determined through the order, with the first order having the lowest / shallowest rate. The reason for using the Butterworth over other is due to the filter *"not only completely rejecting the unwanted frequencies, but should also have uniform sensitivity for the wanted*

frequencies" [6]. Other filters, e.g. Chebyshev and Elliptic, tend to be distorted before or after the cliff edge, and so are not desired as they can give false values

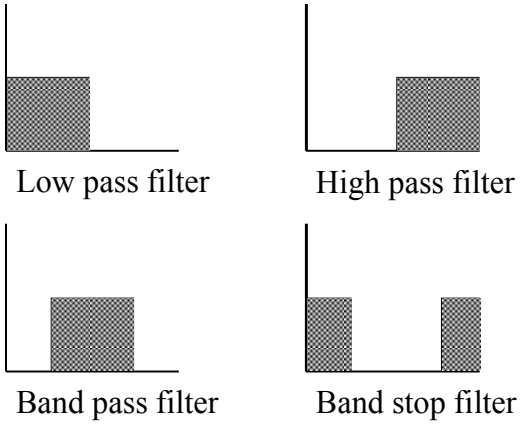

Figure 6-3: The outline of the idealised filter [7]

Irregularities in the signal can conceal or distort the pertinent frequencies through high amplitude, such as the frequency of a bogie at 5Hz and 2 occurrences will be distorted by a 50Hz at 5 occurrences per trace due to the higher frequencies and the noise making the peaks rapidly fluctuate and creating false strain values. The data that has been collected show an electromagnetic frequency (EMC) at 50Hz on all sites causing the time domain trace to be distorted. The irregularities are seen at 50Hz (and multiples of 50Hz), due to the alternating current (AC) generated at 50 cycles/second through the National Grid.

The cut off frequency is a drop off of -3dB through the signal, which is half the maximum power. The cut off was determined by Butterworth in his design of the filter [6]. The values for the filter were calculated using the Matlab Butterworth function *butter(N,Wn),* where N is the order and Wn is the frequency value $0 < Wn < 1$, i.e. a required cut off frequency of 50Hz with a full range of 500Hz would require a $Wn = 50/500 = 0.1$. The nth order is also sometimes called the 'roll off rate' as it tends to impact on the frequencies left behind after filtering. Typically, '*N*' is in the region of two to ten as orders above ten would cause a 'ripple' in the data by achieving a closer fit to the cliff edge as the design could cannot achieve the roll off rate necessary to get the filter.

A 10^{th} order Butterworth filter was applied to the strain data with a low-pass cut off applied to the original data before analysis. SC1 cut off was at 99Hz, and SC2-4 at 49Hz to limit the noise from EMC. The frequency values were selected due to the sampling rate of the systems, 3000samples/s at reference and 1000samples/s at non-reference, and the additional stray frequencies found above 50Hz due to the electrification and distortion through cabling. No

relevant frequencies were found above 100Hz in any case. The 10th order was selected due to the sharpness of the filtering, and the removal of information being nearer the idealised 'cliff-edge' filter. Figure 6-4 shows the comparison of filtering orders, running from first order to tenth order, where |H(r)| is the frequency response. Any order greater than the tenth order should not be used as it distorts the data before and after the cut off frequency, due to generating a spline closer to the vertical cliff edge. Chebyshev filter is included in Figure 6-4, showing a 'ripple' before the cut off limit to achieve a closer fit to the cliff edge. The ripple of the Chebyshev filter is undesirable as it distorts the relevant data section before the cut off and thus the filter will not be used.

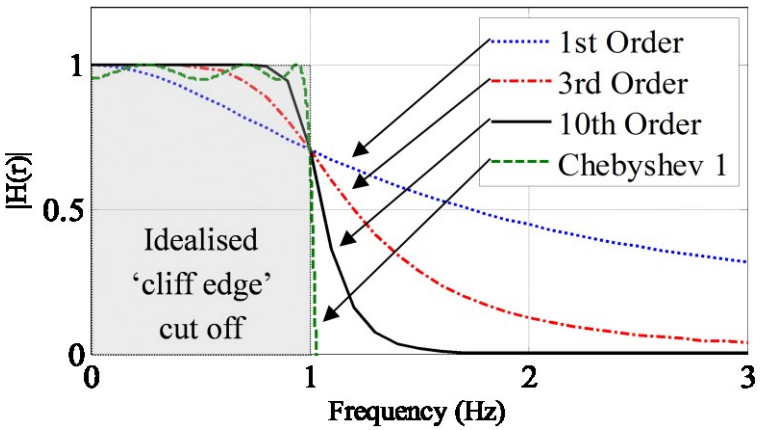

Figure 6-4: The orders of the filtering process and their comparison

From analysing the original experimental data, it was found that the noise of the 50Hz electro-magnetic current within the sample causes a variation of c. 40με as the un-laden gauge output oscillating between -20με and 20με. The oscillation due to EMC noise means that the peak strain without filtering varied by 40με from one vehicle to the next.

6.4 EXPERIMENTAL OUTPUT VALIDATION

A method to validate the strain gauge results is to use Poisson's ratio against that of the material reference. This allows for site validation at an early stage of the experimentation and to monitor the material reaction at the gauge. The validation would show that the connection between the gauge and the rail material is acceptable. Poisson's ratio is the change in lateral length of the material against the change of the vertical length, as materials tend to deform inwards under tensile loading [8]. Poisson ratio is defined as;

$$\boldsymbol{v} = -\frac{\boldsymbol{\varepsilon_{transverse}}}{\boldsymbol{\varepsilon_{axial}}} \qquad (6\text{-}1)$$

Where v is Poisson's Ratio, $\varepsilon_{transverse}$ is the vertical strain and ε_{axial} is the longitudinal strain.

The transverse strains are negative, compression strains, and therefore the ratio is positive. For SC1, the Poisson ratio was consistently between 0.2917 and 0.330. The Poisson's ratio for mild steel is 0.303 [8], and so the values in this simple validation stage can be seen to be acceptable.

6.5 CORRECTED SITE DATA RESULTS

The collected data has been filtered and corrected according to the preceding sections. The results in this section are based on the outputs from the first phase of the instrumentation process, SC1 - 4. Axle weight has been used in the plots of the strain comparison due to the unknown distribution of loads between the two wheels on the axle in the instrumentation outputs.

6.5.1 Assumptions

At this stage of the results, a few of the assumptions that have been made are highlighted.

- The weight of the vehicles are as described in *British Railway Locomotive and Coaching Stock 2012* [9]. A calculated laden weight uses the mass of an average person [10] and the number of seats, with additional weight added for standing passengers and luggage (10kg/person). The maximum weight for diesel locomotives has been derived through maximum fuel tank size and weight of diesel [11].

- The speeds are calculated from the output data peaks and the vehicle bogie spacing, found in [9]. The speed of the trains is used within some of the analysis as it is a significant parameter in the dynamics of the trains. Speed will affect the location of the contact and impact loading through the transfer in the contact and discontinuities.

- The track geometry has been gained from the New Measurement Train (NMT), but the geometry is variable throughout the research. The geometry is known to be a

factor in the degradation [12] of the rail due to the amplified vertical loading caused by the dynamics of the train.

- Peak to peak strain is used in the results section to understand the loading cycle of each wheel over the gauges. Peak to peak strains are used in this section, rather than RMS or mean, to give the strain from the loading of each wheel as it demonstrates loading of each wheel.

6.5.2 Numbering system

The strain gauges have been numbered to ensure that the outputs are comparable across the various sites. The gauges have been placed vertically and horizontally to gain the vertical loading from the wheel and the change in the length of the rail from the contact and the effect that the elongation happens on the change of material response. Each gauge is numbered, with the first number demonstrating the vertical gauge, and the second accounting for the horizontal.

Throughout the switch, there are four rails. To ensure that the gauges are numbered in the same manner for each of the sites, the rails are numbered from one to four. Rail 1 is the rail on the outermost rail of the track, called the ‘cess’ within the rail industry. Rail 2 and 3 are the switch blades; Rail 1 and 4 are fully profiled stock rails.

6.5.3 Process to create results

The graphs for the site analysis show strain against axle load, and the strain against speed for the different vehicles classifications.

For the figures including axle load, error bars demonstrate the possible weight that could be applied through the axle. Axle weight is a commonly used value within the railway industry and divides the total weight of the vehicle by the number of axles. The minimum weight of the error bar is the tare axle weight and the maximum is the values calculated from the assumptions, including fully loaded seats, standing passengers and 10kg luggage per passenger. The axle weight of the sampled vehicles is plotted against the peak to peak strains to be able to monitor any trends between the loading and the material response at each instrumented site. This gave a comparison between similar weights and the corrected strains,

and gauge outputs at the same site. The peak to peak values were found through calculating the maximum distance between strain value of the peak (at the location of the wheel directly over the gauge) and the steady state of the proceeding section of the filtered trace.

Using the same traces as the peak to peak, the speed could also be calculated. The known axle spacing [9] were combined with the determined time between the peaks, which gave speed. The purpose of the strain against speed graphs is to compare to the effect of speed for similar vehicles / masses, to understand the response of the material against changes in loading. The charts have been separated into the various vehicle classifications and similar weights to aid any trend monitoring.

At the sites selected, a function of the S&C unit is to allow freight vehicles to access the mainline railway from a different location / siding. Freight vehicles are typically hauled by Class 66 locomotives. Thus it is assumed that for the freight trains, the first carriage has the specifications of the Class 66 locomotive. Laden freight vehicles are assumed to have a larger mass than passenger vehicles as they are transporting items such as coal to plants. This is significant as it has been found [8] that a heavier mass contributes to a change in wear classification through higher loading forces. The monitoring of the mass will give confidence to the results that were found through statistical studies.

6.5.4 SC1

SC1 is the reference site for the instrumentation. The site was chosen as the reference site as it was installed in May 2011 with the design parameters outlined in the design of experiments. The site will collect the early degradation process as the wheel and the rail become more conformal due to high contact pressures causing localised deformation at the surface of the rail. The reference site has 64 gauges, five geophones, three accelerometers and two thermocouples. SC1 is described in Table 6-1 and shown in Figure 6-5.

6.5.4.1 Site details

Table 6-1: SC1 design of experiments output and specific levels and parameters

Unit Name	Switch Design	Rail Inclination	Line Speed	Track Quality	Traffic Type	Annual Tonnage
SC1	D	Vertical	60kph (40mph)	Good	Passenger: 6.2MGTPA Freight: 5.4MGTPA	17.0 EMGTPA[2]

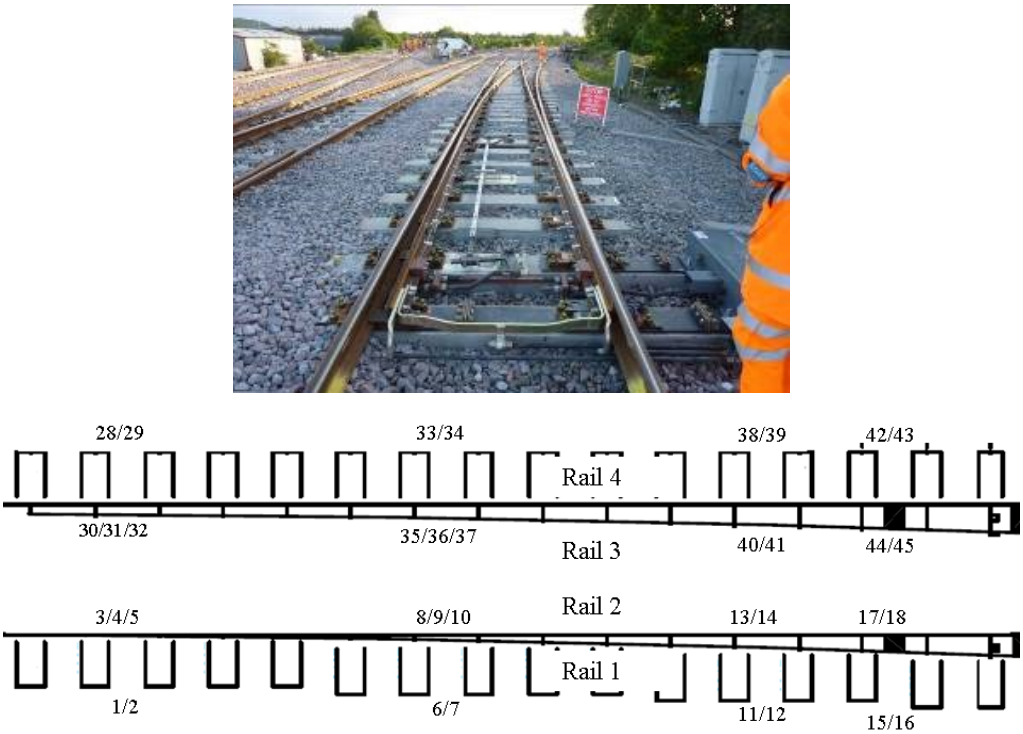

Figure 6-5: Photo of site SC1, facing the points with the direction of traffic coming outwards, the gauge numbers and locations, with Rail 1 on the right (cess), and Rail 4 the left (six foot)

[2] Equivalent Million Gross Tonnes Per Annum – explanation found in Abbreviations

6.5.4.2 Strain Gauge results

The vertical peak to peak strain outputted against axle weight is shown in Figure 6-6.

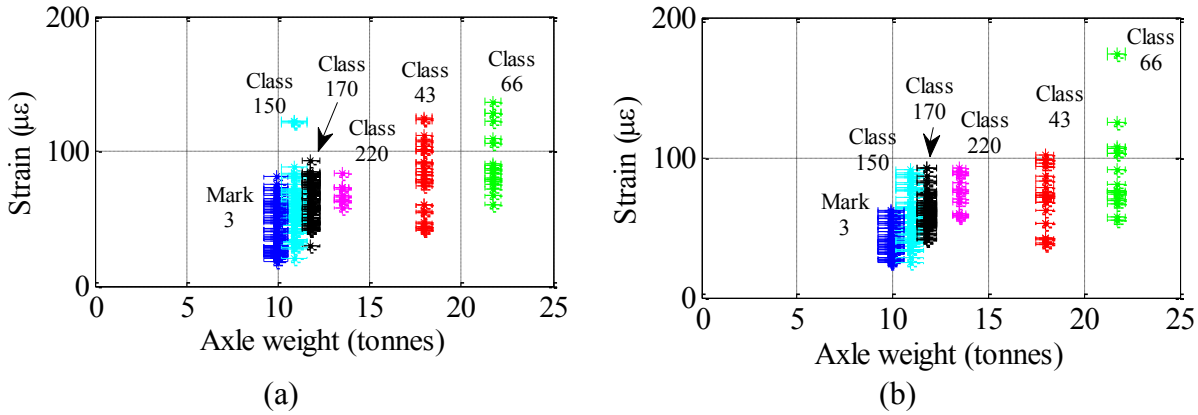

Figure 6-6: Vertical strains against axle weight for various vehicles at (a) Strain Gauge 1 (SG1) on Rail 1 and (b) SG28 on Rail 4 between sleeper 2 and 3

Presently, the outputs from the strain gauges (SGs) at similar locations are within 10%. A few of the class 150 (cyan coloured) are above 10%. The Mark 3 has higher strains on the stock rail with the closed switch blade (SG28), 25% larger in comparison to the other rail at SG1. This is due to the additional dynamics of the vehicle transferring from one rail to another.

Figure 6-7 shows the outputs from strain gauge 1 at SC1. The figure shows the strain generated at the gauge from the various vehicles traversing the points at various speeds, categorised into vehicle type.

For SG1, all the strain is below 200με. Freight vehicles have an increased value of strain at a lower speed, but are still within 200με. The majority of the vehicles passing through the site are passenger (c. 55 tonnes/coach), with the freight having a larger weight / vehicle (c. 90 tonnes/wagon).

Figure 6-8 shows the outputs from SG 28 at SC1, showing the strain from the various weights traversing the points at various speeds.

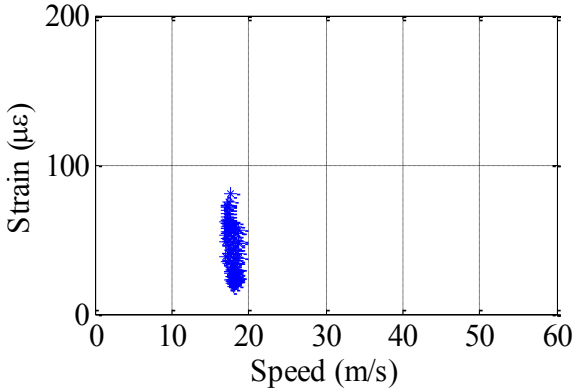

(a) Mark 3 coach, tare weight: 4.6t wheel load

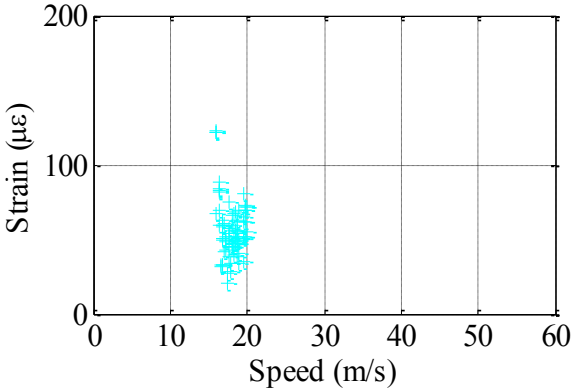

(b) Class 150, tare weight: 5.1t wheel load

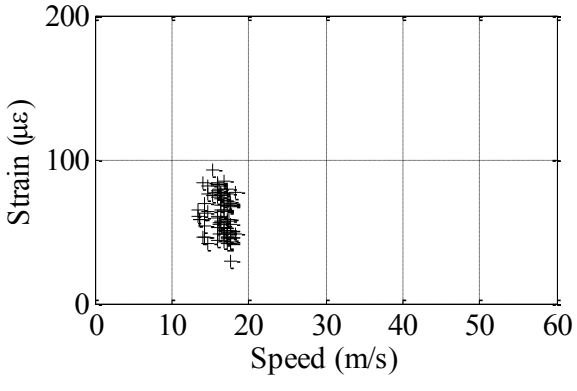

(c) Class 170, tare weight: 5.7t wheel load

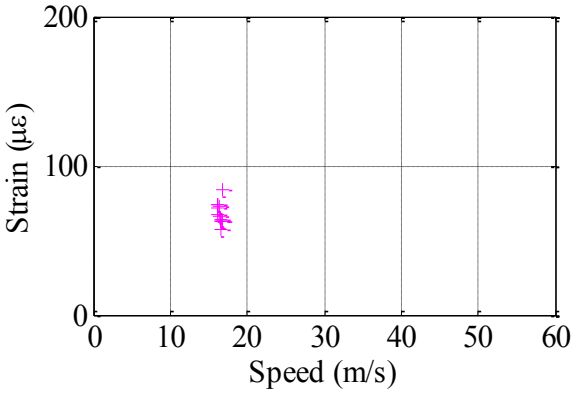

(d) Class 220, tare weight 6.6t wheel load

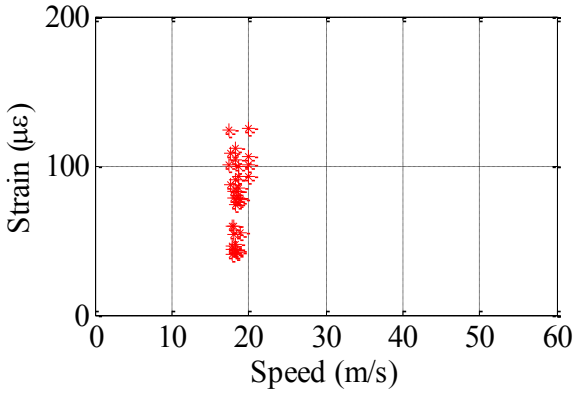

(e) Class 43 loco, tare weight: 8.5t wheel load

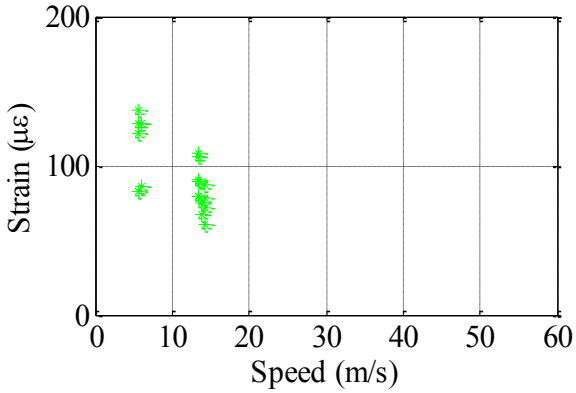

(f) Class 66 Loco, tare weight: 10.2t wheel load

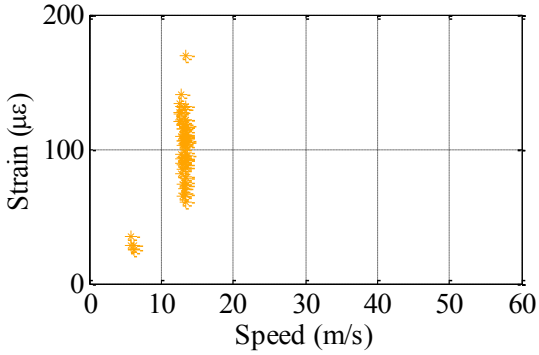

(g) Freight with unknown load

Figure 6-7: Processed peak to peak strain gauge results from Strain Gauge 1 at SC1 grouped in vehicles

The output from SG28 shows that the majority of the peak to peak strain being outputted has a lower value than the SG1 with similar vehicles. Whilst the static loads of the various vehicles are the same, the dynamic effect on the loading can vary due to the contact between the wheel and the rail through the state of wear on the wheels. The state of wear on the wheels affects the size of the contact patch and therefore the stress going. The wear is very difficult to monitor for each vehicle that passes through the site as the measurement of all wheels would be very time consuming.

As the vehicle travel through the switches, the wheel transfers from the switch rail onto the stock rail on a single side to allow for the vehicle to continue. It has been seen in some of the above examples that the loading on the stock rail with the closed switch (Gauge 1) has a higher strain on the through route than the open side (Gauge 28). The Class 66 (Figure 6-7 & Figure 6-8 (f)), traverses the points on the diverging route, towards the right of Figure 6-5, with the majority of the contact on Rail 1 and Rail 3. To understand the increase on the closed switch rail, the reference site put additional gauges at the transfer zone to monitor the process of transfer from the switch rail to the stock rail. Roll and yaw (rotation around axis x and z) generates contact in different locations, caused by the vehicle traversing the asset. As the gauges are in static locations, this would seem to be unlikely due to the trend of vehicles and their contact conditions, seen in Figure 6-8.

One other reason behind the change in contact condition is the lateral position of the rail and the wheel profile. The lateral position and the influence of the contact pressure will be investigated in Chapter 8 – *Modelling and validation*.

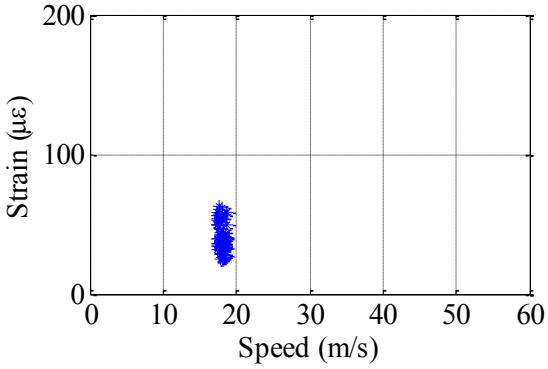

(a) Mark 3 coach, tare weight: 4.6t wheel load

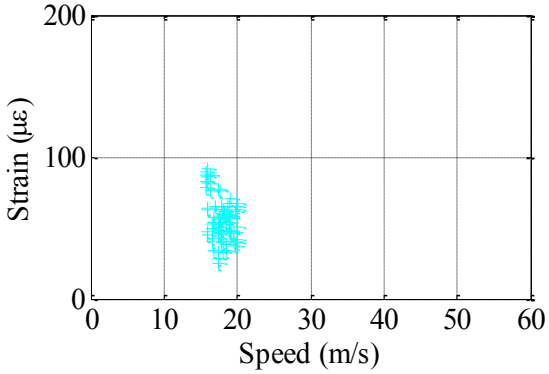

(b) Class 150, tare weight: 5.1t wheel load

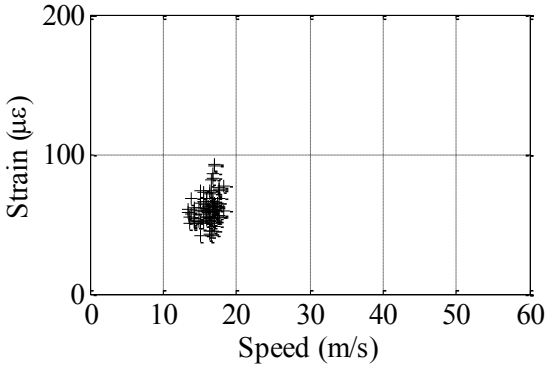

(c) Class 170, tare weight: 5.7t wheel load

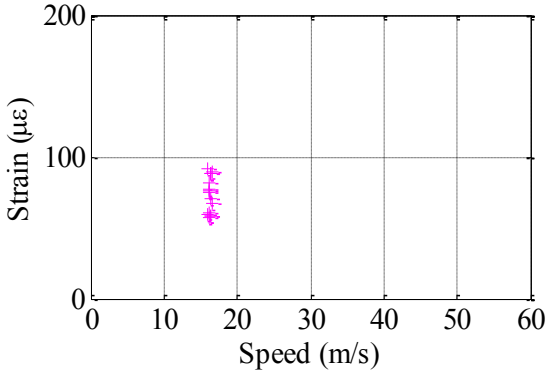

(d) Class 220, tare weight 6.6t wheel load

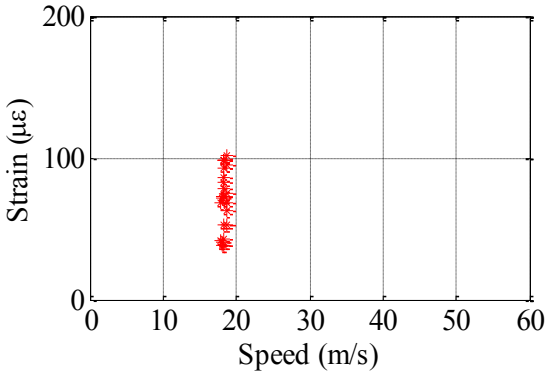

(e) Class 43 loco, tare weight: 8.5t wheel load

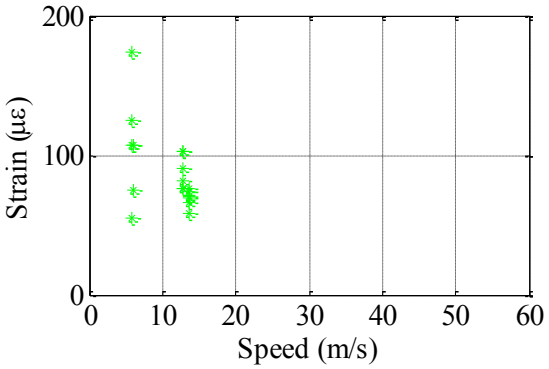

(f) Class 66 Loco, tare weight: 10.2t wheel load

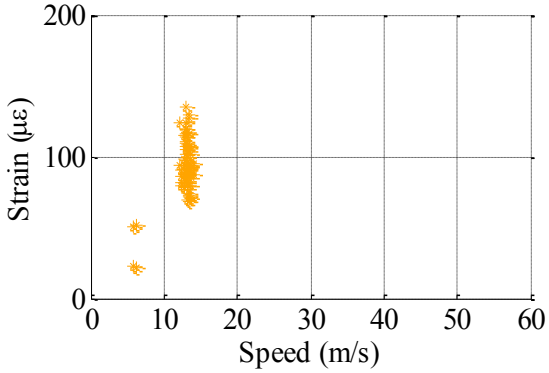

(g) Freight with unknown load

Figure 6-8: Processed peak to peak strain gauge results from Strain Gauge 28 at SC1 grouped into vehicle types

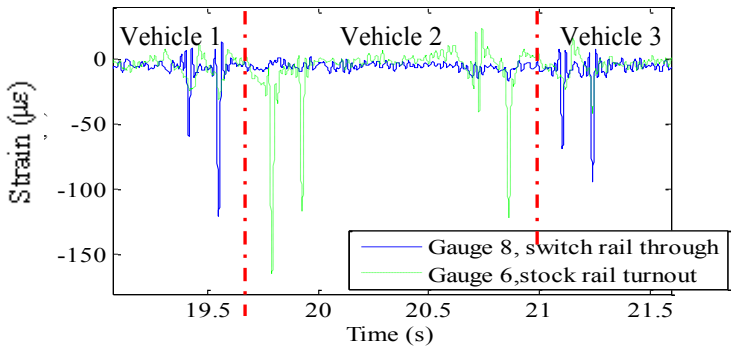

Figure 6-9: An example of a vehicle various contact conditions at SC1 and the loading of different gauges at the transfer zone

Figure 6-9 shows three vehicles of a train at the same location, between sleepers 7 and 8 from the toes, with the outputs from two different gauges; Gauge 6 on Rail 1 (green ---) and Gauge 8 on Rail 2 (blue -). The figure shows that whilst outputs are the same train, the individual wagons do not come into contact on the same rail. The rail contact location is dependent on the bogie angle, wheel and rail profiles, and vehicle offset. As both the gauges on the same side are not loaded at the same time, Figure 6-9 shows the change in strain is due to change in lateral offset of the wheelsets, change in yaw angle of the axles and wheel profiles. This means that the transition from switch to stock rail happens at different locations along the 1m transition length depending on wheel profiles and axle yaw angles, and lateral offset of the vehicle.

Figure 6-10 shows four unfiltered frequency contents through a Fast Fourier Transform (FFT), of the gauge in the switch region, gauges 1, 6, 28 and 33 to understand the frequencies present in the loading. An FFT was completed to understand the frequencies of the loading to understand the major contributions of the vehicle to the strains. The FFT's were completed on the various gauges at SC1 to monitor the change in the loading through the switch panel.

Gauges 6 and 33 have an increased EMC values at 50Hz but this is due to the electrical cabling in close proximity to the instrumentation cables, generating an induced current. The 50Hz have been removed for all time (non-linear) analysis using a Butterworth low pass filter. The EMC has been removed as it does not contribute to the understanding of the change of strain in the material.

The majority of the amplitudes above 1 are below 10Hz, and therefore align with the vehicle loading frequencies that were shown in Figure 5-3. These include bogie spacing and car body spacing at 60kph. The frequency shows that the vehicle speed loading is highly influential in

the non-linear outputs. From the FFT, there are no significant amplitudes above 100Hz, and over 50% of the amplitudes are zero. Therefore, loading from medium (100Hz to 500Hz) and high frequency (above 500Hz) are non-pertinent at the gauge location. The additional frequencies of the wheel / rail contact seen in other literature were not present at the gauge as they would tend to be within the influence of the contact patch. The peak amplitudes show the bogie spacing of 2.6m at 56kph (0.7Hz), the axle spacing (5.68Hz) and the vehicle vertical bounce due to the suspension (7.1-7.9Hz). The peaks at 50Hz show the influence of the EMC.

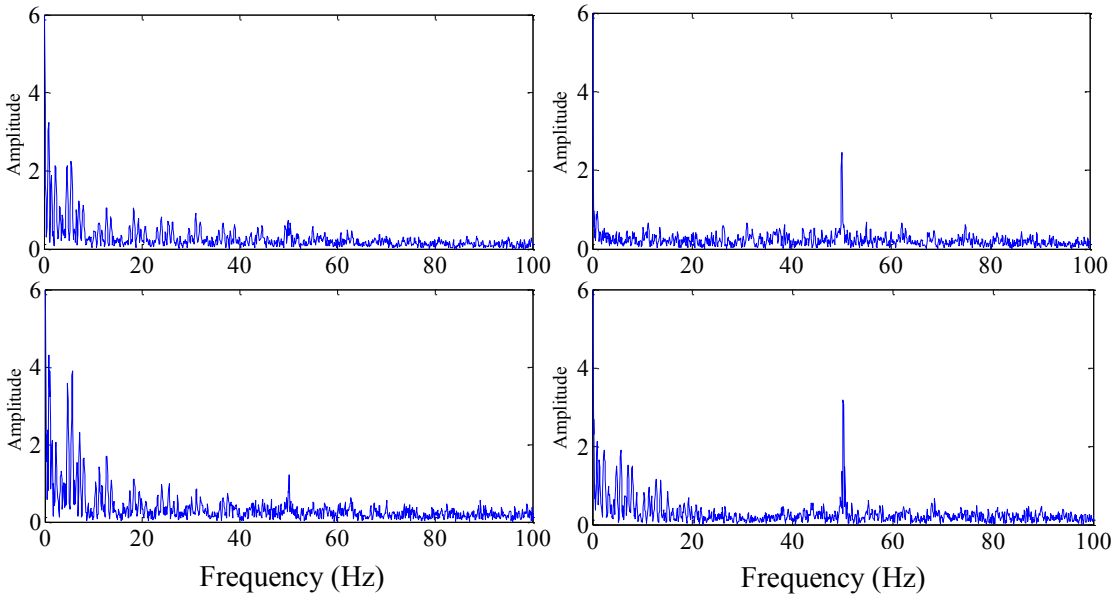

Figure 6-10: Frequency from Gauge 1 (top left), Gauge 6 (top right), Gauge 28 (bottom left) and Gauge 33 (bottom right)

Similar frequencies (depending on speed) and amplitudes are found for all the trains that were analysed from SC1 with variations of frequency of 10% depending on speed. This gives a baseline for the loading type, car body, at this early stage of strain for S&C in service.

6.5.4.3 Geophone results

The geophone results at SC1 have been completed in collaboration with Louis Le Pen (LLP) at the University of Southampton (UoS). Louis Le Pen has agreed to let the collaboration work be used in the thesis. All work completed by LLP has been referenced.

Geophones output velocity of an uni-axial direction. In the field instrumentation, vertical axis was the most pertinent due to understanding the displacement and bending of the structure

due to loading. Using integration of velocity, the displacements of the attached component can be derived after low frequency filtering to standardise the sensitivity. The displacements allow an understanding of the system; rail, sleeper, rail pads and ballast, their conditions under loading and deterioration over time.

Five geophones were installed at SC1 with four of the five on the outside of an 800m radius curve going through the crossing. The main focus for this section of the investigation was to monitor the change in vertical motion of the crossing to monitor the deterioration and the effect on strain, which will be examined in Chapter 7. The locations of the geophones are shown in Figure 6-11. The locations of geophones 22, 57 and 24 were chosen as the variation in the stiffness at the crossing has high industrial relevance due to the high cost of the crossing, and the monitoring of the vertical deflection through the asset longitudinally.

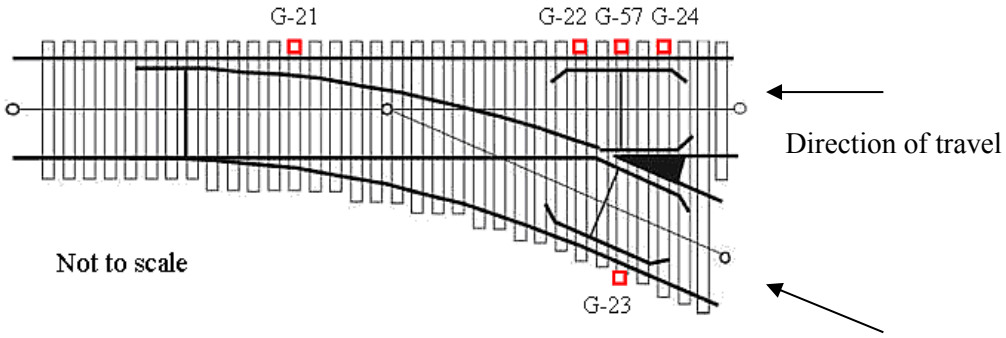

Figure 6-11: Geophone location at SC1; G-21 is on sleeper 11, G-22 on sleeper 41 at the crossing, G-23 and G-57 on the crossing nose sleeper (sleeper 43), and G-24 on sleeper 45

Figure 6-12 shows the converted peak to peak outputs from the geophones on the site, and their location. Geophone 23 gave very small results (less than 0.5mm) and so has not been included in the figure.

Figure 6-12 shows that the largest vertical motion (up to 3.5mm displacement) occurs on the bearer with the crossing, with the switch panel (geophone 21) recording displacements of less than 1mm. The geophones either side of the crossing nose see similar range of motion. The displacements show that the bending of the asset is greatest at the crossing nose due to the additional bending strains of the large and heavy crossing asset. The switch sees less vertical motion due to the irregularities in the transition being over a longer length at the switch (1m rather than 0.2m) and the discontinuities of the running path at the crossing causing high magnitude loading as the vehicle traverses.

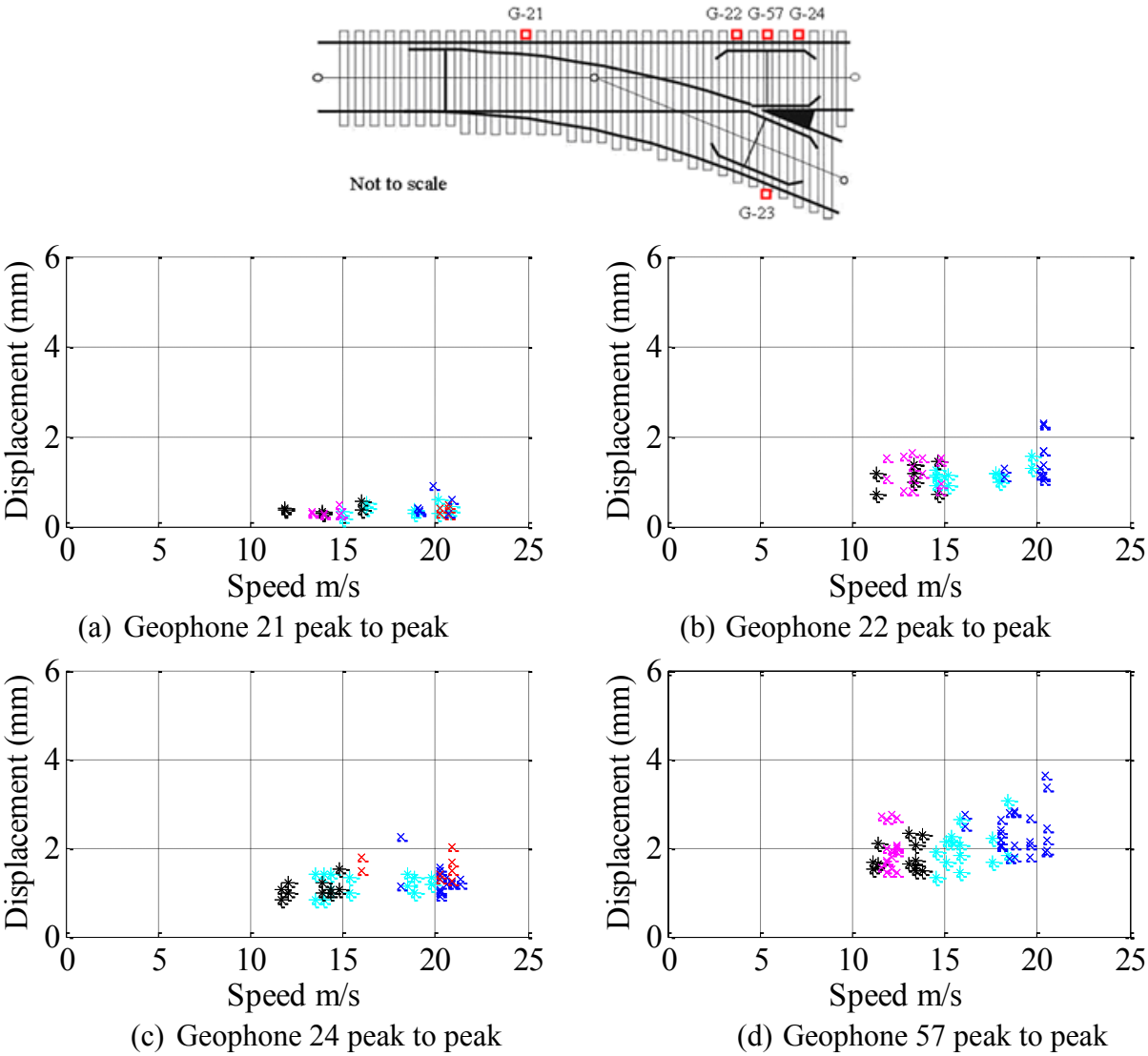

Figure 6-12: Geophone peak to peak outputs at SC1 against speed from the various instruments, with the same legend as the Figure 6-6 for different vehicles

Figure 6-13 shows the results from the crossing geophone courtesy of LLP at UoS. The peak to peak displacements of 1.6mm – 2mm are within 10% of those found at the geophones at geophone 57 in Figure 6-12, (with the black '*'). The comparison gives a validation of the results and the processing from velocity to displacements as UoS results and conversions have been validated against other instruments [4].

The outputs in Figure 6-13 show a vertical displacement of a Class 170 and the variation over 6 months. Network Rail's geophone 24, in the same location, showed a converted displacement of 1.8mm in January 2013. The displacement is within 0.2mm of the data from UoS. This gives confidence that the processing and conversion is correct as the UoS data had additional validation.

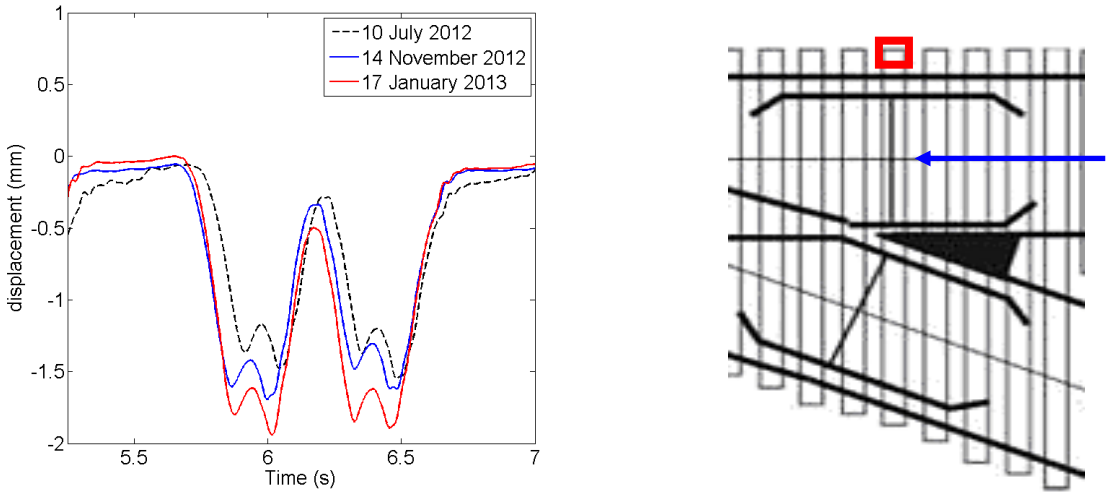

Figure 6-13: An output from the geophones over time with conversion to displacement with the location and direction of travel on the right – Data courtesy of LLP

As the results from the UoS work and the NR instrumentation are within 0.2mm, the validation is acceptable and this gives additional confidence in the outputs and methods of derivation for the other instrumented sites.

6.5.5 SC2

SC2 is a non-reference site that was selected due to the higher annual tonnage that is seen and is not in the initial stages of wear as the wheel and rail should be more conformal. The site has 30 channels, 26 strain gauges, two geophones and two thermo couples. The site sees mainly passenger, but is also sees a high freight tonnage.

6.5.5.1 Site details

Table 6-2: SC2 design of experiments output and specific levels and parameters

Unit Name	Switch Design	Rail Inclination	Line Speed	Track Quality	Traffic Type	Annual Tonnage
SC2	D	Vertical	160kph (100mph)	Poor	Passenger: 9.0MGTPA Freight: 8.2MGTPA	29.4 EMGTPA

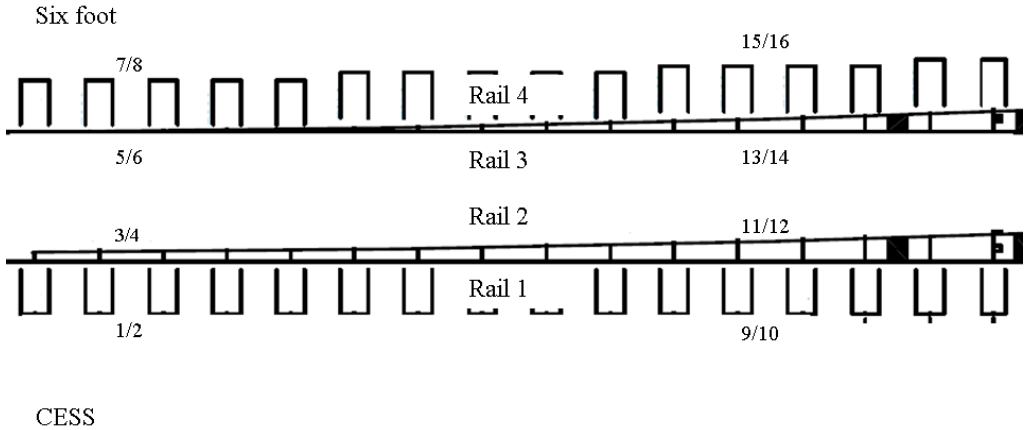

6.5.5.2 Figure 6-14: Photo of site SC2, facing the points with the direction of traffic coming outwards and the location of the gauges numbers on the site

6.5.5.3 Strain Gauge results

Due to damage to the instrumentation and system, no outputs could be collected and therefore no conclusions can be drawn from the results. Considerable difficulties were experienced by contractors fitting the instrumentation for this site due to access to site and high quantity of electrical assets in close proximity to data logger and cabling.

For interference and connections of instrumentation issues, the outputs gained were inconsistent and therefore not used in the investigation.

6.5.6 SC3

SC3 is a non-reference site that was chosen due to the higher line speed and the higher freight percentage. There were 26 strain gauges installed, two geophones and two thermocouples.

6.5.6.1 Site details

Table 6-3: SC3 design of experiments output and specific levels and parameters

Unit Name	Switch Design	Rail Inclination	Line Speed	Track Quality	Traffic Type	Annual Tonnage
SC3	D	Vertical	200kph (125mph)	Satisfactory	Passenger 8.0MGTPA Freight 7.5MGTPA	24.0EMGTPA

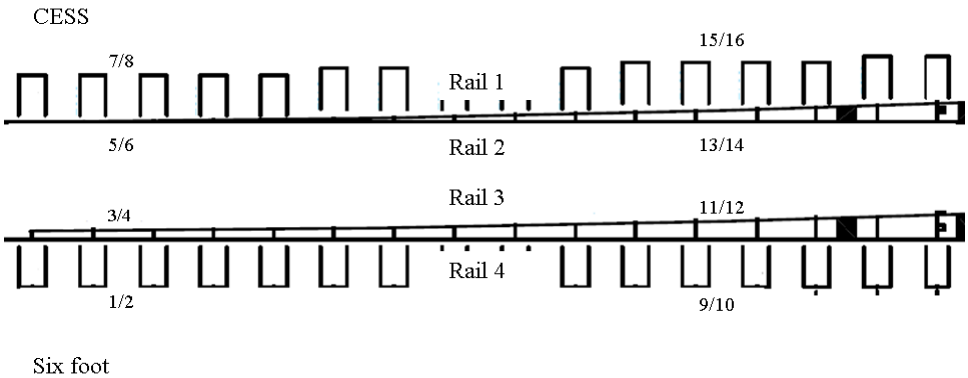

Figure 6-15: Photo of site SC3, with the passenger vehicles travelling outwards and the freight typically on the diverging route inwards and the gauge location on the site

6.5.6.2 Strain Gauge results

The weight of a vehicle is hugely complicated to accurately identify because of additional weights, such as luggage, passengers and fuel for diesel vehicles. Figure 6-16 shows the processed results from Strain Gauge 1 and Strain Gauge 7 with error bars showing the possible range of weights using previous assumptions.

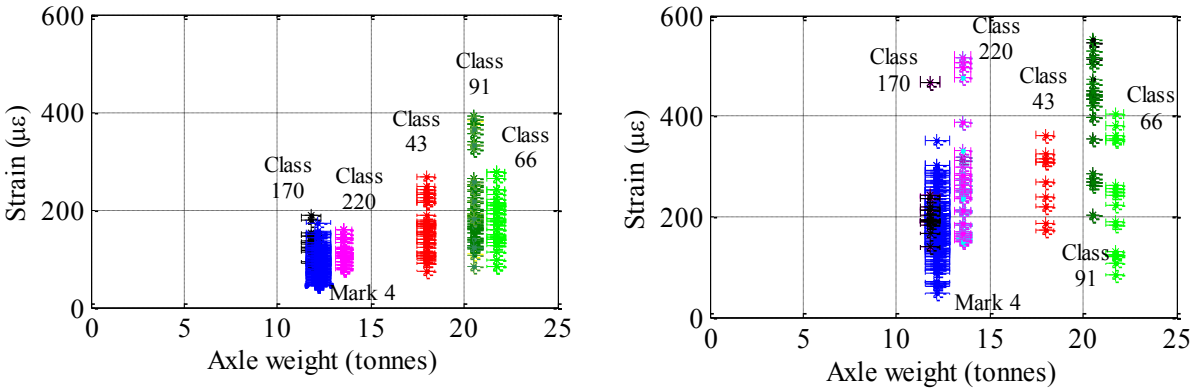

Figure 6-16: Vertical strains against weights for various vehicles at SC3, at (a) SG1 and (b) SG7 with the error bars representing the possible range of weights

Comparing the variance of strains recorded from the different gauges at the switch toes, it can be seen that the closed switch blade (SG7) encounters larger strains, especially the vehicle 'Class 220' (tare wheel weight of 6.6t), with an increase of up to 350με on SG1. The larger strain is due to the additional vehicle dynamics that would be seen by the vehicle having to transfer from one rail to another, and similar to the trends seen at SC1. The variation in strain for similar vehicles is difficult to quantify wear rates as the reasons for the range of strain is unknown. The range of strain is significant as the deterioration of the strain shows a bigger increase compared to the other sites within the research.

The peak values from the vehicles passing over SG1 are shown against speed in Figure 6-17. SG1 is on the open switch blade side for the through route, and therefore reacts similar to a plain line section of vertical track for the through traffic.

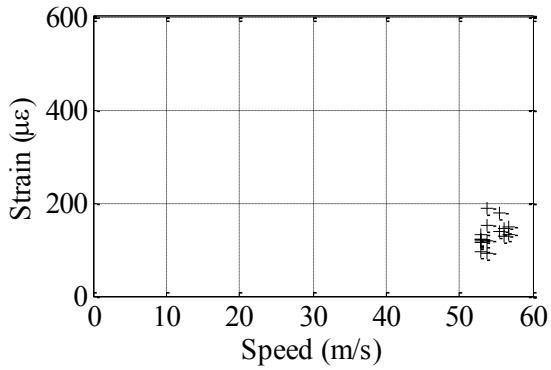

(a) Class 170, tare weight: 5.7t wheel load

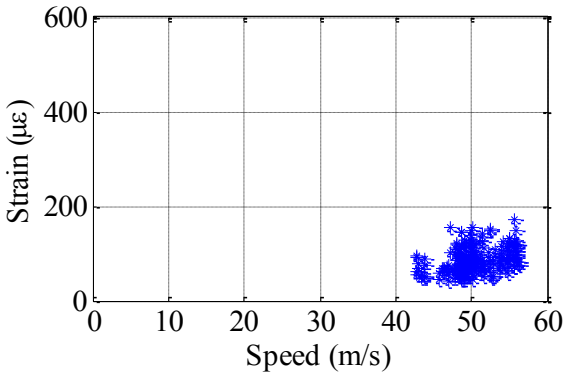

(b) Mark 4, tare weight: 5.9t wheel load

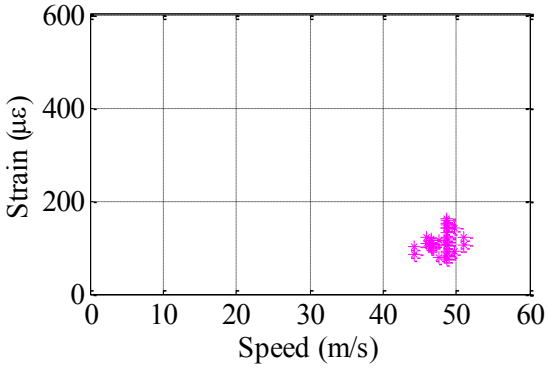

(c) Class 220, tare weight 6.6t wheel load

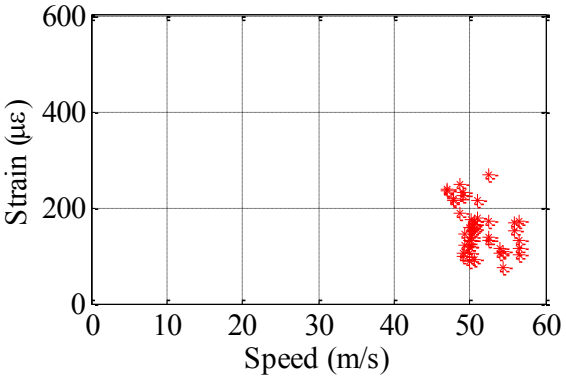

(d) Class 43 loco, weight: 8.8t wheel load

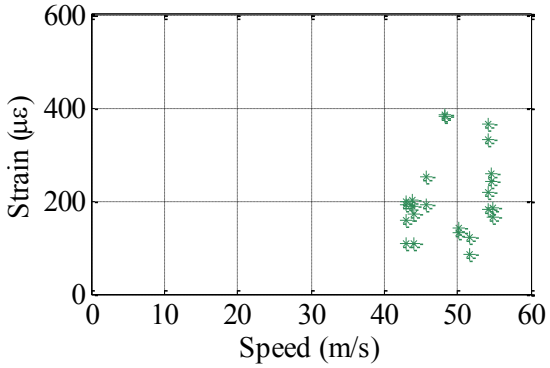

(e) Class 91, tare weight: 10.3t wheel load

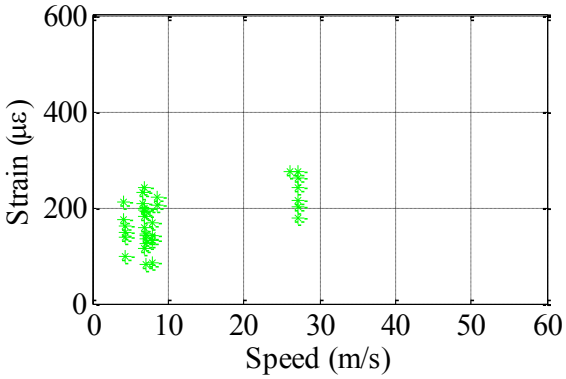

(f) Class 66, tare weight: 10.6t wheel load

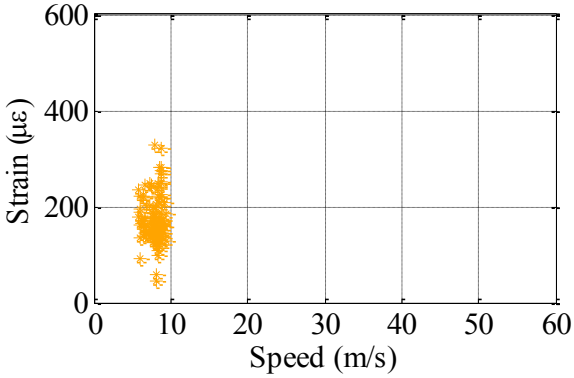

(g) Freight wagon with unknown load

Figure 6-17: Strains against speed separated into various vehicles at SG1 on SC3

The peak values from the vehicles passing over SG7 are shown against speed in Figure 6-18.

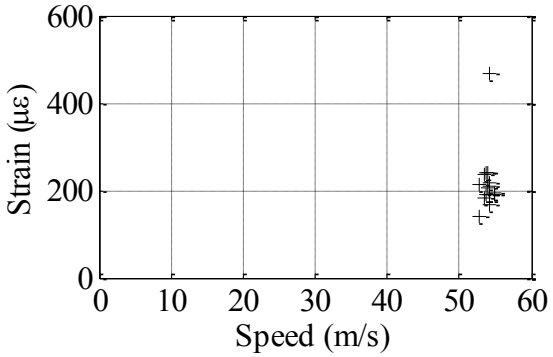

(a) Class 170, tare weight: 5.7t wheel load

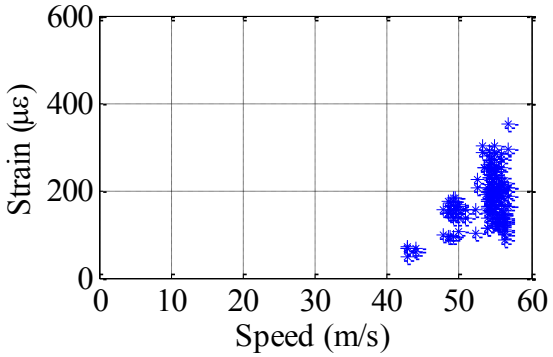

(b) Mark 4, tare weight: 5.9t wheel load

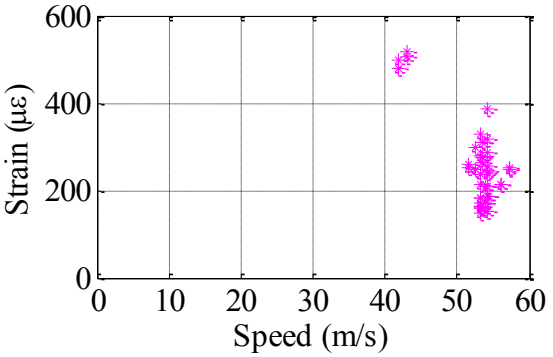

(c) Class 220, tare weight 6.6t wheel load

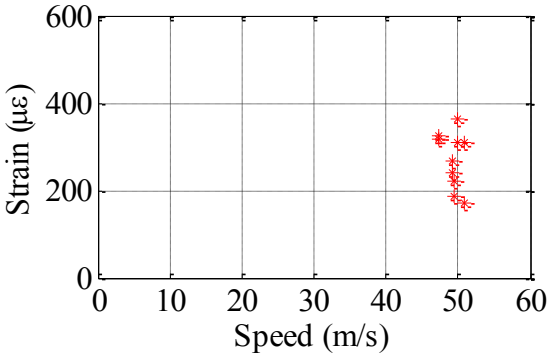

(d) Class 43 loco, weight: 8.8t wheel load

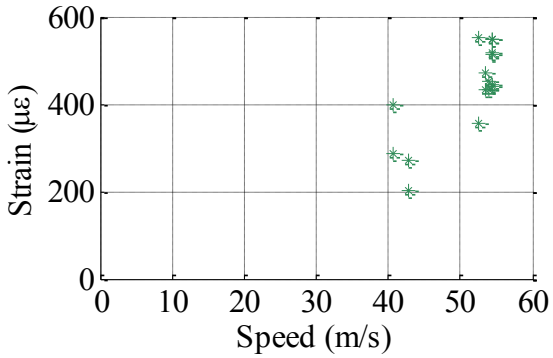

(e) Class 91, tare weight: 10.3t wheel load

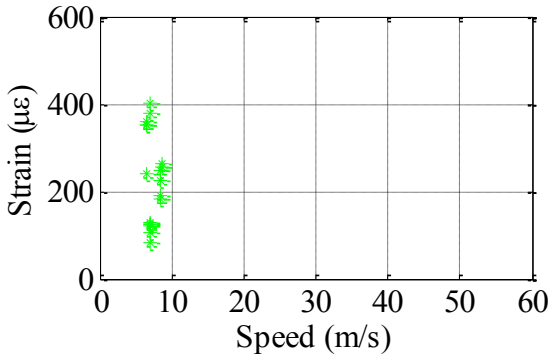

(f) Class 66, tare weight: 10.6t wheel load

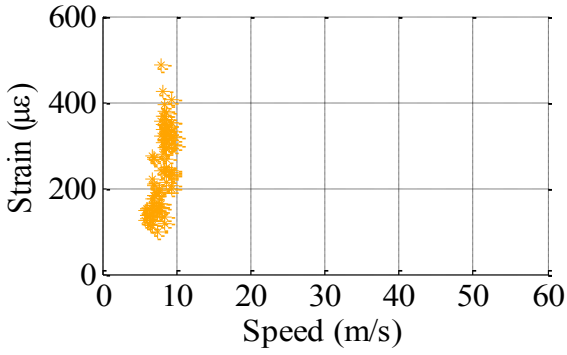

(g) Freight wagon with unknown load

Figure 6-18: Strains against speed separated into various vehicles at SG7 on SC3

The strain gauges at the crossing were removed due to the changing of the crossing shortly into the project. The reason that was given for changing the crossing is;

- Vertical motion of the crossing on the bearer were large (as will be discussed in section 6.5.6.3) due to the low ballast stiffness that was present on site and high frequency vibration that occurred due to the unsupported rail / crossing

- The crossing leg material (the section of the crossing adjoined to the plain line section) was being changed for a high performance (HP) material. The change of the material was to try to reduce the amount of plastic deformation and wear damage that was occurring on the crossing nose and leg section of the panel and so the gauges were removed from the crossing and a smaller amount of data was collected for the crossing compared to the switch.

The gauges were not able to be replaced due to the access to the infrastructure and ended up not being available for the analysis.

A frequency analysis was completed on the vehicles recorded over the site, with an example shown in Figure 6-19. 500Hz is the maximum accurate frequency due to the Nyquist theory with sampling rate of 1000samples/s, c.f. Section 5.3.4 and so the analysis is completed below 500Hz.

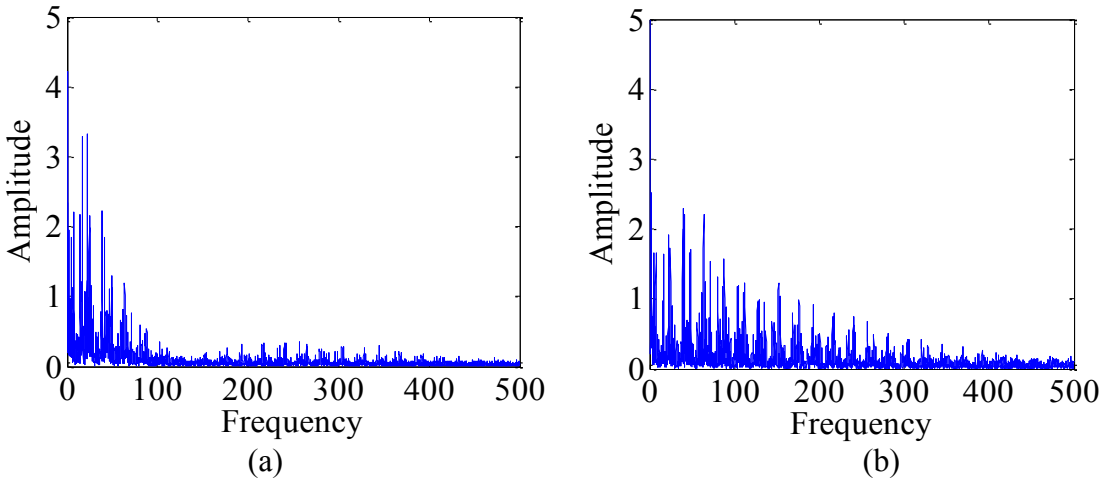

Figure 6-19: frequency of (a) Strain Gauge 1 and (b) Strain Gauge 7 for vehicle 8

The vehicle shown in Figure 6-19 is a Class 91 loco and Mark 4 coaches. The frequency for a passenger vehicle with axle spacing of 2.6m travelling at 175kph (50m/s) is 18.91Hz. The other frequencies that have amplitude greater than one in the system at SC3 are between 40Hz – 70Hz. From the analysis in Chapter 4, the likely cause for these excitements is from the 'unsprung mass' of the vehicle [13] due to the vibrations of the vehicles in direct contact with the rail before the suspension. The unsprung mass for the Class 91 and Mark 4 are 1740kg and 1860kg respectively [9]. The unsprung mass of the vehicle is being excited by

the entry into the S&C unit and the transfer from one rail to another (SG7 is on the closed switch side).

Figure 6-19 (b) shows a wider range of frequencies compared with (a). This means that the loading of the gauges tends to be at a higher frequency on the stock rail with the closed switch blade, up to 150Hz. The higher frequencies would mean additional vibration in the switch, with Berggren [14] showing that stationary rail vibrates at 200Hz. Lower frequencies from the dynamics of the system and loading are from the cyclic loading at 2.6m axle spacing. This shows that the additional dynamics through increased vertical deflection are higher frequency in the switch, tend to be more localised and cause localised deformation.

6.5.6.3 Geophone results

Two geophones were installed at SC3, one at the switch panel, on the end of sleeper 2, and one at the crossing nose. The geophone at the crossing was attached using a resin and anchors. High voltages were seen due to the vibrations and large vertical movements at the crossing nose bearer. The motion of the sleeper was large enough to displace the housing containing the geophone. The geophone was re-attached on four occasions, but the housing became displaced within days on each occasion due to the inability to withstand the high vibration present.

Figure 6-20 shows an early geophone output from the switch tip and the crossing nose. From the data at the crossing, the settled values for the peak to peak displacement are c. 15mm, in comparison with the switch that is c. 2mm. The large displacement at the crossing can include some of the distortion due to the geophone housing becoming displaced, and therefore will not be used in the on-going analysis. The peak in the trace is at 7.7s is due to the conversation and phase lag of the geophone. The peak to peak values of the geophone do not include the first and last peak as the settlement of the instrument due to the mass system causes erroneous readings.

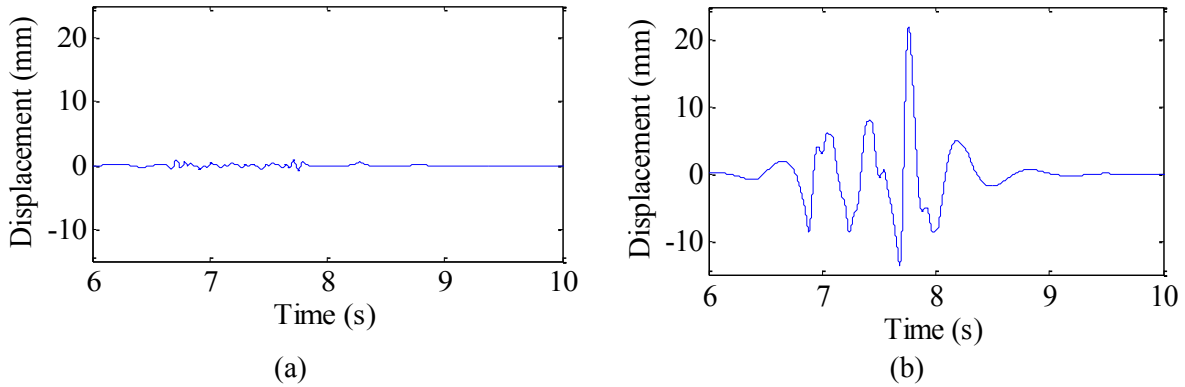

Figure 6-20: Geophone displacement at (a) switch tip and (b) crossing at SC3 for a class 170

The geophone at the switch (sleeper 2) stayed attached and operated throughout the investigation. The converted results that were recorded are shown in Figure 6-21.

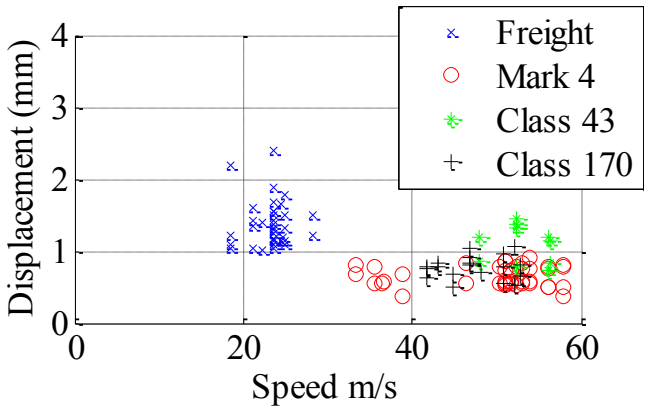

Figure 6-21: Peak to peak vertical displacements from Geophone 1 at SC3 (sleeper 2)

The freight vehicles are creating a larger vertical displacement than the passenger vehicles due to the larger mass of the laden freight vehicles. Mark 4 coach generated lower displacements, between 0.5mm and 1mm due to lower weight of 5 tonnes/wheel compared against the unknown weight of laden freight vehicles.

Freight vehicles cause greater deflections due to the slower speeds, less than 15m/s, exacerbating the poor ground conditions at SC3, and loading of all irregularities.

The displacements at the switch tend to show similar displacements for the Mark 4 vehicles. The variation of strain, from 50με to 350με for a Mark 4 coach at the switch, is an unknown occurrence, and will be investigated in later chapters using modelling techniques.

6.5.7 SC4

SC4 is a non-reference site as was installed in September 2004 and was chosen due to the inclined stock rail with higher freight percentage. The trains use both the through and diverging route, in line with Figure 6-22. There were 26 strain gauges installed, two geophones and two thermocouples. The main difference to the other sites is the stock rails are inclined (at 1:20). The type of switch design is called NR60 (for the 60kg/m stock rail). The inclined rails are used as they are more conformal in shape with the wheels, the tread designed at 1:20, which reduced contact stress with increased contact patch and location.

6.5.7.1 Site details

Table 6-4: SC4 design of experiments output and specific levels and parameters

Unit Name	Switch Design	Rail Inclination	Line Speed	Track Quality	Traffic Type	Annual Tonnage
SC4	D	Inclined	140kph (100mph)	Good	Passenger 5.2MGTPA Freight 3.7MGTPA	13.2EMGTPA

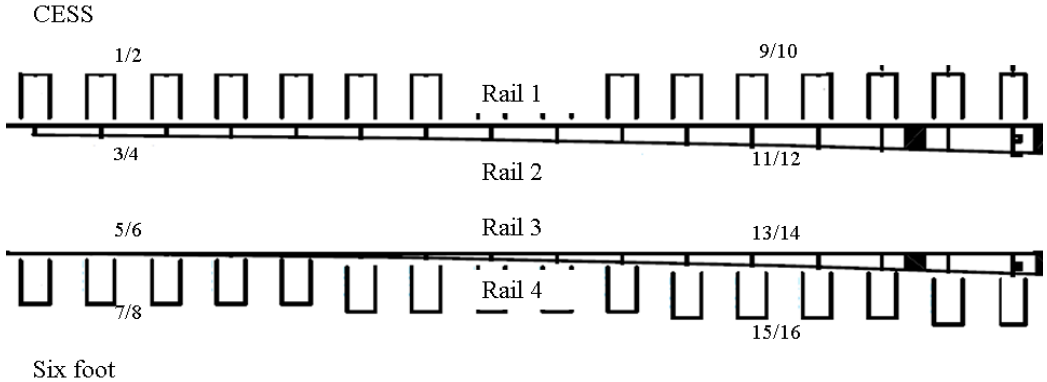

Figure 6-22: Photo of site SC4, facing the points with the direction of traffic going outwards and the location of the gauges

6.5.7.2 Strain Gauge results

A number of the strain gauges are not working due to faults as the instruments are highly sensitive equipment and on an operational railway infrastructure. The faults were not able to be rectified the before the outputs were collected. SG1, 2, 7, 8, 15, 16 and 22 (7 of 26, 27%) were not working. Comparisons with the other sites are therefore limited due to the number of comparable gauges. Figure 6-23 plots the outputs from SG 9 and 17 (on the plain line section at the crossing). The plots show the difference in the loading at an inclined plain line section of the crossing and an inclined section of rail in closure panel, SG9.

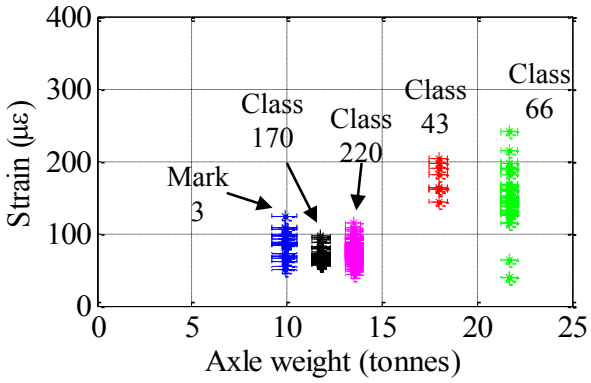

Strain gauge 9 – all vehicle comparison – plain line, sleeper11

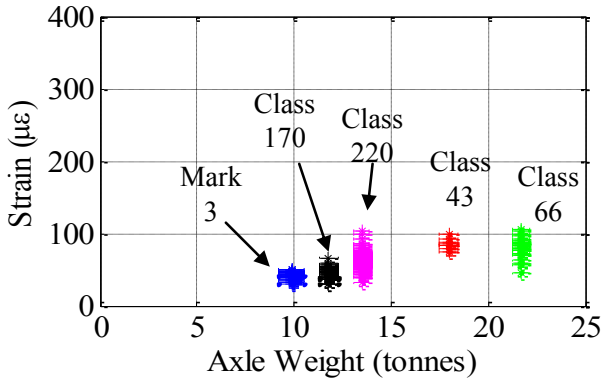

Strain gauge 17 – all vehicles - plain line, sleeper 42 (crossing)

Figure 6-23: A comparison between the switch and the crossing section in terms of the strain generated from various vehicles

The results show change of 10% in the strain that is being generated between the crossing plain line section and the regular inclined rail for the Class 220, but some of the other vehicles, Class 43 in particular, show decreases of greater than 100% of the strains generated at the crossing.

Figure 6-24 show the strain outputs of freight vehicles for the through and the diverging routes at SC4. The vehicles in Figure 6-24 (a) are laden and on the turnout route, which means that the vehicles have an increase in the vertical dynamic loading that the rail is being exerted. Figure 6-24 (b) is on the through route and tare. The turnout rail is seeing c. 400με increase in the strain when compared with the through route. As the gauges are experiencing similar ground condition (as they are attached to the same bearer), the main reason for the strain variation is the dynamic loading of the vehicle is due to weight.

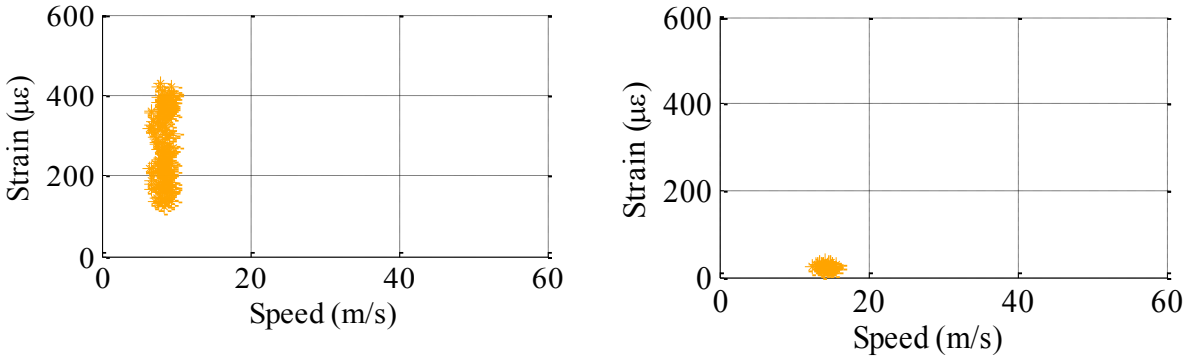

(a) Strain gauge 11 (b) Strain gauge 13

Figure 6-24: Strain gauge results from sleeper 11 at SC4 showing the comparison with the freight on the through route against fraight on the turnout, with higher speed

The frequencies of the contact between the wheel and rail give a greater understanding of the types of loading that are generating the strain. The frequencies from gauges 9 and 13 are shown in Figure 6-25. Frequencies above 100Hz show amplitudes below 1 and are therefore considered to be insignificant.

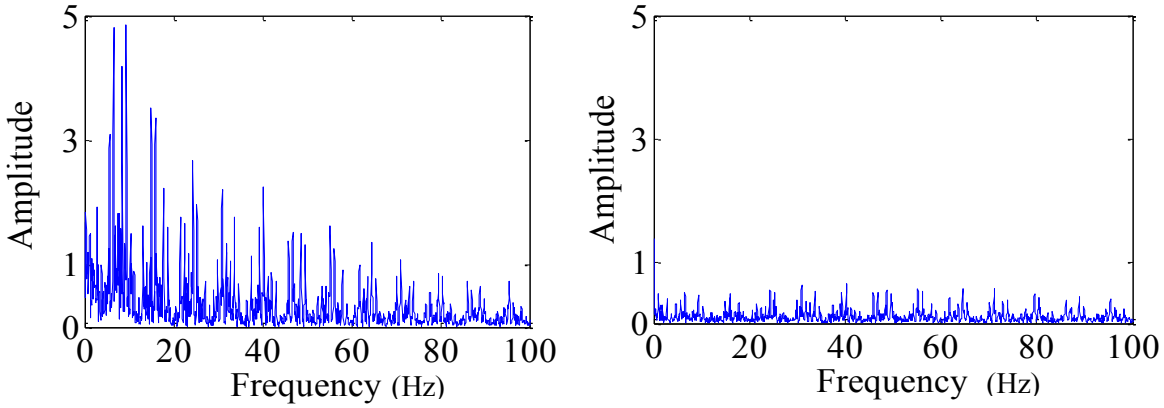

(a) (b)

Figure 6-25: Frequency outputs from Strain Gauge 9 (left) and 13 (right) for SC4

The frequencies that are exciting SC4 are similar to SC3. The lower frequencies (0 - 20Hz) are being excited from the axle spacing and bogie spacing due to the time taken between loading excitations. There are frequencies that are being excited through 40Hz – 65Hz. These frequencies, similar to SC3, are from the unsprung mass and the excitation into the track. There is very little to gain from Figure 6-25 (b) as there are very low amplitudes throughout the frequency range. Strain gauge 13 is showing a limited non-linear time domain, but the FFT results are not as expected. This low frequency content from loading suggests that the gauge results have additional errors in the outputs of the strain gauge.

6.5.7.3 Geophone results

The geophones at SC4 were positioned in the switch panel and at the crossing nose bearer. The outputs from the geophones at these locations are found in Figure 6-26.

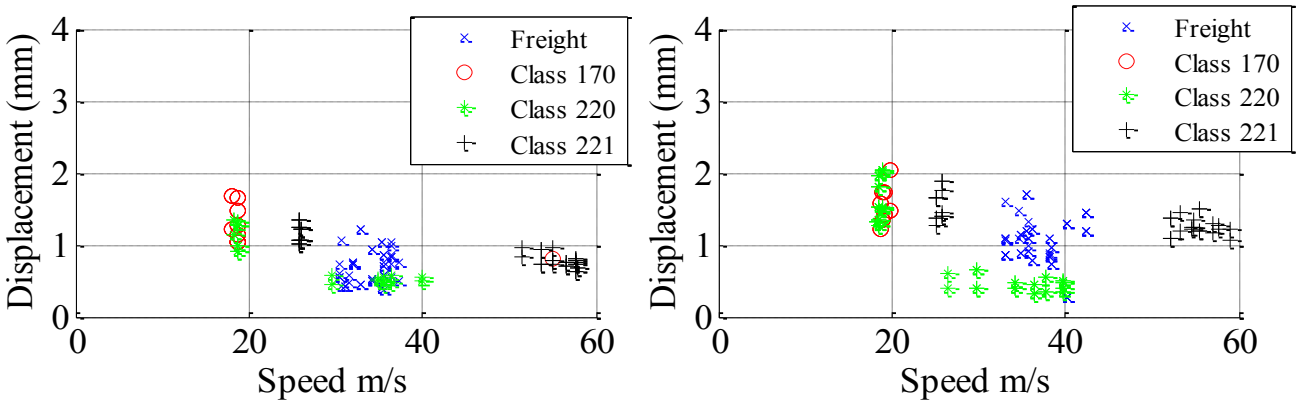

(a) Geophone 1, sleeper 2 (b) Geophone 2, sleeper 42

Figure 6-26: Geophone results from SC4

As seen in the previous sites, the crossing nose tends to show greater displacements for the same vehicles due to the additional mass of the crossing and transfer of wheel creating vertical impact forces. The displacements are low in comparison with SC1, which would see displacements up to 3mm at the crossing. SC4 sees higher speed values so that the combination of higher speeds and inclined rails contribute to lower displacements and lower strains as it was seen in previous areas that higher speed reduced strain outputs.

6.6 DISCUSSION OF FIELD EXPERIMENTAL RESULTS

This field experimental results are the first instance in the UK that S&C have been instrumented for on-going analysis of the material reaction to loading. Instrumentation is vital in developing an understanding the rate of change through current S&C design. Uncertainty of ±1.5% for strain gauges was calculated from the installation of the gauges, gauge factor, fatigue of the gauge and correction through the DAQ.

Filters were applied to the data to remove frequencies that create uncertainty in the outputs, such as EMC and frequencies with small amplitudes (below 1) that contribute to the noise in the signal. Butterworth filters were applied to the instrumentation outputs with two levels, 99Hz for SC1 and 49Hz for SC2 - 4.

SC1 had vertical motion of up to 1mm at the switch under loading and peak to peak strain of up to 200με. SC2 results could not be shown due to considerable difficulties with the instrumentation and high amplitude electrical interference, which generated inconsistent outputs. SC3 had vertical motion of up to 2.5mm at the switch and strain up to 500με. SC4 has vertical motion of up to 1.8mm at the switch and strain up to 150με on the through route, and up to 500με on the diverging route with laden freight vehicles.

The strains were up to 300με larger on the stock rail with the closed switch blade in comparison with the stock rail without switch blade. The reason for the increase is due to the transfer of the contact of the wheel from switch rail to stock rail and the increased dynamics from the change in the contact location and size.

Strain generated at the gauge at the same sites with the same vehicle types show variance of up to 300με. The variance is thought to be due to the lateral loading, the pressure and the geometry as the variations in weight of the vehicle and the speed at each site are considered negligible. A model was generated for plain line rail to understand the change in the strain from lateral loading location and will be covered in Chapter 8.

The continuation of the research is necessary to develop the on-going trends in the existing S&C units in service. The further work includes collecting more outputs, which are used to understand the rate of change from the instrumented sites in place, and completing the second phase of the instrumentation. The second phase is necessary to cover the different parameters of the design of experiments, such as switch length, to monitor deterioration of the current designs. The more data that can be analysed, the confidence of the deterioration trends can be increased.

REFERENCES

1. Vishay Precision Group. TN-508-1, *Fatigue Characteristics of Micro-Measurements Strain Gages,* Toronto. Micro-Measurements; 2010.

2. ION Geophysical Corpotation. *LF-24 Low Frequency Geophone Sensor datasheet.* ION Geophysical Corpotation. 2010.

3. Priest J & Powrie W, Determination of dynamic track modulus from measurement of track velocity during train passage, *Journal of Geotechnical and Geoenvironmental Engineering*, 2009, November: pp1-33.

4. Bowness D, Lock A, Powrie W, Priest J & Richards D, Monitoring the Dynamic Displacements of Rail Track, *Proceedings of the Institution of Mechanical Engineers, Part F: Journal of Rail and Rapid Transit*, 2006; 221 Part F: pp13-22.

5. Shin K & Hammond JK, *Fundermentals of signal processing, for sound and vibration engineers*: John Wiley & Son; 2008.

6. Butterworth S, On the Theory of Filter Amplifiers, *Experimental wireless and the wireless engineer*, 1930; 7: pp536 - 541.

7. Zwanenburg WJ. The Swiss experience on the wear of railway switches and crossings. In: *7th Swiss Transport Research Conference - STRC 07*, Patterson Z. (eds.); September; Monte Verita / Ascona 2007. p. 15.

8. Ashby MF & Jones DRH, *Engineering Materials 1 - An introduction to their properties and application - 2nd Edition*. Butterworth-Heinemann; 2002.

9. Pritchard R & Hall P, *British Railways Locomotives & Coaching Stock 2012: The Rolling Stock of Britain's Mainline Railway Operators and Light Rail Systems*: Platform 5 Publishing Ltd,; 2012.

10. Conrad Quilty-Harper, Andrew Blenkinsop, David Kinross & Dan Palmer. *The world's fattest countries: how do you compare?* : From Telegraph Media Group Limited; 2013 Available from: http://www.telegraph.co.uk/earth/earthnews/9345086/The-worlds-fattest-countries-how-do-you-compare.html [Accessed: 14/05/2013].

11. Walker R. *Mass, Weight, Density or Specific Gravity of Liquids*. 2008 Available from: http://www.simetric.co.uk/si_liquids.htm [Accessed: 17/05/2013].

12. Iwnicki S, Bjorklund S & Enblom R, *Wheel Rail Contact Mechanics*. In: Lewis R., Olofsson U., (eds.) *Wheel-Rail Interface Handbook*. Woodhead Publishing Limited; 2009.

13. Kassa E & Nielsen JCO, Dynamic interaction between train and railway turnout: full-scale field test and validation of simulation models, *Vehicle System Dynamics - International Journal of Vehicle Mechanics and Mobility*, 2008; 46(1): 521-534.

14. Berggren E. G, Martin X.D. Li & Spannar Jan, A new approach to the analysis and presentation of vertical track geometry quality and rail roughness, *Wear - An international journal on the science and technology of friction, lubrication and wear*, 2008, 16th May; 265: 9.

7. PROGRESS OF DETERIORATION

This is the first time that processed instrumentation results have been analysed to understand the key factors in the deterioration of S&C over time. The analysis includes a single train loading through an S&C unit to understand the dynamic loading. Analysis against the design of experiments parameters was completed to understand the progression of deterioration from geometry. The analysis shows higher speed generating lower strain due to change in contact location. The Root Mean Squared strain from the triggered samples was used for the analysis for deterioration against tonnage. Peak to peak strains and displacements were analysed to monitor individual loading cycles and the effect of speed and change in geometry on strain.

7.1 SUMMARY OF RESULTS

The progress of deterioration studies the loading through the S&C unit and the analysis of DOE parameters. A summary of the results that have been found are;

- The trends identified are strong for the data collected, but the deterioration life cycle analysis would have increased strength if more data was collected.
- Strains for 3 sites with varying design of switch, age of asset and vehicle types
    - Stock rails with closed switch blades generate higher strain than open switch blades, which are similar to plain line sections. The increase in strain is due to the transfer of the wheel from the switch rail to stock rail generating higher vertical impact forces through irregular loading.
    - SC1 generates strains up to 200με for all the vehicles, and the frequency of loading through the switch is below 30Hz and due to the car body vertical loading.

- SC3 generated strains of 400με on plain line sections and up to 600με on the stock rail with the closed switch blade. The frequency content is higher than SC1, and includes influences from the unsprung mass and track stiffness, between 40Hz – 80Hz.
- SC4 generates strain up to 200με, and the frequency within the loading is from the car body and unsprung mass, which is similar to SC3.

- Geophones for 3 sites
  - SC1, the reference site, has an increase in vertical motion against time from 1.4mm to 1.95mm over a 6 month time period at the crossing and 0.5mm to 0.7mm at the switch due to settlement of ballast.
  - The maximum displacement at SC3 at the switch is 2.7mm, with the geophone at the crossing reaching the maximum of 20mm of peak to peak displacement before becoming detached due to the large vibrations dismantling the housing.
  - SC4 shows the displacement of 1.8mm at the switch and up to 2mm at the crossing.
  - Increased displacement does not induce greater strain, but there is an increase in the displacement over time for all sites, with a similar gradient.

- Accelerometer for the reference site SC1
  - The value for acceleration at the switch and crossing are small, with values of 0.04g. The value for acceleration has been constant since the start of the investigation.

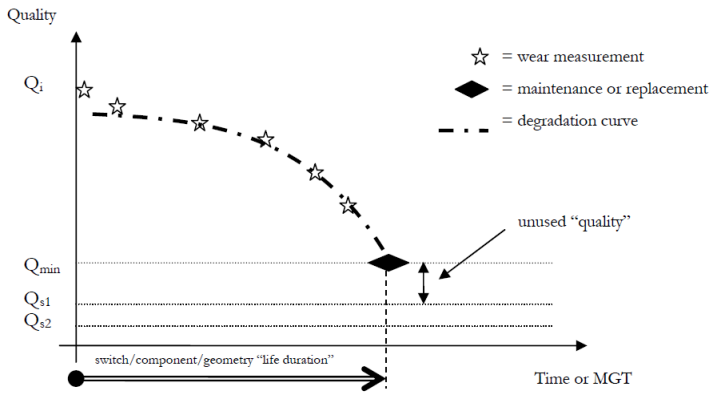

Figure 7-1: Quality during the life of S&C or its components [1]

7.2 SUMMARY OF INDUSTRY KNOWLEDGE ANALYSIS

Zwanenburg [1] found that for 'standard' turnouts (common crossing with turnout design switch) with heavy loading, the life expectancy would decrease with angle. A smaller angle (a large curve) leads to longer life due to the vehicle dynamics generating reduced longitudinal (slip) and lateral forces (angle of attack) through the contact patch. Bad soil quality has a negative linear relationship on the expected life of the asset, due to the increased dynamic forces that are generated through increased loading onto a poor foundation. Figure 7-1 shows the degradation of the life of the asset and the quality of switches and crossings throughout the life of the asset.

Zwanenburg found through renewal data in Switzerland that speed has a negative linear relationship to the life time distribution [2]. The time for the dynamic interaction between the wheel and the rail was extended at lower speeds and exacerbating any foundation irregularities.

Through the chapter, strain values will be compared with Zwanenburg's statistical / replacement analysis and modelling to give a comparison on some of the other research outputs. This comparison and expansion will increase the degradation knowledge of S&C for additional maintenance, and focus for the UK infrastructure.

7.3 LONGITUDINAL LOADING THROUGH SWITCH PANEL

Switches have longitudinal variable profiles to allow for transfer of vehicles from one line to another. There is potential for the strains to vary along the switch panel due to change in the contact location and distribution of load. A comparison of the strains generated through the length of the switch has been completed to show how this change affects the degradation. Figure 7-2 shows the corrected vertical RMS strain through the switch and some axial comparison shown in Table 7-1. The strains in Table 7-1 have been rounded to 1dp due to the gauge outputs and the errors levels showing that any result smaller would be insignificant. The corresponding gauge locations are shown in Figure 6-5.

Table 7-1: RMS axial strains converted to actual strain the various stages through the switch panel for (a) the inside (rail 1 and 2) of the curve and (b) for the outside (rail 3 and 4) of the curve

Axial actual strain					Axial actual strain				
SC1	Vehicle	Freight	Pass Cl220	Pass Cl170	SC1	Vehicle	Freight	Pass Cl220	Pass Cl170
	Speed (kph) / Sleeper	47.8	59.6	56.8		Speed (kph) / Sleeper	47.8	59.6	56.9
CH02	2	90.6	72.7	70.9	CH07	7	81.8	68.5	--
CH04	2	--	--	--	CH09	7	73.4	73.4	73.2
CH29	2	114.8	88.8	86.6	CH34	7	106.3	77.0	78.4
CH31	2	--	--	--	CH36	7	--	--	--
(a)					(b)				

The connecting lines in Figure 7-2 have been used to associate the same rails and do not mean that the strains are linear between the gauge locations.

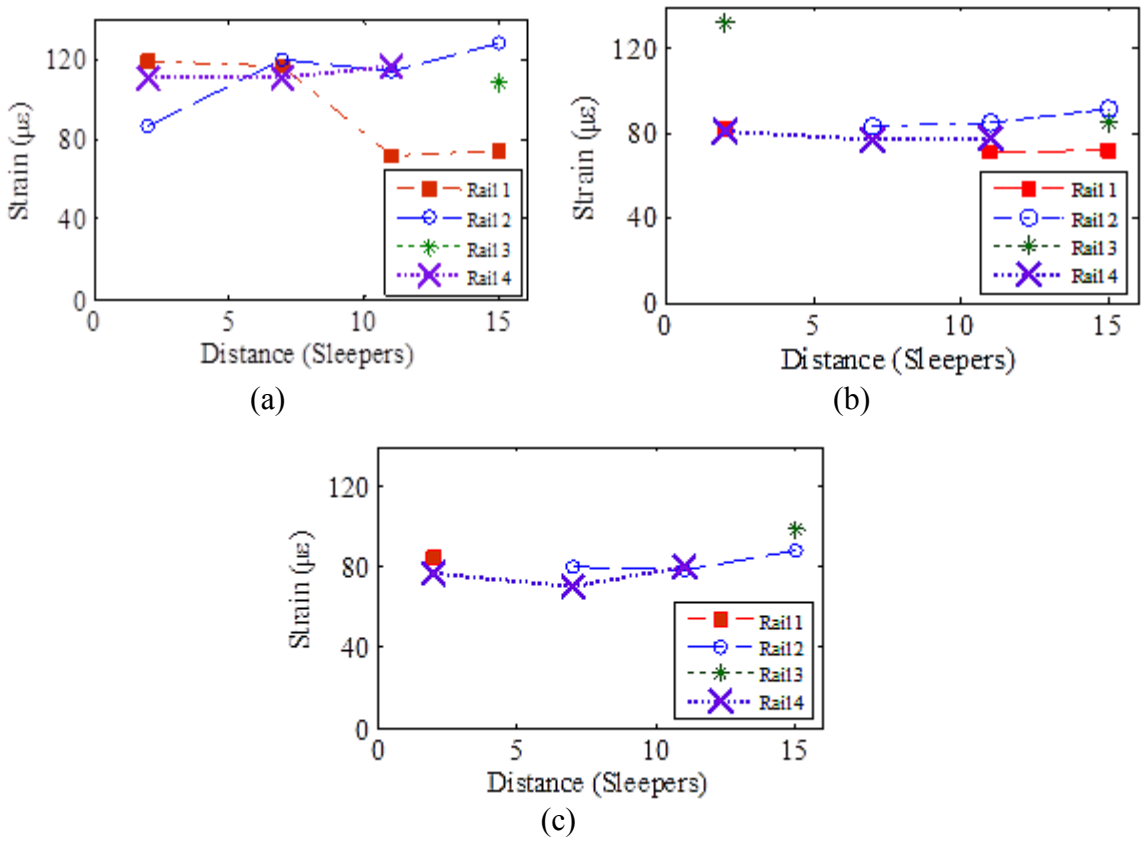

Figure 7-2: Transverse RMS strains for (a) freight vehicle,(b) passenger class 220 and (c) a passenger class 170

At sleeper 6 and 11 for the freight and Class 220, there are strains generated on more than one rail / side, i.e. Rail 3 and 4, or 1 and 2. There are three possible assumptions that can be made;

- There is multi-point / rail contact between the wheels of the vehicles and various rail sections. With multi-point contact, there is an expectation that the loads would be distributed between the contact points as the weight of the vehicle has not changed.
- The whole structure is bending and adjoining / connected assets are vertically displaced. Rail 2 is loaded by a vehicle, the sleepers move vertically and the connected components, Rail 1, traverse in the same direction. This generates a strain at the gauge on Rail 1 through vertical elongation of the unit.
- The stress transfer block, on sleeper 12, causes the strain from one to be transferred into the other rail, seen in Figure 7-3.

Figure 7-2 shows that the cumulative strain is being generated through the switch panel. With additional strain entering the system around the transfer zones, increased degradation would be expected through asymmetrical loading and potential to increase the yield strain of material past the elastic limit and generate plastic flow.

Due to the location of these some of the outputs (sleeper 11 from the switch tips), assumption 1 (multi-point contact) should be ruled out. It is highly unlikely that at the flexible point of the rail (sleeper 11) that there would be more than one rail in contact with the wheel due to the distance between the rails, as shown in Figure 7-3. This assumption could still be feasible closer to the switch tip, where the rails are in contact.

The cumulative values for the low rail (inside of an 880m radius curve, Rail 1 and 2) of the track for the freight have over 200με. Whilst individual strains being generated are less than 120με, the wheels are contacting with more than one rail, giving a total strain in the region of over 200με at sleepers 2 and 7. At sleepers 2 and 7 it is assumed multi point contact is occurring. As vehicle weight cannot change drastically, additional dynamic loading are present at these locations, which would increase the likelihood of deterioration through cyclic loading through exceeding of yield of the rail steel.

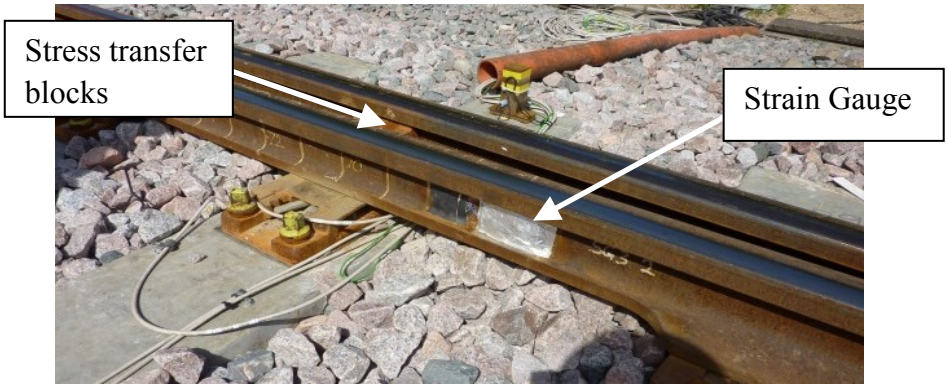

Figure 7-3: Flexible section of the rail a sleeper 11 demonstrating the gap between the rails and location of stress transfer block in relation to gauges

The region that the wheel transfers from switch rail to the stock rail is called the wheel transfer zone. In the wheel transfer zone various vehicle types behave differently. For the Class 220, the outside rails (rail 3 and 4) come into multi point contact around the switch tips. The Class 170 does not seem to have similar results, with one point contact in all strain gauge locations along the switch panel due to the curving ability of the vehicles; the Class 220 with a stiffer yaw suspension. A high (stiff) yaw suspension allows for a stabile yaw motion on straight track, but is more damaging aspects to rail on curves. The transfer of loading of the passenger vehicles occurs between sleeper 6 and 11.

The loading through the switch panel focuses around the wheel transfer zone, with strain at multiple rails at the gauges. The flexible section also sees multiple loading, due to additional rail components and their connection. The axial data shows that freight vehicle generate the highest longitudinal strain, with outputs up to 140με. The transverse loading through the switch shows that there is similar loading through the length of the switch, with additional loading through multi-point contact and strain gauge loading. The areas with multipoint contact and higher magnitude loading are the locations of increased degradation due to the complicated contact through irregularities and distribution of loads.

7.4 RATE OF DETERIORATION

Analysis of the data collected is the first step in condition monitoring process and can set trigger levels in the predictive maintenance development. The analysis section focused on the change of strain under tonnage as tonnage has greater significance to the degradation of the material compared with time due to the degradation occurring from tonnage.

7.4.1 Cumulative tonnage trend analysis against strain

The instrumentation was placed on S&C units with varying time in service and different yearly loading due to the key parameters found in failure statistics and previous studies [2]. The variation in age of the S&C units is to give a representation of the development of strain over the life cycle. The variation in the age and the cumulative tonnage allowed monitoring of the change in strain due to the total tonnage that had traversed the units.

Figure 7-4 (a) – (e) show the vertical RMS strains being generated at the various sites and location. The gauges in each figure are at the same location longitudinally along the sites.

The strains shown in Figure 7-4 (b) demonstrates that there is a162% increase in response due to the contact from one rail to another under 125MGT. When this is compared with the 70% increase from Figure 7-4 (a), it shows that the increase in strain is not wholly due to the cyclic contact, but that additional dynamic forces are increasing the cumulative strain seen within the switch.

Results from Rail 4 have not been shown due to the small (31 of 123 datasets) number of datasets that exceeded the 50με RMS trigger. The change in strain is highest towards the switch tip, seen in Figure 7-4 (b). Figure 7-4 (d) is showing larger strain, however, this is due to loading of heavier axles on the turnout route of laden freight. The trends for each of the rail outputs are completed in a trend fitting function in Excel software. Figure 7-4 (b) shows a positive quadratic and (d) shows a negative linear representation due to the inclined rail at heavier tonnage. The inclined rail causes a change in the contact condition between the wheel and rail, as shown in Figure 7-7. The effect of the change in lateral contact locations are investigated in Chapter 8.

7.4.2 Geophone analysis at the crossing of SC1

The geophone deterioration analysis was completed in collaboration with LLP at the UoS. For the analysis, additional geophones were installed onto the crossing panel at SC1, as shown in Figure 7-5. The locations of the geophones were selected at a higher longitudinal frequency than the experimental monitoring as it was completed as part of another set of research objectives from Track21. The purpose of this section was to see how the vertical displacements and velocity of the units alters longitudinally and with cumulative tonnage.

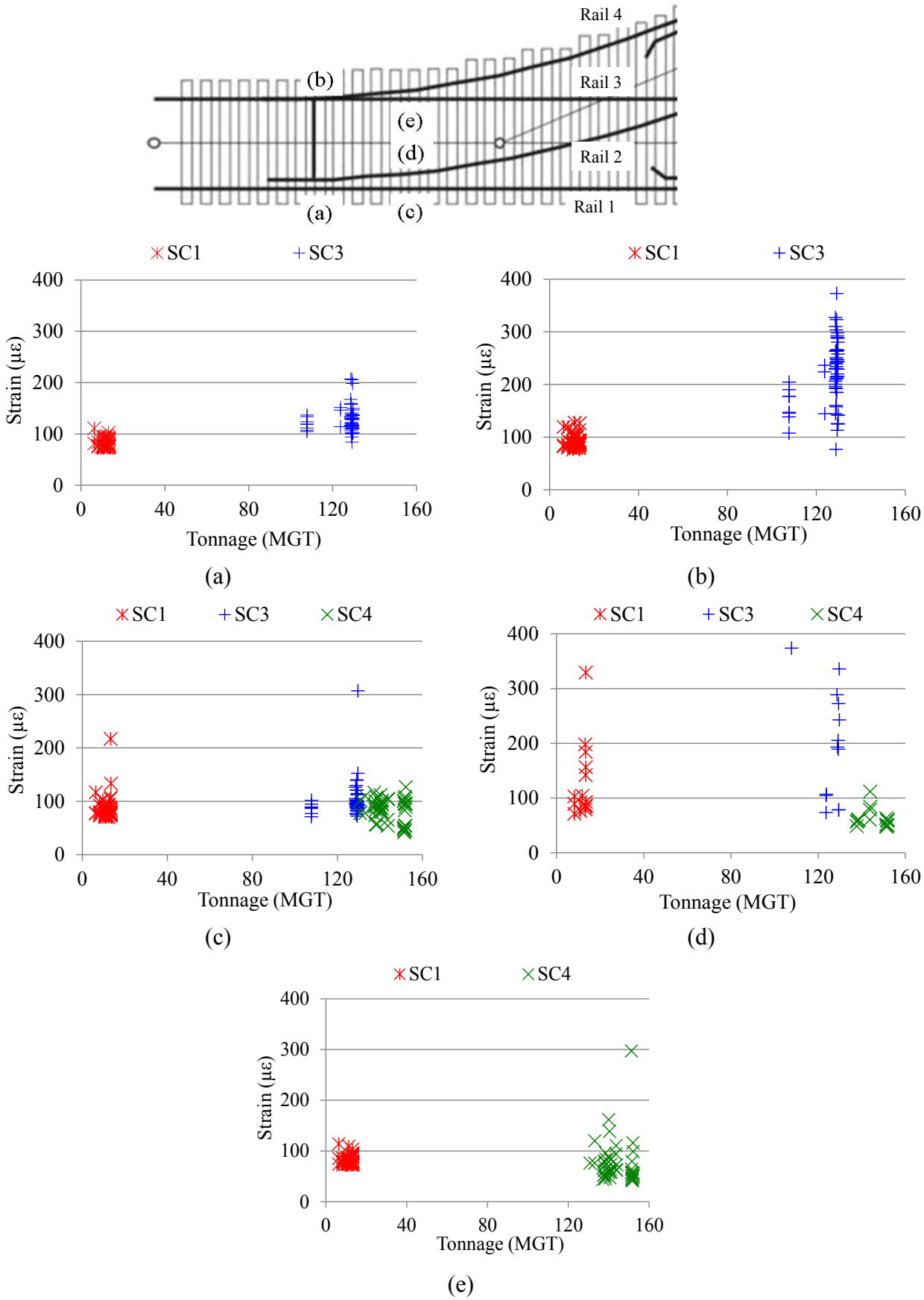

Figure 7-4: Root-mean squared (RMS) strains for the different sites against the total tonnage at the respective sites

The same assumptions, sensitivities and instrumentation noise are present as described in Section 6.2 - *Error levels,* and Section 6.3 - *Instrumentation output and correction factors.* Three visits were completed at SC1 over a 6 month period. Figure 7-5 shows the output from each visit for the various geophones.

The sleeper under the crossing nose moves the up to 2mm vertically, with larger loading on the crossing rather than on the wing-rail. The large deflections are from the high mass of the crossing and the small contact between the wheel and rail due to the variable profiles and discontinuities in the running path on the crossing. A trend for all geophones at SC1 is an increase in the deflection over time, due to the settlement of ballast and degradation of under sleeper stiffness. Over the 6 months of monitoring between July 2012 and Jan 2013, there are insignificant increases in the strain due to this increase in deflection, which can be seen in Figure 7-5 and Figure 7-6.

A correlation between vertical displacement and strain can be achieved through monitoring at the same locations. Vertical displacement, Figure 7-5, and change in strain, Figure 7-6, are collected on the crossing at SC1 to show the change and the correlation between the two parameters. Figure 7-6 shows the RMS bending strain from the gauges at the crossing, and the location of the specific gauges. The gauges are orientated longitudinally, showing bending strains over 1 year. The gauges were positioned over the sleepers, as it was found through failure statistics, that the fracture tends to happen over the sleeper. This is due to the crossing bending more through poor under sleeper conditions, reducing the support and allowing a greater distance between support locations. Gauges 61 and 65 are on the typically used route, and gauges 59 and 63 on the lesser used turnout route. Gauge 59, 61, 63 and 65 outputs are below 200με. Strain gauge 61 has the highest mean value throughout the measurements, but the results over time show a linear representation, with a gradient of zero.

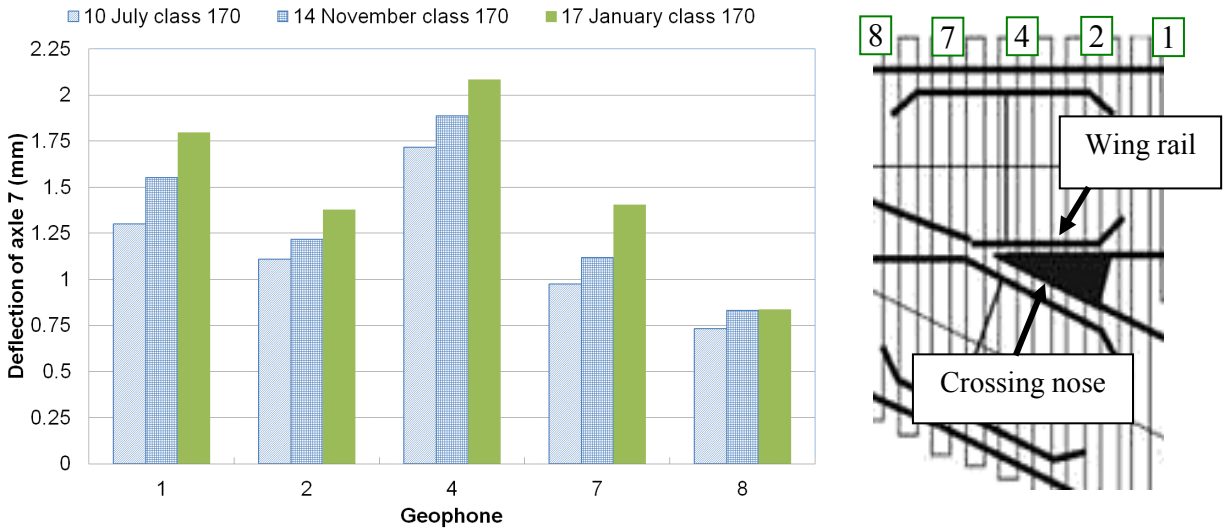

Figure 7-5: Deflection change over time at SC1 for the various geophones and their locations

The comparison between displacements and strain over time has not previously been completed. The strains seen at SG63 are around 65με on the crossing are due to the crossing being loaded on the through route (loading above gauge 65). The bending affects the whole asset, exceeding RMS trigger values at gauge 63. From the analysis of Figure 7-5 and Figure 7-6, the increase in the deflections of the infrastructure, in some cases 0.6mm over 5 months, are not demonstrating similar increases in strain through the crossing.

The reasons for the increase in deflection not affecting the strains are:

- The loading of the vehicles are similar over the crossing, similar weights, similar speeds which contribute to the similarity in strain
- The whole asset is deflecting at similar vertical rate, thus the change in strain is relatively small.

As the vehicles are different, with different mass (but similar speeds) this idea could be ruled out. Thus, the whole crossing unit increased the deflections at a similar rate, maintaining the material deflection at a similar rate.

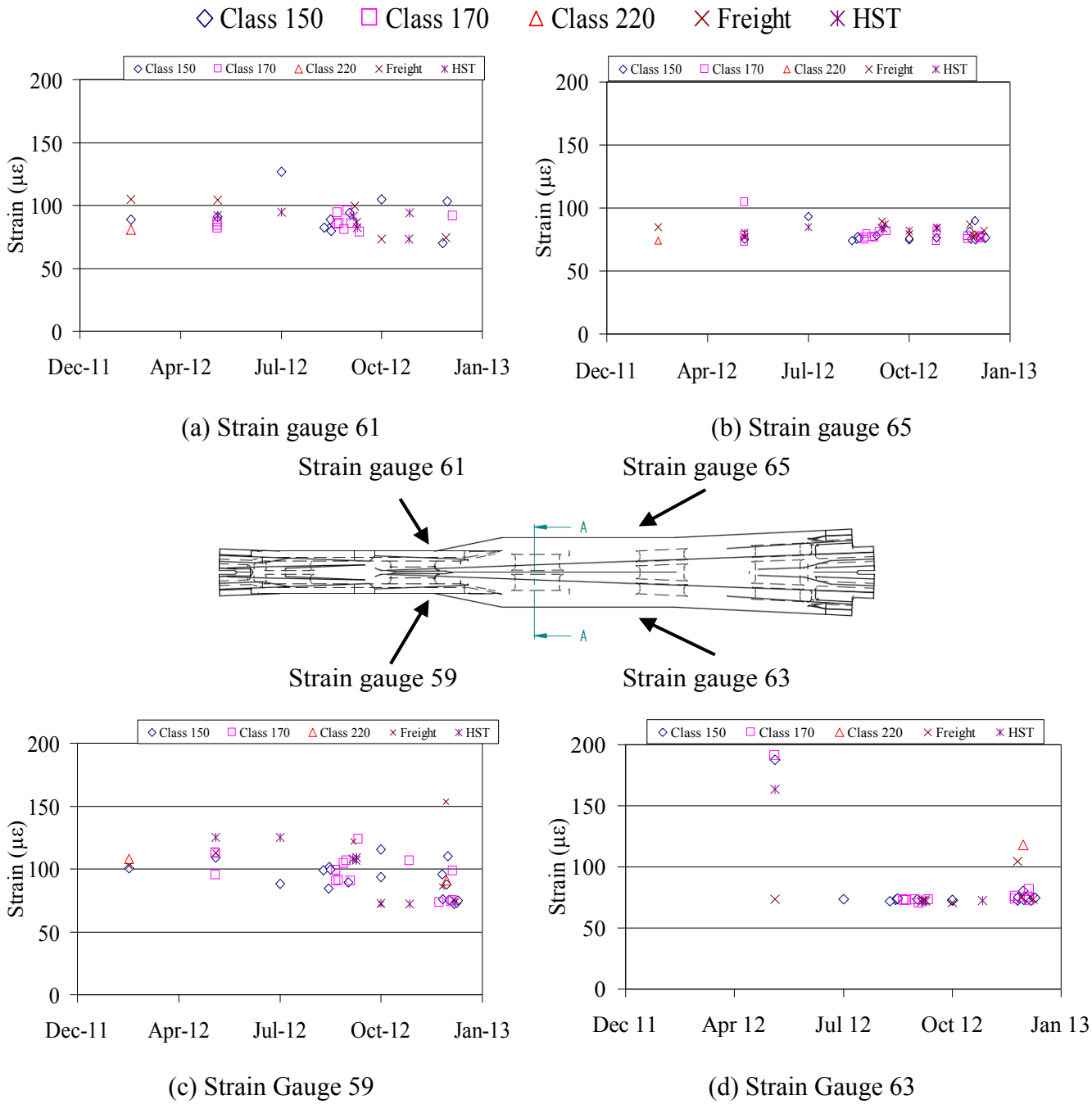

Figure 7-6: Change in strain over time at the crossing on SC1 with an image of the gauge location in the centre

7.5 DESIGN OF EXPERIMENTS ANALYSIS

Within Chapter 6 – *Design of experimentation*, the investigation found six parameters to monitor the deterioration of S&C. The parameters that are analysed in this section are;

- Line speed alters the dynamic effect on the irregularities
- Track quality was shown to exacerbate deterioration
- Annual tonnage with higher annual tonnage tending to experience more plastic deformation.

Switch design, rail inclination and traffic type do not draw conclusions due to the limited instrumentation outputs. The parameters are summarised and the reason for their inclusion in the design of experiments.

The next section will go through the parameters, the levels that have been chosen and instrumented and the effect the parameter has on the strain generated to monitor the degradation on similar loading types.

7.5.1 Switch design

The switch design for sites SC1 to SC4 are all the same angle turnout, D length, vertical design (please refer to Section 5.2.1 for further details). With only the same switch turnout length instrumented in the first phase, any trends are inconclusive for the switch design parameter. It has been previously shown [1, 2] that the longer switch length and long crossing angle generated lower strain on the turnout route due to a reduction in the wheel – rail creepage. It has also been seen [3] that the direction of the traversing move (facing or trailing) generated similar strain results in either direction.

7.5.2 Rail inclination

SC4 had inclined stock rails [4] (at 1:20 inclination, which is common for inclined rail in the UK, Germany has some 1:40) through the length of the switch. *Figure 7-7* shows the difference in contact between the inclined and vertical rails. Sites, SC1, 2 and 3 have vertical stock rails through the S&C. Inclined switches removes any transfer from inclined rail to vertical for the S&C which would alter the contact location and therefore the vehicle dynamics. Switch rails, including inclined S&C, are vertical due to the design of the baseplates and the difficulties of operating the switch on an inclined plane.

The RMS for the gauges 9-20 at SC4 show that on the full section of the rail within the closure panel, the strains generated are lower than those seen on vertical S&C.

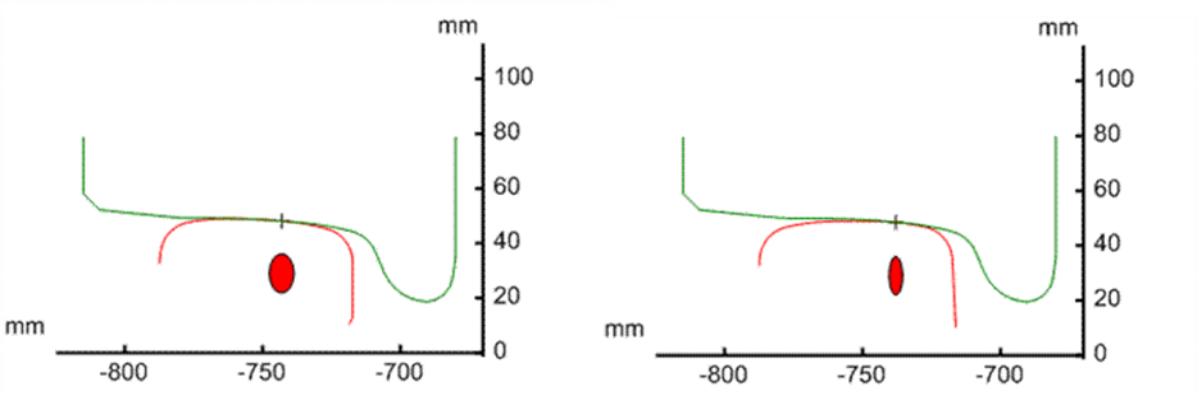

(a) (b)

Figure 7-7: Varying contact conditions for the (a) inclined rail and (b) vertical rail against a common (new P8) wheel profile, processed through Vampire© software

The lower strain seen at the inclined rail shows that the loading due to pressure is smaller at SC4. The larger contact patch on the inclined stock rail is shown in Figure 7-7 which is generated due to the wheel and the rail having increased conformity which increases the contact patch. As the gauges at the switch tips were not working due to damage, no conclusions could be drawn regarding the inclination parameter on the switch blade.

7.5.3 Line speed

From the DOE, the speeds seen at SC1 and SC3 are different, with similar switch lengths and inclination. It can be seen through the strain against speed graphs in Figures 6-7 to 6-16 in Chapter 6. To understand the relationship between the speed and the strain, a polynomial evaluation has been completed giving a relationship between the sites. The relationships will give a greater understanding if speed is a key parameter, on the through route, for maintenance of S&C from the variation in strain.

Peak to peak strains were collected from the site outputs using vertical strain gauges. The values of strain were plotted against the speed in m/s for each site. The peak to peak strains were inputted into Matlab software, and a *polyfit* [5] analysis was run to monitor the representation. *Polyfit* is a function built in Matlab function to fit the various polynomial to the data, with an input being the type of function; linear or quadratic, to give the least squares analysis. Cubic was found to have a small relationship to the data, and so has not been used.

For plotting purposes, the representations have been shown against the original peak to peak strain. For plotting, function *polyval [6]* is used within Matlab. *Polyval* uses the line function calculated from the *polyfit* and determines values for the equivalent polynomials, which is then plotted, as shown in Figure 7-8.

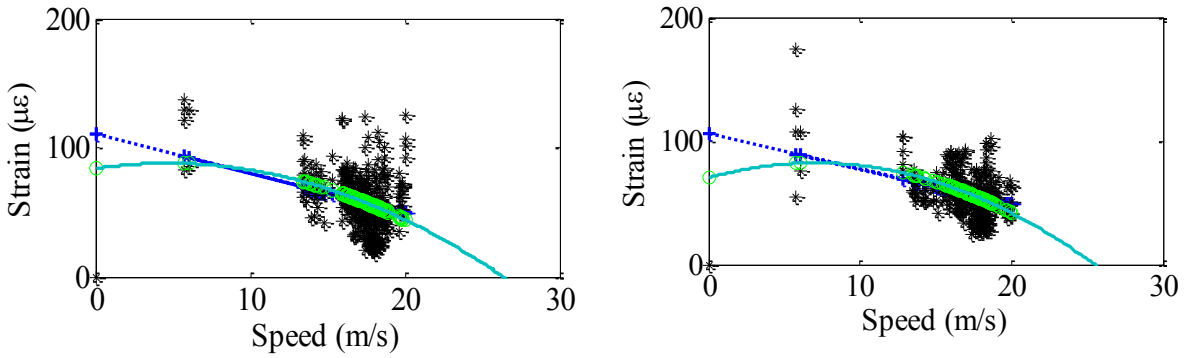

Figure 7-8: A linear (blue) and a quadratic (green) relationship between speed and strain for Strain Gauge (a) 1 and (b) 28 from SC1

The line of 'least squares' is determined from the best fit of the relationship between the strain data and the polynomials. The residuals of each of the points of the polynomial against the original point are calculated, with the smallest total residual giving the best fit.

Figure 7-8 show the relationship between the peak to peak strains and the speed for Strain Gauge one and 28. The linear relationship is negative (i.e. the gradient is decreasing) with a gradient of -2.7x has the best fit. The quadratic lines are similar in shape and quantities but have larger residual in comparison due to the variance at lower speeds.

All the graphs and gradients are similar at SC1, with 3 (out of 16, 19%) gauges in the switch showing a positive linear relationship. The positive linear relationships occurred at Strain Gauge 8, 38 and 44 at SC1, with a mean gradient of 0.6x. The positive linear gauges are all on the outside of the curve. The additional forces generated as the vehicle traverses the switch, outputs the low positive gradient against speed. The gauges are all vertical gauges, within the switch area. The gradient shows that the faster the vehicle is travelling, the strain at the gauge is reducing.

In the SC3 speed analysis, the linear and the quadratic representation were very similar in both shape and initial values. Gauges at the switch tip, on the open switch blade, show a negative linear relationship, and in the closed switch blade it was positive linear relationship. The change in the relationship is due to the increased dynamics that are occurring on the

closed switch blade, generating higher strain at higher speed and transition from one line to the other.

SC4 has very similar representation between linear and quadratic representation again, but with the gauges not being at the switch, the increased dynamics from the transition are not present and a negative linear representation is found.

The analysis has shown that in the majority of cases, there is a negative linear representation of strain with increased speed at the switch. Analysis shows a linear representation with gradient of 0 at the crossing, (c.f. section 7.4.2). This conclusion is different to the results found from the vehicle instrumentation by Kassa [3] that showed increases in the wheel – rail force with speed. The difference in conclusions is with an increase in speed, the point of contact changes location to another section of the crossing due to the dynamics of the vehicle shifting the high magnitude loading further down the track. This reduces the strains seen at the gauge at a fixed location, but would increase those seen from the instrumented wheelset as that would be taking the maximum point over the S&C unit.

7.5.4 Track quality

Track quality can be measured using the track recording vehicles that traverse the infrastructure on a rolling cycle. The New Measurement Train, NMT, is used to collect dynamic geometry whilst running at line speed across the network. In the initial DOE, track geometry was highlighted as a parameter due to Zwanenburg's [1] work on soil quality and degradation of the asset in comparison with geometry. The NMT data was collected over a few years for a few of the sites. With SC1 the NMT was not travelling at a required speed to record the geometry data due to manoeuvring onto another mainline. A single manual geometry reading was collected, using an *Amber*© trolley, which collects unloaded gauge and cross level. Dynamic geometry was not possible due to the weight of the instrument collecting the data not able to dynamically load the infrastructure.

Figure 7-9 shows an example of the change in the geometry against the initial geometry collection and the strain in Figure 7-9 (d).

The distance in metres along the x-axis in the geometry readings is from the origin of the recording run. The S&C have been marked on the distances. The gauge is the distance

between the rails at 14mm below the crown of the rail, with 1432mm for vertical S&C as standard. Cross level is the difference in height between the rails longitudinally, with 35m vertical alignment monitoring the cant / crosslevel of the vehicle over a 35m wavelength.

For SC1 the geometry was aligned to the design parameters that were set at installation in 2011. The rate of change for gauge, the difference between the two rails at 14mm below the crown, is c. 1.5mm for the static gauge and cross level from design. This increase in gauge is over time and has aligned with a very small increase in strain, c.20με. The maximum rate of change in SG1 is 5% increase, which demonstrates non-pertinent change in strain with a 5% difference in the geometry.

With SC3 there are three recordings that can be used to monitor the rate of change in the geometry and compare with the change in strain. The NMT recordings were in January 2011, January 2013 and June 2013. The strains are not recorded up to June 2013 but should be used in on-going analysis to monitor degradation of material.

Figure 7-9 shows the gauge, cross level and vertical alignment variations from the January 2011 recording at SC3, with additional plot of the RMS strain. The SC3 switch toes are at 258420m from the beginning of the geometry run, with the crossing nose at lower mileage to the switch, at 258374m. There was a variation in the recording speeds at which the geometry was collected; January 2011 was recorded at 122mph (196kph), January 2013 at 77mph (123kph) and June 2013 at 123mph (198kph). The variation in speed has an effect on the outputs from the NMT, but it is not considered to be the complete reason for the change in geometry.

For the individual readings that have been taken from the recording car, the gauge and cross level and alignment are within maintenance tolerance according to NR/L2/TRL/001 inspection standard. The outputs from the geometry vehicle show that there is a small change, but this is not significant to change the contact location and the magnitude of the loading, which can happen with a variation in the geometry.

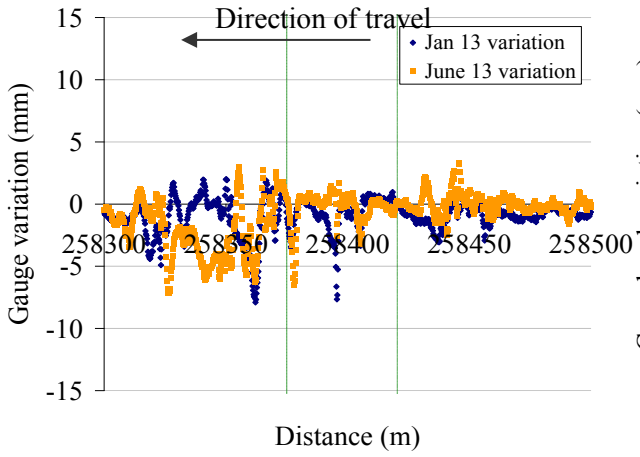

(a) Gauge variation

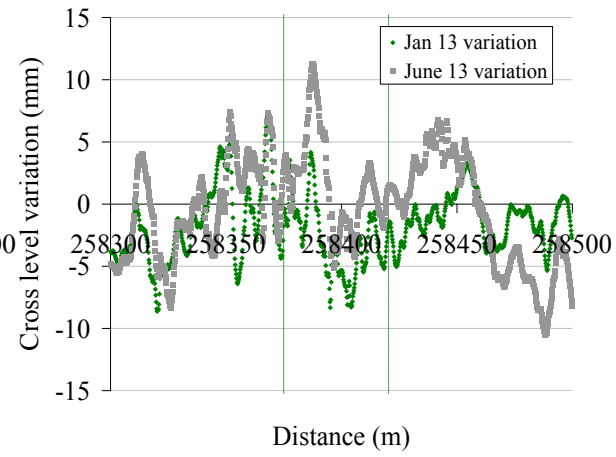

(b) Cross level variation

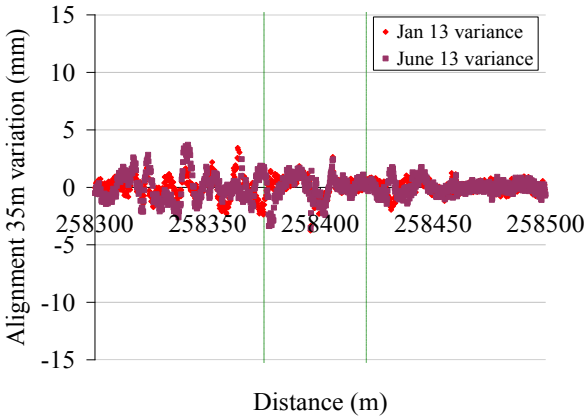

(c) Vertical alignment with 35m wavelength

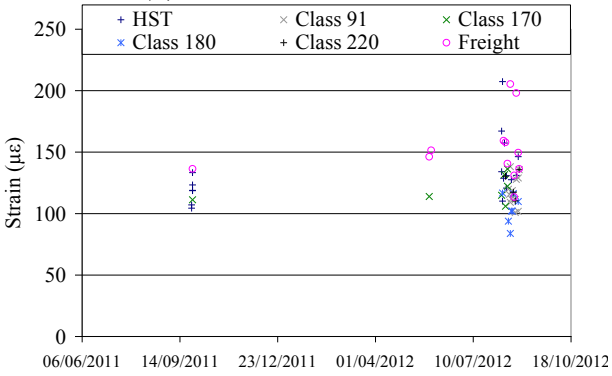

(d) strain results over duration of project

Figure 7-9: (a) – (c) show the variation in the geometry measured on the new measurement train with (a) the gauge variation, (b) the cross level variation and (c) the vertical alignment at 35m wavelength. (d) shows the strain gauge outputs from SG3

The results are only useable at the locations of the gauges, with 2m from toes, 11m from toes and at the crossing (not applicable at the crossing in this example in Figure 7-9). From the strain gauge RMS results shown in Figure 7-9 (d), at 2m from the toes there is a lateral misalignment of 5mm from the original collected data between January 2011 and January 2013. A Class 220 at similar speeds shows a variation of 101% of the strain at SG1. The variation is due to the change in cross level as other geometry outputs are similar for that time.

At SC4 there was a vertical alignment increase of 4.5mm, contributing to an increase in the RMS strain of 60% for the same vehicles in some cases, and zero change in others. The variations show that for maintenance, focus should be on the alignment of cross level, to keep the strain generated by the dynamic loading, with vertical alignment and gauge showing a smaller increase.

From the strain measurements and the study of the track geometry over time, it has been seen that the major contributor to the change in strain is the lateral / cross level loading, with over 100% of the original RMS strain measured with 5mm of variation in measured geometry.

7.5.5 Traffic type

According to Zwanenburg [1], the less freight percentage seen over the infrastructure will reduce the life of the asset, with less than 50% freight seeing the shortest cumulative life due to the S&C track staying in track longer than those with significant passenger vehicles. Percentage of freight vehicles (locomotives and wagons) against the total train tonnage from the ACTRAFF data at each site are shown in Table 7-2.

Table 7-2: Freight percentages for the different sites that have been instrumented

Site	SC1	SC2	SC3	SC4
Freight (%)	*46.5*	*47.7*	*48.4*	*41.6*

The asset database shows that the site with the shortest life in service is SC3, with typical rail replacement every 2.5 years (or on average 60 million gross tonnes (MGT)) due to the rail head being damaged beyond repair through the switch. This tonnage is much less than the examples shown in Zwanenburg's thesis, which shows 200MGT for the lowest percentage of freight, which shows that the other aspects were pertinent to the deterioration at SC3.

Not many conclusions can be drawn from the degradation due to freight percentages due to the information being finite. With an increase in the data, there would be increasing certainty towards the freight percentages against the replacement tonnage.

7.5.6 Annual Tonnage

Annual tonnage has been shown in the analysis under section 7.*4 – Rate of deterioration*. The positive linear representation was the most common relationship over the similar gauge locations at various sites. The influence of some of the factors, such as the rail inclination of SC4 seems to have had a positive effect (reduced strain values) on the degradation over time

with increased contact patches size. Poor geometry at SC3 seems to have increased the strain values by increasing the magnitude of loading.

A extension of the trend analysis will need to be continued to gain some more conclusive outputs from the analysis, and has been highlighted for as future works. The annual tonnages for the sites with currently working instrumentation are;

- SC1 – 11.6MGTPA (17EMGTPA)
- SC3 – 15.5MGTPA (24EMGTPA)
- SC4 – 8.9MGTPA (13.2EMGTPA)

From the outputs shown in Figure 7-4, the increase in the tonnage of SC3 shows that there is a negative effect on the strain generated within the rail, showing higher strain values. The main contribution to the change in strain would be the degradation of the ground geometry / condition that allows the vehicle to increase the shear strain, which would affect the geometry through deterioration.

A least squared analysis was completed for axle weight. With the strain gauge being a linear output device, under zero weight, zero strain is expected. An additional linear relationship (red) has been added to Figure 7-10 to demonstrate the linear relationship that goes through the (0,0) axis. Using the least squares analysis, the quadratic relationship gives the best fit, but has a value of -145με at zero weight. As the negative value at zero weight is unrealistic, the relationship is considered to be linear through (0,0) due to the limitations of the quadratic relationship at lower weights. This is reliable as under zero load, there would be zero strain.

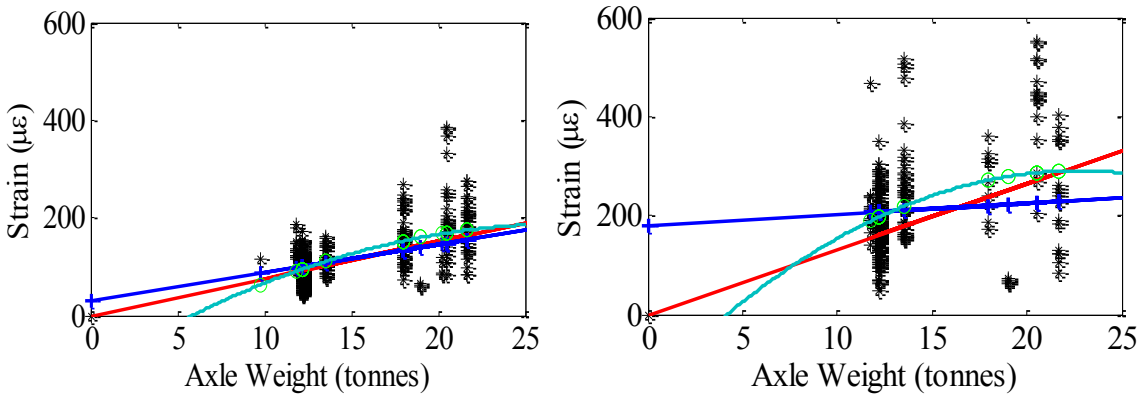

Figure 7-10: A linear (blue), linear through (0,0) (red) and a quadratic relationship (green) for weight against peak to peak strain at strain gauge (a) 1 and (b) 7 for SC3

Figure 7-10 shows the peak to peak strain for gauges 1 and 7 at SC3. The strain is increased with axle weight due to the higher loading applied at the surface. The closed switch blade has a much steeper gradient due to the higher magnitude loading from transferring from one rail to the next. This was shown in Section 7.4.2, and demonstrated that over a period of c. 120MGT, the increase in strain is c. 90% greater on the stock rail with the closed switch against the stock rail with the open switch.

7.6 FAST FOURIER TRANSFORM ANALYSIS

The Fast Fourier Transform (FFT) analysis has only been completed on the strain to monitor the change of excitation through deterioration. Additional work on the frequencies present through the sleepers, using geophones, will be completed at a later date and highlighted as part of the further work from the collaboration work with UoS.

FFT results were shown for the sites in Chapter 6. The results showed that the frequencies range being excited was expanding for SC3 in comparison with the others, due to the ground degradation allowing larger frequency ranges to be excited. The amplitudes are the number of vibrations at certain frequencies within the datasets. SC4 had larger amplitudes than SC1. Explanations for this include;

- SC4 tends to have longer trains than SC1 due to the location on the network and the capacity and scheduled running.
- Increase in the vertical displacement (c. 1mm at SC1 and c. 1.8mm at SC4), although this would tend to change the frequencies that are being excited, which are also present in Figure 6-25.

From the analysis, the increase in the amplitude of the frequency will be due to the increased number of vehicles, with the change in the frequencies that are excited due to the change in vertical displacements and the unsprung mass ability to excite through reduced support of the assets.

7.7 DISCUSSION OF ANALYSIS OF DETERIORATION

The analysis that has been completed on the strain and vertical displacement is novel as the instrumentation outputs that are used in the analysis have not been collected through the S&C panels previously. The conclusions that have been drawn are from the data that was available. An increased confidence could be gained through increased duration of data.

The analysis of the strain data and vertical displacement data show;

- The highest cumulative strain at the locations of the gauge are between 6 and 7 sleepers from the switch tips (4.5m from the tips) due to multiple point contact increasing the loading through increased dynamics.
- Additional strain is found at sleeper 11 for the heavier vehicles due to the rail structure loading vertically and moving attached components, generating a strain.
- Analysis shows that the largest increase in peak to peak and RMS strain over time is at the stock rail with the closed switch blade. The increase in strain is due to the transfer of the vehicle from the switch blade onto the stock rail generating a high magnitude loading.

A polynomial analysis was completed to determine the relationships between the parameters set out in the DOE in Chapter 4. The analysis from the various sites shows that strain has a negative linear relationship with speed due to the contact and the peak forces moving longitudinally away from the directly above the gauge.

Weight has a linear relationship through (0,0) due to the design of gauge, with zero load outputting zero strain (excluding noise). The gradient of the linear polynomial varies depending on the site, with an increase of the gradient at the older sites compared with the newer site. Increased strains are due to the older infrastructure and reduced foundation stiffness.

Track quality, and vertical motion has a damaging (increasing) effect on the gradient of the speed plot at the crossing. The larger the vertical motion, the larger the gradient of the strain against tonnage being generated. This is due to the increasing dynamic loads applied to the system, which increases the degradation rate of the switch and crossing units.

REFERENCES

1. Zwanenburg WJ. *Modelling Degradation Processes of Switches & Crossings for Maintenance & Renewal Planning on the Swiss Railway Network.* PhD Thesis: Delft University of Technology, École Polytechnique Federale De Lausanna; 2009.

2. Zwanenburg WJ. The Swiss experience on the wear of railway switches and crossings. In: *7th Swiss Transport Research Conference - STRC 07*, Patterson Z. (eds.); September; Monte Verita / Ascona 2007. p. 15.

3. Kassa E, Andersson C & Nielsen J, Simulation of dynamic interaction between train and railway turnout, *Vehicle System Dynamics - International Journal of Vehicle Mechanics and Mobility*, 2006; 44(3): 247-258.

4. Jones A, RE/PW/2003, *NR60 Inclined S&C D Switch assembly & machining*, Network Rail, 40 Melton Street, London, NW1 2EE, 2006.

5. Mathworks. *Polyfit - Polynomial curve fitting*. Available from: http://www.mathworks.co.uk/help/matlab/ref/polyfit.html [Accessed: 05/05/2013].

6. Mathworks Document Centre. *Polyval - Polynomial Evaluation*. Available from: http://www.mathworks.co.uk/help/matlab/ref/polyval.html [Accessed: 10/06/2013].

8. MODELLING AND VALIDATION

Modelling allows for a method to validate the conclusions drawn from the instrumentation outputs and monitor the effects that parameters have on the strain and displacement outputs. Validations of five parameters were completed through computer modelling; strain gauge vertical location, closed switch rail strain increase, increased speed decreasing strain, field instrumentation output variation with lateral loading position, and variable ground stiffness. Vampire and Abaqus/CAE software was used to complete the dynamic and finite element modelling respectively.

This section goes through the application of the Finite Element Analysis (FEA) modelling, generated in Abaqus/CAE modelling software and the application of the outputs from the nominal rail part. A railway specific software package, Vampire®, has been used for a standard turnout with similar design to SC1 for the dynamic affects.

8.1 VALIDATION INTRODUCTION

Two commercially available computer packages, Vampire® and Abaqus/CAE, were used for validation. Vampire® is an industry used software application that can calculate the stress being generated in the contact patch using dynamic calculations [1]. Abaqus/CAE is a FEA package that was used for the static modelling and variation in strain at the gauge location. Vampire® is computationally quicker to run against the full multi-body simulation packages due to the 2D nature of the calculation and focus on the head of the rail. FEA is more computationally expensive, but with the ability to understand the strain at a certain location through the full rail section. There are many errors that may occur in the field experimentation as shown in the Section 6.2 *Error Levels* in *Field Experimental Outputs*. To increase the confidence of the outputs from the instrumentation and to understand the contributing parameters in the strain outputs, validation / modelling of the system was completed.

From the analysis section of the field instrumentation outputs, five topics need additional validation through modelling;

- Increased speed reduced strain at the gauge – From the gauge outputs, it was found that the strains decreased with increasing speed. To find out the cause for this, and if there are any detrimental effects on the track, Vampire® was used to validate the speed effect on strain.

- Increased strain from transfer from the switch blade – It was seen in strain outputs and analysis chapters that there was an increased strain as the wheels transferred from the switch blade onto the stock rail. Vampire® was used to model the dynamic loading of the variable switch profiles.

- Vertical strain gauge alignment – The positioning of the gauge in field experimentation is highly complicated to ensure it is equal to the design. FEA is used to monitor the effect of vertical position on the strain gauge and the affect of vertical position of the gauge.

- Contact position laterally on the rail – From experimentation outputs, there is a strain variation of up to 300με for similar vehicles at the same gauge. An explanation for some of the contribution to this could be the lateral location of the contact due to the contact between the wheel and rail. The same static FEA model is used with change in the contact positions to understand the effect that the location has on the output at the expected location of the gauge.

- The strain variations from variable ground stiffness – under rail conditions are another potential explanation for the variation of the variations in strain. The contact position and variable ground conditions are modelled at the same time to monitor the cumulative effect on the strain at the gauge.

8.2 DYNAMIC MODELLING FOR SPEED VALIDATION

Speed was shown in the *Progress of deterioration* chapter to reduce strain at the gauge. To validate the analysis, a vehicle dynamics model of S&C was created within Vampire®. A track model was set up that represented an S&C unit, similar design to SC1 and SC3, as it gave a representation of a non-static loading. The model was created to understand the effect

that speed had on the loading through the complex geometry and discontinuities in the running path through S&C.

8.2.1 Vampire® S&C model design

The model consisted of rail profiles that were collected in track at 0.1m intervals through both the switch and the crossing panels at SC1. The Vampire model interpolated the rail between the measured profiles and outputs a contact region at a frequency of 0.001m longitudinally. To align the model with the reference site, the crossing occurs first, followed by the transition from the switch to the stock rail. The model was aligned to Figure 8-1, with a gauge spread of up to 50mm for the change in the contact found through the crossing to represent the discontinuity in the running path, along with measured rail profiles. A kink (short change in contact lateral conditions) was applied at 100m to represent the switch tips, altering the contact location.

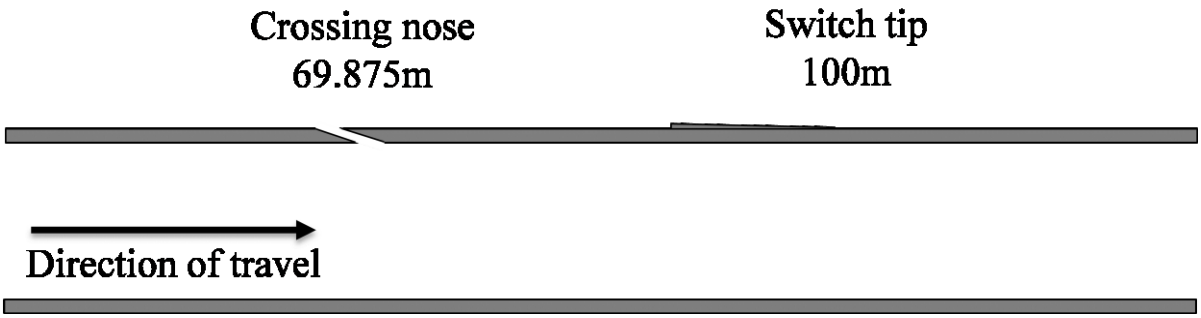

Figure 8-1: Vampire® model schmatic

The crossing nose and the right hand turnout traversing in a trailing direction are the same as SC1. The model was run at a variety of speeds that are found across the network, from 10m/s (36kph) to 60m/s (210kph), at 10m/s intervals. The vehicle used was equivalent to 10 tonne axle load, which is a equivalent to a tare Class 150 vehicle with new wheel profiles, which runs over the site SC1.

8.2.2 Speed validation

Figure 8-2 shows the wear number (Tγ, Creep force multiplied by creepage between the wheel and rail) output at (a) the crossing and (b) the transfer zone to see the surface the

variation in the contact location and stress through the asset under loading. Tγ was chosen as it is the energy within the contact patch and expresses the dynamic loading conditions.

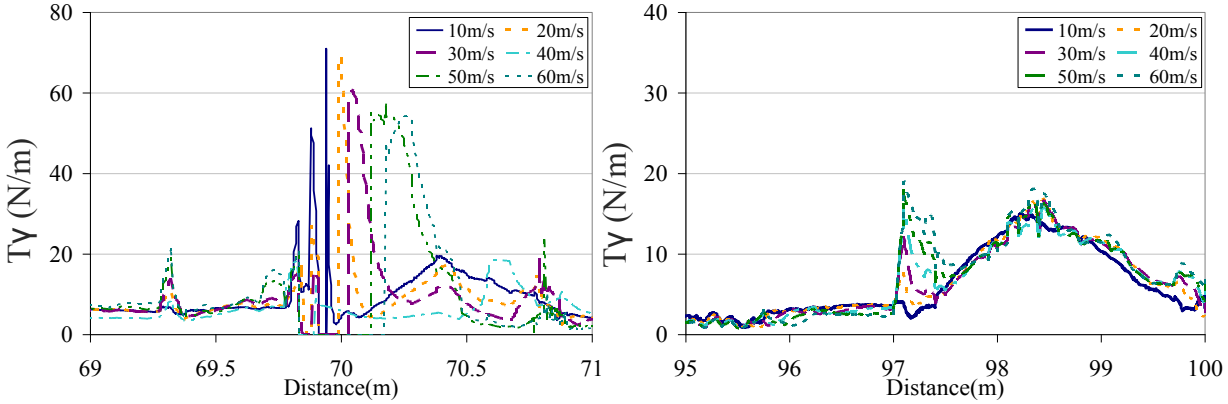

(a) (b)

Figure 8-2: Vampire Tgamma output comparing various speeds at a) crossing and b) switch

The location of the maximum Tγ shifts longitudinally due to the speed and the vehicle reaction to the irregularities. The change in the location of contact is due to the vehicle suspension and the vehicle rapidly transferring from one rail to another. The length of the contact irregularity, or loss of contact between the wheel and rail on the left rail, ranges from 0.03m for 10m/s to 0.140m at 60m/s. This shows the whilst the strains that would be found at the gauge on the crossing nose appeared to be decreasing with the speed, the peak values are shifting longitudinally with the speed, and elongating the location at which the wheel is in contact with the crossing [2].

8.2.3 Switch transfer validation

The switch blade was seen to generate higher strains through the results shown in *Process of deterioration*, which experiences an increase of 100με on each site, and under 130MGT increased the strain by up to 300με. The increase in strain is due to the continuous and repeated transfer of the vehicles from the switch blade onto the stock rail and the increased dynamics of the vehicle which generate a higher vertical shear strain. The Vampire® model was used to validate the increase in dynamics that were being experienced on the track.

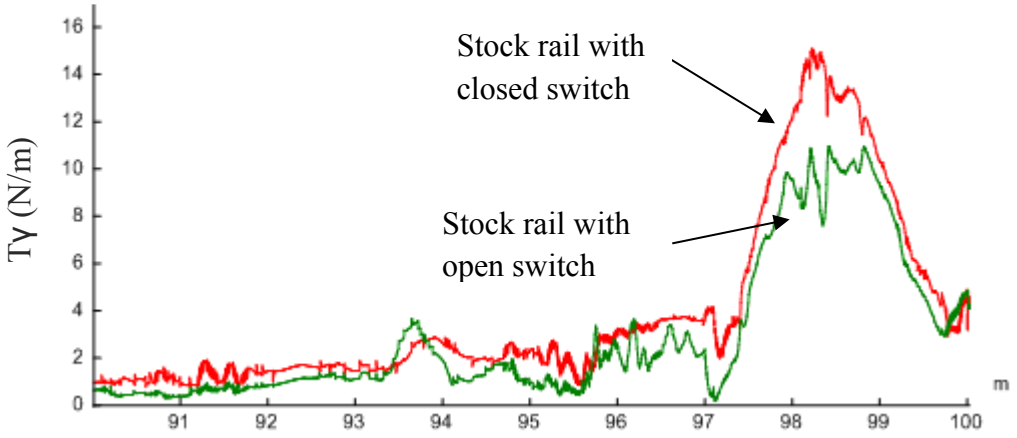

Figure 8-3: Vampire Tgamma output comparing stock rail with open and closed switches

The localised stress outputted from the model show that there is an increase on the left rail through the majority of the switch panel. The effect on site is seen as up to 300με, with the output from the modelling showing an increase of 5N/m. This difference between the modelling and the instrumentation is shown by Coleman [3]. The Vampire® software only calculated a single point of contact location, and therefore has a change in loading magnitudes due to the interpolation for a simplification of a single point completed through complex multipoint contact region. This means that the complex multi-point contact regions are modelled as a single point of contact at a location between the two precise loads and therefore reduce some of the accuracy of loading within the model. The simplifications of the iterations in Vampire® software are used to decrease the computational power needed for the model and are the reason behind the smaller than expected forces generated through the transfer from switch blade to stock rail in the model output.

8.3 FINITE ELEMENT ANALYSIS FOR STRAIN AND DISPLACEMENT

Using FEA allows for parameters to be tested and monitor the outputs due to specific loading conditions and the ability for the body to be loaded internally. The change in contact location and variable pressures would be very difficult to replicate in a lab testing due to the amount of space needed and the inclusion of other variable parameters, such as ground condition.

The purpose of this modelling is to understand some of the differences that have been found from field experimentation, with the same vehicles generating a large difference in strain

values, and validate the ground stiffness against strain conclusions that were drawn from the strain gauge and geophone comparison.

A plain line rail section was modelled in commercially available FEA software package Abaqus/CAE, with a 56kg/m (113lb/ft) profile, typical for plain line sections of track in the UK [4]. The design of rail profile (vertical 56E1) is 'as installed' plain line section found at SC1, the reference site, and SC3. FEA was completed to validate the strain at the gauge due to the ability to change parameters and compare results, such as variable loads and variable under rail stiffness. Under rail stiffness was modelled to increase the accuracy of the outputs by allowing for a deflection in the system under loading. The variable stiffness under sleeper increases the accuracy of the model output as it replicates the non-rigid construction of the railway system.

Displacements of the sleeper node, shown in Figure 8-7 are outputted and aligned with the instrumentation data from site to ensure that the system (rail, sleeper and under rail stiffness) conditions are realistic. Ensuring that the outputs from the nodes are as expected will allow for validation of the instrumentation results in addition to the FEA validation.

Figure 8-4 show the von Mises stress from the steps and the location of the loading from the FEA that has been completed in the Abaqus/CAE modelling software.

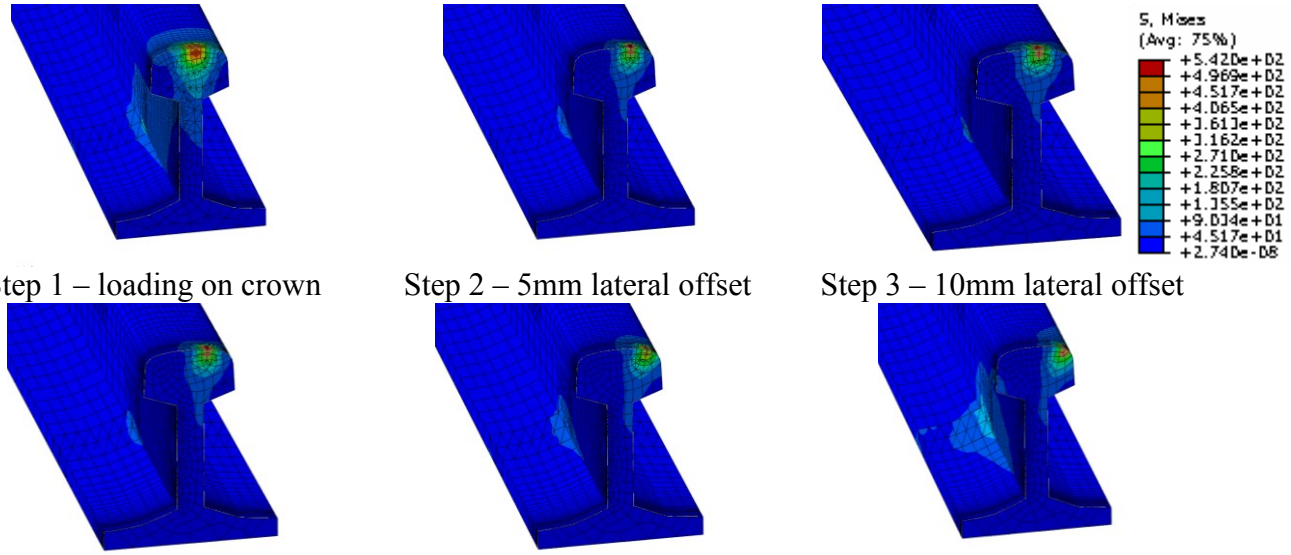

Step 1 – loading on crown | Step 2 – 5mm lateral offset | Step 3 – 10mm lateral offset

Step 4 – 15mm lateral offset | Step 5 – 20mm lateral offset | Step 6 – 25mm lateral offset

Figure 8-4: Progression of steps in the finite element analysis showing the location of maximum stress within the plain line rail section

8.3.1 Finite Element Analysis parameters

FEA has the advantage of generating variations of parameters which for field instrumentation can be expensive and time consuming, either in a lab or in the field. The advantages for FEA allows for parameters to be altered, and strain outputs at a specific location to be created and outputted. The disadvantages include the need for regular validation to ensure accurate high quality outputs. The maximum shear strain from FEA and at the same location as gauge are validated against the peak to peak shear strain values seen at SC1 at the gauge. In the model generated, three variable parameters are investigated;

1. lateral location of contact
2. variable stiffness of one sleeper and variable stiffness of two sleepers
3. variation in pressure being loaded at the surface.

FEA was chosen for completing the loading and variation in the loading as it has the ability to generate strain through the part, as well as output strains at various locations. The computer that the models were run on had the processing as described in Table 8-1;

Table 8-1: Pressure and suspension element flexibility

Computer type	Processor	CPU	Bit rate	RAM
Desktop	i7 – 2600k (8core)	3.4GHz	64	8Gb

All the models were run on the same computer, so the times completed are comparable.

8.3.2 Assumptions and alignment with instrumentation

A summary of the assumptions used when generating the model in Abaqus/CAE are;

- Static analysis is preferred over dynamic analysis within this model due to the reduced computational time for completing the model. The static analysis is completed to understand the strain development due to the loading of the system and affect stiffness has on the strains. This gives a reasonable comparison with the field experimentation output. Additional benefits for completing a dynamic analysis: development of loading and progression of displacement to increase the accuracy;

were deemed less significant in comparison to the additional disadvantages: increased time per analysis and increased computational resources.

- The forces being applied is through a contact patch at 0.0001m^2. A steel wheel and a steel rail are used on the railway as the wear on both parts are reduced due to the similarities in properties and high resistance to wear. The wheel, with an initial radius of 0.45m, generates a contact patch on the rail in which all the traction and braking forces must be applied. The contact patch is typically 0.0001m^2 in size.

- Pressure loading is used as the contact and application of force between the wheel and rail which covers an area (the contact patch). This distributes the load evenly over the area / patch. The pressure loading is applied normal to the surface.

- Rail material is steel with a Young's modulus of 209000MPa and a Poisson's ratio of 0.3 [5, 6].

These assumptions do not include the general assumptions and errors that are included within the FEA programme, which include discritisation of elements within the model, which can cause uncertainty through transfer of stress and strain within the elements and through the model.

8.3.3 Part and mesh

The model of the rail was created from a part supplied by Network Rail. The model is made up of a 5m section of plain line rail, with a head profile of an 113a rail [7], as 5 metres can include multiple under rail support system.

A mesh convergence, analysis to monitor the optimum mesh size at the area of interest, was completed to ensure the model was efficient and accurate. The results from the convergence are shown in Figure 8-5. The percentage change from the previous maximum stress and the time to complete the model, from the 'CPU time' are shown. The pressure of 1000MPa was used on the crown of the rail in the modelling. With the maximum strain occurring at the surface, hand calculations using 10t wheel load give a maximum stress of 980MPa.

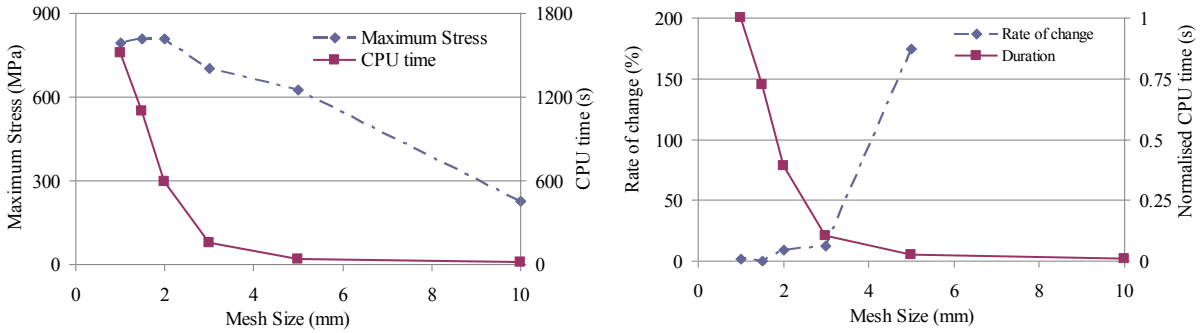

Figure 8-5: Mesh convergence analysis showing the (a)maximum stress and CPU time and (b) strain variation and CPU time against the size of the mesh under the load location

The converged outputs give the maximum von Mises stress at 810MPa. With comparing with hand calculations, the uncertainty is 17%. This uncertainty is due to the simplifications of the hand calculations and not considering any of the rail shape conditions, which causes the variation.

From the convergence analysis, a 2mm mesh is used for the FEA modelling. The mesh convergence showed that there was a variance of 1.8% in the maximum stress between a 2mm mesh and 1mm mesh. The time to complete the model with a 2mm mesh was 40% less than the 1mm mesh.

A variable mesh was applied to the rail longitudinally, with the elements at the significant area of loading and output section of 2mm, in line with convergence. The area further than 300mm away from the contact location is a 25mm hexahedral mesh. A larger mesh decreases the computational time, but it is not within the sensitive area of contact or output. Figure 8-6 shows the element sizes in relation to the gauge, with the loading at the head of the rail, directly above the gauge.

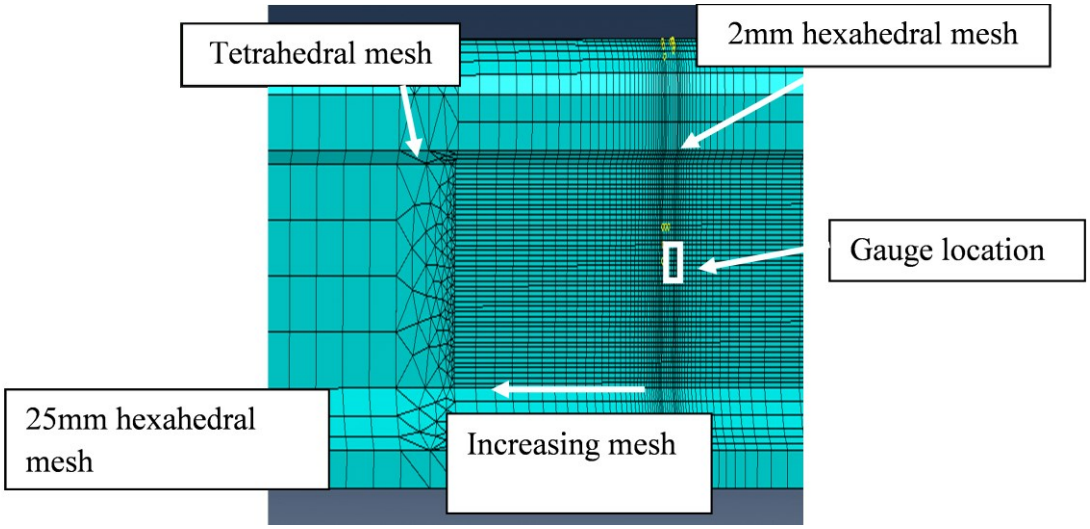

Figure 8-6: The FEA meshing of the model, illustrating types of elements

The small elements at the gauge location increase the accuracy of the model whilst giving outputs from the surface on the neutral axis, similar to the location of the strain gauge on site. Hexahedral meshes (Hex) have six sides and were used over the majority of the rail at varying sizes for quick processing due to the simple shape. Tetrahedral are pyramidal in shape and allow two different hex mesh sizes to be aligned by using varying sized elements due to the shape and compatibility between the elements.

8.3.4 Boundary conditions

An under rail 'suspension system' has been generated to increase the accuracy of the model under loading, as shown in Figure 8-7. The system represents the support under the rail, with the sleeper assumed rigidly attached to the rail, and the variable ballast stiffness supporting the sleeper, with rigid foundation. The purpose of this is to get the output from the gauge through variable under rail stiffness and to validate the results found in Chapter 7, which showed small increase from the response with larger increases in deflection. Vampire® uses the value of 50MN/m for the stiffness of the under contact conditions, i.e. the stiffness of the rail is included in the stiffness value. The value of 50MN/m was derived from the experimental studies [8], with the reference also giving examples of 63MN/m (125MN/m for track stiffness) from British Rail Research. Industry experts claim that the track stiffness varies from 25MN/m (equivalent to a multiple (greater than 4) unsupported sleepers) to 200MN/m (on very firm, contaminated ground) from experimental studies [9, 10].

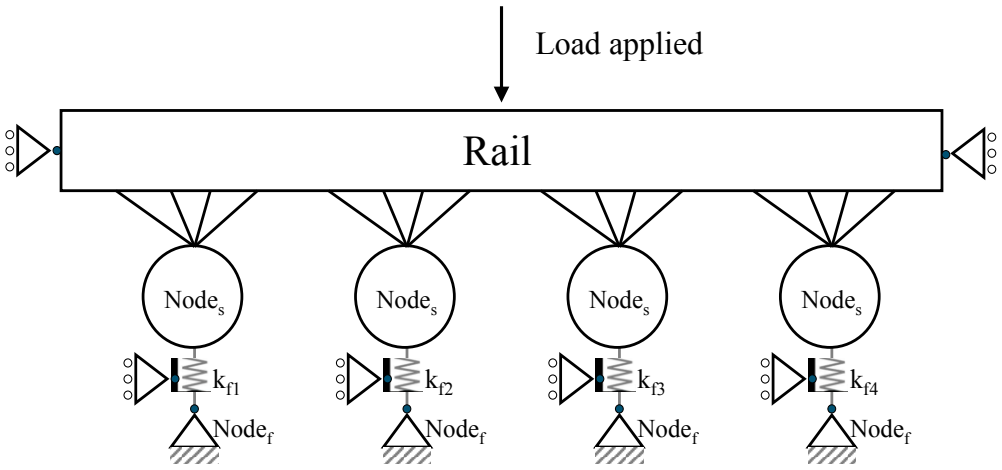

Figure 8-7: Schematic of the ground conditions and elements for modelling

k_f is the stiffness between the sleeper node, $Node_s$, and the foundation node, $Node_f$.

'Node s' (sleeper node) is conditioned to only move vertically, with 'Node f' (foundation node) fully conditioned; boundary conditions in vertical, longitudinal, lateral, yaw, pitch and roll. A stiffness of 50MN/m stiffness has been applied to the connector between the 'Node s' and 'Node f'. Sets, groups of nodes, were created to represent the sleepers, 710mm from centre to centre, and were 300mm wide, which is a typical width of a sleeper under SC1 and SC3.

k_{fx} is variable with the baseline of 50MN/m. The stiffness values are variable as seen in Chapter 6 – *Field Experimental Output.* The increase of displacement has a detrimental effect on the strain found at the switch, increasing from 90με at 1mm to 190με at 2.5mm (on open switch for a Class 220 vehicle from the field experimental results on SC3). In the first simulation, k_{f2} ranges from 10MN/m to 100MN/m, and in the second scenario k_{f2} and k_{f3} are varied, with equal stiffness. The model enables a change of ground condition can be monitored, either with a track defect (single sleeper variation) or geometry irregularity (two sleepers).

A single rail has been modelled for simplicity, to give an indication of the parameters that can cause a change in strain. The variable stiffness can demonstrate the effect of variable track geometry which can be referred back to the instrumentation and analysis. As the ballast and sleepers degrade, the track stiffness will either increasing with contamination, or decreasing with reduced support. The output of the vertical displacement can be used as a validation against field instrumentation. The modelling shows six variable stiffness and the effect that the change in ground stiffness has on the strain and the displacement of the system.

8.3.5 Load

The load is applied to the lateral positions outlined in Figure 8-9. The same pressure load normal to the surface and at a magnitude of 1000MPa was applied. 1000MPa was chosen due to the loading of the Class 91, vehicle on SC3, with an axle load of 20.3 tonnes. The maximum axle weight allowed on the network according to the 'Route Availability' is 25.3 tonnes (from Network Rail Sectional Appendix [11]), which is equivalent to 1230MPa. As only a few vehicles are at the maximum weight, a weight of 20.3 tonnes was chosen to represent the outputs from the instrumentation.

8.3.6 Phase 1: Gauge vertical location verification

The vertical location of the gauge can be a source of uncertainty as the additional bending adds to the strain seen at the gauge. The purpose of this investigation was to identify the level of error that could be incurred from the vertical distance of the gauge from the neutral axis. This would give additional confidence in the gauge output results. Figure 8-8 shows the strain against the reference of the neutral axis, at (0,0).

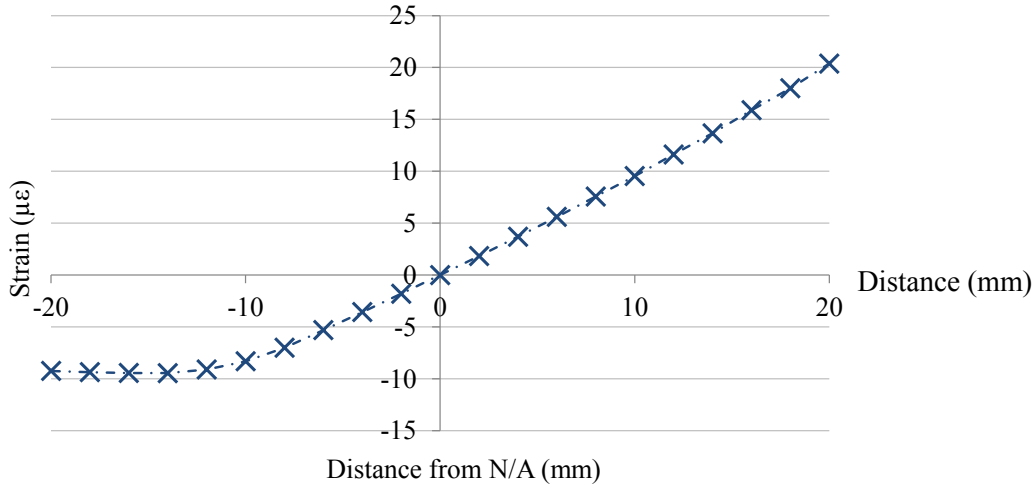

Figure 8-8: Variation in strain across the gauge from the model in Abaqus/CAE with base conditions

With the strains being the change of length of the gauge, the original length of the gauge at 13mm, and the variation over the length of the gauge at the neutral axis is zero. Changes in strain seem to be linear between -10mm and 20mm. The gauges were installed as close to the neutral axis as to allow for increased accuracy.

8.3.7 Phase 2: Strain variation from lateral contact and variable stiffness

The location of the contact laterally is variable due to the wheel and rail profiles, with additional variation through plastic deformation or wear. The FEA modelling monitors the change in strain at the gauge from the variation in the lateral position of the loading on the head of the rail. The model will determine the influence that lateral contact has on the strain and the deterioration of the rail.

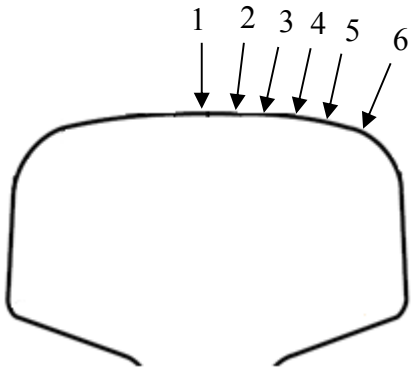

Figure 8-9: Contact location across the head of the rail

Initially, the contact / pressure position will be altered across the cross section of the rail. After the initial cross section / lateral conditions, the stiffness of a single under rail condition (sleeper) is altered, and then of two sleepers. The output gives an indication of the vertical geometry impact on the strain seen at the gauge, and the variation with lateral contact. The strains and vertical displacements from the model are shown in Figure 8-10. The figure shows the loading from the variable cross sections, with *'vertical'* number 1 on Figure 8-9, 5mm equal to number 2, until 25mm offset is number 6. The modelling outputs shows that the vertical loading gets the largest strain response at the gauge, and largest deflections of the rail, which is to be expected as the vertical loading deflects the furthest. The most significant variations in strain from the change in under rail conditions are at 10MN/m stiffness, with a single sleeper variance showing a change in strain of c. 70με. This increase from the lateral loading helps build the conclusion for the large variations in strain output at SC3.

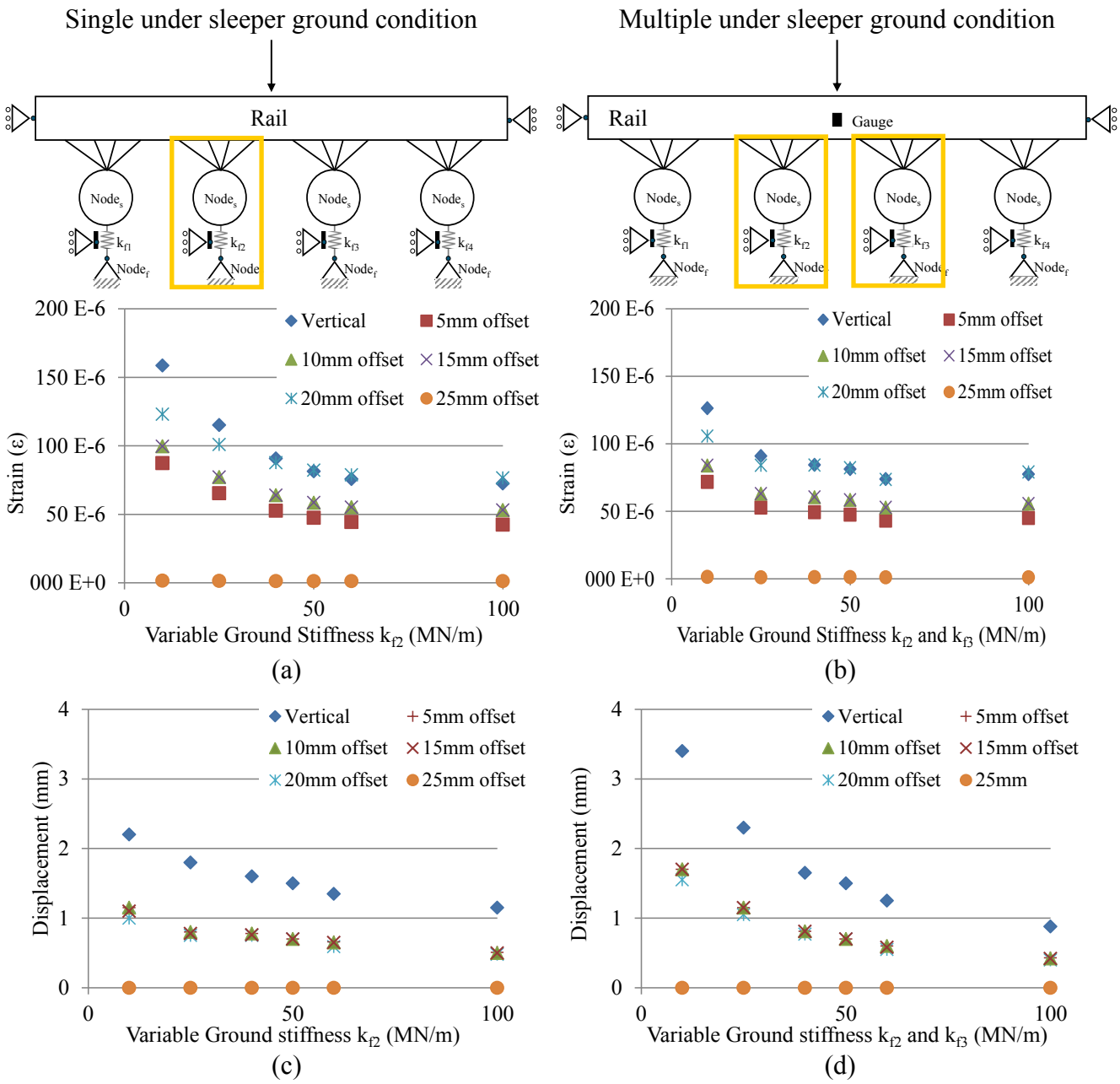

Figure 8-10: Output from FEA modelling with (a) and (b) showing strain change for various ground condition at the gauge and (c) and (d) showing displacement at the base of the rail

8.3.7.1 Variable sleeper stiffness

Variable sleeper stiffness represents the deterioration of the under rail conditions. The modelling aim is to monitor the strain at the gauge depending on the various under rail conditions and system stiffness that might occur on site. For the modelling, a single sleeper and two sleepers, one either side of the gauge, were modelled. A single sleeper variable stiffness represents if there are any issues with the components, either a change in the rail pad

stiffness or missing components, whilst two sleepers would represent the degradation of the track. Variable stiffness of two sleepers was completed as additional sleeper variations yielded similar strain outputs. The maximum deflection was outputted from at the base of the rail under the gauge location.

8.3.7.2 Lateral loading analysis

At 50MN/m, the reference ground condition, the vertical loading and loading at 20mm are similar for strain, and 5mm offset to 15mm offset are similar for strain, with 25mm not generating an output at the gauge. The 25mm loading not recording any strain at the gauge is due to the normal loading of the model not generating a vertical shear strain at the gauge due to the radius at the surface. The changes of radius occur at 6mm and 26mm, shown in Figure 8-11. 5mm to 15mm loading steps are within similar radius sections of the rail so the shear strain at the gauge are constant due to similar loading.

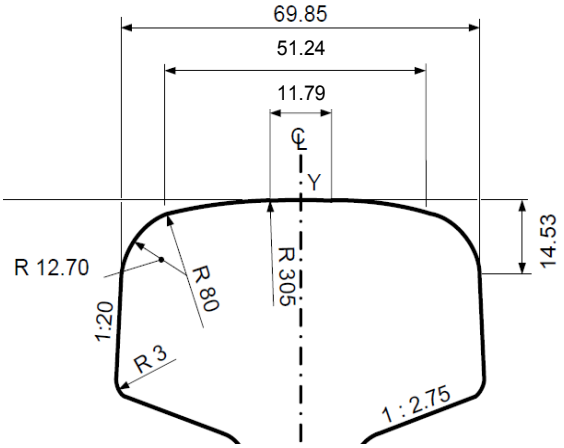

Figure 8-11: The variation in the radii of the 113A (56E1) rail profile [7]

The strain output is influenced by the location of the loading across the head of the rail, which is in relation to the radius of the rail head. The strain shows that the lateral location of the rail head contact can contribute to a increase in the gauge loading from 50με to 75με, which is a 50% increase. The increase in strain shown from the same vehicles on the field instrumentation would be due to the contact location between the wheel and rail.

8.3.7.3 Ground stiffness analysis

For stiffness greater than 50MN/m, the strain output is constant for the single and double sleeper variation. The similar strains are due to the rail part not being able to deform much over the gound condition of 50MN/m. With 40MN/m and below, the strain output changes with a exponential decreasing relationship. The decrease in stiffness under rail allows for larger (from 2.2mm at 10MN/m to 1.5mm at 50MN/m) vertical displacement.

The displacement was measured at the bottom of the rail and shows that the two under-rail variable stiffness does have a increasing effect on the vertical motion as the stiffness decreases. The increase of motion for two variable stiffness shows the displacement reducing by over a 1mm with one sleeper variable. The variation in the vertical motion below one and two under rail conditions (1.8mm for two variable conditions and 0.7mm for a single variation) are due to the rail being restrained by attached components. The results show that the increase in displacement, through multiple under rail stiffness variance, does not represent an increase in the shear strain being generated. Similar to the crossing as seen in section 7.4.2 - *Geophone analysis at the crossing of SC1*, the additional length that is allowed to vertically move keeps the strain internally lower than small lengths of stiffness variation due to the change in length at the gauge.

8.3.8 Phase 3: Variable loading pressures

Loads vary with vehicles and contact profiles. A load analysis was completed to check to see if the gauge location generated an output linear with load similar to the instrumentation linearity. The relationship from field instrumentation showed strain gauge output was linear with the load. Using the same assumptions as noted in Section 8.3.2, the head / centre line of the rail was loaded with incrementally increasing loads. The strains from the gauge location are found in Figure 8-12. The location of loading was 10mm from centre, to give a realistic contact location found at SC1, and the ground stiffness was at the reference of 50MN/m for all sleepers, as per the reference description.

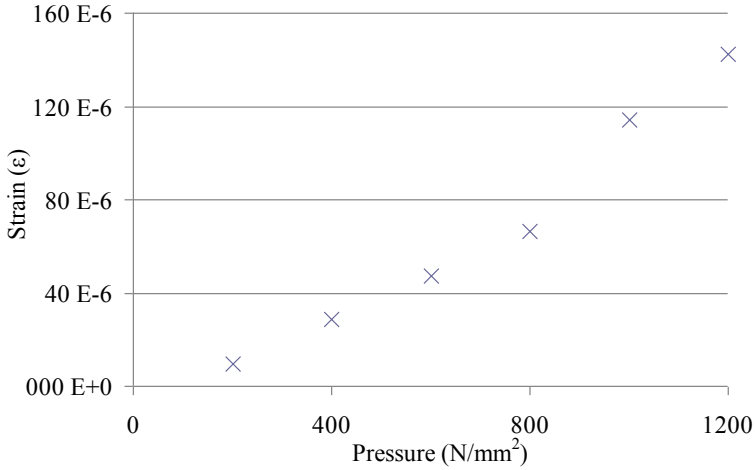

Figure 8-12: The strain output from varying pressure applied 15mm from the head of the rail with 50MN/m reference on all under rail stiffness

The outputs show that there is a good linear relationship between pressure at the rail head and strain output at the strain gauge location. The weight of the vehicles running over SC1 is between 400kN/m^2 and 850kN/m^2 per wheel, which give outputted results of between 40με and 75με from the modelling. The simplified model gives strain between 40με and 75με and the strains seen on SC1 are between 50με and 90με. This gives 86% accuracy, which is acceptable as the assumptions within the modelling and the effect on the suspension system. The variation in the output of the model against the instrumentation is due to unknown stiffness at SC1 through the S&C unit.

The size of the mesh is an additional source of error that might cause a small variation, with the convergence showing 2% error from the strain output in Figure 8-5.

8.3.9 Analysis and Calculation of contact forces

From the hand calculations seen in Chapter 5, the estimated shear stress found in a rail was c. 7.97MN/m^2. From the numerical calculations from the finite element analysis, the mean principal stress was 8.4MN/m^2. This gives an uncertainty level of 6% from the hand calculations. This is seen as acceptable due to the simplifications and assumptions that were used in the hand calculations such as profile change, and solid ground conditions.

The strains that are seen from the outputs at the gauge location show that from a Class 91, and the ground stiffness within 50MN/m, the reference range, the strains should be between 50με and 100με.

8.4 SUMMARY OF THE FORCES NUMERICALLY GENERATED AND THEIR VALIDATION WITH EXPERIMENTAL DATA

Static Finite Element Analysis (FEA) and vehicle dynamics computational modelling methods were completed to validate five of the conclusions drawn from the instrumentation outputs. Five field monitoring conclusions were validated using the two different modelling methods; increased speed decreases strain at the gauge, stock rail with closed switch generates higher strain than the stock rail with open switch, lateral position alters the loading, increase of vertical motion increase strain, and magnitude of the loading increases strain.

From vehicle dynamics modelling software package, Vampire®, speed moves the peak loading longitudinally, relocating the peak away from the gauge locations at the crossing through wheel transfer dynamics. The slower speeds allow the dips, and transfers from one rail to another, to be impacted on a higher frequency through the vehicle traversing.

The Vampire model shows that there is a small increase in the Tγ (Wear number) being generated with regards to the switch blade position against the stock rail. The experimental results showed a significant increase of up to 300με. The increase of 5J/m within the model is due to the software not being designed to cope efficiently with multipoint contact, which changes the vehicle dynamics and increases the strain in the rail with the closed switch blade.

The FEA static model was completed with pressure on a standard rail profile, applying variable ground stiffness conditions through boundary conditions and springs. A 1000MN/m pressure was applied at the surface, with the lateral position across the head of the rail of the loading showing a fluctuation in the strain of up to 35με. The maximum strain output was at the crown of the rail as the normal loading had a direct impact on the length of the gauge. An exponential decay relationship is shown against increasing ground stiffness and strain, with greater than 50MN/m showing a constant strain output.

As pressure at the same location increases, the strain increases at the gauge. The linear increase of strain was expected due to the design of the gauge being linear with load. The ground conditions cause an anomaly at pressure of 800MN/m, with errors around the mesh size and the initial compression of the springs contributing to the effect.

REFERENCES

1. DeltaRail Group Ltd, *Vampire Help Manual*. Hudson House, 2 Husdon Way, Derby, DE24 8HS, United Kingdom, DeltaRail Group Ltd. 2012.

2. British Rail Board. GM/TT0088 *Permissible Track Forces for Railway Vehicles,* Railway Technical Centre, Derby. Group Standards; 1993.

3. Coleman I, Kassa E & Smith RA. Algorithm for wheel/rail contact detection at railway switches and crossings. In: *22nd International Symposium on Dynamics of Vehicles on Roads and Tracks*, Iwnicki S., Goodall R., Mei T. X. (eds.), Manchester, Manchester Metropolitan University, 2011, p.6

4. Ventry D, RE/PW/792, *CEN56E1 Rail section and drilling details*, Network Rail, 40 Melton Street, London, NW1 2EE, 1986.

5. Tata Steel, *Rail Material Property Comparisons*: Tata Steel, 2010.

6. Ashby MF & Jones DRH, *Engineering Materials 1 - An introduction to their properties and application - 2nd Edition*. Butterworth-Heinemann; 2002.

7. Ventry D, RE/PW/620, *BS113A Rail section and drilling details*, London. Network Rail, 40 Melton Street, London, NW1 2EE, 2005.

8. Jenkins HH, Stephenson JE, Clayton EA, Morland GW & Lyon D, The Effect of Track and Vehicle Parameters on Wheel/Rail Vertical Dynamic Forces, *The Railway Engineering Journal, Institute of Mechanical Engineers*, 1974, January; 3(1).

9. Priest J & Powrie W, Determination of dynamic track modulus from measurement of track velocity during train passage, *Journal of Geotechnical and Geoenvironmental Engineering*, 2009, November: pp1-33.

10. Le Pen L. Research Fellow, University of Southampton. Personal communication. 26/02/2013.

11. Network Rail (Network Rail employees only). *Network Rail Sectional Appendix (NESA)*. From Network Rail; Available from: http://www.networkrail.co.uk/aspx/10563.aspx [Accessed: 08/09/2013].

9. CONCLUSIONS

A review of the thesis describes the main outputs of the research. Contributions towards developing knowledge within life time monitoring of switches and crossings through field experimentation are discussed. The implications of the research completed are described, with recommendations for further work arising from the thesis.

9.1 THESIS REVIEW

The research motivation was to understand the forces going through the S&C and how the deterioration develops under dynamic loading throughout the life cycle. This is important as S&C are a 'hungry asset', taking up £410m in maintenance and renewal in 2011/12, which includes 24% of the maintenance budgets for 5% of the network. S&C units allow manoeuvrability within the network whilst keeping the railway safe and operational. The costs come from the complexities within the design and the operations of S&C and the budget percentage shows the significance of the asset within the rail infrastructure company.

The understanding of life cycle deterioration within S&C has not previously been monitored due to the complexities in design and implementation, and the industrial research focusing on other areas, such as damage mechanisms. The lack of information on the deterioration rates through S&C means that the current maintenance practices are cyclic or reactive because the current predictive practices lack the necessary knowledge of deterioration. The outcome from this investigation can be used to provide a finely calibrated pre-emptive schedule for more effective S&C maintenance and investment, which will optimise the replacement regime and maintenance practices.

The objectives for the research were set out as:

- Evaluate performance of current in-services S&C.
- Determine deterioration of S&C over time.

- Determine the key factors that change the deterioration rate of S&C.

The gaps of current knowledge, found through the literature review, centred on:

- Optimisation of maintenance for S&C found through existing practices due to the current cyclic inspections.

- Increase the knowledge of UK field instrumentation. Currently, instrumentation is used infrequently to understand the forces on the rail network. In late 1970s and early 1980s, crossings were instrumented, but focused on specific designs and for short periods. These designs are no longer pertinent and need updating to include the modern rolling stock.

- Performance of current S&C in UK. A failure analysis was completed in 2007 [1], which focused on failures due to traffic type. To understand the current S&C, an update was necessary.

- Critical parameters in the degradation of S&C. S&C have over 200 design possibilities, which are currently replaced like for like in service. Development of parameter knowledge will optimise the design and location to increase the efficiencies of the network.

In order to reach the objectives and fill the gaps of knowledge found in Chapter 3, field experimentation was designed and installed to find the strains through in-services S&C units.

In Chapter 4, the Network Rail failure statistics were analysed from 2011 to 2013. Through statistical analysis of the delays to the trains due to S&C, the failures covered a wide geographical area and the switch rail was found to be the highest component failure. The delay and rectification costs were combined to get a 'failure cost'. The mid speed switches, C and D length switch, were chosen for further investigation due to the significant population, 63% of total S&C population, and preferred design of the infrastructure owner, operator and maintainer going forward, the D switch (see Table 2-3 for definition).

Chapter 5 looked at the field instrumentation design. The design of the instrumentation and experimentation was novel to the S&C in the UK. Eight sites were selected which had six parameters using a design of experiments technique. In Phase 1, four of the sites were instrumented, with the limitation on implementation due to access to infrastructure. Of the four sites with instrumentation, three gained clear and useable data with the final site

generating un-filterable amounts of noise. Strain gauges, geophones and accelerometers were installed at strategic locations determined through hand calculations, and failure statistics. Two sampling techniques are analysed to reduce the huge number of datasets, whilst the outputs remaining pertinent. The Latin Hypercube method was selected due to the semi-randomised nature of selection.

Chapter 6 studies the data collection, conversion and filtering of the raw data selected. The instrumentation outputs were stored at each site in a data logger for manual download due to the amount of data collected and limited telecom network availability to transfer the data via a remote network. Peak to peak strain and displacements were shown and analysed. The frequency from the reference site and one non-reference site were analysed to show the change in the frequency of loading through deterioration of the S&C units.

The effect on the deterioration from the outputs was investigated in Chapter 7 through completing an analysis on the design of experiment parameters. The development of strain with cumulative tonnage showed an increase, whilst the bending strain through the crossing did not develop with increases in vertical displacement of the structure.

The investigation in Chapter 8 validated the outputs from the instrumentation using computational modelling. FEA and dynamic modelling were used to understand the relationship between the location of contact, speed and the strain being generated at the gauge. The modelling was completed to establish key parameters in the deterioration of S&C.

9.2 SWITCH AND CROSSING LOADING AND THEIR IMPLICATIONS

S&C deterioration is dependent on the magnitude of loading between the wheel and the switch / crossing, as with all cumulative loading and fatigue. This research has investigated four areas with the implication pertinent to the railway industry.

9.2.1 Location of failure

As was seen in Chapter 4, the last four years have shown that S&C account for between 6.5% and 10.4% of the annual delay minutes nationally, although 70-85% of these occur in the points operating equipment (POE). Whilst the majority of the failure minutes occur within the POE, the focus of this research is on the Pway components due to the safety critical

nature of their failures. Failure statistical analysis from switches and crossings showed that the switch blade was highly significant. The main failure mode was dependant on the length of the switch, with wear causing c. 45% of failure at higher speed and plastic deformation at c. 44% of failure at lower speed. This is due to the variation in vehicles, with freight vehicles tending to generate plastic deformation from high loading less likely to traverse higher speed switches. The switch rail has a significant influence on the S&C unit as it is the moveable section of the railway, with longitudinal profiled rails that allow for a transition from the through route, to the turnout.

9.2.2 Loading as the vehicle traverses the switch and crossing unit

Chapters 6 and 7 monitored the outputs from the instrumentation and compared the loading through a single S&C unit for multiple vehicles. The RMS shear strain seen for all vehicles through the unit were greater than 80με, with the freight generating 120με at the gauge at sleeper six. The loading at sleeper six is significant due to the multiple point contact that occurred and high strain. This means that the management of the wheel / rail contact conditions at sleeper 6 are vital to maintain a high capacity railway.

Chapter 7 shows that the transfer from the switch rail to the stock rail generates a larger vertical loading, which generates a much larger cumulative strain over time / under tonnage. This is shown by an 85% increase in the strain under the same tonnage between the stock and transferred section. The turnout route often experiences larger vertical strains through laden freight, but is traversed less often. This leads to larger amounts of plastic deformation rather than abrasive wear and removal of material or fatigue as the plastic flow of the material occurs before the abrasive wear removes the material.

The strain values of the S&C unit have benefits to the industry by understanding the increased rate of the strain, which leads to failures. This is due to the increased vehicle loading that occurs with the transition of the vehicle from the switch rail onto the stock rail.

Five conclusions arose from the instrumentation that needed validating through vehicle dynamics package Vampire® and finite element package Abaqus/CAE;

- The vertical installation of strain gauges. This was completed to understand some of the uncertainty that came with the field installation of the gauges. It was found,

through FEA that with a 10mm offset from the neutral axis, there was a variance of ±10με. The relationship was linear between displacement and variance of ±12mm vertically.

- Strain decreased with increasing speed. This was found to be true at the gauge location through dynamics modelling. Vampire® software showed that the wheel traversing the crossing would lift vertically from the rail through the irregularities, with the distance of lift elongated by the increased speed. This variation moves the contact away from the gauge location. The contact increases the loading further along the rail, but decreases the strain at the gauge location.

- The stock rail with closed switch blade had higher strain than the open switch stock rail. The increased strain is due to the transferring of the wheel from the switch rail onto the stock rail and generating an increased dynamic loading including multi point contact. The maximum increase in mean strain of 150με shows that the stock rail with the closed switch blade deteriorates quicker, including the below rail conditions, and then continues to degrade at an accelerated rate. The strain values of the stock rail and the position of the switch rail have not previously been quantified. Computational models that are used in the railway do not fully model this transfer due to the complexities in multipoint contact, which means that they exclude some of the dynamic conditions and peak loading conditions.

There is a variation at some of the gauges of up to 300με under similar vehicles. To gain a greater understanding of this variance, the topic was broken down into smaller phases of research using FEA, which was used due to the accuracy of the FEA for the elastic modelling, and the ability to output strains at various locations.

- Phase one and two: the variable contact conditions across the head of the rail and variable ground condition showed the location of the contact of similar pressure and under good rail stiffness can induce a change of 40με at the gauge. With the change in the ground conditions and reduced stiffness the change in the strain could grow up to 80με.

- Phase three: Strain reaction was linear with load and weight variation. From the modelling, the variation in the strain, up to 300με, found from instrumentation is unlikely to be caused by a variation in the load from the similar vehicles.

From the analysis carried out, the contact conditions and the ground stiffness are highly important in the variation in the shear strain generated at the gauge on the neutral axis.

9.2.3 Design of experimentation evaluation

The design of experiments was built on the failure statistics in Chapter 4 and the expert knowledge gained from inside Network Rail [2]. Chapter 5 outlines six parameters, with three levels in each of the parameters. The instrumentation outputs were analysed in Chapter 7 to show a lower strain was generated on the through route, but the transfer from switch to stock rail generated an increased strain on either route. The lateral / cross level geometry also has a negative effect on the strain in the rail, with a 5mm lateral shift doubling the strain. An increase in the tonnage has also been confirmed to increase the loading in a linear relationship through FEA.

Speed was found to have a negative linear relationship with strain, with an increase in the speed decreasing the strain at the gauge, which was unexpected, as an increase with speed would increase the strain on plain line through increased vehicle loading. Chapter 8 modelled this phenomenon and found that the location of the contact was changing longitudinally through the irregularity, and away from the gauge, but with an increased magnitude.

The design of experiments benefit the industry through knowing the parameters the exacerbate S&C deterioration and their effect on the strain generated through loading. With knowledge of the lateral geometry having an increased dynamic effect on the strain, additional focus can be put on the geometry through the S&C unit. Understanding the speed affect will allow any new designs of S&C to focus on the transition, at the crossing wing rail, and the switch rail to the stock rail and ensure support and reduced irregularities through the length of the transition.

9.2.4 Crossing vertical geometry and associated strain

The increase vertical displacement at the crossing was compared against the change in strain in Chapter 7. There was a steady increase in the vertical displacement from 1.8mm to 2.2mm at the crossing nose, which seemed to have a negligible effect on the bending strains across the crossing over a 7 month period. This was found to be due to the constant increase in the

vertical displacement and therefore having the variation on the change of strain less than 10με.

The rate of change of the geometry is the key contributor to the development of knowledge, with a similar increase in deflection generating no increase in the strain. Chapter 8 compared the strain and displacement of a variable sleeper stiffness configuration to show the effect of rate of stiffness change. The modelling showed that with two sleepers with equal lower stiffness (at 20MN/m) had a reduced strain (85με to 120με) than with one variable sleeper stiffness.

9.3 CONTRIBUTIONS TO KNOWLEDGE

The contribution to knowledge of life time monitoring of switches and crossings through field experimentation have been covered in three areas;

- **Performance of current S&C** – Analysis of the existing failure modes have been made using recent delay data from the network. Previous analyses focused on renewal rates of S&C in Switzerland, or historic, which are covered in the literature review. The outputs from the failure analysis were used to contribute to the design of experiments technique. The outputs from the instrumentation also contribute to the performance of current S&C, with a comparison against the design of experiments parameters used.

- **UK field instrumentation of S&C** – For the first time, field instrumentation has been completed on the highly complex S&C unit due to the historic research interests not focusing around S&C. The thesis includes the design of experimentation which focused over 20,300 S&C units on the network into eight pertinent sites. The outputs from the instrumentation have been processed to give strain and vertical velocity that has not been available previously because the outputs from the instrumentation were not available. Corrected data from three of the four sites in the initial phase have been compared with analysis of the design of experiment parameters. Further work is required in the field instrumentation data collection to strengthen any conclusions that were made during the timeframe of the research. The vertical deflection of crossings against the strain has also been analysed, which has not been completed before.

- **Critical parameter study** – An evaluation of the design of experiments parameters have not previously been completed due to the lack of available instrumentation data as it was not available. The outputs from the instrumentation have been used to understand the parameters that have a greater influence on the deterioration of the S&C. The contribution to the knowledge has been validated through computational modelling, with FEA and dynamic modelling. Both modelling types are well known and have been validated; however, the outputs from the modelling have not been used for the analysis of S&C.

9.4 FURTHER WORK

This research shows that four areas would benefit from further research.

- Develop deterioration trends through on-going analysis of instrumentation outputs. This would allow for limits and trends / patterns to be used to develop a predictive maintenance routine. With increased quantity of instrumentation outputs covering a longer period of time, the conclusions can be supported with increased confidence. Instrumentation data was used from January 2011 to March 2013 due to the duration of the live data logging systems. Whilst varying ages of S&C were instrumented in this research, a full life-cycle has not been covered by the data collected. Additional data from the current instrumented sites will allow for developments in the knowledge to be broadened and strengthen and quantify the conclusions.

- An expansion of the instrumentation to the second phase, examining different lengths of S&C and various tonnages to strengthen the conclusions found. The instrumentation that is currently in place covers four of the eight sites outlined in the design of experiments due to time constraints and access to the sites. The first phase of the instrumentation covered similar S&C turnout length and so an analysis was completed with other parameters. With additional research completed in field experimentation outlined in the DOE, the further work will close some of the gap of forces and deterioration through various designs. To develop the research, the output from the instrumentation on different length of S&C should be investigated to give a greater understanding of a parameter outlined in the initial design. Further work is required in the switch length to develop the knowledge of existing S&C units and the

variation on the instrumentation output on the diverging route, rather than a focus on the through route for this research.

- The development of a risk based maintenance practice leading to predictive maintenance. The risk based maintenance practices would need to take the failure statistics and develop levels for the detection, sensitivity and occurrence. As a result of the failure statistics and limited understanding of the current failures through S&C, risk based maintenance operations can be developed to close some of the gaps found through inspections and failure statistics. While the failure statistics and necessary information were collected, the development of the risk-based maintenance operations was outside the scope of the research. Future work is needed on the development of the levels within the three risk classification categories, and then implementation and trail schedule to increase the predictive maintenance knowledge.

- Development of a theoretical S&C loading model. Coleman [3] studied the effect of dynamic loading on a crossing. The combination of the instrumentation outputs and the development of a switch dynamic model would increase the validation and the total knowledge of deterioration through S&C. A single rail was modelled with a suspension system to represent plain line under a pressure load. As a result of the simplifications that were modelled, further research is needed to develop and validate the model which will allow for in-depth parameter studies for studying new design.

REFERENCES

1. Williams J, Gordon D & Harrison J, *S&C Failure and Delay Analysis*, Report No: SA/TSS/17754/S3/R001, Serco Assurance Thornson House, Birchwood Park, Warrington, Cheshire, WA3 6GA. 2007.

2. South G. Principal Switch and Crossing Engineer. Personal communication. 7th January 2011.

3. Coleman I, Kassa E & Smith RA. Algorithm for wheel/rail contact detection at railway switches and crossings. In: *22nd International Symposium on Dynamics of Vehicles on Roads and Tracks*, Iwnicki S., Goodall R., Mei T. X. (eds.), Manchester, Manchester Metropolitan University, 2011, p.6

APPENDIX 3.A – SWITCH INSPECTION HAZARDS

Details for the NR/C/S/053 and the inspection criteria that define a 053 failure.

Switch side wear inspection S053 and some of the signs of failure

Hazard Number	Details	Tell tale signs
1	Sideworn stock rail associated with a little used switch rail	− The switch tip projects above the bottom of the sidewear scar − The switch tip has been struck by wheels − The switch tip has been deformed by wheels into the sideworn stock rail
2	Stock rail and switch rail both worn	− The switch rail may be more worn and display a flatter sidewear angle than the stock rail − The wheels have formed a ramp on the switch rail − Markings have been left by the wheel flange as it has begun to climb the switch rail nd then slipped back
3	Stock rail headwear associated with less headworn switch	− The switch tip has been stuck by wheels
4	Switch rail damage	− Lipping is present on the gauge face of the stock rail and / or the back edge of the switch rail − There is evidence of: o Horizontal longitudinal cracking under lipping on the switch rail; o Small prices of metal are starting to lift out of the switch rail; o Numerous pieces having broken out of the switch rail o Hogged switch rails associated with lipped components
5	Switch rail with a sharp gauge corner profile	− Associated with austenitic manganese and mill heat treated rail steels − Any profile forming a noticeable edge or faceted surface at the gauge corner − Dust / shavings of steel in proximity of switch − Bright marking indicating wheel contact with a sharp radius.

APPENDIX 5.A – ALIAS AND ORDER CALCUTIONS

Aliasing is the shifting of frequency content that are larger than the Nyquist frequency into the area of interest, when converting from analogue to digital. This is an undesirable effect which can be filtered out with the use of anti-alias filters. This filtering is completed within the DAQ and does not need to be considered for the sampling calculations.

R_s = Sampling rate

N_s = Nyquist frequency, the maximum reliable, useable frequency, $R_s/2$

F_s = Frequency of the singal using the data acquisition system

R_{int} = round(F_s / R_s)

F_{alias} = Absolute((Rs*Rint) - Fs), which give the alias frequency of the system.

The order of the system should be between 1 and 6. These can be increased with the use of doubling the filtering, but become useless about order 10.

When plotted on logarithmic scales, the Butterworth filter response is flat within its pass-band and then rolls off with an ultimate linear roll off rate of -6 dB per octave (-20 dB per decade). A second-order filter decreases at -12 dB per octave, etc. The ultimate roll off rate is actually the same for all low pass and high pass filters.

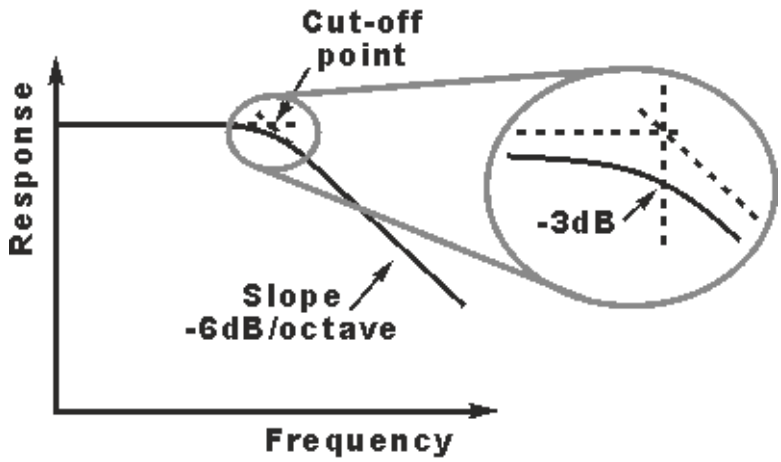

(http://www.radio-electronics.com/info/rf-technology-design/rf-filters/butterworth-rf-filter-basics.php)

The N^{th} order Butterworth filter: The magnitude response of the N^{th} order Butterworth filter with cut-off frequency $\grave{U}_c$ is given by

$$|H(j\Omega)| = \frac{1}{\sqrt{1+(\Omega/\Omega_c)^{2N}}}$$

With the normalized frequency variable defined as r = W / Wc , the MATLAB segment below plots the magnitude response for 1st, 3rd, and 10th order filters, that is, N = 1, 3, and 10, respectively. Note that as the filter order increases the response becomes flatter on either side of the cut-off; and the transition (cut-off) becomes sharper.

r = 0: 0.1: 3;

H1 = 1./sqrt(1.+ r .^2); H3 = 1./sqrt(1.+ r .^6); H10 = 1./sqrt(1.+ r .^20);

(http://www.expertsmind.com/learning/butterworth-filter-assignment-help-7342873922.aspx)